PERFORMANCE OF HIGH-STRENGTH STEEL REINFORCEMENT IN SHEAR FRICTION APPLICATIONS

Final Report

PROJECT SPR 805

Oregon Department of Transportation

PERFORMANCE OF HIGH-STRENGTH STEEL REINFORCEMENT IN SHEAR FRICTION APPLICATIONS

Final Report

SPR-805

by

Andre Barbosa, Ph.D.
David Trejo, Ph.D.
Nicolas Matus
and
Naga Pavan Vaddey, Ph.D.

Oregon State University
School of Civil and Construction Engineering
101 Kearney Hall
Corvallis, OR 97331

for

Oregon Department of Transportation
Research Section
555 13th Street NE
Salem OR 97301

and

Federal Highway Administration
1200 New Jersey Avenue SE
Washington, DC 20590

September 2020

Technical Report Documentation Page

1. Report No. FHWA-OR-RD-21-02	2. Government Accession No.	3. Recipient's Catalog No.
4. Title and Subtitle Performance of High-Strength Steel Reinforcement in Shear Friction Applications		5. Report Date -September 2020- 6. Performing Organization Code
7. Author(s) Andre Barbosa, Ph.D., P.E.; 0000-0003-4547-531X David Trejo, Ph.D., P.E.; 0000-0001-8647-8096 Nicolas Matus Naga Pavan Vaddey, Ph.D., 0000-0002-1999-0003		8. Performing Organization Report No.
9. Performing Organization Name and Address Oregon State University School of Civil and Construction Engineering 101 Kearney Hall Corvallis, OR 97331		10. Work Unit No. (TRAIS) 11. Contract or Grant No.
12. Sponsoring Agency Name and Address Oregon Dept. of Transportation Research Section 555 13th Street NE, Suite 1 Salem, OR 97301 Federal Highway Admin. 1200 New Jersey Avenue SE Washington, DC 20590		13. Type of Report and Period Covered Final Report 14. Sponsoring Agency Code
15. Supplementary Notes		

16. Abstract: The use of high strength steel reinforcement has the potential to provide economic and constructability benefits when used in reinforced concrete structures. Current design provisions limit the nominal yield strength of reinforcing steel bars to 60 ksi (420 MPa) for many bridge design applications. This report presents results from a laboratory testing program designed to evaluate the performance of concrete interface shear reinforced with ASTM A706 Grade 60 (420 MPa), ASTM A706 Grade 80 (550 MPa), ASTM A615 Grade 100 (690 MPa), and ASTM A1035 Grade 120 (830 MPa) reinforcing steel bars. Results are reported on the influence of reinforcing steel bar size, reinforcing steel bar spacing, shear interface surface preparation, and nominal concrete strength on shear friction performance. This report provides a summary of previous research regarding shear friction theory, a description of the test specimen design, and an overview of the materials used. Results indicate that using high-strength steel reinforcing bars did not have a significant impact on the peak loads reached, however they did allow for the development of greater post-peak sustained loads due to dowel action in the post-peak stage of the test specimen responses. Significant variation was observed when analyzing the effect of surface preparation. Additionally, in some cases, an exposed aggregate surface preparation enhanced the aggregate interlock and allowed it to contribute to the post-peak shear capacity. Overall, the results presented indicate that an increase in allowable nominal yield strength to 80 ksi (550 MPa) maintains a conservative design per AASHTO and ACI 318-14 code provisions.

17. Key Words	18. Distribution Statement Copies available from NTIS, and online at www.oregon.gov/ODOT/TD/TP_RES/

19. Security Classification (of this report): Unclassified	20. Security Classification (of this page): Unclassified	21. No. of Pages 247	22. Price

SI* (MODERN METRIC) CONVERSION FACTORS

APPROXIMATE CONVERSIONS TO SI UNITS

Symbol	When You Know	Multiply By	To Find	Symbol
		LENGTH		
in	inches	25.4	millimeters	mm
ft	feet	0.305	meters	m
yd	yards	0.914	meters	m
mi	miles	1.61	kilometers	km
		AREA		
in^2	square inches	645.2	millimeters squared	mm^2
ft^2	square feet	0.093	meters squared	m^2
yd^2	square yards	0.836	meters squared	m^2
ac	acres	0.405	hectares	ha
mi^2	square miles	2.59	kilometers squared	km^2
		VOLUME		
fl oz	fluid ounces	29.57	milliliters	ml
gal	gallons	3.785	liters	L
ft^3	cubic feet	0.028	meters cubed	m^3
yd^3	cubic yards	0.765	meters cubed	m^3
~NOTE: Volumes greater than 1000 L shall be shown in m^3.				
		MASS		
oz	ounces	28.35	grams	g
lb	pounds	0.454	kilograms	kg
T	short tons (2000 lb)	0.907	megagrams	Mg
		TEMPERATURE (exact)		
°F	Fahrenheit	(F-32)/1.8	Celsius	°C

APPROXIMATE CONVERSIONS FROM SI UNITS

Symbol	When You Know	Multiply By	To Find	Symbol
		LENGTH		
mm	millimeters	0.039	inches	in
m	meters	3.28	feet	ft
m	meters	1.09	yards	yd
km	kilometers	0.621	miles	mi
		AREA		
mm^2	millimeters squared	0.0016	square inches	in^2
m^2	meters squared	10.764	square feet	ft^2
m^2	meters squared	1.196	square yards	yd^2
ha	hectares	2.47	acres	ac
km^2	kilometers squared	0.386	square miles	mi^2
		VOLUME		
ml	milliliters	0.034	fluid ounces	fl oz
L	liters	0.264	gallons	gal
m^3	meters cubed	35.315	cubic feet	ft^3
m^3	meters cubed	1.308	cubic yards	yd^3
		MASS		
g	grams	0.035	ounces	oz
kg	kilograms	2.205	pounds	lb
Mg	megagrams	1.102	short tons (2000 lb)	T
		TEMPERATURE (exact)		
°C	Celsius	1.8C+32	Fahrenheit	°F

*SI is the symbol for the International System of Measurement

ACKNOWLEDGEMENTS

The authors would first like to acknowledge the Oregon Department of Transportation (ODOT) for providing the funding for this research project. At ODOT, we would like to acknowledge Matthew Mabey, Tanarat Potisuk, Craig Shike, and other engineers at the ODOT's Bridge Standards and Bridge Design units. The authors thank Jeff Gent and James Batti for their technical assistance during testing at Oregon State University. Several graduate and undergraduate students also contributed at various levels to work performed in the laboratory; their help on this project is truly appreciated. Special thanks to Cascade Steel (McMinnville, OR) for continued support on the products and specifications related to high-strength reinforcing steel bars.

DISCLAIMER

TABLE OF CONTENTS

LIST OF TABLES

LIST OF FIGURES

1.0 INTRODUCTION

High strength steel (HSS) reinforcing bars are commercially available, but limited research has been performed to justify and provide confidence for its use. When used in reinforced concrete elements, HSS reinforcing bars have the potential to provide economic and constructability benefits. However, the lack of laboratory testing results on the performance of HSS reinforcing bars in concrete elements is a cause for concern. Because of this, current design code provisions, such as American Association of State Highway and Transportation Officials (AASHTO) Load Resistance Factored Design (LRFD) Bridge Design Specifications and ACI 318-14 limit the nominal yield strength of reinforcing steel bars to 60 ksi (420 MPa) for many bridge design applications. Previous research has reported that using nominal yield strength greater than 60 ksi (420 MPa) in shear interfaces results in unconservative estimates of the shear interface capacity of the specimens (Zeno 2009, Harries et al. 2012, Barbosa et al. 2017). More recent research by Barbosa et al. (2017) has reported that AASHTO LRFD could potentially increase the limit of nominal yield strength values up to 80 ksi (550 MPa) but results were mixed and depended on other variables not tested in the original research.

1.1 OBJECTIVE OF THE RESEARCH

The objective of this research is to evaluate and define the performance of HSS reinforcing bars in shear friction applications. The report focuses on the use of the use of American Society of Testing and Materials (ASTM) A706 Grade 80 (550 MPa), ASTM A615 Grade 100 (690 MPa), and ASTM A1035 Grade 120 (830 MPa) reinforcing steel bars, since these are representative of the range of strengths expected in future bridge design and construction. To successfully implement the use of HSS reinforcement to current design provisions for reinforced concrete structures, it is critical to understand and define its performance. A total of forty-five (45) push-off specimens were designed and tested at the Structural Engineering Research Laboratory at Oregon State University to gain more insight into the effects of reinforcing steel bar grade, shear interface surface preparation, reinforcing steel bar spacing, reinforcing steel bar size, and nominal concrete strength in concrete interface shear behavior.

1.2 OUTLINE OF THE RESEARCH REPORT

This report consists of seven chapters. Chapter 1 (this chapter) provides an introduction, objectives of the research, and a brief description of what is included in each chapter. Chapter 2 presents a literature review of previous research regarding shear friction theory, code review regarding current design code provisions, experimental research, and research with full-scale composite beam specimens. Chapter 3 presents the experimental program and specimen design. Descriptions of the test specimen dimensions, reinforcement layout, experimental test matrix, and test setup and procedures are provided. Chapter 4 is an overview of the materials used in this research, including specifications and standards considered for evaluating the reinforcing

steel bars and concrete mixtures used in this study. Additionally, this chapter provides results from testing performed on reinforcing steel bars and concrete cylinders of the push-off test specimens that were constructed and tested. Chapter 5 presents experimental results and main findings based on the results obtained in terms of the effects of high-strength reinforcing steel on shear friction, including the influence of reinforcing steel bar grade, reinforcing steel bar spacing, and reinforcing steel bar size. Chapter 6 presents experimental results and main findings from tests of specimens focusing on effects of surface preparation and nominal concrete strength on shear friction. Finally, chapter 7 presents the main conclusions of the research program findings.

2.0 LITERATURE REVIEW

This chapter presents a review of the literature on concrete-concrete shear interface behavior. Shear friction is defined in this document as the resistance to displacement of an interface of two elements when acted upon by a shear force. The force is parallel to a given plane at an existing or potential crack location, an interface between dissimilar materials, an interface between two concretes cast at different times, or the interface between different elements of the cross-section (AASHTO 2015). Examples are corbels, bearing shoes, ledger beam bearings, and connections between precast concrete elements (Mansur et al. 2008).

In this chapter, the review of shear friction theory of concrete-concrete interfaces is presented first. A review of the research with push-off test specimens is then presented before research results from full-scale composite beam specimens are presented. Finally, current code equations for predicting in-service performance are reviewed.

2.1 SHEAR FRICTION THEORY

Shear friction theory is used to predict the strength of concrete-to-concrete interfaces under longitudinal shear stresses. It assumes that friction arising from the roughness of the concrete-to-concrete interface controls the shear force transfer mechanism. Figure 2.1 shows a saw-tooth model used to represent this theory. Harries et al. (2012) described shear friction as a "wedging action" arising from the relative motion between rough concrete interfaces, referring to the seminal Birkeland and Birkeland (1966) publication. This motion forces a crack to open in the direction perpendicular to the shear interface. As the crack opening increases, the reinforcing steel engages, thus creating a clamping force acting perpendicularly to the shear interface.

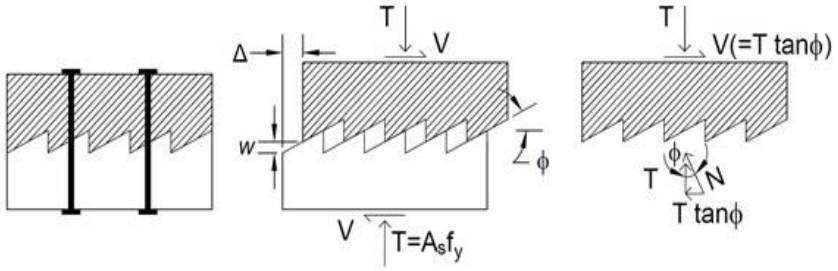

Figure 2.1: Shear friction reinforcement analogy (adapted from Birkeland and Birkeland, 1966)

Santos and Julio (2012) reported that the four main parameters included in the shear friction model are adhesion (chemical bond), cohesion (aggregate interlock), friction, and dowel action, like those described in Zilch and Reinecke (2000). The effect of these parameters on the shear

capacity can be explained by the following three load carrying mechanisms: (1) adhesion and cohesion, τ_a; (2) aggregate interlock shear friction, τ_{sf}; and (3) dowel action of the reinforcing steel bars that cross the interface, τ_{sr}. Figure 2.2 shows the influence of these three load-carrying mechanisms as a function of the relative displacement between concrete-to-concrete shear interfaces. As reported in Santos and Julio (2012), the roughness of the concrete surface has a significant impact on the concrete-to-concrete bond strength. This effect of the surface roughness is considered in code design equations as a combination of a cohesion coefficient and friction coefficient. Santos and Julio (2014) reports that even though it is well known that the load transfer mechanism in concrete-to-concrete interfaces depends on cohesion, friction, and dowel action, current design codes do not consider the dowel action mechanism explicitly.

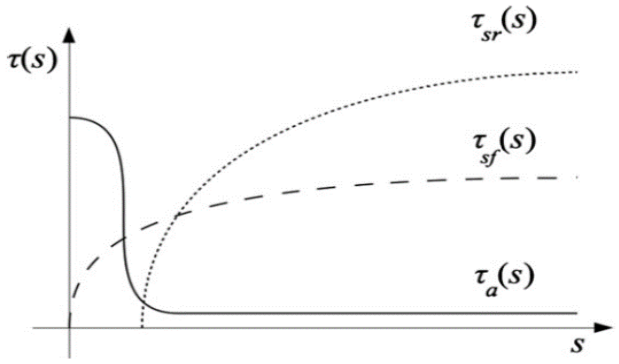

Figure 2.2: Load transfer mechanisms (adapted from Zilch and Reinecke, 2000)

As shown in Figure 2.2, when the relative displacement, s, between two concrete interfaces is low, the main load carrying mechanism is the adhesion and cohesion between concrete interfaces, τ_a. During this stage, the bond between the two concrete surfaces is unbroken and the interface exhibits its highest resistance, with little to no cracks being visible across the interface. Both concrete strength and concrete-to-concrete interface roughness are factors influencing the bond between these concrete surfaces and therefore the shear capacity of the interface.

The second load carrying mechanism shown in Figure 2.2 is the shear-friction mechanism (τ_{sr}). As the relative displacement between the concrete interfaces increases, the aggregates interact and force the crack between the concrete surfaces to increase. This causes the interface separation to further widen, thus engaging the reinforcing bars crossing the concrete-to-concrete interface. The opening at the interface generates a clamping force and increases the friction forces across the interface. The combination of the clamping force and the effect of the surface roughness result in aggregate interlock. The strength and size of the aggregates and roughened surface at this interface, and the clamping force provided by the reinforcing bars, are factors that influence the magnitude of the aggregate interlock mechanism load carrying capacity. Harries et al. (2012) reported that the crack width across the interface is critical in the interface shear friction behavior and that the crack width must be large enough to cause the reinforcing steel to strain. As a result, the crack width is directly proportional to clamping force. However, as crack

width increases, the cohesion generated at the interface by the roughened surface is reduced and therefore the crack width is inversely proportional to the cohesion component of shear friction.

Kim et al. (2010) determined that the aggregate type is a critical factor influencing aggregate interlock. The authors reported that larger aggregate interlock was observed in concrete mixtures containing river ravel compared to concrete mixtures containing limestone aggregate, for self-consolidating concrete (SCC) and conventional concrete (CC) mixtures. Figure 2.3 shows the observed behavior of the crack width-normal stress relationship and the crack width-crack slip; it can be seen that normal stress (Figure 2.3a) and crack slip (Figure 2.3b) increase as crack width increases.

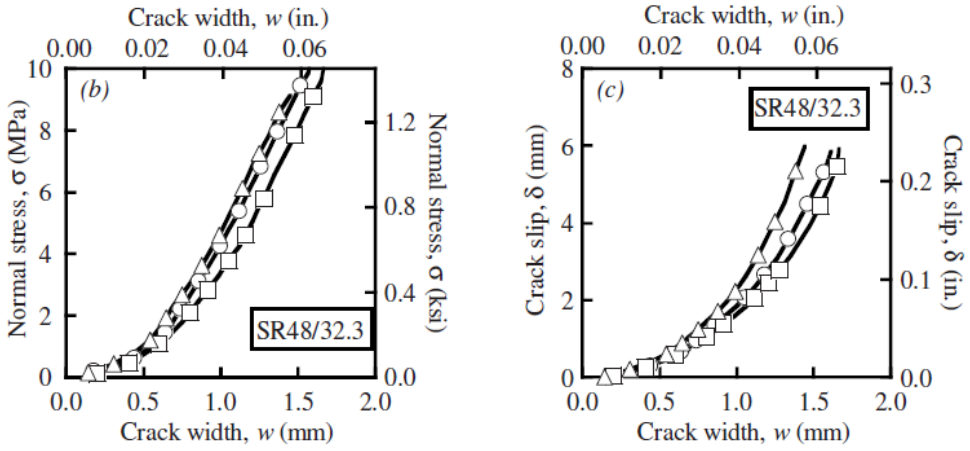

Figure 2.3: Typical plots of measured parameters in interface shear friction tests. Results presented are from Kim et al. (2010), and SR48/32.3 corresponds to a mixture tested that is a self-consolidated [S] concrete mixture, with river gravel [R], 48 MPa strength, and 32.3% coarse aggregate volume.

The last load carrying mechanism shown in Figure 2.2 is the shear reinforcement dowel action. The relative displacement between concrete interfaces will cause the reinforcement crossing the interface to be subjected to shear, in what is usually referred to as dowel action. Figure 2.4 illustrates three different dowel modes described in Park and Paulay (1975): flexure, shear, and kinking. The moment resistance of the reinforcing bar resists flexure dowel action, while the shear resistance of the reinforcing bar resists shear dowel action. Kinking is resisted by tensile resistance at an angle between the two plastic hinges, therefore creating both horizontal and vertical resistance. Each of these mechanisms require substantial slip on the interface for the dowel action to engage significantly.

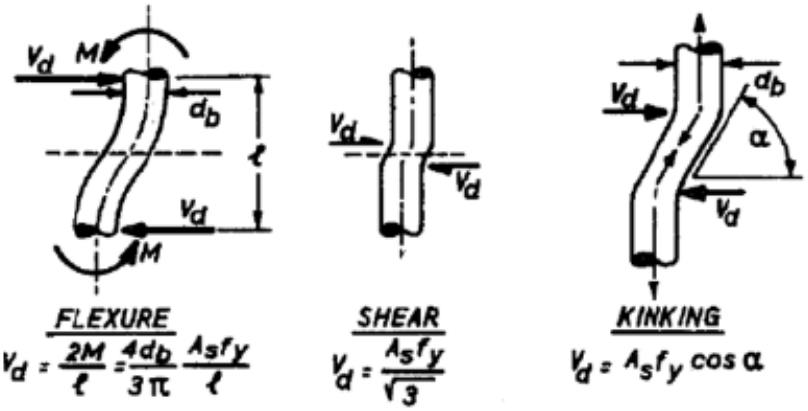

Figure 2.4: Three mechanisms of dowel action (Park and Paulay 1975)

Walraven and Reinhardt (1981) reported that dowel action is not a contributing load carrying mechanism at smaller crack widths, as can be seen in Figure 2.5. This indicates that cohesion and aggregate interlock are the main load carrying mechanisms at small crack widths. Although not shown in Figure 2.5, dowel action becomes the main contributor to the interface shear strength as the contribution of aggregate interlock is reduced due to increasing crack width.

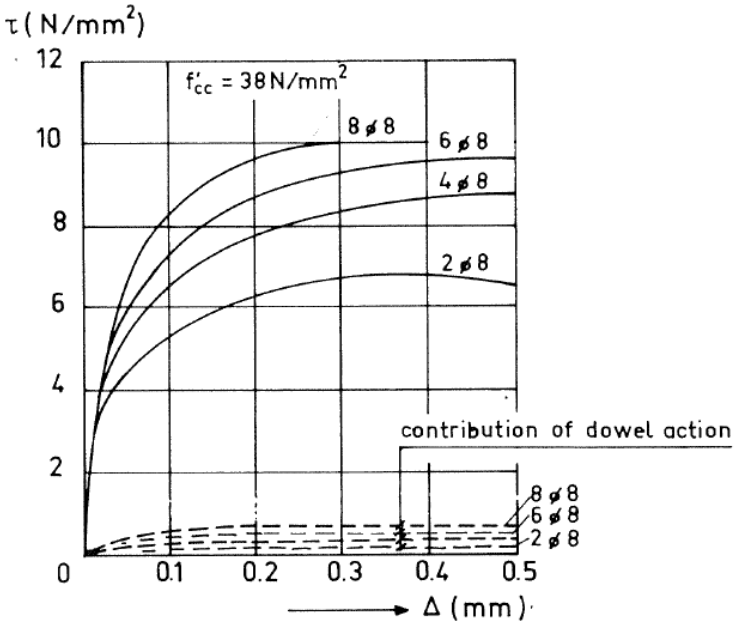

Figure 2.5: Contribution of dowel action to the total shear stress in a crack (Walraven and Reinhardt, 1981)

2.2 CODE REVIEW

This section reviews the main codes used for structural engineering design across the world, including the AASHTO (2014) standard design specification, American Concrete Institute (ACI) 318-14 design specification, Precast Concrete Institute (PCI) Design Handbook, and the International Federation for Structural Concrete (FIB) Model Code 2010. While the latter is not an actual code, it provides the basis of what is adopted in the Eurocodes and the national design documents in Europe.

2.2.1 AASHTO Design

The equations in AASHTO (2014) Section 5.8.4.1 for nominal shear resistance, V_{ni}, are presented in Equation (2-1) through Equation (2-5). Equation (2-1) consists of two terms. The first term refers to the contribution from cohesion and/or aggregate interlock with a cohesion coefficient, *c*. The second term refers to the contribution of the net normal clamping force through a friction coefficient, μ. The nominal shear resistance, V_{ni}, is given by:

$$V_{ni}=cA_{cv}+\mu\left(A_{vf}\,f_y+P_c\right) \tag{2-1}$$

and shall not be greater than the lesser of:

$$V_{ni} \le K_1\,f_c'A_{cv} \tag{2-2}$$

$$V_{ni} \le K_2\,A_{cv} \tag{2-3}$$

in which

$$A_{cv} = b_{vi}\,L_{vi} \tag{2-4}$$

Where

c = cohesion factor specified in Article 5.8.4.3;

A_{cv} = area of concrete considered to be engaged in interface shear transfer (in.^{2} [mm^2]);

μ = friction factor specified in Article 5.8.4.3;

A_{vf} = area of interface reinforcement crossing the shear plane (in.^{2} [mm^2]);

f_y = yield stress of reinforcement but design value not to exceed 60 ksi [420 MPa];

P_c = permanent net compressive force normal to the shear plane; if force is tensile, P_c is taken equal to 0.0 (kip [kN]);

b_{vi} = interface width considered to be engaged in shear transfer (in. [mm]);

L_{vi} = interface length considered to be engaged in shear transfer (in. [mm]);

f_c' = specified 28-day compressive strength of the weaker concrete on either side of the interface (ksi [MPa]);

K_1 = fraction of concrete strength available to resist shear specified in Article 5.8.4.3;

K_2 = limiting interface shear resistance specified in Article 5.8.4.3.

AASHTO (2014) states that the interface shear resistance is limited to 60 ksi [420 MPa], due to an overestimation of interface shear capacity when higher values are used, even though limited number of tests have been carried out.

Factors for Equation 2-2 to 2-4 are listed in AASHTO (2014) Section 5.8.4.3 and here in Table 2.1. The limits in the AASHTO provisions is strictly dependent on the interface condition and each interface condition has a corresponding K_1 and K_2 factor. K_1 accounts for the fraction of concrete strength available to resist interface shear. K_2 represents a limiting interface shear resistance. Based on the values listed in AASHTO provisions, K_1 has varies very little for different interface conditions (0.2 to 0.3), while K_2 varies considerably (800 to 1800). Overall, equation (2-2) is implemented to prevent crushing or shearing of aggregate along the shear plane, and equation (2-3) is implemented to account for the sparseness of available experimental data.

AASHTO (2014) Section 5.8.4.4 provides minimum area of interface reinforcement required across the interface given by:

$$A_{vf} \geq \frac{0.05A_{cv}}{f_y} \qquad \textbf{(2-5)}$$

Table 2.1: Cohesion and Friction Factors from AASHTO Section 5.8.4.3.

Interface Preparation	c, ksi (MPa)	μ	K_1	K_2, ksi (MPa)
Cast-in-place concrete slab on clean concrete girder surfaces, free of laitance with surface roughened to an amplitude of 0.25 in. (6.35 mm).	0.28 (1.93)	1.0	0.30	1.8 (12.4)
Normal-weight concrete placed monolithically.	0.40 (2.76)	1.4	0.25	1.5 (10.3)
Normal-weight concrete placed against a clean concrete surface, free of laitance, with surface intentionally roughened to an amplitude of 0.25 in. (6.35 mm).	0.24 (1.65)	1.0	0.25	1.5 (10.3)
Concrete placed against a clean concrete surface, free of laitance, but not intentionally roughened.	0.075 (0.52)	0.6	0.20	0.8 (5.52)

The minimum interface shear reinforcement, A_{vf}, need not exceed the lesser of the amount determined using Equation (2-5) and the amount needed to resist $1.33V_{ni}/\phi$ (ϕ from AASHTO 2014, Article 5.5.4.2.1) as determined using Equation (2-1) in this report. This is intended as an over strength factor as the minimum is waived or lowered if the shear resistance without reinforcing steel exceeds $1.33V_{ni}/\phi$. Additionally, the minimum reinforcement provisions specified shall also be waived for girder/slab interfaces with surface roughened to an amplitude of 0.25 in. [6 mm] where the factored interface shear stress, v_{ni} of AASHTO (2014) Equation 5.8.4.2-1 is less than 0.210 ksi [1.45 MPa], and all vertical (transverse) shear reinforcement required by AASHTO (2014) Article 5.8.2.5 is extended across the interface and adequately anchored in the slab.

2.2.2 American Concrete Institute (ACI) Design Specifications

The horizontal shear capacity specified in the ACI 318-14 Section 16.4.4 is presented in Equation (2-6) through Equation (2-11). Equation (2-6) consists of two terms. The first term assumes a cohesion factor of 260 psi [1.79 MPa] multiplied by the area being investigated. The second term refers to the contribution of the reinforcing steel to the horizontal shear strength multiplied by a factor of 0.6, all multiplied by the area being investigated. The requirements for a surface intentionally roughened to 0.25 in. (6 mm) amplitude are based on tests discussed in Kaar et al. (1960), Saemann and Washa (1964), and Hanson (1960).

$$V_{nh} = \lambda\left(260 + 0.6\frac{A_v f_{yt}}{b_v s}\right) b_v d \qquad \textbf{(2-6)}$$

Where

λ = modification factor for lightweight concrete from Section 19.2.4;

f_{yt} = specified yield strength of transverse steel reinforcement (psi [MPa]);

A_v = area of shear reinforcement within spacing s, (in.^{2} [mm^2]);

b_v = width of shear interface (in. [mm]);

s = center-to-center spacing of transverse reinforcement (in. [mm]);

d = distance from the top face of the beam to the centroid of the tensile longitudinal reinforcement (in. [mm]).

ACI 318-14 does not specify a limit of 60 ksi (420 MPa) for the yield stress of reinforcing steel, which is the case in AASHTO (2014). However, it does have an upper limit for V_{nh} , as shown in Equation (2-7).

$$V_{nh} \leq 500\, b_v d \tag{2-7}$$

If this limit is surpassed, V_{nh} shall be calculated in accordance to ACI 318-14 Section 22.9, shown in Equation (2-8), which does specify the yield stress of reinforcing to 60 ksi (420 MPa), and where the coefficient of friction μ shall be taken according to ACI 318-14 Table 22.9.4.2.

$$V_n = \mu\, A_{vf}\, f_y \tag{2-8}$$

In addition to the upper limit presented in Equation (2-7), a minimum area $A_{v,min}$ of shear reinforcement within spacing s should be provided in accordance to ACI 318-14 Section 16.4.6, shown in Equation (2-9), for concrete placed against hardened concrete intentionally roughened to a full amplitude of approximately 0.25 in. (6 mm) and concrete placed against hardened concrete not intentionally roughened.

$$A_{v,min} = \max\left\{0.75\sqrt{f_c'}\frac{b_w s}{f_y};\, 50\frac{b_w s}{f_y}\right\} \tag{2-9}$$

When concrete contact surfaces are clean and free of laitance, and concrete is placed against hardened concrete not intentionally roughened and minimum area of shear reinforcement is provided, V_{nh} has an upper limit as shown in Equation (2-10). When minimum area of shear reinforcement is not provided, V_{nh} is limited per Equation (2-10).

$$V_{nh} \leq 80 b_v d \tag{2-10}$$

For normal-weight concrete, placed either monolithically or placed against an intentionally roughened concrete surface as specified in ACI 318-14 Section 16.4.4, V_n needs to comply with Equation (2-11), where A_c is area of concrete considered to be engaged in interface shear transfer.

$$V_n < \min \begin{cases} 0.2\, f_c' A_c \\ (480 + 0.08\, f_c') A_c \\ 1600\, A_c \end{cases}$$

(2-11)

2.2.3 PCI Handbook

The PCI Handbook in Section 5.3.6 states that shear friction shall be calculated according to ACI 318-14 Section 22.9, as shown in Equation (2-8). In scenarios where load reversal does not occur, the use of an effective shear-friction coefficient, μ_e, is permitted when the concept is applied to monolithic or concrete with roughened surfaces.

$$\mu_e = \frac{1000\, \lambda\, A_{vf}\, \mu}{V_n}$$

(2-12)

Where

λ = factor for use with lightweight concrete (PCI Section 5.3.3);

A_{vf} = area of shear reinforcement perpendicular to the assumed crack plane (in.^{2} [mm^2]);

μ = shear-friction coefficient (PCI Table 5.3.1);

V_n = nominal interface shear resistance.

2.2.4 FIB Model Code 2010

The FIB Model Code 2010 states that the main parameters determining the actual load bearing capacity observed in tests (large scale and small scale) are interface roughness, cleanliness of surface, concrete strength and quality, eccentricity/inclination of shear force, strong bond/pre-cracking/de-bonding before testing, and ratio of reinforcement crossing the interface. The overall shear resistance results from the following main mechanisms:

- Mechanical interlocking and adhesive bonding,
- Friction due to:

- External compression forces perpendicular to the interface,
- Clamping forces due to reinforcement and/or connectors,

- Dowel action of reinforcement and/or connectors crossing the interface.

FIB Model Code 2010 describes two indicators to quantify the surface roughness of concrete: (1) the mean roughness parameter, R_m, and (2) the mean peak-to-valley height parameter R_z. Figure 2.6 illustrates these two indicators. The mean roughness parameter represents the mean deviation of the profile from a mean line and is calculated as:

$$R_m = \frac{1}{l}\int_0^l |y(x)-\bar{y}|\cdot dx \approx \frac{1}{n}\sum_{i=1}^{n}|y_i-\bar{y}|$$
$$\bar{y} = \frac{1}{l}\int_0^l y(x)\cdot dx \approx \frac{1}{n}\sum_{i=1}^{n} y(x)$$

(2-13)

The mean peak-to-valley height represents the mean difference between peak and valley measurements within a certain number of assessment lengths as shown in Equation (2-14).

$$R_z = \frac{1}{n}\cdot\sum_{i=1}^{n} R_{zi}$$

(2-14)

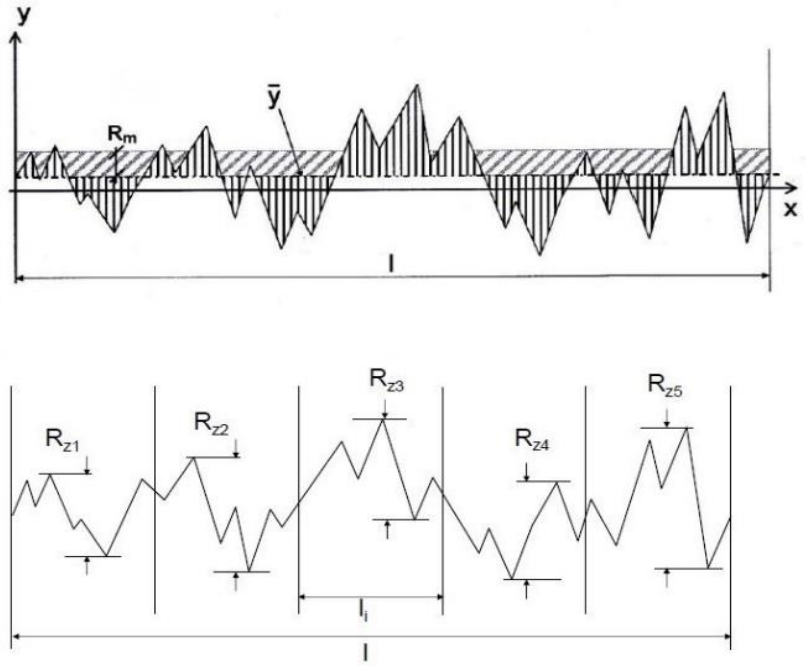

Figure 2.6: Average roughness, R_m, and mean peak-to-valley height, R_z (FIB Model Code 2010)

The design limit for interface shear, with no reinforcing steel crossing the interface, is given by:

$$\tau_{Rdi} = c_a f_{ctd} + \mu \sigma_n \leq 0.5 \nu f_{cd}$$

(2-15)

Where:

c_a = coefficient for adhesive bond;

μ = coefficient of friction;

σ_n = lowest compressive stress resulting from a normal force acting on the interface;

f_{ctd} = design value for concrete tensile strength;

f_{cd} = design value of the concrete strength, f_c.

If reinforcement is required to cross the interface, the design limit is:

$$\tau_{Rdi} = c_r f_{ck}^{1/3} + \mu \sigma_n + \kappa_1 \rho f_{yd}(\mu \sin\alpha + \cos\alpha) + \kappa_2 \rho \sqrt{f_{yd} f_{cd}} \leq \beta_c \nu f_{cd}$$

(2-16)

Where:

The surface roughness coefficients to be used with Equation 2-16 are listed in Table 2.2 and correspond to:

c_r = coefficient for aggregate interlock effect at rough interfaces;

f_{ck} = characteristic value of the compressive strength of concrete;

f_{yd} = reinforcing steel tensile design yield strength;

κ_1 = interaction coefficient for tensile force activated in the reinforcement;

κ_2 = interaction coefficient for flexural resistance;

ρ = ratio of reinforcement steel crossing the interface;

α = angle of inclination of reinforcing steel crossing the interface;

β_c = coefficient for the strength of the compression strut;

ν = effectiveness factor for the concrete.

Table 2.2: Coefficients for Different Surface Roughness as Presented in FIB Model Code 2010

Surface roughness	Example	R_m, in. (mm)	c_a	c_r	κ_1	κ_2	β_c	μ	
								$f_{ck} \geq 20$	$f_{ck} \geq 35$
Very rough	High pressure water jetting, indented	≥ 0.12 (3)	0.5	0.2	0.5	0.9	0.5	0.8	1.0
Rough	Sand blasted, high pressure water blasted, etc.	< 0.06 (1.5)	0.4	0.1	0.5	0.9	0.5	0.7	
Smooth	Untreated, slightly roughened	≥ 0.06 (1.5)	0.2	0	0.5	1.1	0.4	0.6	
Very smooth	Cast against steel formwork	Not measurable	0.025	0	0	1.5	0.3	0.5	

There is a limit set on the tensile force in the reinforcement due to simultaneous bending and/or reduced anchorage of bars, and because shear failure can occur at low slip values, and thus:

$$\kappa_1 = \frac{\sigma_s}{f_y} \leq 1.0 \qquad \textbf{(2-17)}$$

2.3 EXPERIMENTAL RESEARCH

This section provides a summary of the literature where experimental research was conducted with push-off test specimens to assess shear. Table 2.3 provides an overview of the published research and identifies test and experimental parameters considered in each study to assess interface shear. The table is in chronological order. A description of each study is provided.

Hofbeck et al. (1969) investigated the shear transfer strength of reinforced concrete specimens with and without cracking along the shear plane. The objective of the study was to determine the influence of pre-existing cracks in the shear plane on the shear transfer strength, to determine the influence of strength, size, and arrangement of reinforcement on the shear transfer strength, and to examine the possible contribution of the dowel action on shear transfer strength. Test results indicated that a pre-existing crack along the shear interface increased the slip and reduced the ultimate shear strength when compared with uncracked specimens. The reduction in ultimate shear strength decreased as the reinforcement ratio increased. Additionally, test specimens reinforced with higher strength steel bars reported higher shear transfer strength, except for the specimen with the highest reinforcement ratio. The authors concluded that shear-friction theory

provided a reasonable and conservative estimate of shear transfer strength in pre-cracked normal weight concrete.

Mattock et al. (1976) tested push-off specimens, both uncracked and pre-cracked, using lightweight concrete to develop shear transfer design recommendations. The types of aggregate used were naturally occurring gravel and sand, rounded lightweight aggregate, crushed angular lightweight aggregate, and sanded lightweight aggregate. Test results indicated that diagonal tension cracks in uncracked specimens began to appear at shear stresses of 400 psi (2.76 MPa) to 700 psi (4.8 MPa). No diagonal cracks formed in pre-cracked specimens. The authors noted that the ultimate shear capacity increased for larger reinforcement ratio values. The authors reported a lower shear transfer strength for concrete specimens with lightweight aggregate when compared with specimens containing normal-weight gravel aggregate and sand concrete mixtures.

Kahn and Mitchell (2002) tested fifty push-off specimens with uncracked, pre-cracked, and cold joint interfaces. The objective of the study was to extend the existing provisions presented in ACI 318-99 to high-strength concrete. Concrete design strengths investigated were 4 ksi (27.6 MPa), 7 ksi (48.3 MPa), 10 ksi (68.9 MPa), and 14 ksi (96.5 MPa), and the reinforcement ratio varied from 0.37% to 1.47%. The authors recommended the yield stress, f_y, be taken as 60 ksi (420 MPa) rather than using the measured yield stress. This recommendation is due to the results of normal-weight and high-strength concretes showing lower scatter and reaching larger capacities when compared to the ACI 318 design equation values. The authors concluded that the current ACI 318 provisions were conservative in estimating interface shear strength for high-strength concrete. They recommended fy be taken as 60 ksi (420 MPa) to limit the slip along the smooth cracks in high-strength concrete. An upper limit of 20% was proposed for shear stress.

Wallenfelsz (2006) and Scholz et al. (2007) assessed the horizontal shear strength of a deck panel to prestressed concrete beam connection. Figure 2.7 provides a schematic of the horizontal push-off tests described in both publications. Figure 2.8 shows three cases of the typical load versus slip testing results. Figure 2.8(a) presents the case where the horizontal shear resistance of the shear connector is lower than the cohesion shear resistance. The shear-slip response is characterized by a sharp drop in shear load after the interface cracks, followed by a sustained load phase. Figure 2.8(b) presents the case where the steel shear connectors' resistance is approximately equal to the cohesion resistance. The shear-slip response is characterized by a small drop in shear load after cracking, followed by a sustained growth phase. Figure 2.8(c) presents the case where the steel shear connector resistance is higher than the cohesion resistance. The shear-slip response is characterized by an initial slope change after cracking occurs which represents the load transferring from cohesion to the shear connectors. The load continues to grow until peak load is reached, at which point the shear connectors begin to yield. Results indicated that the resistance provided by shear friction did not occur until cracking begins, which occurred when the adhesion bond was broken. This observation led the authors to recommended modifications of the current equation in AASHTO (2014), described in the next section, by separating the two components.

Table 2.3: Reference Parameters for Push-off test Specimens.

Reference	Specimen size, in. (mm)	Number of specimens	Bar Size, in. (mm)	Steel ratio, ρ, %	Yield Stress, f_y, ksi (MPa)	Design Concrete Strength, f_c', ksi (MPa)
Hofbeck et al. (1969)	21.5 x 10 x 5 (546 x 254 x 127)	38	1/8 (3.2), #2 (6.4 mm), #3 (#10M), #4 (#13M), #5 (#16M)	0.00% -2.64%	48.0-66.1 (331-456)	4 (27.6)
Mattock et al. (1976)	22 x 12 x 12 (559 x 305 x 305)	62	#3 (#10M)	0.00%-3.79%	47.7-53.6 (328.9-369.6)	2.5 (17.2), 6.0 (41.4)
Kahn and Mitchell (2002)	24 x 12 x 10 (610 x 305 x 254)	50	#3 (#10M)	0.37%-1.47%	69.5 (479.2), 83.0 (572.3)	6.8 (46.9), 17.9 (123.4)
Scholz et al. (2007)/ Wallenfelsz (2006)	48 x 18 x 16 (1219 x 457 x 406)	26	#4 (#13M), #5 (#16M)	0.10%, 0.16%	73 (503.3)	4.3-6.0 (29.6-41.4)
Mansur et al. (2008)	29.5 x 15.75 x 5.9 (750 x 400 x 150)	19	0.315 in. (8 mm), #3 (#10M)	0.45%-2.67%	43.5 (300)	10.6 (73.1), 12.3 (84.8), 13.8 (95.1), 15.4 (106.2)
Scott (2010)	50 x 18 x 16 (1270 x 457 x 406)	36	#4 (#13M), #5 (#16M), #6 (#19M)	0.00%, 0.10%, 0.5%, 1.2%	60 (410)*	5.7-6.2 (39.3-42.7)
Trejo and Kim (2011)	48 x 18 x 16 x (1219 x 457 x 406)	8	#4 (#13M), #5 (#16M)	0.10%	62 (428)	5.9-7.5 (40.7-51.7)
Harries et al. (2012)	44 x 24 x 10 (1118 x 610 x 254)	8	#3 (#10M), #4 (#13M)	0.41%, 0.75%	61.5 (424.0)-140.0 (965.3)	5 (34.5)

Shaw and Sneed (2014)	24 x 12 x 5.5 (610 x 305 x 140)	36	#3 (#10M)	1.33%	66.2 (456)	5, 8 (34, 55)
Krc et al. (2016)	24 x 12 x 5.5 (610 x 305 x 140)	52	#3 (#10M)	0.009% 0.013% 0.017% 0.022%	72.2 (498)	4.4-5.6 (30.3-38.6)
Barbosa et al. (2017)	44 (52) x 24 x 24 (1118 (1321) x 610 x 610)	20	#4 (#13M) #5 (#16M)	0.42% 0.65%	64.5 (445)-89 (614)	4.2-5.2 (29.0-35.9)
Li et al. (2017)	33 x 18 x 12 (24) (838 x 457 x 305 (610))	16	#5 (#16M)	0.22% 0.43% 0.86%	72 (496) 140 (965)	5.0-7.5 (34.5-51.7)

*Actual yield stress not reported. Nominal yield stress stated.

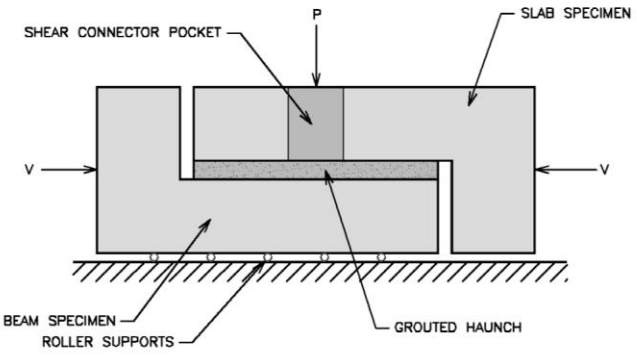

Figure 2.7: Horizontal push-off test (Wallenfelsz, 2006)

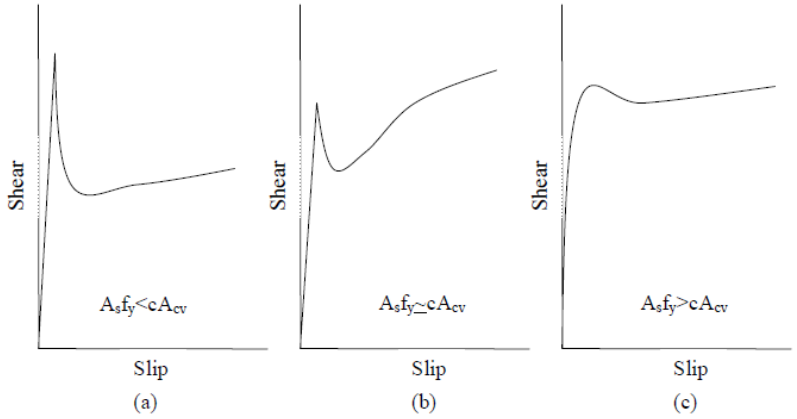

Figure 2.8: Typical Load versus Slip Plots (Wallenfelsz, 2006)

Mansur et al. (2008) conducted tests on 19 pre-cracked push-off specimens. The two major parameters considered in the research were the compressive strength of the concrete, f_c', and the reinforcement parameter, $\rho_v f_y$, through the shear interface. Figure 2.9 shows the typical load-deformation response of the test specimens. It is characterized by the four (4) events shown in Figure 2.9. Results indicated that an increase in the concrete strength increased the stiffness of Branch I, increased the load achieved in the Branch I, and increased the peak shear stress (strength). Results also indicated that an increase in the reinforcement parameter, $\rho_v f_y$, generated changes in response like when the concrete strength was increased. The authors noted that a balanced reinforcement parameter and concrete strength parameter could be achieved to result in higher shear resistance values.

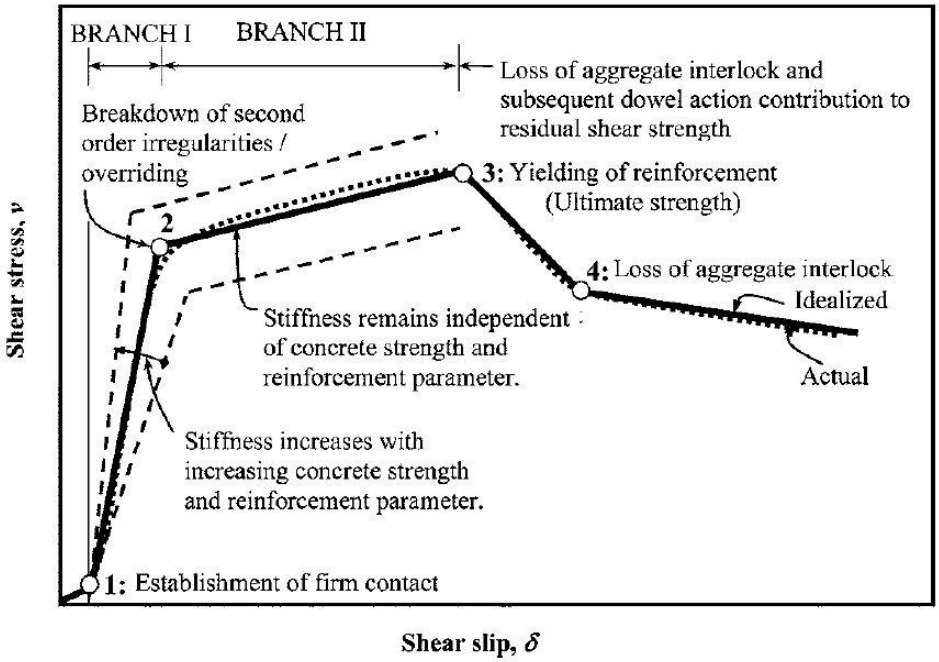

Figure 2.9: Response in terms of slip/separation under increasing load (Mansur et al. (2008))

Scott (2010) evaluated the accuracy of the current AASHTO LRFD provisions in predicting horizontal shear strength of precast girders and cast-in-place decks for both normal weight and lightweight concrete. The experimental program included testing 36 push-off specimens. The tests investigated the steel reinforcement ratio and the combination of deck and girder concrete. From the results of the push-off tests, the author concluded that the AASHTO (2007) provisions were conservative in predicting interface horizontal shear strength for a precast concrete girder and cast-in-place concrete deck. The authors noted that if higher values of reinforcement area crossing the shear interface were used, the strain values in the reinforcement either right before or right after cracking were lower than with lower reinforcement area. However, the reinforcement still reached strain levels that suggested yielding. The author noted that the modifications proposed in Wallenfelsz (2006) provided a better fit to their test data.

Trejo and Kim (2011) conducted 24 push-off tests to assess the shear transfer behavior of the girder-haunch-deck systems. Results indicated that there were five different stages of a typical failure mode, as shown in Figure 2.10. These stages included: (1) adhesion loss, where interface slips at constant load, V_{loss}; (2) engagement of shear key components; (3) peak load shear key failure, V_{peak}; (4) dowel action of connectors or beginning of sustained load, V_{sus}; and (5) system failure (not shown in Figure 2.10).

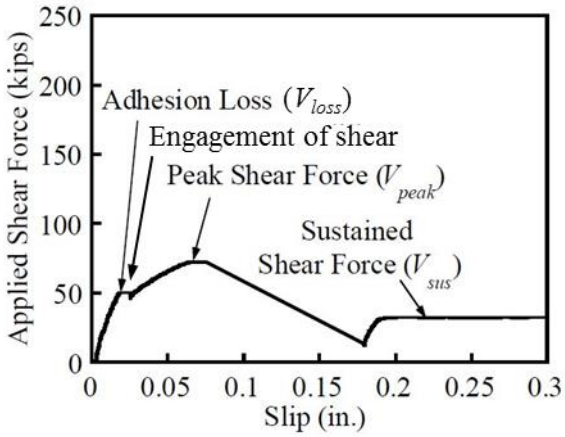

Figure 2.10: Typical failure mode and the plot of the system (Graph recreated from Trejo and Kim 2011)

Harries et al. (2012) and Zeno (2009) summarized a research program developed to study the shear interface behavior when using with high-strength reinforcing steel bars across the interface. The objective of the research was to compare the behavior of the horizontal shear capacity of specimens containing ASTM A615 and ASTM A1035 reinforcing steel. The experimental program included push-off test specimens with 60 ksi (420 MPa) and 100 ksi (690 MPa) reinforcing steel with reinforcement steel ratios varying from 0.40 to 0.75%. The bar sizes were #3 (#10M) and #4 (#13M) bars, and the concrete-to-concrete surface was prepared with a 1/4 in. (6.35 mm) amplitude roughness and cleared of laitance before the second layer was cast. Results from the testing showed that three of the four specimens reinforced with ASTM A615 Grade 60 (420 MPa) reinforcing steel reached the design values determined per AASHTO (2007). On the other hand, none of the specimens reinforced with ASTM A1035 Grade 100 (690 MPa) specimens reached the design values when using 100 ksi (690 MPa) to compute the shear capacity. However, when f_y was limited to 60 ksi (420 MPa), the A1035 specimens did reach the design values per AASHTO (2007).

Test results reported by Zeno (2009) indicate that the shear-friction mechanism occurs in stages, as shown in Figure 2.11. The author reported that the concrete component had the highest contribution to the load transfer mechanism before cracking occurred. After cracking, the contribution of the reinforcing steel bars ("steel component" in the figure) increased. These results indicate that the load transfer through the concrete and reinforcing steel bars of the shear-friction mechanisms do not act simultaneously, as suggested by the shear-friction equation in AASHTO (2014).

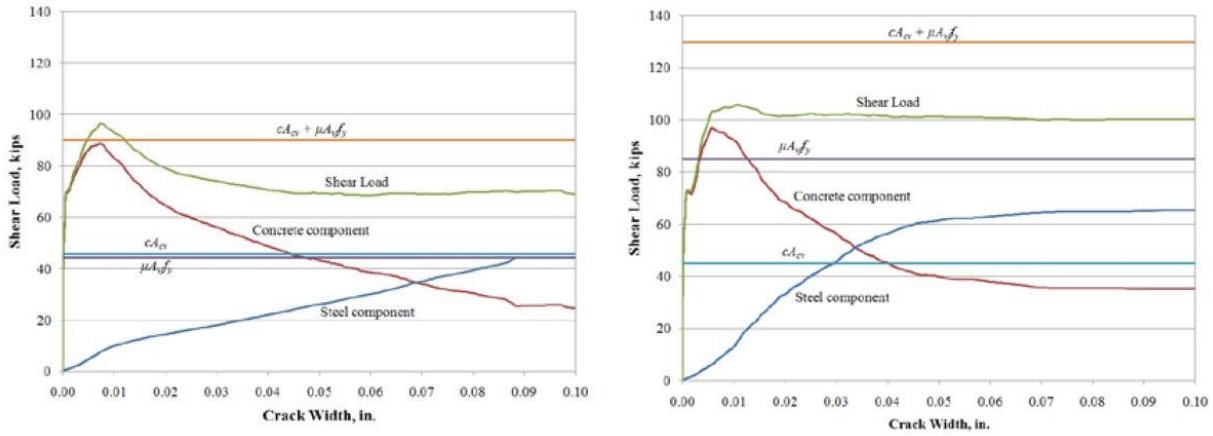

(a) (b)

Figure 2.11: Components of shear-friction shear load vs crack width for specimens with reinforcing steel bars consisting of (a) A615 #3 (#10M), and (b) A1035 #3 (#10M) (Zeno (2009))

Figure 2.12 to Figure 2.15 can be used to summarize the main observations in the research described in Harries et al. (2012). Figure 2.12 shows results of shear load versus mean shear displacement. The strain measurements are shown in Figure 2.14. The authors reported that the shear-friction capacity did not increase considerably with the use of ASTM A1035 Grade 100 (690 MPa) reinforcing steel. The researchers concluded that this occurred because the specimens reached the ultimate load before the reinforcing steel yielded. Based on these findings, the authors recommend the clamping force should be considered as a function of the steel modulus rather than the yield strength.

Figure 2.13 and Figure 2.15 show the linearized results of shear load versus mean shear displacement behavior and strains, respectively, where the three stages can be clearly identified:

1. Stage 1: this stage covers the behavior before cracking occurs. It is characterized by a linear shear load versus shear displacement behavior in all the specimens. During this stage, the applied load is resisted by the concrete component, controlled by the concrete-to-concrete bond between the two surfaces.

2. Stage 2: this stage covers the behavior from cracking to reaching the ultimate capacity. It is characterized by softening, observed in the change of slope. During this stage, the applied load is resisted by the friction originated from the interface surface roughness. Due to the low values of strain reached in the reinforcing steel bars crossing the interface, the clamping force across the interface is still low and does not have a considerable contribution to resisting the applied load.

3. Stage 3: this stage covers the post ultimate behavior. It is characterized by a sustained load carrying capacity in the ASTM A1035 Grade 100 (690 MPa)

specimens. The ASTM A615 Grade 60 (420 MPa) specimens exhibited a faster degradation of the post ultimate load carrying capacity.

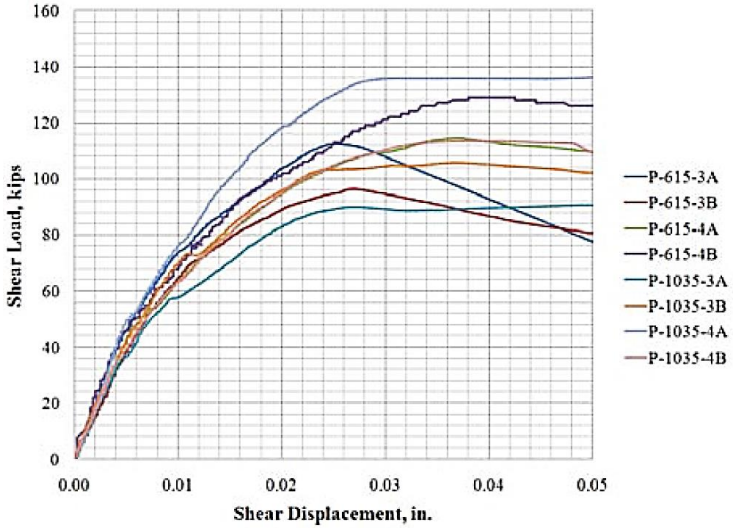

Figure 2.12: Shear load versus shear displacement showing the described stages of the shear friction mechanism (Zeno 2009) [1 in. = 25.4 mm]

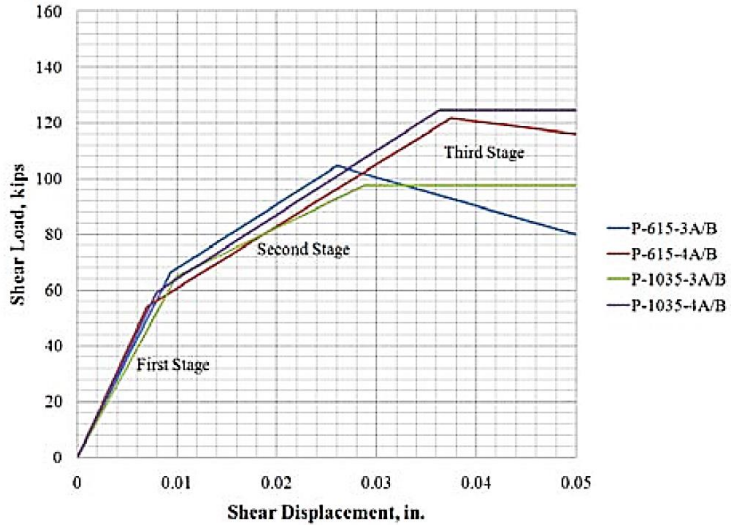

Figure 2.13: Linearization of shear load versus shear displacement showing the described stages of the shear friction mechanism (Zeno 2009) [1 in. = 25.4 mm]

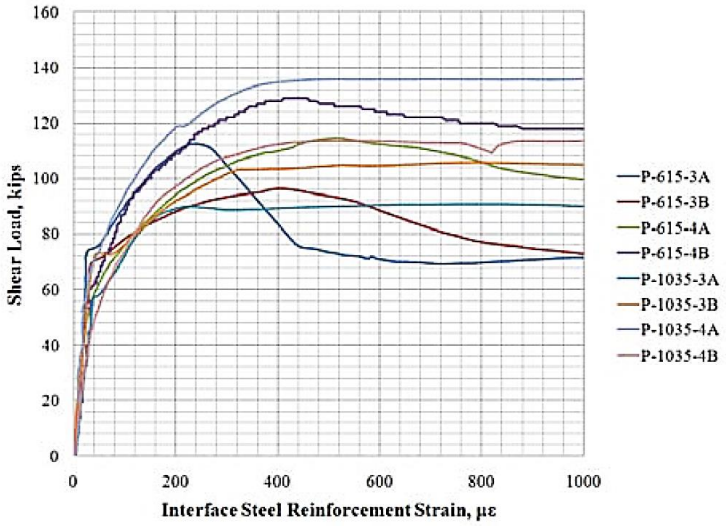

Figure 2.14: Shear load versus mean interface steel strain showing described stages of the shear friction mechanism (Zeno 2009) [1 kip = 4.448 kN]

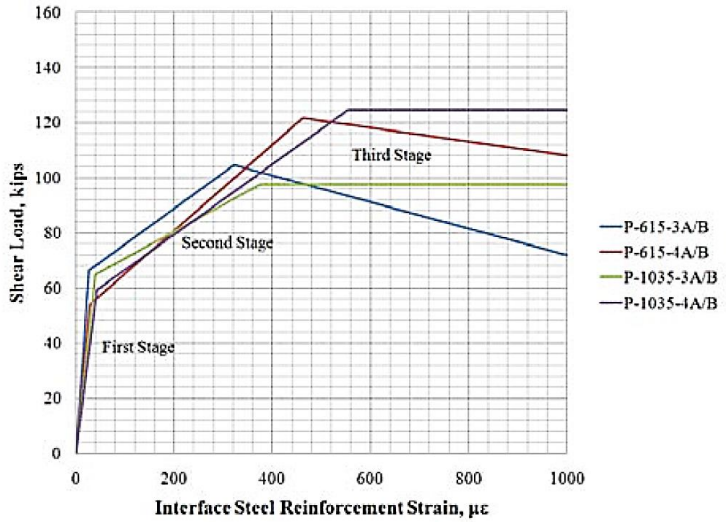

Figure 2.15: Linearization of shear load versus mean interface steel strain showing described stages of the shear friction mechanism (Zeno 2009) [1 kip = 4.448 kN]

In summary, Harries et al. (2012) concluded that the design values calculated per AASHTO (2007) were only reached by specimens reinforced with ASTM A615 Grade 60 (420 MPa) reinforcing steel. The results showed that increasing the yield stress of the reinforcing steel did not increase the peak load capacity due to the reinforcing bars not reaching their yielding strain before reaching the peak load, as indicated by the strain measurements collected via strain gages. However, the peak load did increase with a higher bar size. This was attributed to a higher interface stiffness resulting from a higher reinforcing bar area.

Shaw and Sneed (2014) researched the direct shear transfer across an interface of lightweight aggregate concretes cast at different times. The experimental program consisted in testing 36 push-off test specimens with test variables such as concrete type, concrete compressive strength, and surface preparation. Shear strengths obtained from the experimental tests were compared to PCI Design Handbook and ACI 318-11 code provisions. The authors reported that concrete type had no influence on the shear strength of the test specimens; however, concrete compressive strength had a significant impact on shear strength of the test specimens. The authors noted that PCI and ACI 318-11 provided conservative estimates of shear strengths for the sand-lightweight and all-lightweight cold-joint test specimens. The authors noted that additional research is needed to assess the impact of the reinforcement ratio in shear strength for all-lightweight and sand-lightweight concrete cold-joint test specimens.

Krc et al. (2016) compiled a database of shear friction test results from previous research performed with push-off test specimens subjected to monotonic loading without external normal forces. The authors compared the database results to PCI Design Handbook and ACI 318-14 shear friction design provision to validate these provisions. Test variables considered were concrete type, lightweight aggregate material, shear interface surface preparation, reinforcement ratio, and crack interface condition. The authors reported that values of Vtest/Vcalc indicate that the effective shear friction coefficient, μe, approach presented in PCI is more accurate than the conventional shear friction coefficient, μ, approach presented in both PCI and ACI 318-14 for normal weight, sand-lightweight, and all-lightweight concrete with monolithic uncracked, monolithic pre-cracked, and cold-joint roughened interface conditions. PCI and ACI 318-14 conventional shear friction coefficient, μ, approach provides a conservative shear friction capacity estimation for cold-joints with a smooth interface preparation for sand lightweight and all-lightweight concrete. The authors recommend removing the modification factor λ used to calculate the coefficient of friction, μ, to obtain more accurate shear friction capacity estimations.

The second phase of Krc et al. (2016) entailed an experimental program with 52 push-off test specimens and test variables such as concrete type, lightweight-aggregate material, surface preparation, reinforcement ratio, and crack interface condition. The authors reported that cold-joint specimens with a roughened interface reached a larger ultimate shear stress than cold-joint specimens with a smooth interface. Additionally, the ultimate shear stress reached by the cold-joint specimens with a smooth interface appeared to be independent of concrete type. The authors reported that the use of λ in the coefficient of friction, μ, approach presented in PCI and ACI 318-14 are conservative for all lightweight-aggregate specimens. The authors recommend the use of the effective coefficient of friction, μe, and approach presented in PCI.

Barbosa et al. (2017) investigated the effect of high-strength steel (HSS) reinforcement on concrete-to-concrete shear interface capacity. Four sets of five push-off test specimens were used with reinforcing steel ratios varying from 0.42 to 0.64%, #4 (#13M) and #5 (#16M) bar sizes and reinforcing steel grade 60 (420 MPa) and grade 80 (550 MPa), per ASTM A615 and A706. All the specimens were designed to have similar peak shear loads per AASHTO (2014). The authors concluded that the specimens reinforced with #5 (#16M) reinforcing bars showed an increase in shear friction resistance when HSS was used. However, the same change was not

observed in the specimens reinforced with #4 (#13M) reinforcing bars. Figure 2.16 shows the mean interface shear force versus reinforcing steel strain for all the specimens tested. The specimen label 4G60 corresponds to the reinforcing steel bar size [#4 (#13M)], and the reinforcing steel bar grade [G60 (420)]. All the specimens show linear behavior until approximately 50 microstrain, where a substantial change in slope is observed. This change in slope occurs at a higher load for specimens reinforced with #4 (#13M) reinforcing bars. The authors attributed this difference to the lower concrete area present in the #5 (#16M) bar specimens, thus having less contribution from concrete-to-concrete cohesion. For specimens reinforced with grade 60 (420 MPa) reinforcing steel, the specimens reinforced with #4 (#13M) reinforcing bars reached the nominal yield strain after the peak interface shear load was reached. However, the specimens reinforced with #5 (#16M) reinforcing bars reached the nominal yield strain before the peak interface shear load was reached.

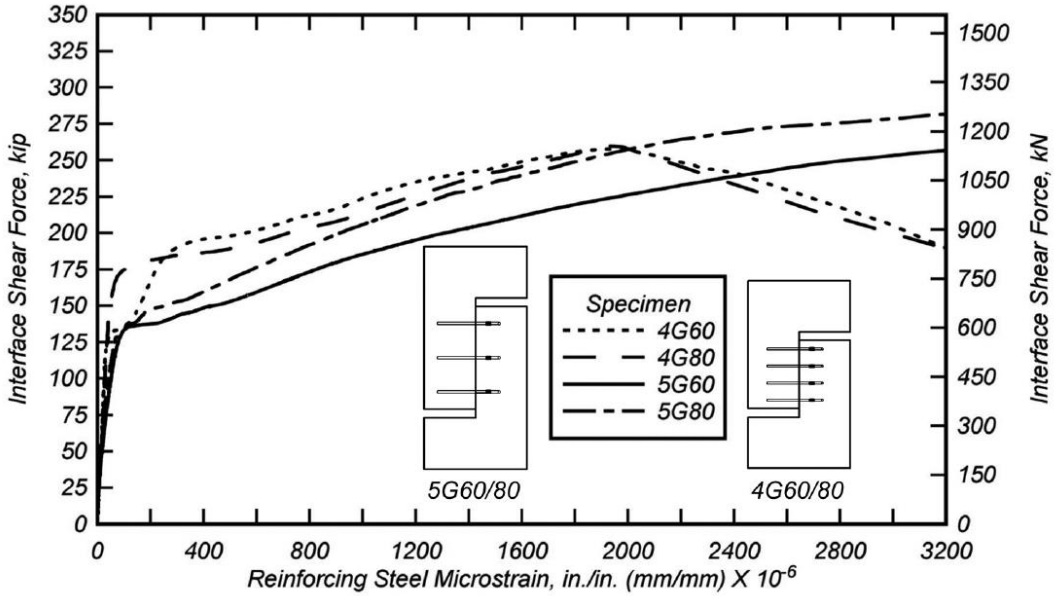

Figure 2.16: Interface shear force versus reinforcing steel strain (Barbosa et al. 2017)

Figure 2.17 shows a plot of data points normalized by the concrete strength versus the reinforcement ratio normalized by concrete strength and Young's modulus of the reinforcing steel. The specimens reinforced with #4 (#13M) bars, with both grade 60 (420 MPa) and grade 80 (550 MPa) reinforcing steel, did not reach their yield stress until reaching the ultimate capacity; therefore, the authors concluded that the clamping force can be described as a function of the elastic modulus instead of the yield strength (Harries et al. 2012). The thick line represents the design equation proposed by AASHTO (2015), with a maximum value limited by the shear value corresponding to $K_1 A_{cv} f_c'$ per AASHTO (2015). The cohesion and friction coefficients, c and μ, respectively, were obtained through linear interpolation between the case of a surface roughened to 1/4 in. (6.35 mm) and the case of a surface not intentionally roughened, as there is no case in AASHTO (2015) for directly accounting for the surface roughened to 1/8 in. (3.175 mm) The authors pointed out that all the data points collected were above the line

defined by AASHTO (2015), thus indicating that the design equation is conservative. The data points are also above the line defined by the design equation using f_y = 80 ksi (550 MPa), which indicates that allowing the use of this stress would still be considered conservative. It is worth noting, however, that the vertical axis in Figure 2.17 is normalized by the concrete strength and not only the interface shear area, which is used in AASHTO (2015) to characterize the cohesion factor used in the equations.

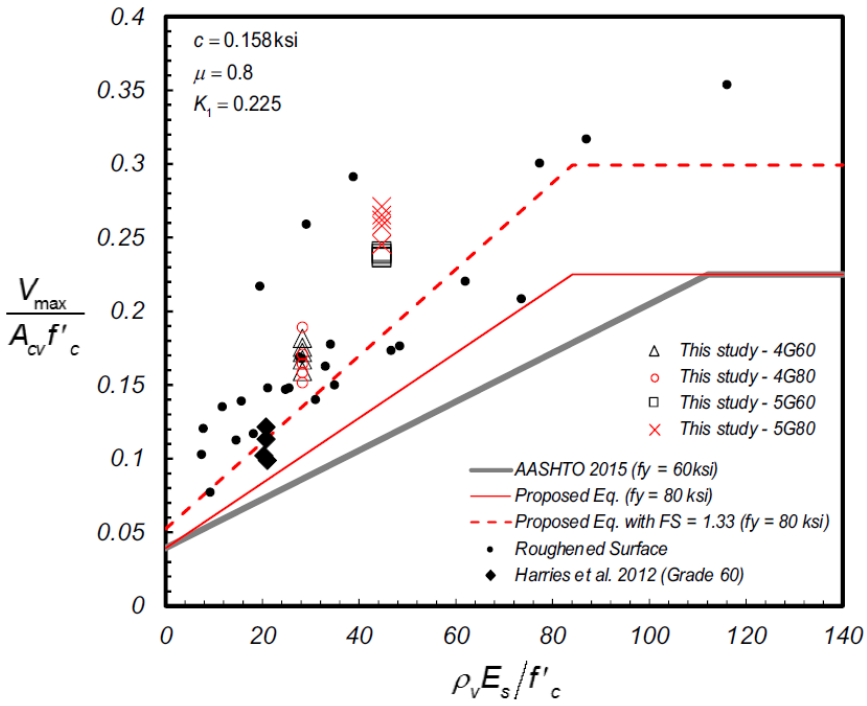

Figure 2.17: Experimental normalized peak shear stress versus normalized reinforcement stiffness across the interface (Barbosa et al. 2017)

Li et al. (2017) tested 16 small-scale push-off test specimens to study how horizontal shear transfer between precast and cast-in-place concrete surfaces were influenced by surface preparation, bond breakers (epoxy and roofing felt), and interface reinforcement properties (yield strength, reinforcement amount, and means of anchorage). Three different surface preparations were tested: (1) fully roughened surface with 1/4 in. (6.35 mm) grooves, (2) troweled surface, and (3) middle 6 in. (152.4 mm) or 12 in. (304.8 mm) of the surface roughened with 1/4 in. (6.35 mm) groves. Two debonding agents were used: (1) epoxy, which was applied to the concrete of the bottom piece after initial set and again prior to casting of the top piece, and (2) roofing felt. Two types of reinforcing steel were used: (1) normal-strength (ASTM A615/A615M-16 Grade 60 [420 MPa]), and (2) high-strength (ASTM A1035/A1035M-16 Grade 120 [830 MPa]). Two types of spacing were used: (1) 6 in. (152.4 mm) spacing for specimens with two pairs of interface reinforcement bars, and (2) specimens with a single interface reinforcement bar placed at the center of the 12-inch-long (304.8 mm) interface. All interface reinforcement bars used were #5 (#16M) reinforcing bars. Reinforcing steel ratios varied from 0.22 to 0.86%.

Results from the Li et al. (2017) experimental program indicated that surface preparation and interface area had a large influence over the peak strength. The highest peak strength was achieved by specimens with fully roughened surfaces, followed by middle surface roughened specimens, and troweled and debonded specimens. Figure 2.18 illustrates this observation where the higher initial stiffness, in terms of force versus slip, can be observed in specimens with fully roughened surfaces. Specimen labels consist of five terms: (1) surface preparation (R is rough, T is troweled, RM is rough middle); (2) specimen width (12 in. [304.8 mm], 24 in. [609.6 mm]); (3) bond breaker (NB is no bond breaker, F is roofing felt, E is epoxy); (4) shear reinforcement spacing (12 in. [304.8 mm] means one pair of #5 [#16M] bars, 6 in. [152.4 mm] means two pairs of #5 [#16M] bars); and (5) reinforcement parameters (NR is normal-strength hooked, HR is high-strength hooked, HB is high-strength headed). The large drop in force after the peak force is reached led to a sustained load behavior controlled by dowel action in the reinforcement. As expected, the peak force in partially roughened specimens was lower than the peak force in fully roughened specimens. However, when compared in terms of stress (force divided by the area of roughened concrete), partially roughened specimens had higher first cracking and peak strength than comparable fully roughened specimens. The authors concluded that shear transfer performance should be considered in terms of stress. Figure 2.19 illustrates that an essentially bilinear behavior was observed in specimens with a partially roughened surface and fully roughened surface, representing the behavior before and after cracking of the interface. In this study, the contributions of cohesion and reinforcement to peak strength were estimated working under the assumption that shear strength can be expressed as the sum of both contributors. The values obtained for cohesion were approximately double and equal to values recommended in AASHTO Specification for roughened and troweled surfaces, respectively. The contribution of normal strength steel was estimated at $1.1A_sf_y$, where the coefficient of 1.1 is larger than the coefficient recommended by AASHTO Specifications (1.0 and 0.6 for roughened and troweled surfaces). Post-testing observations showed that the failure plane was primarily located in the side with lower strength concrete. This observation led the authors to conclude that the lower concrete strength should be used when calculating shear strength.

Results in Li et al. (2017) indicated that the use of high-strength reinforcing steel did not transform into a significant effect on stiffness, cracking strength, peak strength and post-peak strength. In comparison, the increase of reinforcement area had a more important impact. The authors concluded that additional studies are required due to the small number of specimens tested.

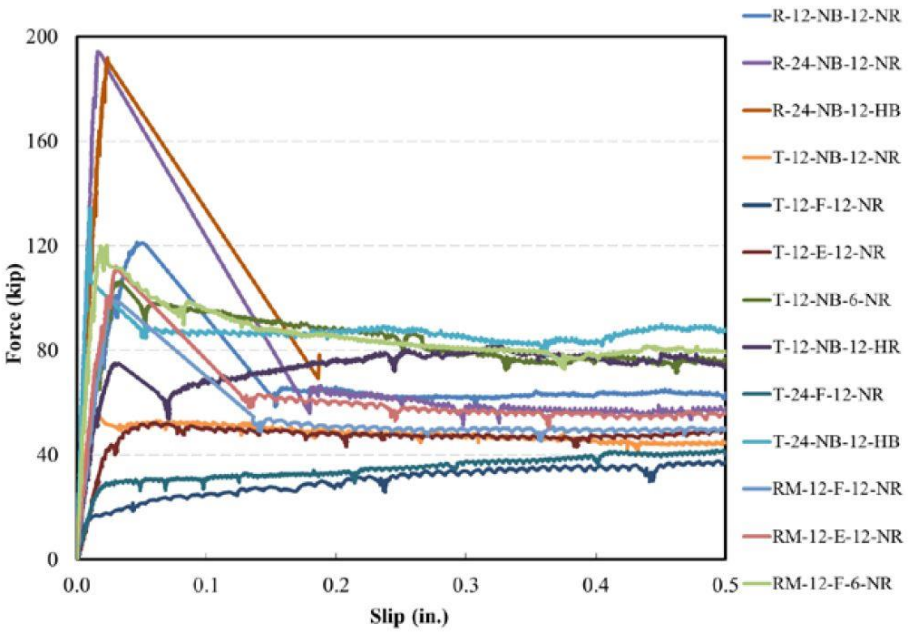

Figure 2.18: Force vs slip (Li et al. 2017) [1 in = 25.4mm]

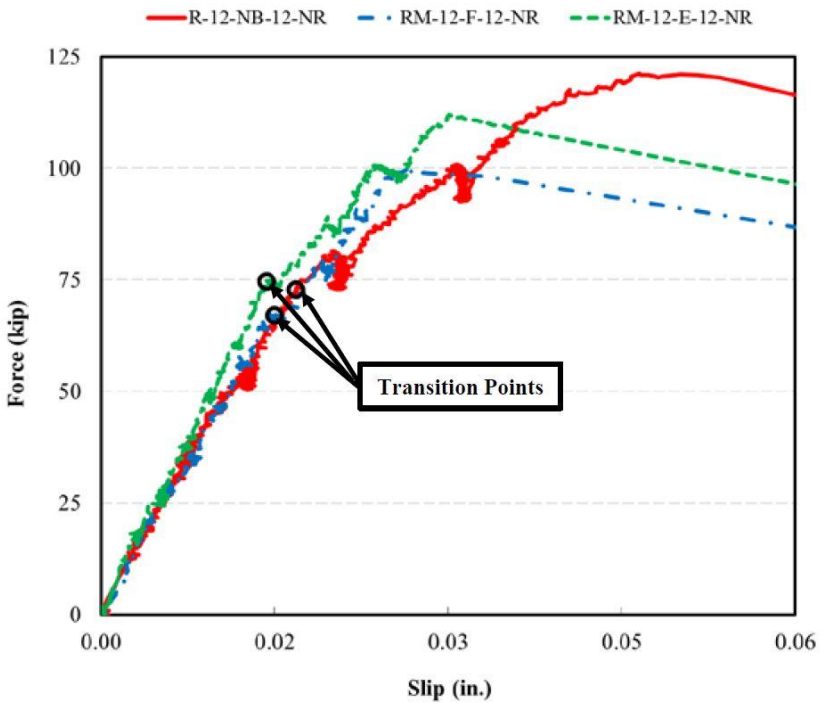

Figure 2.19: Force vs slip zoomed region up to 0.06 in. (1.52mm) slip (Li et al. 2017) [1 in = 25.4mm]

Soltani and Ross (2017) created a database of experiments carried out to evaluate the interface shear transfer on uncracked reinforced concrete specimens. Data from 774 tests were studied and gathered into a database with the objective of evaluating the accuracy of the interface shear transfer provisions per AASHTO LRFD Bridge Design Specifications, Eurocode 2, and CSA A23.3. The authors filtered the data to create code-specific databases for the three mentioned code provisions. The authors found that all codes evaluated are conservative, although the degree of conservatism varied depending on design variables such as concrete compressive strength, steel reinforcement ratio across the interface, and test specimen dimensions. The results of the analysis showed that when strength reduction factors are not considered, unconservative results were observed in 8.2%, 1.6%, and 7.6% of the specimens for AASHTO LRFD, Eurocode 2, and CSA A23.3, respectively. When strength reduction factors are considered, the percentage of unconservative results observed were 1.8%, 1.6%, and 2.3%, for AASHTO LRFD, Eurocode 2, and CSA A23.3, respectively. The authors determined that AASHTO LRFD provisions presented a decrease in level of conservatism as concrete compressive strength decreased, Eurocode 2 presented an inverse relationship between level and conservatism and the interface reinforcement index (ρf_y), and CSA A23.3 presented the most alarming observation as 69% of the specimens heavily reinforced (ρf_y > 1305 psi (9 MPa)) showed unconservative strength ratios.

2.4 RESEARCH WITH FULL-SCALE COMPOSITE BEAM SPECIMENS

This section provides a summary of research performed using full-scale composite beam tests. Table 2.4 provides an overview of the published research and identifies test and experimental parameters provided by each reference.

Seamann and Washa (1964) researched the strength of the joint between precast concrete beams and cast-in-place concrete slabs. The experimental program involved testing 42 beams to provide insight into the following test variables: (1) concrete interface roughness; (2) joint position with respect to the neutral axis; (3) length of shear span; (4) reinforcing ratio across the interface; (5) shear key effect; and (6) concrete strength. The authors reported that the ultimate shear strength increased as the concrete surface roughness increased from smooth to intermediate roughness. The ultimate shear strength also increased when the reinforcement ratio of reinforcement steel bars crossing the interface increased. On the other hand, the ultimate shear strength was approximately equal between beams with intermediate rough surface and beams with shear keys. Additionally, the authors reported that the ultimate shear strength presented a subtle increase when concrete strength increased from 3 ksi (20.7 MPa) to 5.5 ksi (37.9 MPa).

Loov and Patnaik (1994) investigated the behavior of "rough" joints in composite concrete beams and their capacity to develop interface shear for different reinforcing steel ratios. The experimental program involved testing 16 composite concrete beams with two main test variables: clamping stress, and concrete strength. The joint preparation was described as "well compacted having a rough surface, clean and free of laitance, with coarse aggregate protruding but firmly fixed in the matrix" (Loov and Patnaik 1994). All beams were designed to fail in

horizontal shear. The authors recommended a parabolic equation for shear resistance based on the test results. The equation combines the effects of concrete strength and clamping stress. The authors proposed an equation that represents the test results more accurately compared to the design equation in ACI Code in 1963.

Patnaik (2001) studied the behavior of shear friction behavior of composite concrete beams with smooth interfaces. The experimental program consisted in testing 18 rectangular-shaped section beams and six T-shaped section beams with a smooth interface. Test variables include interface width, concrete strength and the ratio of depth of the tensile reinforcing steel to spacing of the horizontal shear reinforcing steel (d/s), and clamping stress, among other. The author reported that 'd/s' had no significant influence on the horizontal shear strength. The author concluded that the ACI 318 provisions for horizontal shear in composite concrete beams is conservative.

Kahn and Slapkus (2004) evaluated the AASHTO (1998) and ACI 318-02 horizontal shear strength design provisions for the use of high-strength concrete at the interface created by a precast concrete beam and a cast-in-place deck. The experimental program consisted in testing six composite beams with precast webs with nominal strength 12 ksi (83 MPa). Test variables were concrete strength, and transverse reinforcement ratio. The authors reported results that indicated that AASHTO (1998) and ACI 318-02 provisions for horizontal shear are conservative for static loads. The authors recommend that current design provisions for shear friction and for interface shear in composite beams can be extended to high-strength concrete.

Kovach (2008) researched the horizontal shear stress of composite concrete beams without horizontal shear ties. The experimental program consisted in two phases totaling 32 test specimens. The test variables considered were roughness of the composite interface surface finish and concrete strength of the slab. The author concluded that interface roughness has a significant influence on the horizontal shear capacity; therefore, it is important to properly roughen the interface surface. It is important to note that the author mentioned some issues that may arise from push-off tests. Even though the point load applied to the test specimen is aligned in a way to avoid eccentricities, these can occur and result in an overturning moment causing the loaded element to pull away near the loaded edge. Stress concentrations can arise depending on the accuracy and correct alignment of the test setup, which can lead to unconservative estimates of horizontal shear capacity.

Fang et al. (2018) researched the interface shear behavior of normal weight and lightweight concrete composite T-beams and compared these to AASHTO and ACI design code provisions. An experimental program was developed where 12 T-beams were tested with the variables of interface preparation, clamping stress, and lightweight slab concrete strength. The authors reported that most composite beams failed at the horizontal shear interface in which the main test variables influencing the horizontal shear capacity were the interface preparation and clamping stress. The authors determined that AASHTO and ACI design code provisions conservatively predicted the interface shear capacity. The authors proposed a new equation to predict a more accurate interface shear capacity for different types of concrete with both smooth and rough shear interface preparations.

Table 2.4: Reference Parameters for the Full-scale Composite Beam Specimens.

Reference	Specimen size, in. (mm)	Number of specimens	Bar Size	Reinforcement ratio, ρ, %	Yield Stress, f_y, ksi (MPa)	Concrete Quality, f_c', ksi (MPa)
Seamann and Washa (1964)	96, 144, 240 x 17 x 15 (2438, 3658, 6096 x 432 x 381)	42	#3 (#10M), #4 (#13M)	0.00-1.07%	42.6 (293.7), 53.7 (370.2)	3 (20.7), 4.5 (31.0), 5.5 (37.9)
Loov and Patnaik (1994)	118.1 x 15.75 x 13.78 (2999.7 x 400 x 350)	16	#3 (#10M)	0.10-1.89%	59.0-63.5 (407-438)	2.8-7.5 (19.3-51.7)
Patnaik (2001)	Rectangular Beams: 106.3 x 13.78 x 9.84 (2700 x 350 x 250) T-Section Beams: 126.0 x 13.78 x 15.75 (3200 x 350 x 400)	18	0.22 in. (5.6 mm), 0.25 in. (6.4 mm), 0.34 in. (8.7 mm), 0.35 in. (8.9 mm), 0.56 in. (14.1 mm)	0.05-1.05%	49.3-102.1 (339.9-704.0)	2.5-5.0 (17-34.8)
Kahn and Slapkus (2004)	120 x 16.5 x 15.5 (3048 x 419 x 394)	6	#3 (10M)	0.19-0.37%	80.7 (556)	7.3 (50.3), 11.3 (77.9)
Kovach (2008)	130 x 12 x 11.5 (3302 x 305 x 292)	35	N/A	0.00%	N/A	3 (20.7), 6 (41.4)
Fang et al. (2018)	94.5 x 15.7 x 13.8 (2400 x 400 x 300)	12	#3 (#10M)	0.00-0.698%	50 (345.86)	7.3 (50)

2.5 SUMMARY

This chapter reviewed available information related with shear friction theory and the effect of surface roughness and high-strength reinforcing steel. This comprehensive literature review compiled information on shear friction behavior and load transfer mechanisms, experimental programs using push-off test specimens and the equations in the main design specifications.

Previous research has shown that before the peak shear capacity is reached the controlling parameters in concrete-to-concrete interfaces are cohesion and aggregate interlock. Aggregate interlock is influenced by surface roughness, clamping force, and aggregate size. After the peak shear capacity is reached, dowel action becomes the controlling parameter.

Limited research has been performed on specimens containing high strength steel. Research is needed to gain a better understanding of its behavior in shear friction applications (Zeno 2009, Harries et al. 2012). Results from these experimental programs show that the shear interface capacity of the specimens can be overestimated when a yield strength higher than 60 ksi (420 MPa) is used. Barbosa et al. (2017) reported results that indicated that if the reinforcing bars crossing the interface yield, a stress higher than 60 ksi (420 MPa) may be used to calculate the shear friction resistance. However, a group of test specimens from the same project reported that when the reinforcing bars did not yield the results agree with findings reported by Harries et al. (2012). Barbosa et al. (2017) determined that the reinforcement bar size and spacing might have an important effect over the results obtained. Surface preparation was not considered as a test variable in Harries et al. (2012) or Barbosa et al. (2017). Therefore, there is limited information on the influence it has on the behavior of shear friction interfaces.

3.0 EXPERIMENTAL PROGRAM AND SPECIMEN DESIGN

3.1 INTRODUCTION

Although HSS reinforcement is commercially available today, its use is still limited. Currently, AASHTO limits the design yield stress of horizontal shear concrete interface reinforcing bars to 60 ksi (420 MPa). Some research on the application of HSS reinforcement bars in bridges (Trejo et al. 2014, Barbosa et al. 2017) has been performed but limited research has been done on the application of HSS reinforcement in concrete horizontal shear interface connections (Zeno 2009, Harries et al. 2012, Barbosa et al. 2017).

The objective of this study is to provide new data on the behavior of concrete cold joint interface connections reinforced with ASTM A706 Grade 80 ksi (550 MPa), ASTM A615 Grade 100 ksi (690 MPa), and ASTM A1035 – 16b Grade 120 ksi (830 MPa) reinforcing steel subjected to horizontal shear loading. To do this, specimens were designed based on ODOT (2014) BR300 standard drawing. These specimens simulated a girder-deck connection. Testing of these specimens provided data on the performance of horizontal shear interface connections reinforced with HSS reinforcement. Additional test variables not considered in previous research, such as interface preparation, reinforcing steel bar size, reinforcing steel bar spacing, and nominal concrete strength, are included to provide further insight into the behavior of concrete cold joint interface connections.

3.2 EXPERIMENTAL DESIGN

An experimental program was developed to assess the performance of A706 Grade 60 ksi, (420 MPa), A706 Grade 80 ksi (550 MPa), ASTM A615 Grade 100 ksi (690 MPa), ASTM A1035 – 16b Grade 120 ksi (830 MPa) reinforcing steel performance in shear friction applications. This experimental program included testing 45 push-off test specimens separated into five groups depending on the test parameter being tested in each specimen. All 45 specimens were designed using ODOT (2014) section 1.17.8.2, which refers to AASHTO (2014) 5.8.4 for design. The test variables included grade of reinforcing steel, interface preparation, bar spacing, bar size, and concrete nominal strength. The steel reinforcement ratios in the specimens tested ranged from 0.33% to 0.78%. Figure 3.1 shows the naming convention for the specimens.

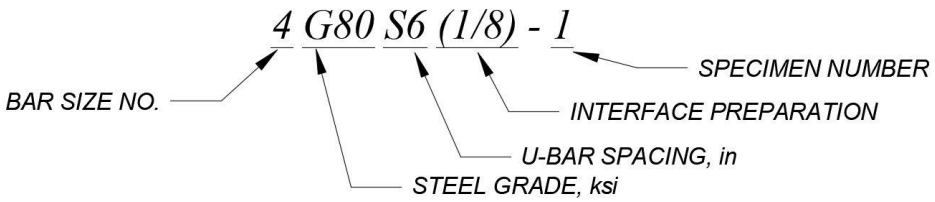

Figure 3.1: Naming convention of the push-off test specimen series

The experimental test matrix is shown in Table 3.1. Details of different specimen groups are summarized in Table 3.1 in five different sections, namely the (a), (b), (c), (d), and (e), where each section refers to a specific test variable. The specimen groups shown in the first row of sections (a) and (b) were used to assess the influence of more than one test variable on shear interface capacity. Hence, these groups were referred in different sections of the table as 1(a) and 1(b), where '1' represents the first row of the section.

Table 3.1 Experimental Test Matrix.

(a) Influence of Reinforcing Grade

Reinforcement Type	Grade, ksi	Nominal f_c' ksi	Interface Preparation	Rebar Spacing in.	Rebar Size	# of Specimens	Specimen Group Label
A706	60	5	1/8" IR	6	#4	3	4G60S6(1/8)
A706	80	5	1/8" IR	6	#4	3	4G80S6(1/8)
A615	100	5	1/8" IR	6	#4	3	4G100S6(1/8)
A1035	120	5	1/8" IR	6	#4	3	4G120S6(1/8)

(b) Influence of Interface Preparation

Reinforcement Type	Grade, ksi	Nominal f_c' ksi (MPa)	Interface Preparation	Rebar Spacing, in. (mm)	Rebar Size	# of Specimens	Specimen Group Label
A706	80	5	As Cast	6	#4	3	4G80S6(AC)
A706	80	5	1/8" IR	6	#4	See 1(a)	4G80S6(1/8)
A706	80	5	1/4" IR	6	#4	3	4G80S6(1/4)
A706	80	5	EA	6	#4	3	4G80S6(EA)

(c) Influence of Bar Spacing

Reinforcement Type	Grade, ksi	Nominal f_c' ksi (MPa)	Interface Preparation	Rebar Spacing, in. (mm)	Rebar Size	# of Specimens	Specimen Group Label
A706	80	5	1/8” IR	4	#4	3	4G80S4(1/8)
A706	80	5	1/8" IR	6	#4	See 1(a)	4G80S6(1/8)
A706	80	5	1/8" IR	12	#4	3	4G80S12(1/8)

(d) Influence of Reinforcing Bar Size

Reinforcement Type	Grade, ksi	Nominal f_c' ksi (MPa)	Interface Preparation	Rebar Spacing, in. (mm)	Rebar Size	# of Specimens	Specimen Group Label
A706	80	5	As Cast	6	#4	See 1(b)	4G80S6(AC)
A706	**80**	**5**	**As Cast**	**6**	**#5**	**3**	**5G80S6(AC)**
A706	80	5	1/8" IR	6	#4	See 1(a)	4G80S6(1/8)
A706	**80**	**5**	**1/8" IR**	**6**	**#5**	**3**	**5G80S6(1/8)**
A706	80	5	1/4" IR	6	#4	See 1(b)	4G80S6(1/4)
A706	**80**	**5**	**1/4" IR**	**6**	**#5**	**3**	**5G80S6(1/4)**
A706	80	5	EA	6	#4	See 1(b)	4G80S6(EA)
A706	**80**	**5**	**EA**	**6**	**#5**	**3**	**5G80S6(EA)**
(e) Influence of Nominal Concrete Strength							
Reinforcement Type	**Grade, ksi**	**Nominal 2ksi (MPa)**	**Interface Preparation**	**Rebar Spacing, in. (mm)**	**Rebar Size**	**# of Specimens**	**Specimen Group Label**
A706	**80**	**3**	**1/8" IR**	**6**	**#4**	**3**	**4G80S6F3(1/8)**
A706	80	5	1/8" IR	6	#4	See 1(a)	4G80S6(1/8)
A706	**80**	**6**	**1/8" IR**	**6**	**#4**	**3**	**4G80S6F6(1/8)**
Total # of specimens (a) + (b) + (c) + (d) + (e) = 45 tests							

Legend: * Reinforcing steel grade – 60 ksi, 80 ksi, 100 ksi, 120 ksi. Nominal concrete strength – 3 ksi, 5 ksi, 6 ksi. IR – Intentionally roughened; *As Cast*: surface was leveled and not intentionally roughened; 1/8" IR: surface roughened to an amplitude of 1/8 in.; 1/4" IR: surface roughened to an amplitude of 1/4 in.; EA: Euclid Chemical Surface Retarder Formula S was utilized to expose the aggregate of the surface resulting in a surface roughened up to an amplitude of 1/4 in. Rebar spacing – 4 in., 6 in., 12 in. Rebar size – #4, #5.

Figure 3.2 shows the layout of the push-off test specimen with the deck (top) or girder (bottom) halves of the push-off test specimen, which are illustrated in the figure and referred to in this report as side 2 and side 1, respectively. The specimen in this figure had three (3) U-Bars, at a spacing of 6 in. (152.4 mm) on center.

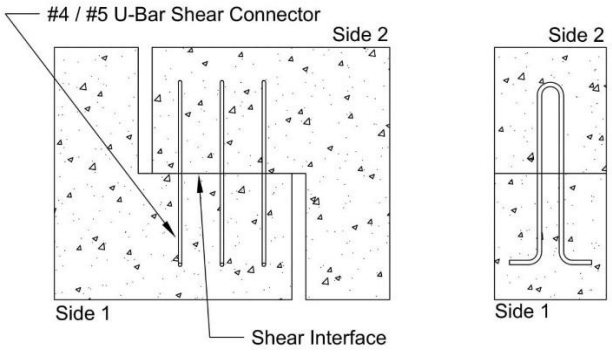

Figure 3.2: Simplified elevation schematic of push-off test specimen containing 3 U-bars to show side 2 (top), side 1 (bottom), reinforcing steel bars, and shear interface

In the experimental design the actuator selected had a capacity limit (500 kips [2224 kN]), and to limit the probability of exceeding the actuator capacity during testing, an area of 2 in. (50.8 mm) by 20 in. (508 mm) on the specimen sides was debonded on the interface of each specimen. Ultra-high-molecular-weight polyethylene (UHMW) strips with dimensions 2 in. (50.8 mm) by 20 in. (508 mm) by 0.25 in. (6.35 mm) were used to create the debonded area. Figure 3.3 shows the debonded area of the specimens along with the overall dimensions of the test specimens and the direction of the applied load.

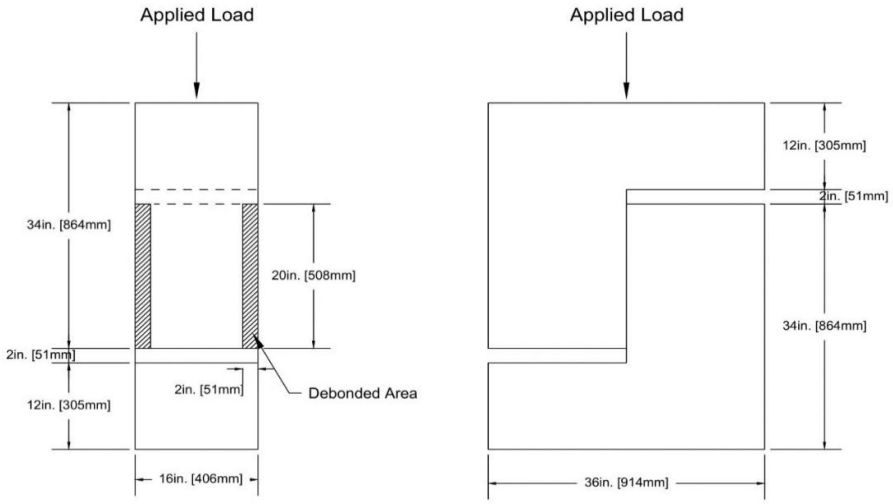

(a) (b)

Figure 3.3: (a) Front view elevation, (b) side view elevation

3.3 PUSH-OFF TEST SPECIMENS DESIGN

Push-off test specimens were designed using ODOT (2014) section 1.17.8.2, which refers to AASHTO (2014) Section 5.8.4. A Strut-and-Tie model was developed to design the steel reinforcement layout, not including the U-bars crossing the shear interface. Detailed designed procedure is shown in Appendix A

3.3.1 Interface Shear Capacity Design

The interface shear capacity for all test specimens was calculated per AASHTO (2014) Section 5.8.4. Mathcad sheets were developed for each specimen group depending on the characteristics such as reinforcing steel bar grade, shear interface surface preparation, reinforcing steel bar spacing, reinforcing steel bar size, and nominal concrete strength. The Mathcad sheets are presented in Appendix A

Out of all the specimens listed in Table 3.1, the maximum interface shear force was 410 kips (1824 kN) Thus, the experimental peak load is estimated to be 500 kips (2224 kN) assuming an over strength factor of 2.0 is used.

3.3.2 Interface Preparation

Four (4) different interface preparations were implemented to aid in the study of the influence of interface preparation on shear friction: (i) As Cast: surface was leveled and not intentionally roughened; (ii) surface roughened to an amplitude of 1/8 in. (3.175 mm); (iii) surface roughened to an amplitude of 1/4 in. (6.35 mm); and (iv) Exposed aggregate: Euclid Chemical Concrete Surface Retarder Formula S was utilized to expose the aggregate of the surface resulting in a surface roughened up to an amplitude of 1/4 in. (6.35 mm). The As Cast surface preparation was obtained by screeding the fresh concrete on the shear interface with a 2x4 piece of lumber. The surfaces roughened to an amplitude of 1/8 in. (3.175 mm) and 1/4 in. (6.35 mm) were roughened with a trowel notched to the specific dimensions to obtain the required roughness. The Exposed Aggregate surface preparation was obtained by spraying the Euclid Chemical Concrete Surface Retarder Formula S on the fresh concrete. The chemical was washed off the shear interface after 18-24 hours, thus exposing the aggregate to an amplitude of 1/4 in. (6.35 mm).

3.3.3 Reinforcing Steel Layout

Figure 3.4 shows the reinforcing steel layout for all specimen types. The differences between specimens are the size, grade, and spacing of the reinforcing steel U-bars crossing the interface. The U-bars terminate in 90-degree standard hooks that satisfy AASHTO (2014) Section 5.10.2.1 and all bend diameters satisfy AASHTO (2014) Table 5.10.2.3-1. All other reinforcing steel (i.e. the reinforcement that did not cross the interface) met ASTM A706 Grade 60 ksi (420 MPa). Stirrups were designed to be #4 (#13M) bars. Longitudinal reinforcing steel was designed to be #6 (#19M) bars. All longitudinal bars terminate with 90-degree hooks. All transverse stirrups

end with 135-degree hooks. Figure 3.5 shows a section view of specimens build with three #4 (#13M) bars.

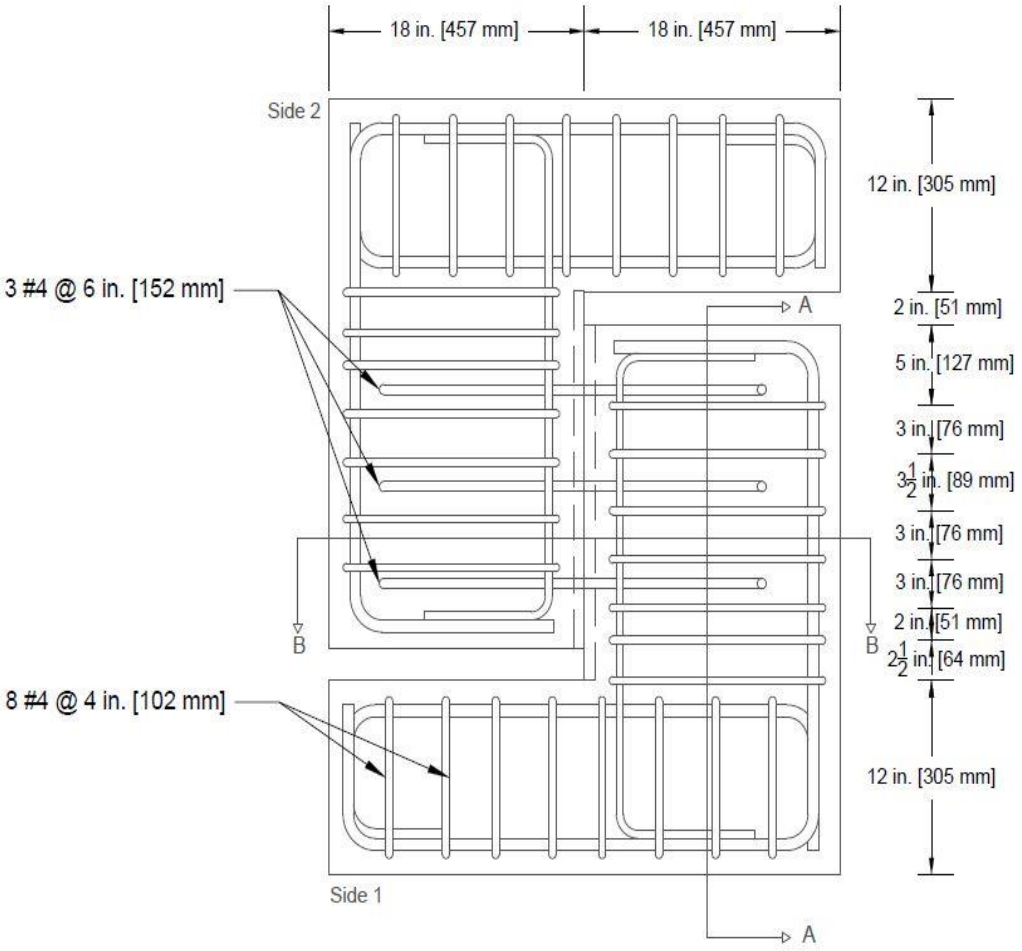

Figure 3.4: Steel layout for a specimen containing three #4 U-bars spaced at 6 in. (152 mm)

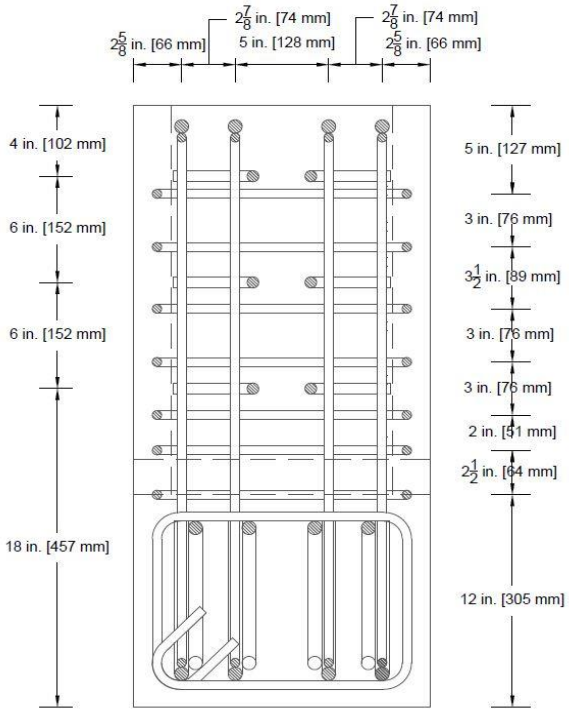

Figure 3.5: Section A-A steel layout for a specimen containing three #4 U-bars spaced at 6 in. (152 mm)

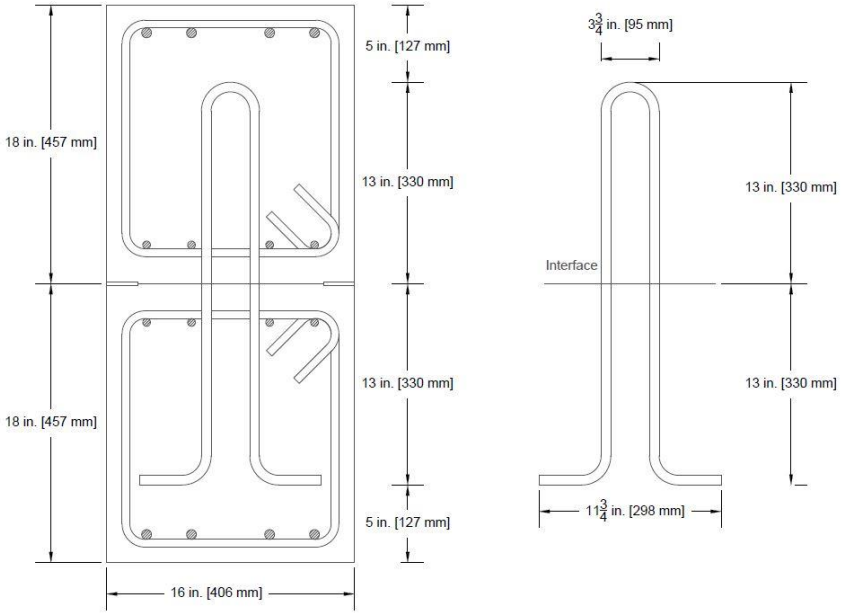

Figure 3.6: Section B-B steel layout for a specimen containing three #4 U-bars spaced at 6 in. (152 mm).

3.4 PUSH-OFF TEST PROCEDURES

The following section discusses the push-off test setup, instrumentation, and testing procedures. Setup procedures, instrumentation for stress and displacement measurement, and rate of loading during the test are presented.

3.4.1 Push-off Test Setup

Figure 3.7 shows an overall view of the specimen and Figure 3.8 shows a photograph of the test setup. Appendix C shows isometric views of the test specimen setups. These figures illustrate the actuator, test specimen, top roller and plates, base plates, roller supports, actuator displacement transducer (LVDT), and reaction frame. Elevation views are shown in Figure 3.9 and Figure 3.10.

Each test was initiated by placing the test specimen in the center of two 4 in. wide steel plates resting on top of the main load transfer base steel plates. It was important to ensure that the specimen interface shear plane was aligned with the load path of the actuator, thus minimizing local stresses due to an eccentric load. A laser level was used to maximize alignment accuracy by aligning the center of the actuator with the specimen interface shear plane. Once the specimen was aligned in the direction parallel to the shear interface, the rollers supports were adjusted to hold the specimen in place. To align the specimen in the direction perpendicular to the shear interface the roller supports on the south side of the specimen were adjusted. Once the rollers were temporarily in place, the specimen was lowered into position. After the test specimen was in position, the reaction frame on the north side was set into place with the overhead crane. The roller guides on all sides were adjusted to be within 0.125 in. (3.2 mm) of the specimen on each side, with the exception of the top roller on the north side reaction frame which was set 2 in. (51 mm) to allow the top side to move, and therefore for cracks to form across the interface being tested, during the tests. Once all the rollers were in place, the top load transfer plates were placed and aligned with the axis of the actuator. External instrumentation was put into place, then all instrumentation was connected, using wire splicers, to the DAQ.

The actuator was placed on manual displacement and lowered to be 0.125 in. (3.2 mm) above the top loading plate. The test rate was then set to 0.001 in/sec (0.0254 mm/sec). The actuator was lowered and stopped when an initial force of 0.5 kip (2.2 kN) was reached to ensure the top plate is tight in place. The pumps were turned off momentarily to adjust the LVDT measuring actuator displacement. This ensured the LVDT would capture the testing displacements within the actuator stroke length limits.

The sensors data started being logged once the pumps were turned back on. The loading rate was set to 0.001 in/sec (0.0254 mm/sec) and the test was initiated in displacement control. The test was paused when the actuator force is approximately 20 kip (89 kN) to ensure all sensors were working properly. Testing was then continued until a displacement of 0.5 in. (13 mm) was reached, after which the test rate was set to 0.005 in/sec (0.127 mm/sec). The test ended when

the 2 in (51 mm) gap between the top and bottom sides of the specimen was closed, or when all the reinforcing steel U-bars across the interface ruptured.

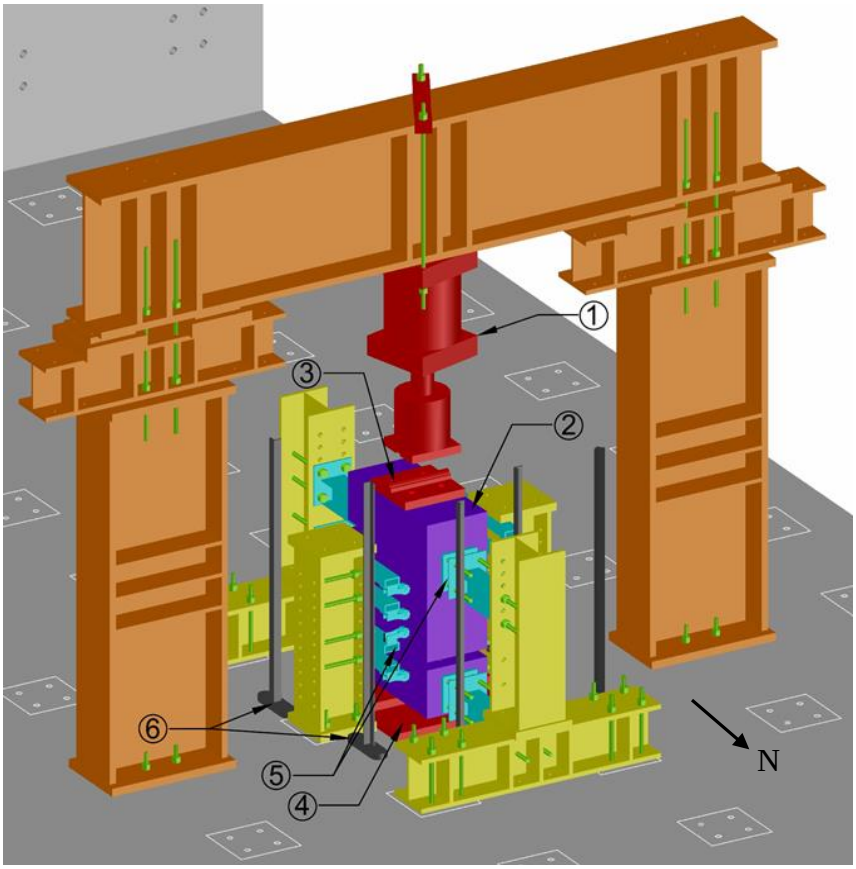

Figure 3.7 General test setup facing southwest. Legend – 1: Actuator; 2: test specimen; 3:roller plate; 4: base plate; 5: roller support for safety (gap provided between rollers and specimen); 6: LVDT sensor supports

Figure 3.8: Photograph of specimen facing southwest before testing

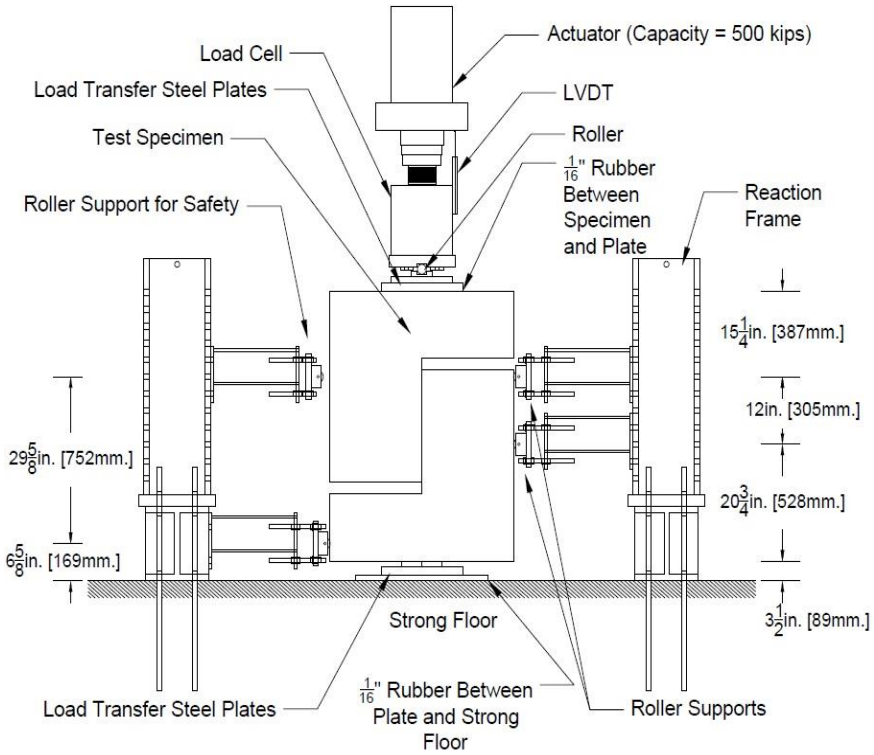

Figure 3.9: North-south elevation view of test setup

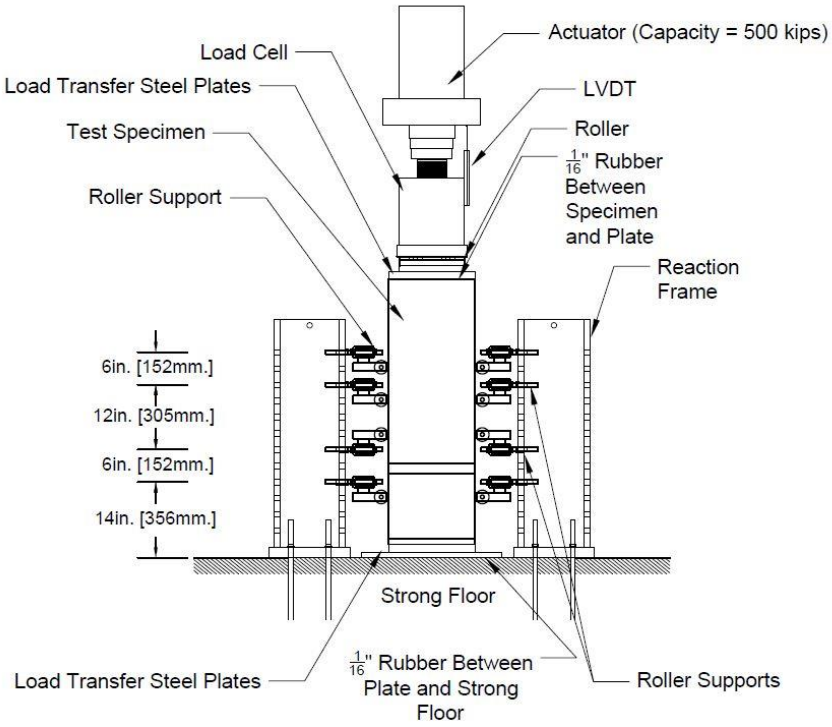

Figure 3.10: East-west elevation view of test setup [1 in. = 25.4mm; 1 kip = 4.48 kN]

3.5 INSTRUMENTATION

Instrumentation was used to monitor the movement of the test specimen and the strains of the U-bars during testing. Figure 3.11 shows the external instrumentation used and Table 3.2 lists the external instrumentation used with the corresponding measurement that was targeted. The vertical displacement of the top L-shape was measured with two (2) string potentiometers (label 1) attached on the face of the specimen and 8 in. (203 mm) from the vertical alignment of the shear interface. The shear interface separation was measured with two (2) Duncan pots (label 2). The tip of the Duncan pot plungers rested on UHMW plastic plates to minimize friction. The base movement was measured using four (4) Duncan pots (labels 3 and lower label 5) placed at 2 in. (51 mm) from the side edge and bottom edge. Two (2) 6 in. (152 mm) LVDTs (label 4) were used to measure the vertical movement of the top L-shape. Their measurements were used to determine if there was rotation of the top L-shape. The plunger of the LVDTs rested on top of UHMW plastic strips to minimize friction. Two (2) Duncan pots were attached 3 in. (76 mm) from the top face to measure potential lateral movement of the top L-shape (upper label 5). One (1) string potentiometer was used to measure the reaction frame beam displacement (label 6). The actuator displacement was measured by an LVDT attached to the actuator (label 7). Prior to the first test, all instruments were calibrated with a Mitutoyo Absolute Digimatic Height Gage (Series 570).

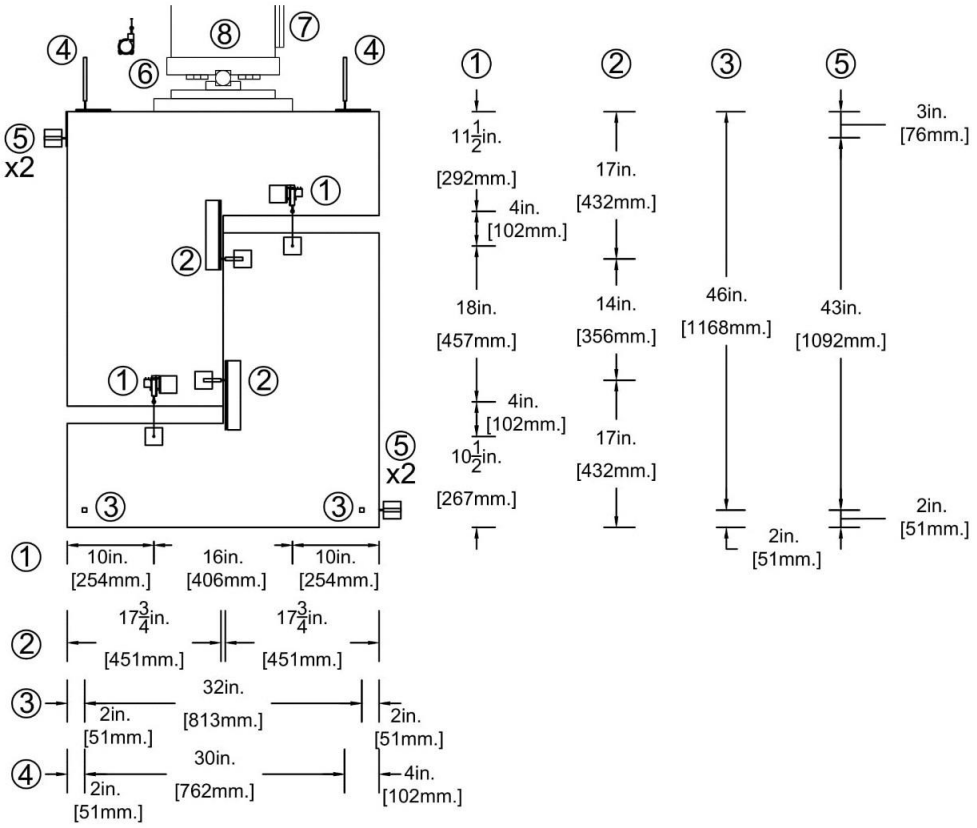

Figure 3.11: North-south external instrumentation elevation view

Table 3.2: Summary of Measure Observations and Instrumentation.

Instrumentation	Objective	Figure 3.11 label
4 Duncan pots (1.5" stroke)	Specimen base movement	3 & 5
2 Duncan pots (1.5" stroke)	Specimen top lateral movement	5
2 LVDT's (6" stroke)	Specimen top vertical movement	4
2 String pots (2" stroke)	Shear interface vertical movement	1
2 Duncan pots (1.5" stroke)	Shear interface horizontal movement	2
1 Actuator	Applied shear load	8
1 LVDT (12" stroke)	Actuator displacement	7
1 string pot (2" stroke)	Reaction frame beam displacement	6

Internal instrumentation used consisted of strain gauges placed on the reinforcing bars crossing the shear interface for all specimens. Strain gauges were placed at 3 in. (76 mm) from the interface on both legs of every U-bar to ensure data collection after initiation of cracking of the concrete interface. An additional strain gauge was placed at 1 in. (25 mm) on one U-bar. All

strain gauges were placed on the inside of the 90° bend of the reinforcing steel U-bars. Strain gauges were labeled s1 to s5, s1 to s7, and s1 to s9 in specimens constructed with two, three, and four reinforcing steel U-bars, respectively. Table 3.3 to Table 3.5 present descriptions of the strain gauge labels and locations for specimens constructed with two, three, and four reinforcing steel U-bars, respectively. Figure 3.12 illustrates the strain gauges applied on specimens containing two U-bars crossing the interface. Figure 3.13 illustrates the strain gauges applied on specimens containing three U-bars crossing the interface. Figure 3.14 illustrates the strain gauges applied on specimens containing four U-bars crossing the interface.

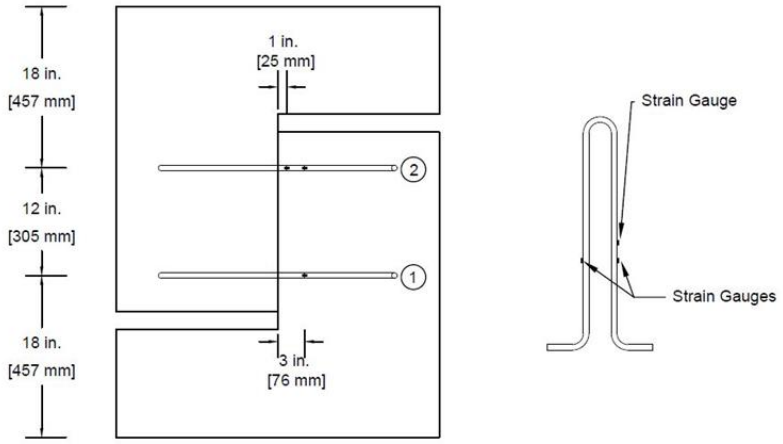

Figure 3.12: Internal instrumentation elevation for specimens built with two U-bars.

Table 3.3: Strain Gauge Labels for Specimens Containing 2 Reinforcing Steel U-bars.

Strain gauge label	Bar Number	Side	Distance from interface, in. (mm)
s_1	1	West	3 (76)
s_2	2	West	3 (76)
s_3	2	West	1 (25)
s_4	1	East	3 (76)
s_5	2	East	3 (76)

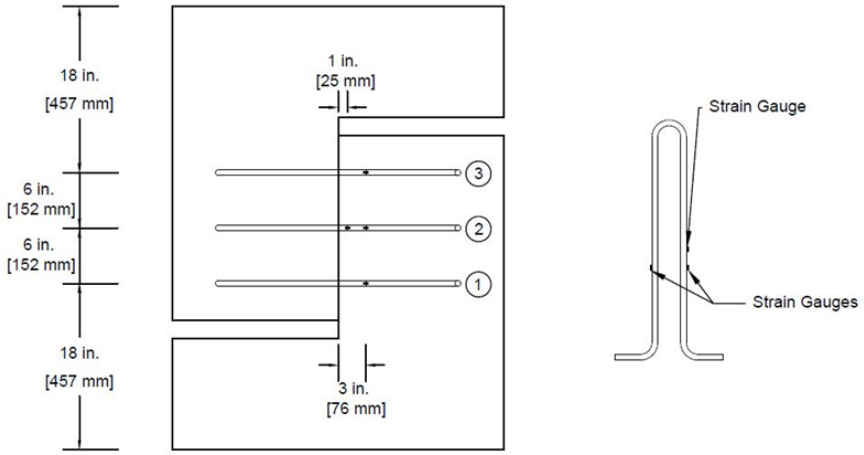

Figure 3.13: Internal instrumentation elevation for specimens built with three U-bars

Table 3.4: Strain Gauge Labels for Specimens Containing 3 Reinforcing Steel U-bars.

Strain gauge label	Bar Number	Side	Distance from interface, in. (mm)
s_1	1	West	3 (76)
s_2	2	West	3 (76)
s_3	3	West	3 (76)
s_4	2	West	1 (25)
s_5	1	East	3 (76)
s_6	2	East	3 (76)
s_7	3	East	3 (76)

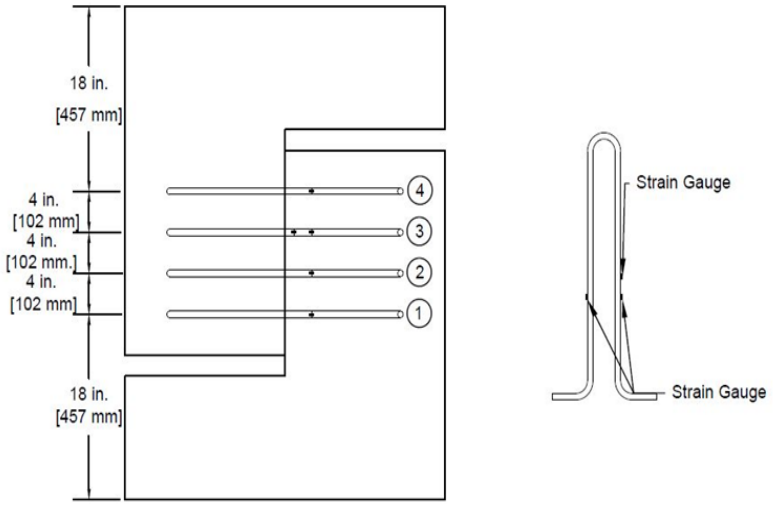

Figure 3.14: Internal instrumentation elevation for specimens built with four U-bars.

Table 3.5: Strain Gauge Labels for Specimens Containing 4 Reinforcing Steel U-bars.

Strain gauge label	Bar Number	Side	Distance from interface, in. (mm)
s_1	1	West	3 (76)
s_2	2	West	3 (76)
s_3	3	West	3 (76)
s_4	4	West	3 (76)
s_5	3	West	1 (25)
s_6	1	East	3 (76)
s_7	2	East	3 (76)
s_8	3	East	3 (76)
s_9	4	East	3 (76)

(a) (b)

Figure 3.15: Strain gauges applied to U-bar reinforcing (a) view of strain gauge with initial protective coating and (b) view of U-bars after strain gauges are installed

3.6 CONSTRUCTION PROCEDURE

The push-off test specimens were fabricated in the Structural Engineering Research Laboratory at Oregon State University. The test specimens were cast in two concrete placements. The construction of the specimens is summarized below.

1. Installation of strain gauges on U-bars as shown in Figure 3.15;

2. Construction and assembly of formwork as shown in Figure 3.16. Formwork for side 1 was placed on a level surface, squared, and strapped;

3. Assembly of reinforcing steel L-cages. Stirrup locations were measured and marked. Rebar tie wire was used to tie steel cages. A construction square was used to ensure

the cages were square. As specimens were symmetrical, both side 1 and side 2 had the same L-shape cage configuration. Example specimen cages are shown in Figure 3.17;

4. Placement of the L-cages in the formwork. The L-shape cage was placed into formwork with plastic spacer guides. Loose ties and other objects were cleaned out of the formwork before casting. Figure 3.18 shows the cages in the formwork;

5. Placement of reinforcing steel U-bars. Plywood pieces marked with the correct reinforcing bar spacing were placed under the U-bars to ensure that they were normal to the interface and at the designed spacing, as shown in Figure 3.19;

6. Casting of side 1 (representing the girder side). Concrete was cast and consolidated, struck level with the surface, and interfaces finished accordingly. For the initial curing phase, burlap and plastic were placed over the concrete immediately after casting and wetted once in the morning and once in the evening. Plastic sheets were placed immediately after casting. Wetting of the specimen started on the day after casting and went on for three days. After three days, the burlap and plastic were removed. Cast specimens are shown in Figure 3.20;

7. Assembly and placement of Side 2 L-cages. L-shape cages for side 2 were assembled and placed on top of side 1, as shown in Figure 3.22.

8. Placement of Side 2 formwork. The second set of formworks was installed, and plastic spacers (not shown) were used to ensure the correct cover is achieved as shown in Figure 3.23.

9. Casting of Side 2. Concrete was cast, consolidated, and struck level with the top of the formwork. Curing followed the same procedure explained in step 6. After three days, the burlap and plastic were removed.

10. The formwork was removed 7 days later. The specimens were all labelled immediately after formwork was removed. Figure 3.24 shows a test specimen after formwork removal.

Figure 3.16: Formwork construction

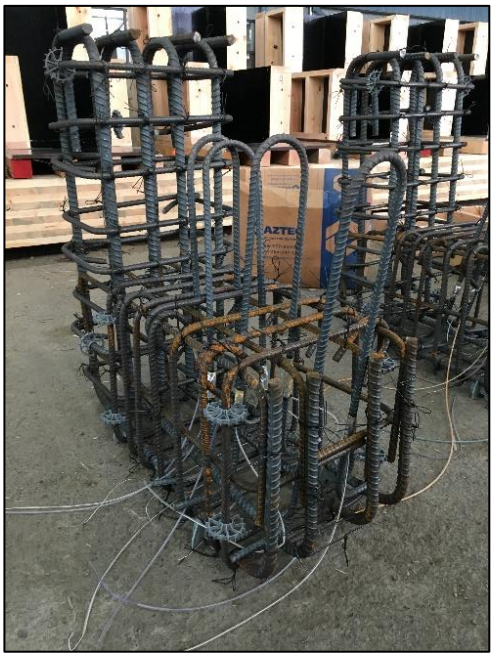

Figure 3.17: Cage for a specimen containing #4 (#13M) reinforcing bars across the interface

Figure 3.18: Cage is inserted into formwork

Figure 3.19: The L-shape half of a specimen containing #4 (#13M) U-bars at the correct location

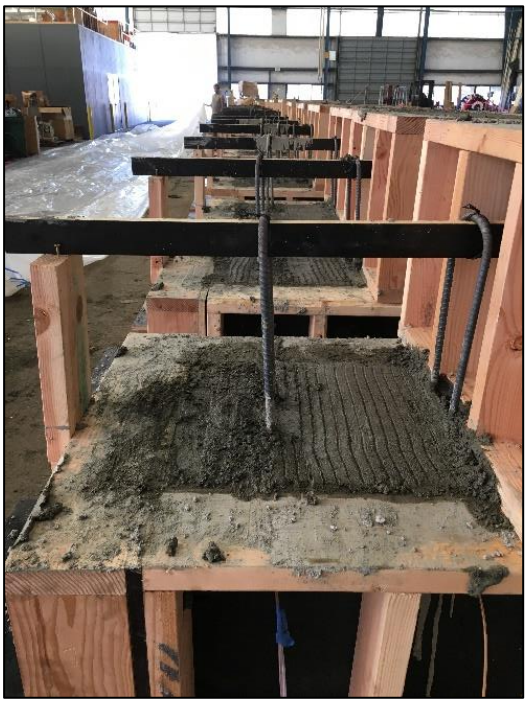

Figure 3.20: Cast specimens after the concrete pour of side 1

(a) (b) (c) (d)

Figure 3.21: Photographs of cast specimens showing surface treatment: (a) as cast, (b) 1/8 in, (c) 1/4 in, and (d) exposed aggregate.

Figure 3.22: Top L-shaped cage is placed on top of specimen

Figure 3.23: Top L-shaped cage is placed inside formwork

Figure 3.24: Constructed specimens after formwork removal

3.7 POST-PROCESSING OF EXPERIMENTAL RESULTS

The results of the force-displacement, force-crack width, and force-strain response for each push-off test specimen are reported in the following sections. The displacement of the shear interface was measured to gain a better understanding of the effect of concrete cohesion, aggregate interlock, and dowel action at the different stages of deformation. The strain in the reinforcing steel U-bars is measured because it was useful in computing the clamping force generated by the reinforcing steel U-bars, which has a direct effect on aggregate interlock. Crack width is an important parameter to measure due to its relation to the concrete-to-concrete cohesion component and the clamping force generated by the reinforcing steel U-bars. Crack width has an inverse relation to the cohesion component, in other words the cohesion component degrades as crack width increases. In contrast, the clamping force in the reinforcing steel U-bars will increase as crack width increases. Section 3.5 provides a detailed explanation of the instrumentation used to measure these parameters.

The typical force-displacement response of a push-off test specimen can be seen in Figure 3.25. There are five important points to highlight from the response, which are: (i) Δ_{cr}, V_{cr}: loss of cohesion identified as described in this section; (ii) V_{ult}, Δ_{ult}: peak interface shear load and corresponding displacement, respectively; (iii) $V_{sus,min}$: minimum sustained interface shear force during post-peak response; (iv) $V_{sus,max}$: maximum sustained interface shear force during post-peak response; and (v) V_b, Δ_b: interface shear force and displacement at the moment the first bar fractures, respectively. The tabulated values for each important point of interest are obtained from the response curves of each individual specimen.

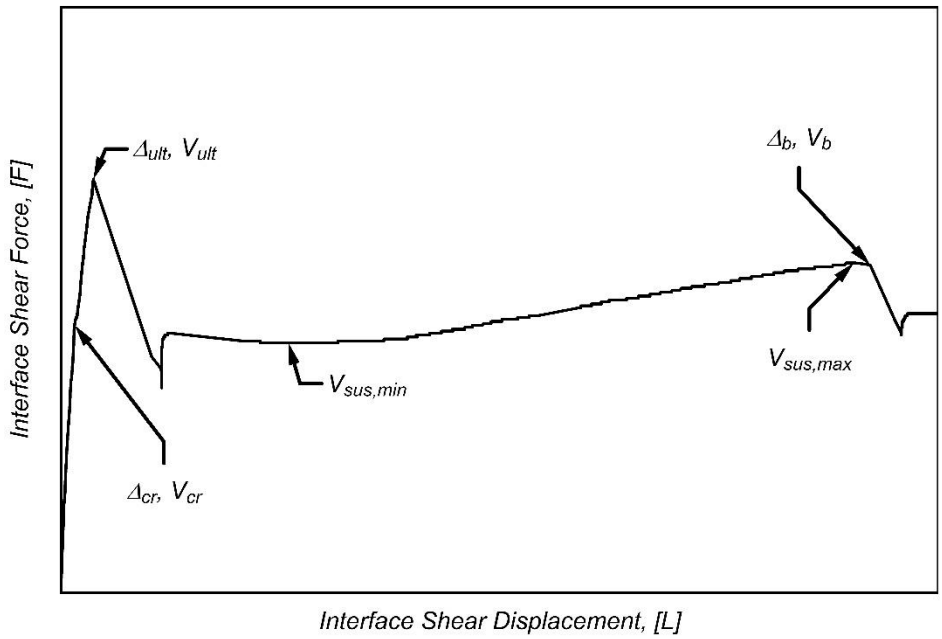

Figure 3.25: Typical force-displacement response of push-off tests and definition of notable parameters.

A standardized method was developed to determine the cracking interface shear force at the point of loss of cohesion; V_{cr}. Figure 3.26 presents a graph illustrating the standardized method for a typical test specimen force-strain response. The standardized method consists of the following four steps: (1) the interface shear force versus reinforcing steel microstrain relationship is plotted. The reinforcing steel microstrain used corresponds to readings from the strain gauge located at 1 in. (25.4 mm) from the interface, as it provides the closest measurement of the strain on the reinforcing steel bar; (2) the values of the interface shear force versus reinforcing steel microstrain curve between $0.1\varepsilon_y$ and $0.2\varepsilon_y$ are isolated to be used to develop a curve fit. These limits were chosen due to their proximity to the inflection point identifying the reduction of stiffness that results from the loss of cohesion, and because they are both within the limits of the reinforcing steel bars being well engaged and linear-elastic behavior of the reinforcing steel bar; (3) the value of the cracking interface shear force at the point of loss of cohesion, V_{cr}, is taken as the y-intercept of the resulting linear fit; and, (4) the corresponding cracking displacement at the point of loss of cohesion, Δ_{cr}, is determined as the interface shear displacement corresponding to the cracking interface shear force load in the interface shear force versus interface shear displacement response.

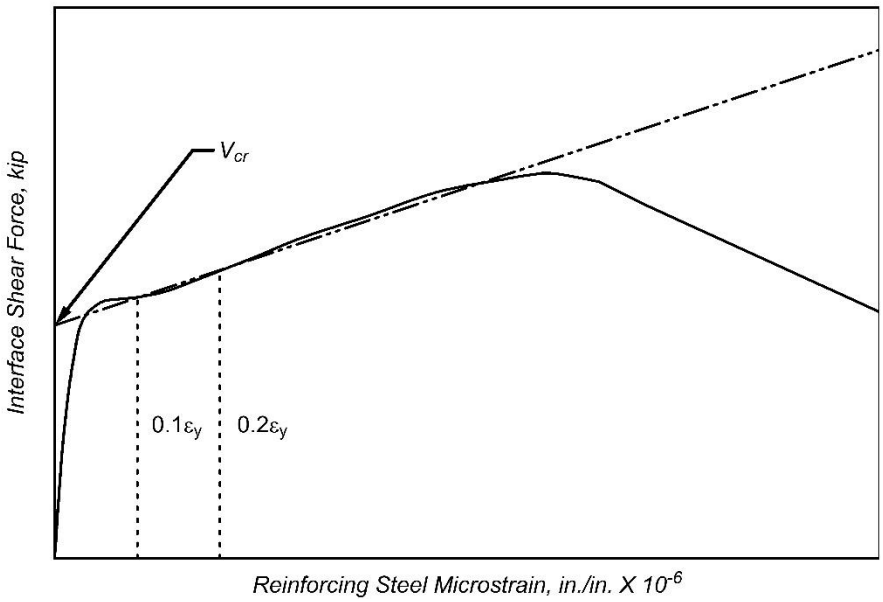

Figure 3.26: Illustration of the points used to determine the point of loss of cohesion.

4.0 MATERIALS

4.1 REINFORCING STEEL

Test specimens were constructed using three types of reinforcing steel U-bars (ASTM A615, ASTM A706, and ASTM A1035) and four grades (60 ksi (420 MPa), 80 ksi (550 MPa), 100 ksi (690 MPa), and 120 ksi (830 MPa)). For ASTM A706 Grade 80, two bar sizes were used, #4 (#13M) and #5 (#16M). For all other grades, #4 (#13M) bars were used. All the reinforcing U-bars were provided by Cascade Steel located in McMinnville, Oregon. Farwest Steel, Eugene, Oregon provided and bent all other specimen reinforcing bars used to construct the specimen rebar cages, while U-bars were cut and bent at Oregon State University.

Table 4.1 and 4.2 summarize the information on the mechanical properties and the chemical compositions of different reinforcing steels as provided by the manufacturers. The tensile test results for different steels listed in Table 4.1 are summarized in Table 4.3. The tensile testing followed ASTM E8/E8M-13a (ASTM 2013). Three (3) specimens were tested for each size and grade of reinforcing steel. All specimens were marked using a metal punch and tested in a 56 kips (250 kN) INSTRON universal testing machine (UTM) Model 5985 at an 8-in. (203.2 mm) grip-to-grip length, per the specifications defined in ASTM A615/A615M-16 (ASTM 2016a), ASTM A706/A706M-16 (ASTM 2016b), and ASTM A1035/A1035-16b (ASTM 2016c). A 3 in. (76 mm) grip length on both ends of the specimen was maintained for all tests. All specimens were tested at a constant displacement rate of 0.0003 in/sec (0.00762 mm/sec) until rupture. A static axial clip-on extensometer that meets the requirements of ASTM E83-16 (ASTM 2016d) was connected at the center of the specimen for strain measurements. The UTM force, the UTM displacement, and the extensometer output were recorded at 100 millisecond intervals. The extensometer was removed at a strain value of 0.08 for the ASTM 706 Grade 60 (420 MPa), the ASTM 615 Grade 80 (550 MPa), the ASTM 706 Grade 80 (550 MPa), and the ASTM 615 Grade 100 (690 MPa) specimens. For ASTM 1035 (CRX4100 and CRX9100) specimens, the extensometer was removed at strain values of 0.03 and 0.06, respectively. A curve-fitting technique was used to establish relationship between the extensometer strain and the UTM displacement-computed-strain measured prior to extensometer removal. Using the fitted function, the post extensometer-removal strains were extrapolated based on the displacement of the UTM head recorded during the test.

Table 4.3 provides a summary of tensile test results, including the elastic modulus, yield point stress and strain, and percentage elongation over an 8-inch gauge length for the specimens tested. The yield stress was determined using both (1) the 0.2% offset method and (2) the 'Extension Under Load' (EUL) method, as described in ASTM E8/E8M-13a (ASTM 2013). A strain value of 0.0035 in/in (mm/mm) strain was chosen for the EUL method. For the elastic modulus, data falling in the stress range of 20 ksi (140 MPa) to 60 ksi (420 MPa) were considered for the elastic modulus calculations of ASTM 706 Grade 60 (420 MPa) steel reinforcing bars, while for

all other grades, the stress range of 20 ksi (140 MPa) to 80 ksi (550 MPa) was considered in the estimation of the Young's modulus. It is important to note that ASTM A1035-16b Type CM Grade 100 (690 MPa) reinforcing steel, as described in the steel mill data, met the tensile property requirements for a Grade 120 denomination per standard ASTM A1035/A1035M-16b, even though the mill data denominates it as Grade 100, as shown in

Table 4.3. Therefore, this material will be referred to as A1035/A1035M-16b Grade 120 (830 MPa) reinforcing steel. Figure 4.1 through Figure 4.8 show the stress-strain curves of each bar type and sizes tested.

Table 4.1: Mechanical and Physical Properties of Reinforcing Bar (Mill Data).

Product ID	Grade	Rebar Size	Heat #	Yield strength, ksi (MPa)	Tensile strength, ksi (MPa)	Elong. % 8 in. (0.2 m)*
#4 706/60	ASTM A706-16 Grade 60	#4 (#13M)	195517	67.5 (465)	95 (655)	18
#5 706/60		#5 (#16M)	211217	67 (462)	94.5 (652)	16
#4 615/80	ASTM A615-16 Grade 80	#4 (#13M)	013517	89.5 (617)	125 (862)	11
#5 615/80		#5 (#16M)	220817	87.5 (603)	121 (834)	12
#4 706/80	ASTM A706-16 Grade 80	#4 (#13M)	062517	91 (627)	116 (800)	14
#5 706/80		#5 (#16M)	042517	89.5 (617)	116 (800)	13
#4 615/100	ASTM A615-16 Grade 100	#4 (#13M)	511215	103 (710)	131 (903)	12
#5 615/100		#5 (#16M)	503615	108 (745)	141 (972)	9.5
#4 CRX4100	ASTM A1035-16b Type CM Grade 100**	#4 (#13M)	179817	119 (820)	160 (1103)	9
#5 CRX4100		#5 (#16M)	059417	136 (938)	165 (1138)	9
#4 CRX9100	ASTM A1035-16b Type CS Grade 100**	#4 (#13M)	166016	133 (917)	170 (1172)	11
#5 CRX 9100		#5 (#16M)	165916	131 (903)	164 (1131)	10

*According to ASTM A706;

** Meets tensile properties requirements for Grade 120 denomination per subsequent reinforcing bar tensile test summary shown in Table 4.3. These were therefore relabeled as Grade 120.

Table 4.2: Chemical Composition of Reinforcement (Mill Data).

Product ID	C	Mn	P	S	Si	Cu	Ni	Cr	V	Mo	Sn	N2	CE*
#4 706/60	0.28	1.22	0.03	0.02	0.23	0.24	0.06	0.17	0.03	0.02	0.02	-	0.5
#5 706/60	0.28	1.28	0.02	0.02	0.23	0.24	0.08	0.13	0.03	0.02	0.01	-	0.52
#4 615/80	0.44	1.27	0.02	0.02	0.26	0.28	0.08	0.16	-	0.02	0.02	-	0.67
#5 615/80	0.43	1.22	0.02	0.02	0.28	0.29	0.07	0.16	-	0.02	-	-	0.66
#4 706/80	0.27	1.33	0.20	0.01	0.24	0.28	0.05	0.16	-	0.01	0.02	-	0.51
#5 706/80	0.27	1.35	0.02	0.02	0.24	0.28	0.06	0.15	-	0.11	-	-	0.51
#4 615/100	0.34	1.34	0.02	0.02	0.25	0.27	0.09	0.12	0.17	0.02	0.02	-	0.57
#5 615/100	0.37	1.34	0.30	0.02	0.27	0.22	0.07	0.14	-	0.15	-	-	0.60
#4 CRX4100	0.10	1.33	0.01	0.01	0.35	0.18	0.06	4.15	0.01	0.02	0.01	0.01	0.74
#5 CRX4100	0.09	0.87	0.01	0.01	0.36	0.14	0.04	4.68	0.01	0.01	0.01	0.01	0.71
#4 CRX9100	0.11	0.58	0.01	0.01	0.39	0.14	0.10	9.54	0.03	0.01	0.01	0.02	1.17
#5 CRX9100	0.09	0.58	0.01	0.01	0.39	0.16	0.10	9.42	0.03	0.02	0.01	0.02	1.14

*CE: Carbon Equivalent determined as shown in ASTM A706/A706M-14.

Table 4.3: Reinforcing Bar Tensile Test Results Summary.

Product ID	Elastic Modulus ksi (MPa)	Yield point (0.2% offset)		Yield point (0.0035 EUL)		Tensile strength point		Ultimate strain		% Elong. in 8 in. (203 mm)
		Stress, ksi (MPa)	Strain, in/in (-)	Stress, ksi (MPa)	Strain, in/in (-)	Stress, ksi (MPa)	Strain, in/in (-)	Stress, ksi (MPa)	Strain, in/in (-)	
#4 706/60	28964 (199700)	64.04 (442)	0.0043	64.08 (442)	0.0035	92.42 (637)	0.121	65.74 (453)	0.157	17.23
#5 706/60	28296 (195094)	65.15 (449)	0.0043	65.15 (449)	0.0035	94.56 (652)	0.112	71.87 (496)	0.170	15.79
#4 615/80	29254 (201699)	85.95 (593)	0.0049	95.88 (661)	0.0035	120.87 (833)	0.091	93.86 (647)	0.132	12.71
#5 615/80	30131 (207746)	85.63 (590)	0.0048	85.74 (591)	0.0035	121.46 (837)	0.092	110.40 (761)	0.126	11.72
#4 706/80	28203 (194453)	88.63 (611)	0.0052	88.37 (609)	0.0035	114.25 (788)	0.098	83.42 (575)	0.135	13.51
#5 706/80	27704 (191012)	88.94 (613)	0.0053	89.11 (614)	0.0035	113.50 (783)	0.103	98.18 (677)	0.143	15.03
#4 615/100	29188 (201244)	103.92 (717)	0.0056	97.73 (674)	0.0035	132.54 (914)	0.085	114.99 (793)	0.103	11.52
#5 615/100	29865 (205912)	105.03 (724)	0.0055	102.02 (703)	0.0035	137.73 (950)	0.081	122.20 (843)	0.104	11.91
#4 CRX4100	28451 (196163)	126.63 (873)	0.0064	92.10 (635)	0.0035	159.73 (1101)	0.041	95.47 (658)	0.086	6.79
#5 CRX4100	31168 (214896)	131.75 (908)	0.0062	101.46 (700)	0.0035	163.02 (1124)	0.060	99.13 (683)	0.091	7.25
#4 CRX9100	29575 (203913)	134.29 (926)	0.0066	100.38 (692)	0.0035	176.06 (1214)	0.054	115.78 (798)	0.093	8.04
#5 CRX9100	27219 (187668)	125.89 (868)	0.0065	92.57 (638)	0.0035	164.25 (1133)	0.056	111.80 (771)	0.096	8.92

Table 4.4: Reinforcing Bar Strain Hardening Results Summary.

Product ID	Grade	Strain hardening point	
		Stress ksi (MPa)	Strain in./in. (mm/mm)
#4 706/60	ASTM A706-16 Grade 60	64.02 (441)	0.011
#5 706/60		65.24 (450)	0.006
#4 615/80	ASTM A615-16 Grade 80	85.69 (591)	0.009
#5 615/80		86.04 (593)	0.007
#4 706/80	ASTM A706-16 Grade 80	88.07 (607)	0.011
#5 706/80		88.32 (609)	0.012
#4 615/100	ASTM A615-16 Grade 100	104.45 (720)	0.009
#5 615/100		105.39 (727)	0.007
#4 CRX4100	ASTM A1035-16b Type CM Grade 120	71.45 (493)	0.002
#5 CRX4100		82.41 (568)	0.003
#4 CRX9100	ASTM A1035-16b Type CS Grade 120	87.94 (606)	0.003
#5 CRX9100		84.33 (581)	0.003

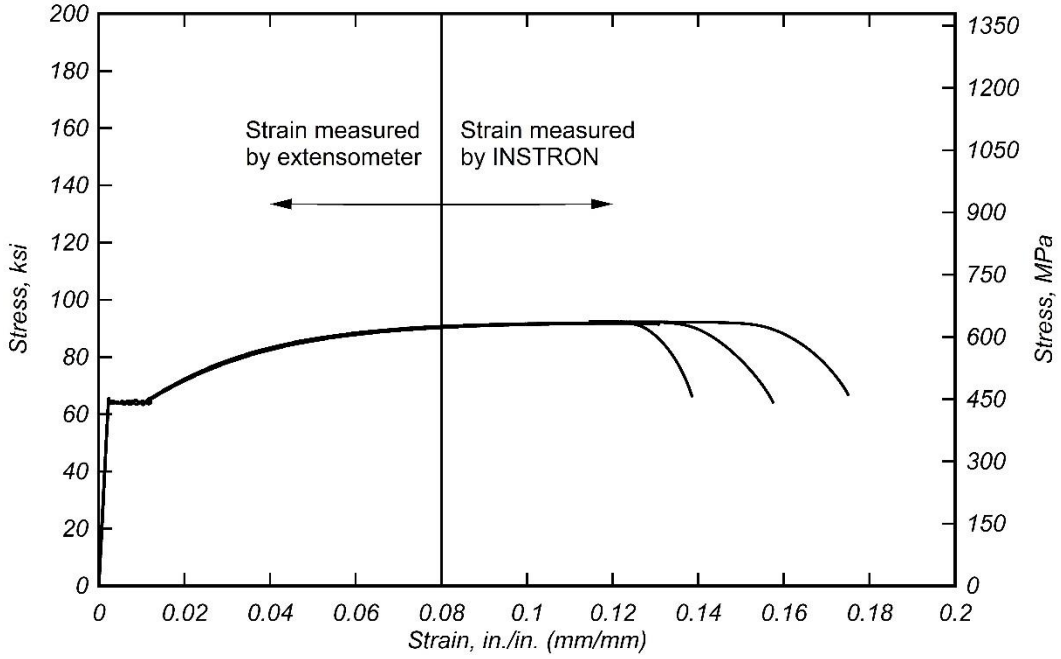

Figure 4.1: Stress-strain plot of #4 (#13M) A706 Grade 60 reinforcing steel bar

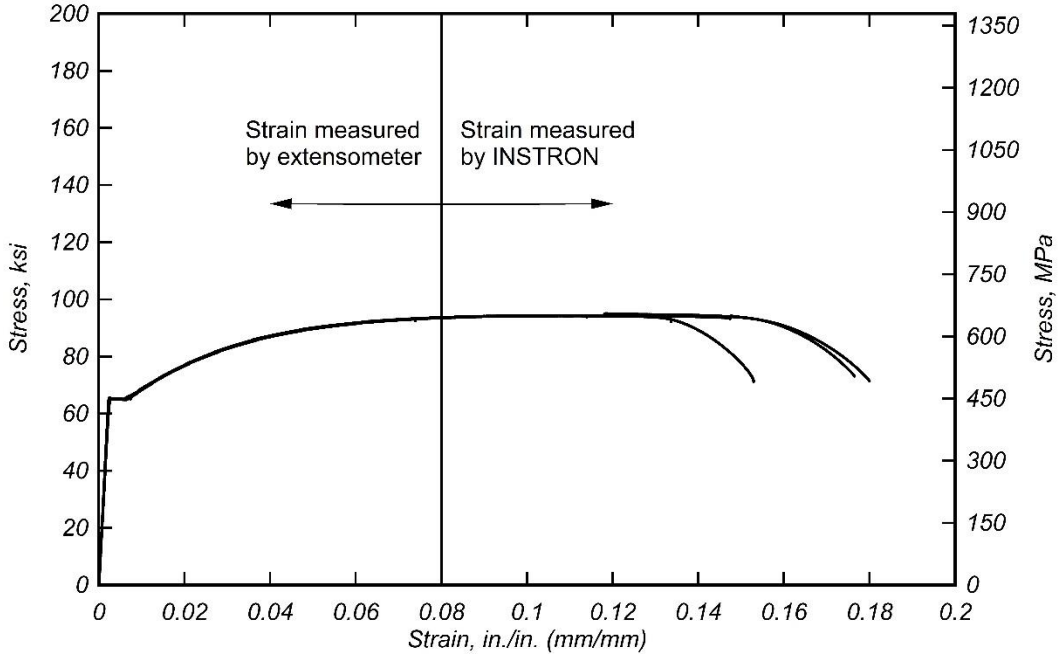

Figure 4.2: Stress-strain plot of #5 (#16M) A706 Grade 60 reinforcing steel bar

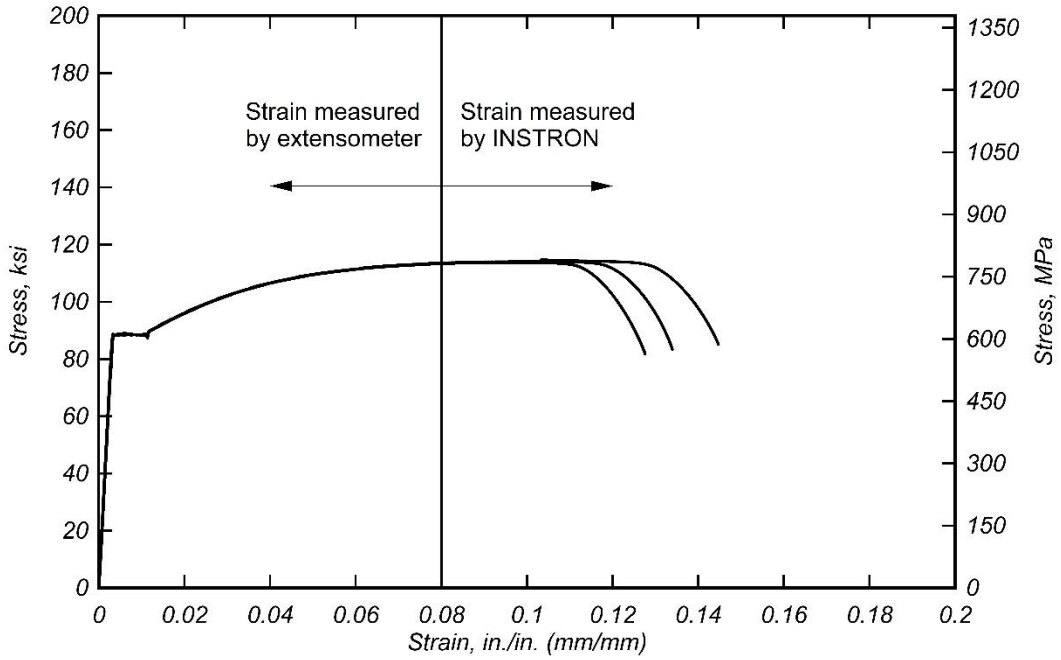

Figure 4.3: Stress-strain plot of #4 (#13M) A706 Grade 80 reinforcing steel bar

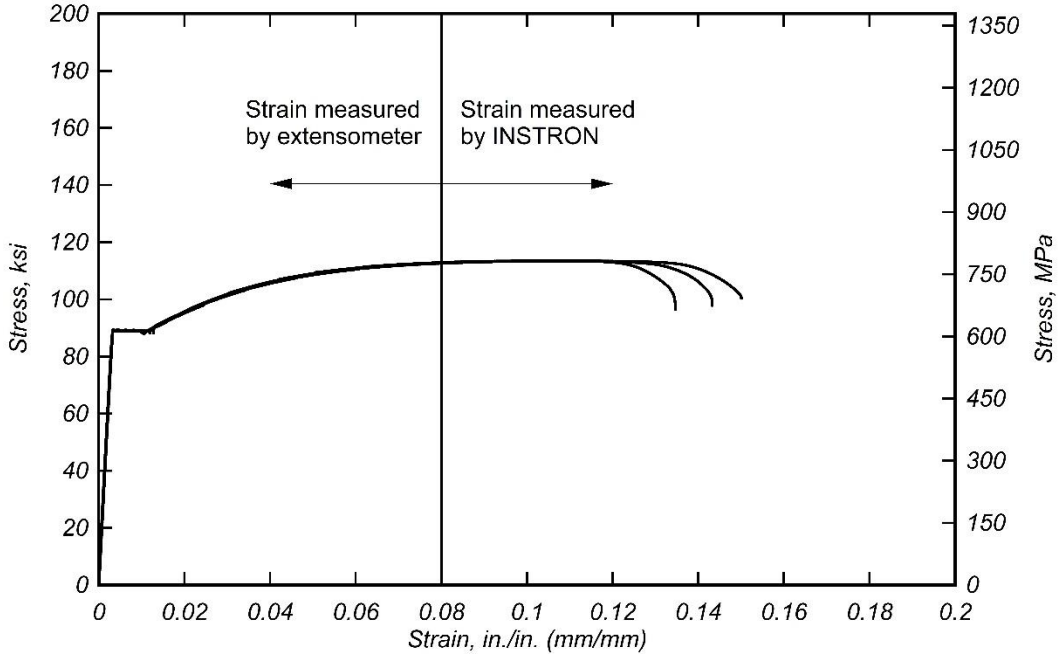

Figure 4.4: Stress-strain plot of #5 (#16M) A706 Grade 80 reinforcing steel bar

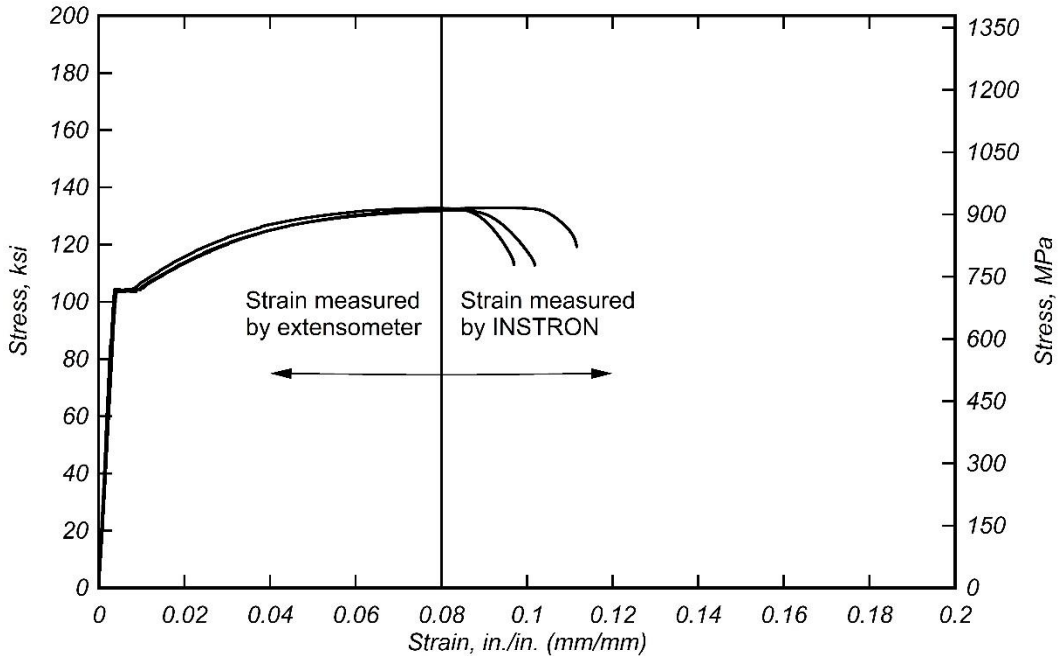

Figure 4.5: Stress-strain plot of #4 (#13M) A615 Grade 100 reinforcing steel bar

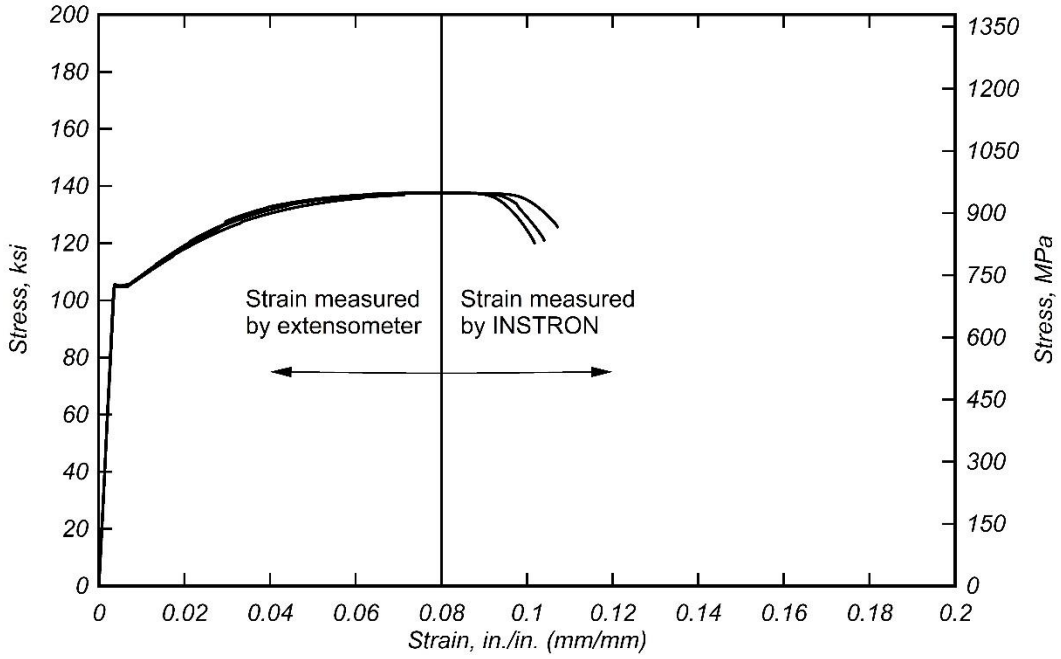

Figure 4.6: Stress-strain plot of #5 (#16M) A615 Grade 100 reinforcing steel bar

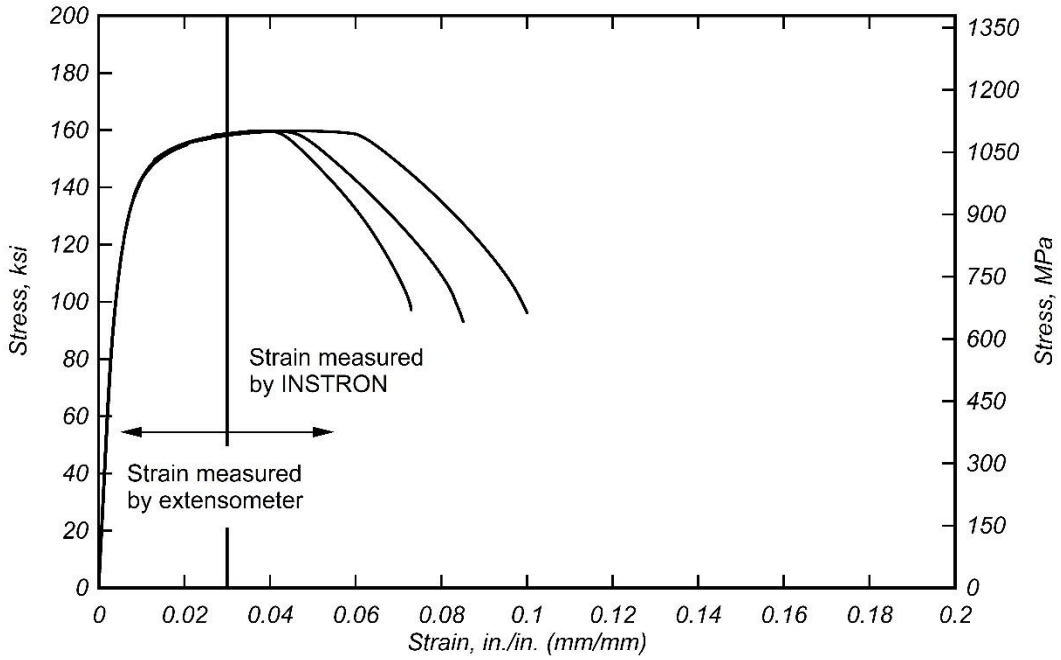

Figure 4.7: Stress-strain plot of #4 (#13M) A1035 CM Grade 120 reinforcing steel bar

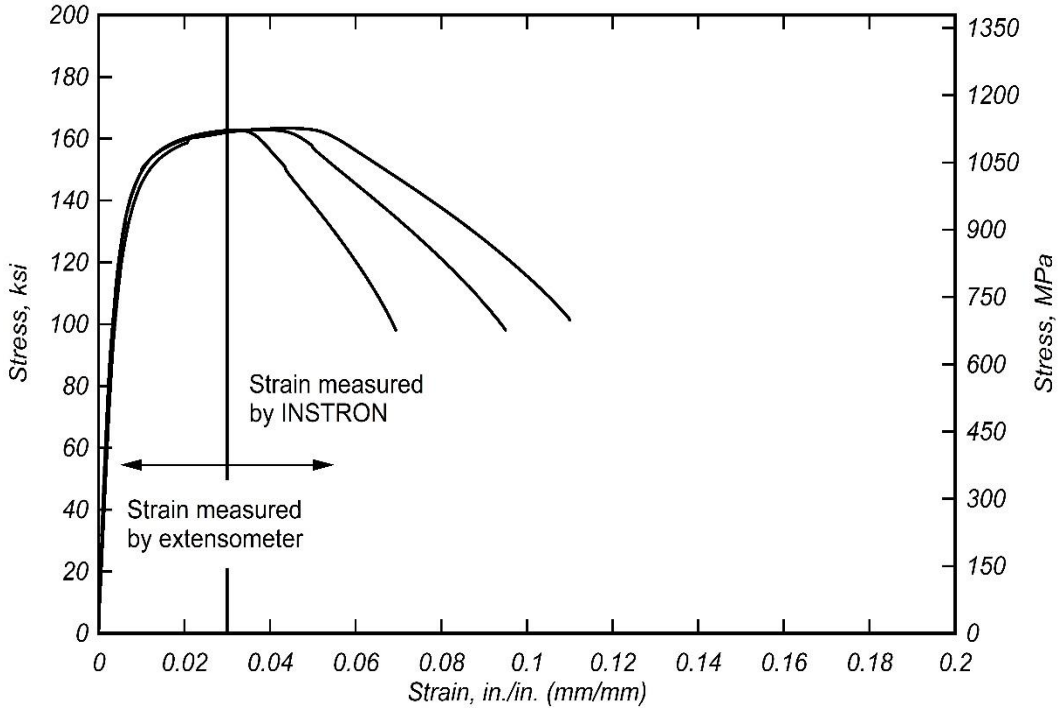

Figure 4.8: Stress-strain plot of #5 (#16M) A1035 CM Grade 120 reinforcing steel bar

4.2 CONCRETE

For each specimen, the push-off test specimens were cast on two different cast dates. The same concrete mixture proportions were used for both casts. The maximum aggregate size was 3/8 in. (9.5 mm) for all mixtures. Table 4.5 shows the concrete mixture proportions for different mixtures used in the study. All the concrete used in this study was provided by Knife River Corporation. The concrete was mixed at the dry batch plant and delivered by truck. The 28-day design/nominal compression strength for Mix #1, Mix #2, and Mix #3 were 5000 psi (35 MPa), 6000 psi (40 MPa), and 3000 psi (20 MPa), respectively.

Table 4.5: Concrete Mixture Proportions per Cubic Yard (Meter).

Mix #	Design f_c', psi (MPa)	W/CM	Coarse agg. lbs. (kg)*	Fine agg. lbs. (kg)	Cement, lbs. (kg)	Slag, lbs. (kg)	Fly ash, lbs. (kg)	Water, lbs. (kg)	Ad. Mix. 1 (WRDA-64), oz (g)	Ad. Mix. 2 (V-MAR3), oz (g)
1	5000 (35)	0.388	1250 (567)	1479 (671)	695 (315)	-	80 (36)	300.6 (135.3)	31 (879)	-
2	6000 (40)	0.438	1100 (499)	1692 (767)	590 (268)	115 (52)	-	309 (139)	24.7 (700)	-
3	3000 (20)	0.525	1200 (544)	1840 (835)	525 (238)	-	-	275.6 (124)	21 (595)	21 (595)

*Maximum aggregate size of 3/8 in. (9.5 mm).
Legend: W/CM – Water to Cementitious Materials Ratio.

Table 4.6 shows the slump and the 28-day mean compressive strengths of concrete. The slump was evaluated using ASTM Standard C143-12 (ASTM 2012c). Concrete cylinder samples were cast in accordance to ASTM C31/31M-12 (ASTM 2012a), Standard Practice for Making and Curing Concrete Test Specimens in the field and were 4 in. (102 mm) diameter by 8 in. (203 mm) tall cylinders. Twenty-four hours after the concrete cast, cylinders were stripped from the molds and stored in the casting area, close to the push-off test specimens. Cylinders were tested for compressive strength following ASTM C39/39M-12a (ASTM 2012b), Standard Test Method for Compressive Strength of Cylindrical Concrete Specimens.

Table 4.6: Fresh Concrete Characteristics.

Mix #	Cast Date	Slump, in. (mm)	28-day mean compressive strength, psi (MPa)
1	07/21/2017	7.75 (197)	6849 (47.5)
1	08/04/2017	6.50 (165)	6778 (46.7)
1	09/12/2017	7.25 (184)	6718 (46.3)
1	10/25/2017	4.25 (108)	6037 (41.6)
1	12/05/2017	7.50 (191)	5540 (38.2)
2	12/06/2017	7.50 (191)	4040 (27.9)
3	12/07/2017	7.00 (179)	3203 (22.1)
1	12/14/2017	6.50 (165)	5661 (39.0)
2	12/15/2017	6.25 (159)	4471 (30.8)
3	12/15/2017	6.75 (171)	2519 (17.4)
1	04/12/2018	7.50 (191)	6261 (43.2)
1	05/03/2018	6.00 (152)	5815 (40.1)

The compressive strength at the time of testing for each push-off specimen is presented in Table 4.7. Each row corresponds to one specimen group where the compressive strength values at the time of testing for the bottom and top casts are presented for the three identical specimens conforming each specimen group. Note that Mix #1, which had a specified nominal concrete strength of 5 ksi (35 MPa) exhibited compressive strengths at the time of testing of 5.6 ksi (38 MPa) and above. Mix #2, with a specified concrete strength of 6 ksi (40 MPa) exhibited compressive strengths at the time of testing of 4.7 ksi (32.4 MPa). Mix #3, with a specified concrete strength of 3 ksi (20 MPa), exhibited a compressive strength at the time of testing of 2.8 ksi (19.5 MPa). The measured mean strength of mix #2 was found to be lower than the 28-day design/nominal strength.

Table 4.7: Concrete Compressive Strength at Time of Shear Specimen Testing.

Specimen label	Adopted value f_c', psi (MPa)
4G80S12(1/8)	6190 (42.68)
4G80S4(1/8)	6190 (42.68)
4G80S6(EA)	5977 (41.21)
4G80S6(1/4)	6190 (42.68)
4G80S6(1/8)	6190 (42.68)
4G80S6(AC)	6190 (42.68)
4G60S6(1/8)	5954 (41.05)
4G100S6(1/8)	5954 (41.05)
5G80S6(AC)	5954 (41.05)
5G80S6(1/8)	5954 (41.05)
5G80S6(EA)	5609 (38.68)
5G80S6(1/4)	5954 (41.05)
4G120S6(1/8)	5977 (41.21)
4G80S6F6(1/8)	4701 (32.41)
4G80S6F3(1/8)	2823 (19.46)

5.0 EFFECT OF HIGH-STRENGTH REINFORCING STEEL ON SHEAR FRICTION

5.1 INTRODUCTION

This chapter presents test results from push-off test specimens with a focus on the effect of high-strength reinforcing steel on shear friction. The effects analyzed in this section are: (1) influence of reinforcing steel grade, (2) influence of reinforcing steel bar spacing, and (3) influence of reinforcing steel bar size. The details of each push-off test specimen discussed in this chapter can be found in the test matrix presented in Table 3.1, section (a), (c), and (d). The discussion in this chapter focuses on results for interface shear force versus interface shear displacement, interface shear force versus strain, and interface shear force versus crack width. The methods implemented for data collection and the instrumentation utilized are presented in Section 3.5. The typical force-displacement response of a push-off test specimen is shown in Figure 3.25.

5.2 INFLUENCE OF REINFORCING STEEL GRADE

This section focuses on the influence of reinforcing steel grade on shear friction. All specimens discussed in this section have an interface roughness of 1/8 in. (3.175 mm), contain three (3) #4 (#13M) reinforcing steel U-bars spaced at 6 in. (152.4 mm), and have a design (nominal) concrete strength of 5000 psi (35 MPa). Because the variable of interest in this discussion is the reinforcing steel grade, the experimental results and discussion focuses on test specimens containing Grade 60 ksi (420 MPa), Grade 80 ksi (550 MPa), Grade 100 ksi (690 MPa), and Grade 120 (830 MPa) reinforcing steel U-bars labeled 4G60S6(1/8), 4G80S6(1/8), 4G100S6(1/8), and 4G120S6(1/8), respectively. Details of the specimens, such as bar size, bar spacing, and interface preparation can be found in section (a) of Table 3.1; drawings showing dimensions of the specimens, as well as location of the reinforcing steel U-bars are presented in Chapter 3. Properties of the reinforcing steel used, and the concrete used are presented in Section 4.1 and Section 4.2, respectively.

5.2.1 Interface Shear Force versus Interface Shear Displacement

Figure 5.1 to Figure 5.4 show the interface shear force versus interface shear displacement relationship curves for the three specimens making up each specimen group constructed with Grade 60 (420 MPa), Grade 80 (550 MPa), Grade 100 (690 MPa), and Grade 120 (830 MPa) reinforcing steel U-bars. The corresponding specimen group labels are 4G60S6(1/8), 4G80S6(1/8), 4G100S6(1/8), and 4G120S6(1/8), respectively. Table 5.1 to Table 5.4 show values of the main characteristic points of the test results for the specimens. The tabulated values were computed as a mean value of the three specimens per group for the characteristic point.

From inspection of Figure 5.1 to Figure 5.4, it can be observed that all tested specimens present similar behavior with a linear initial response until the cracking interface shear load, V_{cr}, is reached, followed by a subtle reduction of stiffness caused by the loss of cohesion, even though the V_{cr} value is slightly different for all specimens. Following this point, V_{cr}, the stiffness remains roughly constant until the peak load is reached. As the displacement increases, the reinforcing steel U-bars crossing the shear interface are engaged and generate a clamping force that holds both pieces of the test specimen together. After the peak load, the shear interface undergoes a significant slip accompanied by a reduction in interface shear force. This big reduction in interface shear force is due to the sudden failure of the aggregate interlock mechanism. It is also related to the stiffness and strain energy released by the test setup. Beyond this level of displacement, the response is controlled by the dowel action mechanism, as cohesion is lost, and aggregate interlock is significantly reduced as the crack width gradually increases. However, as reinforcing steel bars engage with increased displacement, a steady increase in shear load until first bar fracture is observed, indicating a hardening phase as the dowel action mechanism develops.

Figure 5.2 presents the interface shear force versus interface shear displacement relationship for specimen group 4G80S6(1/8). In this figure, it can be observed that specimen 4G80S6(1/8)-2 presents a significantly higher peak load. The load at cracking, however, is like that of the other specimens. This indicates that the higher peak load may be due to the variability originating from roughening the surface to an amplitude of 1/8 in. (3.175 mm), in this case causing the aggregate interlock mechanism to have a higher impact on the force-displacement response. Similarly, in Figure 5.4 specimen 4G120S6(1/8)-2 also exhibited a significantly higher peak load. This behavior can also be explained by the variability originating from the interface roughening process.

The post-peak phase of the mean interface shear force versus interface shear displacement response is also affected by the grade of reinforcing steel. First, as it can be observed in Table 5.5, the post-peak sustained strength increases with increasing reinforcing steel grade. The post-peak sustained strength at first bar fracture values, V_b, are lowest for the 4G60S6(1/8) specimens [123.65 kip (550.01 kN)] and are highest for the 4G120S6(1/8) specimens [213.37 kip (949.10 kN)]. Even though the increase in strength is observable with an increase in reinforcing steel grade, the 4G80S6(1/8) and 4G100S6(1/8) specimens present very similar mean sustained load, exhibiting V_b values of 148.87 kip (662.19 kN) and 169.42 kip (753.63 kN), respectively. In contrast with the differences in mean interface shear force at first bar fracture, V_b, the mean displacement at first bar fracture, Δ_b, for the tested specimens range between 1.018 in. (25.85 mm) and 1.082 in. (27.48 mm), except for the 4G100S6(1/8) specimens which had an mean Δ_b value of 0.918 in. (23.32 mm). The energy dissipated until first bar fracture, E_b, which is calculated as the area under the interface shear force versus interface shear displacement curve until first bar fracture, is a parameter where significant differences can be observed. The mean E_b is the highest in 4G120S6(1/8) specimens, with a value of 16.85 kip-ft. (22.85 kJ), and is lowest in the 4G60S6(1/8) specimens, where the mean value was 10.25 kip-ft. (13.90 kJ). This corresponds to a 64% increase in work done by the 4G120S6(1/8) specimens over the 4G60S6(1/8) specimens. Overall, these results indicate the dowel action mechanism controls the

E_b response and it is characterized by a steady increase in strength and stiffness with increased strength of the reinforcing steel bars.

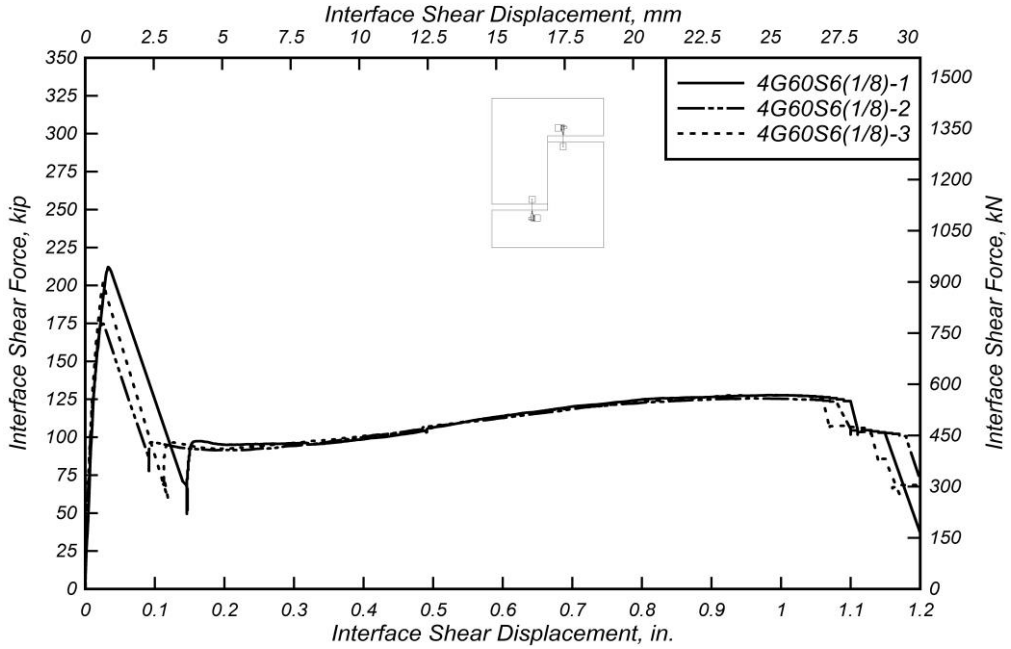

Figure 5.1: Interface shear force versus interface shear displacement for 4G60S6(1/8) specimens.

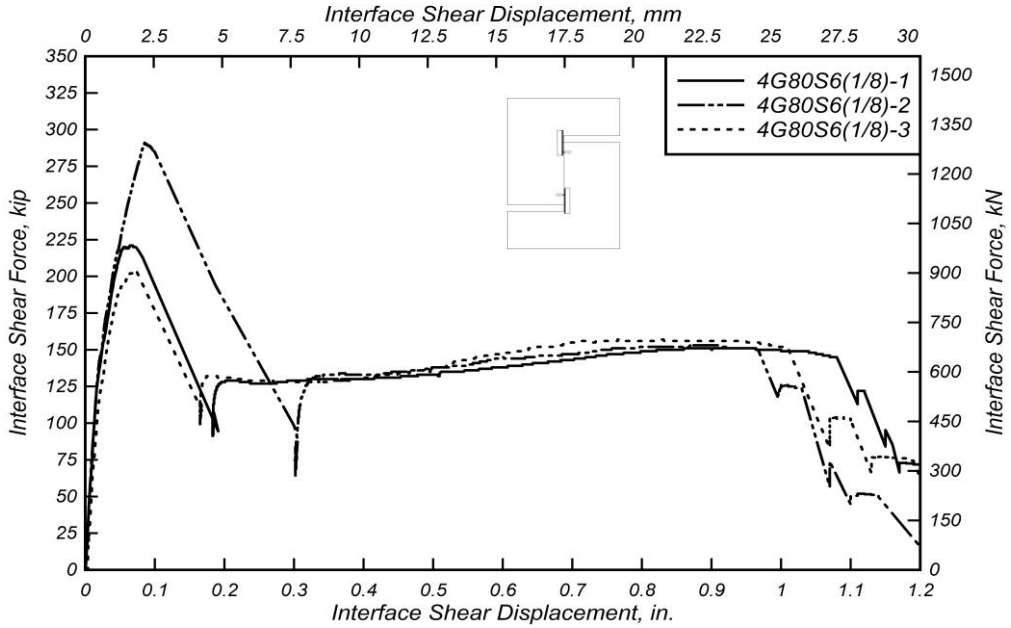

Figure 5.2: Interface shear force versus interface shear displacement for 4G80S6(1/8) specimens

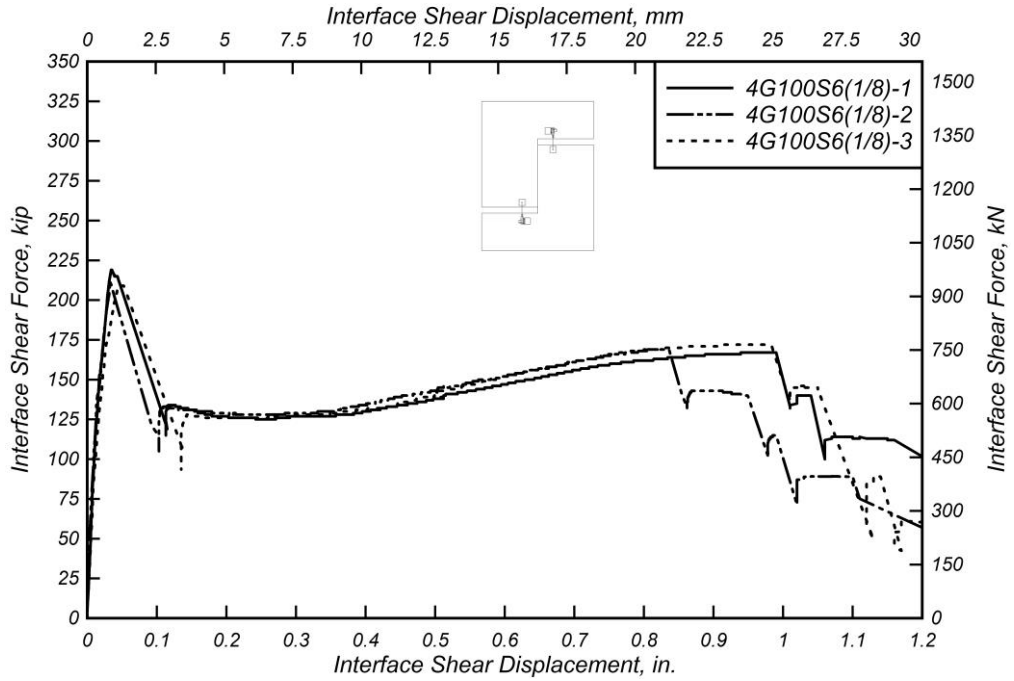

Figure 5.3: Interface shear force versus interface shear displacement for 4G100S6(1/8) specimens.

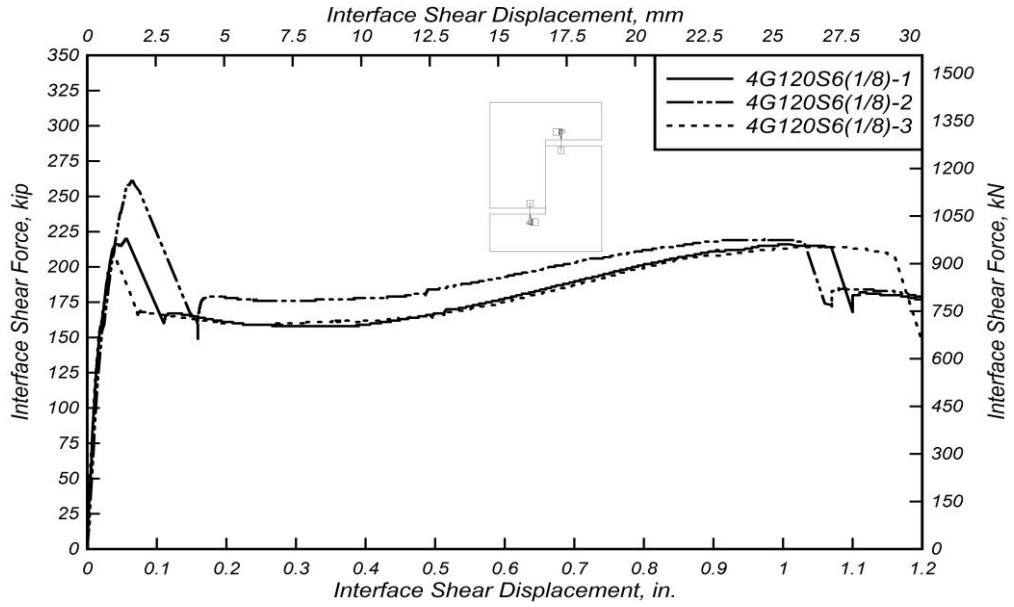

Figure 5.4: Interface shear force versus interface shear displacement for 4G120S6(1/8) specimens

Table 5.1: 4G60S6(1/8) Specimen Shear Test Results.

Specimen	Δ_{ult}, in. (mm)	V_{ult}, kip (kN)	σ_{ult}, ksi (MPa)	$V_{sus,min}$, kip (kN)	$V_{sus,max}$, kip (kN)	Δ_{cr}, in. (mm)	V_{cr}, kip (kN)	Δ_b, in. (mm)	V_b, kip (kN)	E_b, kip-ft (kJ)
4G60S6 (1/8)-1	0.033 (0.838)	212.19 (943.87)	0.884 (6.096)	94.96 (422.40)	127.78 (568.39)	0.013 (0.333)	134.80 (599.62)	1.096 (27.84)	123.45 (549.13)	10.64 (14.43)
4G60S6 (1/8)-2	0.025 (0.635)	174.84 (777.73)	0.729 (5.023)	91.47 (406.88)	125.80 (559.59)	0.010 (0.259)	121.30 (539.57)	1.081 (27.46)	122.83 (546.37)	10.06 (13.64)
4G60S6 (1/8)-3	0.026 (0.660)	202.00 (898.54)	0.842 (5.803)	92.43 (411.15)	127.78 (568.39)	0.007 (0.185)	102.10 (454.16)	1.056 (26.82)	124.66 (554.52)	10.05 (13.63)
Mean	0.028 (0.711)	196.34 (873.38)	0.818 (5.641)	92.95 (413.48)	127.12 (565.46)	0.010 (0.259)	119.40 (531.12)	1.078 (27.37)	123.65 (550.01)	10.25 (13.90)
Median	0.026 (0.660)	202.00 (898.54)	0.842 (5.803)	92.43 (411.15)	127.78 (568.39)	0.010 (0.259)	121.30 (539.57)	1.081 (27.46)	123.45 (549.13)	10.06 (13.64)
STDEV	0.0044 (0.111)	19.307 (85.88)	0.0805 (0.555)	1.803 (8.020)	1.143 (5.085)	0.0029 (0.074)	16.43 (73.10)	0.0202 (0.513)	0.9307 (4.140)	0.3385 (0.459)
COV	16%	10%	10%	2%	1%	28%	14%	2%	1%	3%

Table 5.2: 4G80S6(1/8) Specimen Shear Test Results.

Specimen	Δ_{ult}, in. (mm)	V_{ult}, kip (kN)	σ_{ult}, ksi (MPa)	$V_{sus,min}$, kip (kN)	$V_{sus,max}$, kip (kN)	Δ_{cr}, in. (mm)	V_{cr}, kip (kN)	Δ_b, in. (mm)	V_b, kip (kN)	E_b, kip-ft (kJ)
4G80S6 (1/8)-1	0.065 (1.651)	221.21 (983.99)	0.922 (6.355)	126.72 (563.68)	151.44 (673.64)	0.015 (0.373)	112.5 (500.42)	1.079 (27.41)	145.00 (644.99)	12.92 (17.52)
4G80S6 (1/8)-2	0.085 (2.159)	290.99 (1294.4)	1.212 (8.360)	132.37 (588.81)	152.83 (679.82)	0.016 (0.396)	119.00 (529.34)	0.962 (24.43)	150.57 (669.77)	12.73 (17.26)
4G80S6 (1/8)-3	0.070 (1.778)	203.91 (907.04)	0.850 (5.858)	127.94 (569.11)	156.60 (696.59)	0.016 (0.414)	96.81 (430.63)	1.012 (25.70)	151.03 (671.81)	12.19 (16.53)
Mean	0.073 (1.863)	238.70 (1061.8)	0.995 (6.858)	129.01 (573.86)	153.62 (683.35)	0.016 (0.395)	109.44 (486.80)	1.018 (25.85)	148.87 (662.19)	12.61 (17.10)
Median	0.070 (1.778)	221.21 (983.99)	0.922 (6.355)	127.94 (569.11)	152.83 (679.82)	0.016 (0.396)	112.50 (500.42)	1.012 (25.70)	150.57 (669.77)	12.73 (17.26)
STDEV	0.0104 (0.264)	46.10 (205.06)	0.1921 (1.324)	2.973 (13.22)	2.670 (11.88)	0.0008 (0.020)	11.41 (50.74)	0.0587 (1.491)	3.357 (14.93)	0.377 (0.512)
COV	14%	19%	19%	2%	2%	5%	10%	6%	2%	3%

Table 5.3: 4G100S6(1/8) Specimen Shear Test Results.

Specimen	Δ_{ult}, in. (mm)	V_{ult}, kip (kN)	σ_{ult}, ksi (MPa)	$V_{sus,min}$, kip (kN)	$V_{sus,max}$, kip (kN)	Δ_{cr}, in. (mm)	V_{cr}, kip (kN)	Δ_b, in. (mm)	V_b, kip (kN)	E_b, kip-ft (kJ)
4G100S6 (1/8)-1	0.035 (0.889)	218.87 (973.58)	0.912 (6.288)	125.08 (556.38)	166.89 (742.36)	0.0156 (0.396)	139.70 (621.42)	0.944 (23.98)	166.65 (741.30)	12.08 (16.37)
4G100S6 (1/8)-2	0.033 (0.838)	211.69 (941.64)	0.882 (6.081)	127.77 (568.35)	169.47 (753.84)	0.0135 (0.344)	136.00 (604.96)	0.836 (21.23)	169.47 (753.84)	10.09 (13.68)
4G100S6 (1/8)-3	0.048 (1.219)	209.42 (931.55)	0.873 (6.016)	125.56 (558.52)	172.28 (766.34)	0.0108 (0.274)	95.16 (423.29)	0.974 (24.74)	172.15 (765.76)	12.19 (16.53)
Mean	0.039 (0.982)	213.33 (948.92)	0.889 (6.128)	126.14 (561.08)	169.55 (754.18)	0.0133 (0.338)	123.62 (549.89)	0.918 (23.32)	169.42 (753.63)	11.45 (15.53)
Median	0.035 (0.889)	211.69 (941.64)	0.882 (6.081)	125.56 (558.52)	169.47 (753.84)	0.0135 (0.343)	136.00 (604.96)	0.944 (23.98)	169.47 (753.84)	12.08 (16.37)
STDEV	0.0081 (0.207)	4.933 (21.943)	0.0206 (0.142)	1.4347 (6.382)	2.6958 (11.99)	0.0024 (0.061)	24.716 (109.94)	0.0726 (1.844)	2.7503 (12.23)	1.182 (1.602)
COV	21%	2%	2%	1%	2%	18%	20%	8%	2%	10%

Table 5.4: 4G120S6(1/8) Specimen Shear Test Results

Specimen	$\Delta_{ult,}$ in. (mm)	V_{ult}, kip (kN)	σ_{ult}, ksi (MPa)	$V_{sus,min}$, kip (kN)	$V_{sus,max}$, kip (kN)	$\Delta_{cr,}$ in. (mm)	V_{cr}, kip (kN)	Δ_{b}, in. (mm)	V_{b}, kip (kN)	E_{b}, kip-ft (kJ)
4G120S6 (1/8)-1	0.056 (1.422)	220.21 (979.14)	0.917 (6.324)	158.00 (702.82)	215.99 (960.77)	0.013 (0.325)	126.00 (560.48)	1.066 (27.08)	213.49 (949.65)	16.18 (21.94)
4G120S6 (1/8)-2	0.065 (1.651)	261.45 (1163.0)	1.089 (7.511)	175.75 (781.77)	219.51 (976.43)	0.017 (0.427)	130.50 (580.49)	1.026 (26.06)	218.05 (969.93)	16.75 (22.71)
4G120S6 (1/8)-3	0.037 (0.940)	208.06 (925.50)	0.867 (5.977)	158.79 (706.33)	214.24 (952.99)	0.016 (0.417)	152.00 (676.13)	1.154 (29.31)	208.56 (927.72)	17.61 (23.88)
Mean	0.053 (1.338)	229.88 (1022.5)	0.958 (6.604)	164.18 (730.31)	216.58 (963.40)	0.015 (0.389)	136.17 (605.70)	1.082 (27.48)	213.37 (949.10)	16.85 (22.85)
Median	0.056 (1.422)	220.12 (979.14)	0.917 (6.324)	158.79 (706.33)	215.99 (960.77)	0.016 (0.417)	130.50 (580.49)	1.066 (27.08)	213.49 (949.65)	16.75 (22.71)
STDEV	0.0143 (0.363)	28.00 (124.55)	0.1167 (0.804)	10.03 (44.61)	2.684 (11.94)	0.0022 (0.056)	13.90 (61.81)	0.0655 (1.663)	4.746 (21.11)	0.720 (0.976)
COV	27%	12%	12%	6%	1%	14%	10%	6%	2%	4%

Table 5.5: Summary of Mean Values of Specimen Groups Analyzing Influence of Reinforcing Steel Grade.

Specimen	Δ_{ult}, in. (mm)	V_{ult}, kip (kN)	σ_{ult}, ksi (MPa)	$V_{sus,min}$, kip (kN)	$V_{sus,max}$, kip (kN)	Δ_{cr}, in. (mm)	V_{cr}, kip (kN)	Δ_b, in. (mm)	V_b, kip (kN)	E_b, kip-ft (kJ)
4G60S6 (1/8)	0.028 (0.711)	196.34 (873.38)	0.818 (5.641)	92.95 (413.48)	127.12 (565.46)	0.010 (0.259)	119.40 (531.10)	1.078 (27.37)	123.65 (550.01)	10.25 (13.90)
4G80S6 (1/8)	0.073 (1.863)	238.70 (1061.8)	0.995 (6.858)	129.01 (573.86)	153.62 (683.35)	0.016 (0.395)	109.44 (486.80)	1.018 (25.85)	148.87 (662.19)	12.61 (17.10)
4G100S6 (1/8)	0.039 (0.982)	213.33 (948.92)	0.889 (6.128)	126.14 (561.08)	169.55 (754.18)	0.013 (0.338)	123.62 (549.89)	0.918 (23.32)	169.42 (753.63)	11.45 (15.53)
4G120S6 (1/8)	0.053 (1.338)	229.88 (1022.5)	0.958 (6.604)	164.18 (730.31)	216.58 (963.40)	0.015 (0.389)	136.17 (605.70)	1.082 (27.48)	213.37 (949.10)	16.85 (22.85)

5.2.2 Interface Shear Force versus Strain

Figure 5.5 to Figure 5.8 show the interface shear force versus reinforcing steel strain response for specimen groups 4G60S6(1/8), 4G80S6(1/8), 4G100S6(1/8), and 4G120S6(1/8). In these figures, it can be observed that the behavior for all specimens is linear until the cracking shear force, V_{cr}, is reached at the point of nominal loss of cohesion. These figures also show that the strain in the reinforcing steel U-bars begins to increase at a much higher rate after cracking occurs, which indicates that this region of the response corresponds to an instant at which transition between controlling shear force transfer mechanisms from cohesion to aggregate interlock. Beyond this point, a reduction in slope (stiffness) is observed, and the stiffness remains essentially unchanged until peak load is reached. It is important to note that at peak load none of the measurements from the strain gauges located on the U-bars indicated that the specimens had reached their respective nominal yield strain.

The post-peak behavior is where the difference between test specimen groups becomes more apparent. In this post-peak behavior stage, the force-strain response is characterized by an initial softening phase that precedes a hardening phase. The 4G60S6(1/8) specimens display a rapid shear force capacity reduction and the lowest mean value of the maximum sustained interface shear load at 127.12 kip (565.46 kN). In contrast, the 4G120S6(1/8) specimens exhibit a smooth post-peak transition into the sustained load stage with the highest mean value of the maximum sustained interface shear load of 215.12 kip (956.88 kN). It is important to note that even though at the peak load none of the specimens reached their respective nominal yield strain, results indicate that the U-bars exceeded the yield strain limit in this stage of the response.

Table 5.6 to Table 5.9 present the strain measurements at peak load, V_{ult}, for all the strain gauges contained in each test specimen. Table 5.10 lists the mean value of strain gauges measurements. It is important to note that many strain gauge readings exhibited high COV values, thus indicating the innate variability of the distribution of strain within the test specimen. Additionally, there were several strain gauges that were damaged before the peak load was reached, which limits the additional analysis that can be performed with these specimens.

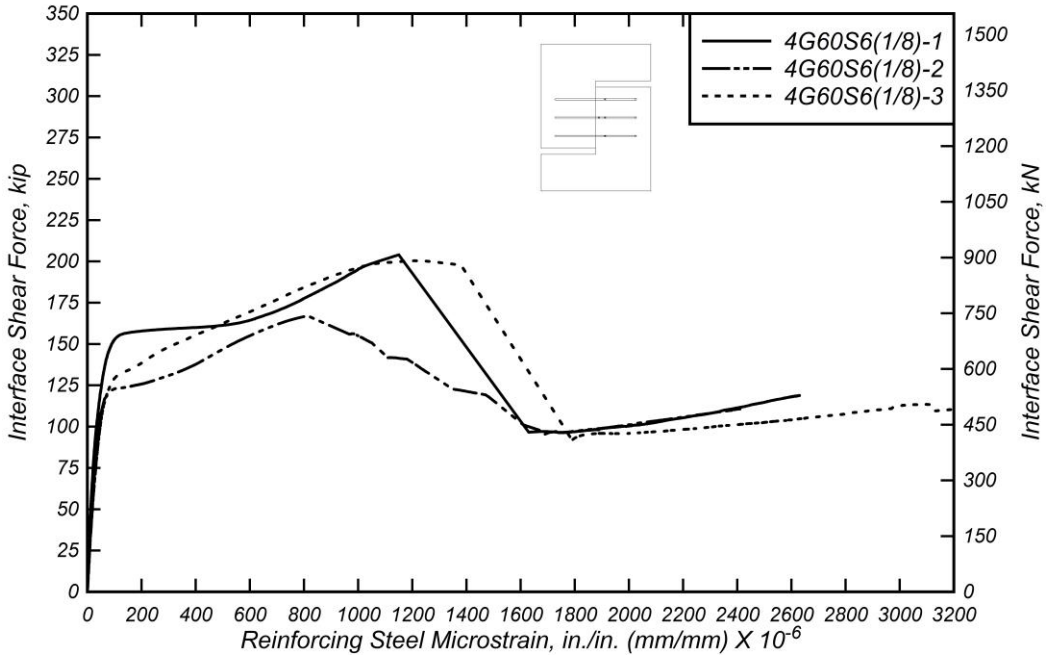

Figure 5.5: Interface shear force versus mean reinforcing steel microstrain for 4G60S6(1/8) specimens

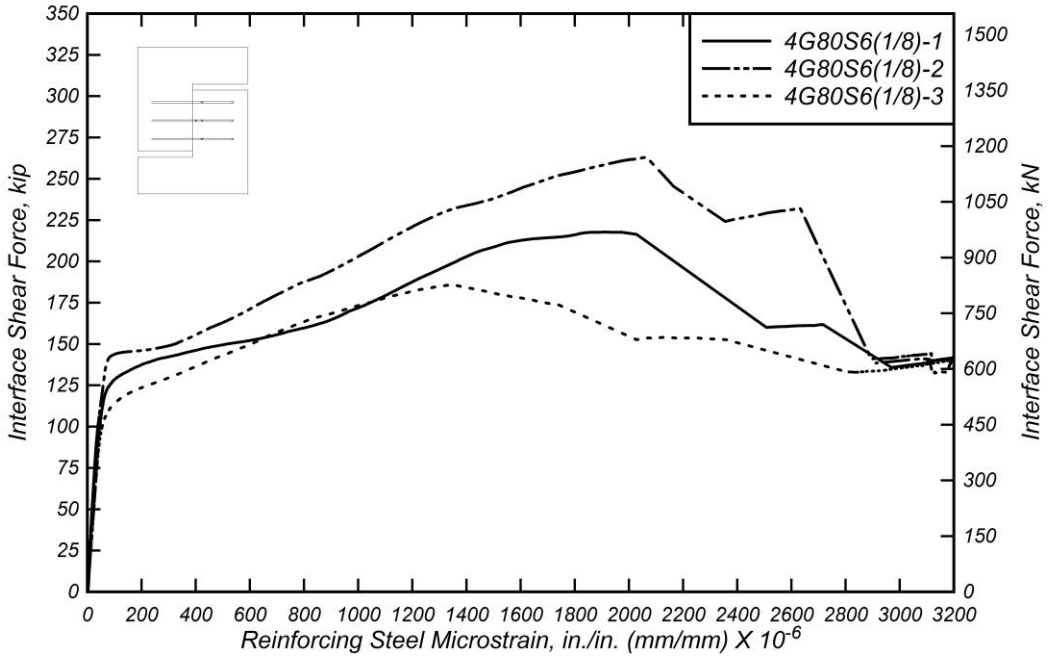

Figure 5.6: Interface shear force versus mean reinforcing steel microstrain for 4G80S6(1/8) specimens

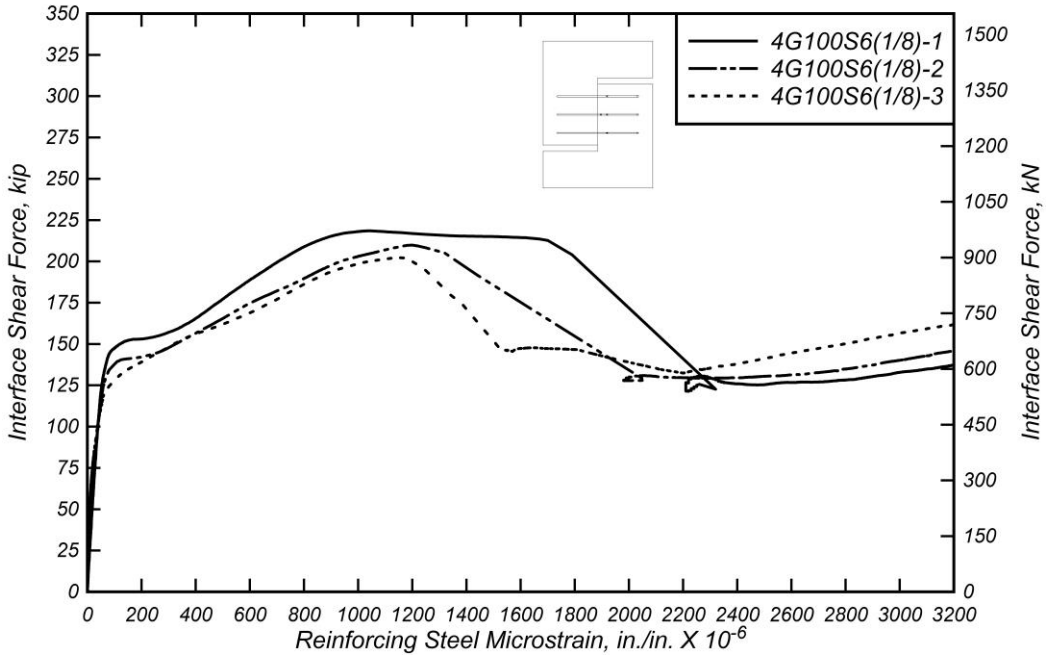

Figure 5.7: Interface shear force versus mean reinforcing steel microstrain for 4G100S6(1/8) specimens

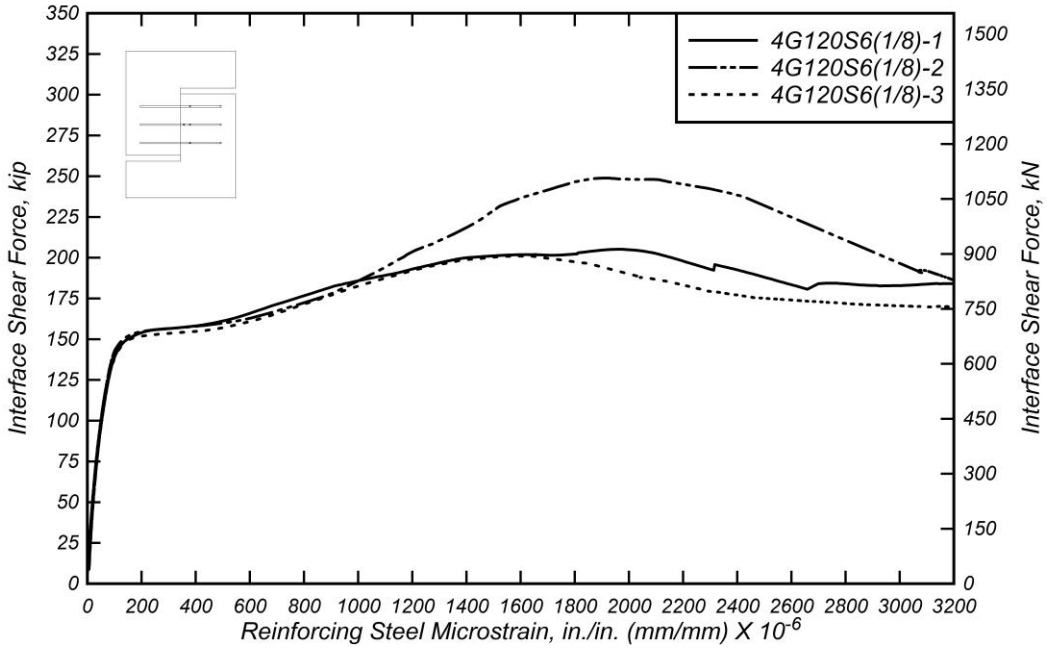

Figure 5.8: Interface shear force versus mean reinforcing steel microstrain for 4G120S6(1/8) specimens

Table 5.6: 4G60S6(1/8) Specimen Strain Gauge Readings at Peak Interface Shear Force.

Specimen	s_1, in./in. (mm/mm)	s_2, in./in. (mm/mm)	s_3, in./in. (mm/mm)	s_4, in./in. (mm/mm)	s_5, in./in. (mm/mm)	s_6, in./in. (mm/mm)	s_7, in./in. (mm/mm)
4G60S6(1/8)-1	0.0010	-	0.0014	0.0018	-	0.0013	0.0014
4G60S6(1/8)-2	0.0007	0.0009	0.0013	0.0011	-	0.0011	0.0011
4G60S6(1/8)-3	0.0010	0.0011	0.0013	0.0016	-	0.0012	N/A
Mean	0.0009	0.0010	0.0013	0.0015	-	0.0012	0.0012
Median	0.0010	0.0010	0.0013	0.0016	-	0.0012	0.0012
STDEV	0.0002	0.0001	0.0001	0.0003	-	0.0001	0.0002
COV	17%	12%	7%	22%	-	9%	16%

Table 5.7: 4G80S6(1/8) Specimen Strain Gauge Readings at Peak Interface Shear Force.

Specimen	s_1, in./in. (mm/mm)	s_2, in./in. (mm/mm)	s_3, in./in. (mm/mm)	s_4, in./in. (mm/mm)	s_5, in./in. (mm/mm)	s_6, in./in. (mm/mm)	s_7, in./in. (mm/mm)
4G80S6(1/8)-1	-	-	0.0019	-	0.0025	0.0018	-
4G80S6(1/8)-2	-	-	-	-	0.0030	0.0025	0.0017
4G80S6(1/8)-3	-	0.0022	-	0.0026	-	0.0018	0.0012
Mean	-	0.0022	0.0019	0.0026	0.0028	0.0021	0.0015
Median	-	0.0022	0.0019	0.0026	0.0028	0.0018	0.0015
STDEV	-	-	-	-	0.0004	0.0004	0.0004
COV	-	-	-	-	13%	19%	26%

Table 5.8: 4G100S6(1/8) Specimen Strain Gauge Readings at Peak Interface Shear Force.

Specimen	s_1, in./in. (mm/mm)	s_2, in./in. (mm/mm)	s_3, in./in. (mm/mm)	s_4, in./in. (mm/mm)	s_5, in./in. (mm/mm)	s_6, in./in. (mm/mm)	s_7, in./in. (mm/mm)
4G100S6(1/8)-1	0.0010	-	0.0012	0.0015	0.0010	0.0011	-
4G100S6(1/8)-2	0.0011	-	0.0017	-	0.0010	0.0012	0.0012
4G100S6(1/8)-3	0.0012	-	0.0011	0.0020	0.0010	-	0.0011
Mean	0.0011	-	0.0013	0.0018	0.0010	0.0012	0.0011
Median	0.0011	-	0.0012	0.0018	0.0010	0.0012	0.0011
STDEV	0.0001	-	0.0003	0.0003	0.0000	0.0001	0.0001
COV	8%	-	26%	19%	0%	11%	9%

Table 5.9: 4G120S6(1/8) Specimen Strain Gauge Readings at Peak Interface Shear Force.

Specimen	s_1, in./in. (mm/mm)	s_2, in./in. (mm/mm)	s_3, in./in. (mm/mm)	s_4, in./in. (mm/mm)	s_5, in./in. (mm/mm)	s_6, in./in. (mm/mm)	s_7, in./in. (mm/mm)
4G120S6(1/8)-1	0.0016	0.0033	0.0019	0.0029	0.0013	0.0031	0.0020
4G120S6(1/8)-2	0.0021	0.0022	0.0027	0.0026	0.0015	0.0019	0.0023
4G120S6(1/8)-3	0.0011	0.0017	0.0013	0.0021	0.0022	0.0015	0.0015
Mean	0.0016	0.0024	0.0020	0.0025	0.0017	0.0022	0.0020
Median	0.0016	0.0022	0.0019	0.0026	0.0015	0.0019	0.0020
STDEV	0.0005	0.0008	0.0007	0.0004	0.0004	0.0008	0.0004
COV	31%	33%	34%	16%	26%	39%	21%

Table 5.10: Summary of mean value of strain readings at peak interface shear force of specimen groups analyzing influence of reinforcing steel grade.

Specimen	s_1, in./in. (mm/mm)	s_2, in./in. (mm/mm)	s_3, in./in. (mm/mm)	s_4, in./in. (mm/mm)	s_5, in./in. (mm/mm)	s_6, in./in. (mm/mm)	s_7, in./in. (mm/mm)
4G60S6(1/8)	0.0009	0.0010	0.0013	0.0015	-	0.0012	0.0012
4G80S6(1/8)	-	0.0022	0.0019	0.0026	0.0028	0.0021	0.0015
4G100S6(1/8)	0.0011	-	0.0013	0.0018	0.0010	0.0012	0.0011
4G120S6(1/8)	0.0016	0.0024	0.0020	0.0025	0.0017	0.0022	0.0020

5.2.3 Interface Shear Force versus Crack Width

Figure 5.9 to Figure 5.12 show the interface shear force versus crack width response for all 4G60S6(1/8), 4G80S6(1/8), 4G100S6(1/8), and 4G120S6(1/8) test specimens. Each figure shows the force-crack width response for the three test specimens in each group. The overall characteristics of the response are very similar within each test specimen group. In the initial stages of the test, crack width is negligible due to the concrete-to-concrete cohesion bond controlling the response and limiting shear interface displacements. After interface cracking occurs, the crack width grows causing cohesion to degrade and aggregate interlock begins to control until the peak load is reached. At peak load, the main identifiable trend is crack width increases as reinforcing steel U-bar grade increases, except for the 4G80S6(1/8) specimens.

Table 5.11 to Table 5.14 present crack width values at points of interest for each specimen group. From these tables, crack width values at peak load, w_{ult}, and crack width values at first bar fracture, w_b, exhibit COV values ranging from 12% to 33% and 14% to 28%, respectively. On the other hand, the values of peak load, V_{ult}, and load at first bar fracture, V_b, exhibit lower variability with COV values ranging from 2% to 19% and 1% to 2%, respectively.

Table 5.15 presents a summary of the mean values of the results for all four of the specimen groups. The mean crack width at peak load, w_{ult}, is 0.0106 in. (0.2692 mm), 0.0152 in. (0.3857 mm), and 0.0207 in. (0.5262 mm), in specimen groups 4G60S6(1/8), 4G100S6(1/8), and 4G120S6(1/8), respectively, while the mean crack width at peak load in specimen group 4G80S6(1/8) is 0.0297 in. (0.7532 mm), which is significantly higher than the other specimen groups. These results indicate that while using higher strength steel does translate into higher capacity, the bond characteristics of the different reinforcing steel grades may play a role at these levels of loading. Thus, even though the use of high-strength reinforcing steel tends to increase the clamping force, its use may also induce larger crack widths. This tends to reduce the contributions of the aggregate interlock mechanism to the interface shear force.

The post-peak behavior exhibits significant differences in behavior between specimen groups. Specimens in group 4G120S6(1/8) exhibit an mean crack width at first bar fracture of 0.1112 in. (2.824 mm) at the sustained load of 216.58 kip (963.40 kN). Specimens in group 4G60S6(1/8) exhibit an mean crack width at first bar fracture of 0.1110 in. (2.820 mm), which is like the value obtained for the 4G120S6(1/8) specimens, even though the post-peak sustained load was significantly lower [127.12 kip (565.46 kN)]. Specimen groups 4G80S6(1/8) and 4G100S6(1/8) present very similar post-peak crack width responses, with the 4G80S6(1/8) having an mean crack width at first bar fracture of 0.2039 in. (5.178 mm), while the 4G100S6(1/8) specimens exhibited an mean crack width at first bar fracture of 0.1813 in. (4.605 mm). This indicates that for every case in which the reinforcing steel U-bars grades were higher than grade 60, the mean value of sustained load capacity increased without resulting a reduction in crack width.

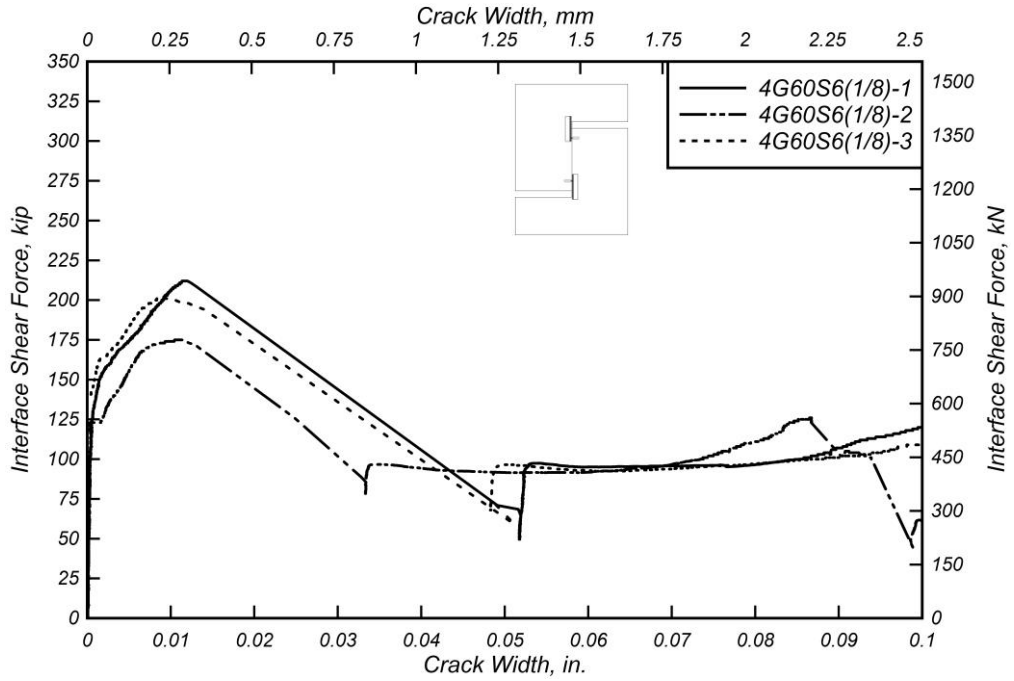

Figure 5.9: Interface shear force versus crack width for 4G60S6(1/8) specimens

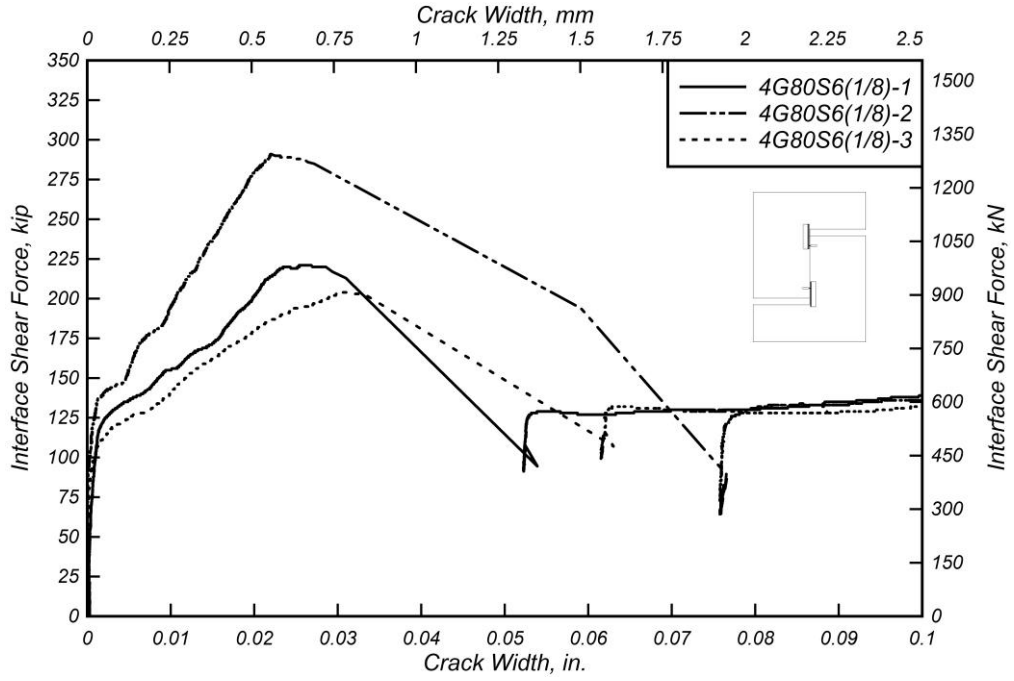

Figure 5.10: Interface shear force versus crack width for 4G80S6(1/8) specimens

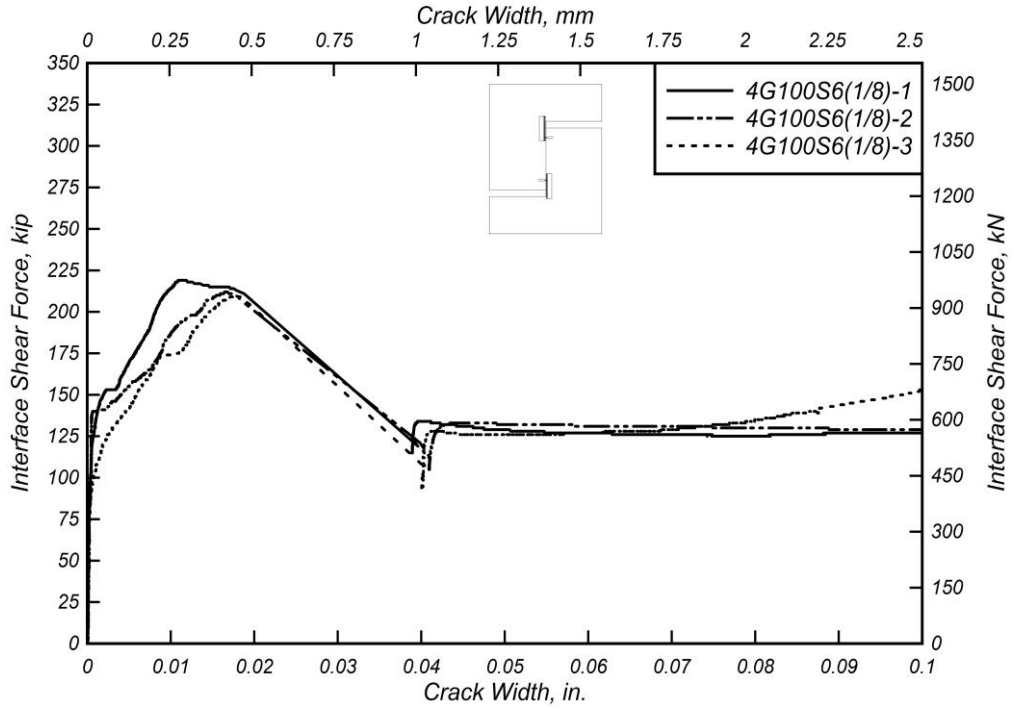

Figure 5.11: Interface shear force versus crack width for 4G100S6(1/8) specimens

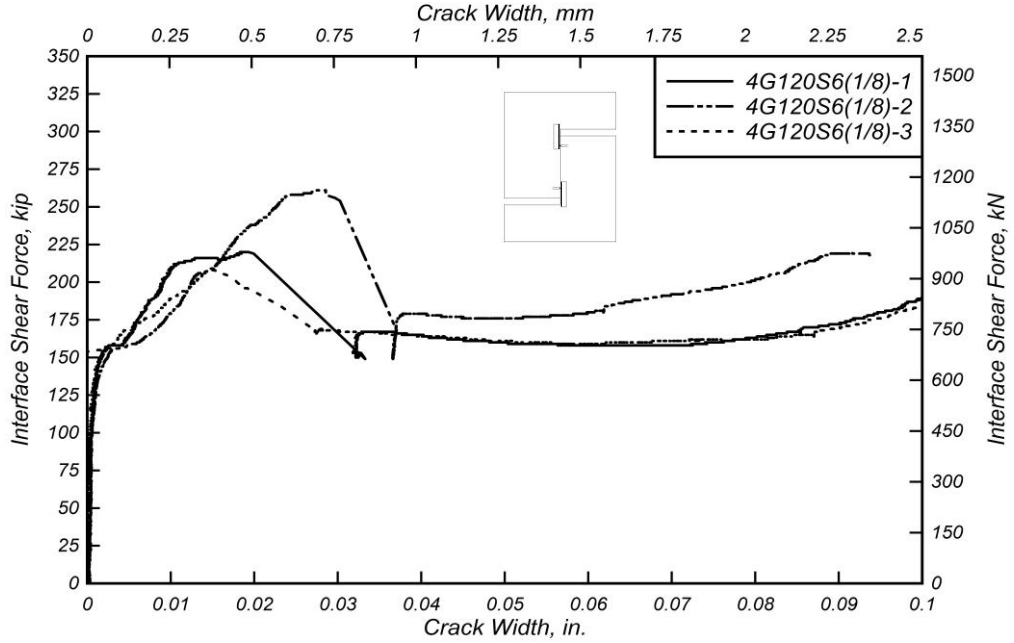

Figure 5.12: Interface shear force versus crack width for 4G120S6(1/8) specimens

Table 5.11: 4G60S6(1/8) Specimen Crack Width Measurements.

Specimen	w_{ult}, in. (mm)	V_{ult}, kip (kN)	w_b, in. (mm)	V_b, kip (kN)
4G60S6(1/8)-1	0.0117 (0.2972)	212.19 (943.87)	0.1184 (3.007)	123.45 (549.13)
4G60S6(1/8)-2	0.0112 (0.2845)	174.84 (777.73)	0.0867 (2.202)	122.83 (546.37)
4G60S6(1/8)-3	0.0089 (0.2261)	202.00 (898.54)	0.1280 (3.251)	124.66 (554.52)
Mean	0.0106 (0.2692)	196.34 (873.38)	0.1110 (2.820)	123.65 (550.01)
Median	0.0112 (0.2845)	202.00 (898.54)	0.1184 (3.007)	123.45 (549.13)
STDEV	0.0015 (0.0379)	19.31 (85.88)	0.0216 (0.5490)	0.9307 (4.140)
COV	14%	10%	19%	1%

Table 5.12: 4G80S6(1/8) Specimen Crack Width Measurements.

Specimen	w_{ult}, in. (mm)	V_{ult}, kip (kN)	w_b, in. (mm)	V_b, kip (kN)
4G80S6(1/8)-1	0.0256 (0.6510)	221.21 (983.98)	0.1732 (4.398)	145.00 (645.01)
4G80S6(1/8)-2	0.0327 (0.8314)	290.99 (1294.4)	0.2602 (6.610)	150.57 (669.77)
4G80S6(1/8)-3	0.0306 (0.7771)	203.91 (907.04)	0.1782 (4.526)	151.03 (671.81)
Mean	0.0297 (0.7532)	238.70 (1061.8)	0.2039 (5.178)	148.87 (662.20)
Median	0.0306 (0.7771)	221.21 (983.98)	0.1782 (4.526)	150.57 (669.77)
STDEV	0.0036 (0.0926)	46.10 (205.07)	0.0489 (1.242)	3.354 (14.92)
COV	12%	19%	24%	2%

Table 5.13: 4G100S6(1/8) Specimen Crack Width Measurements.

Specimen	w_{ult}, in. (mm)	V_{ult}, kip (kN)	w_b, in. (mm)	V_b, kip (kN)
4G100S6(1/8)-1	0.0111 (0.2828)	218.87 (973.60)	0.2369 (6.017)	166.65 (741.29)
4G100S6(1/8)-2	0.0166 (0.4207)	211.69 (941.64)	0.1669 (4.239)	169.47 (753.84)
4G100S6(1/8)-3	0.0179 (0.4537)	209.42 (931.53)	0.1401 (3.558)	172.15 (765.78)
Mean	0.0152 (0.3857)	213.33 (948.93)	0.1813 (4.605)	169.42 (753.63)
Median	0.0166 (0.4207)	211.69 (941.64)	0.1669 (4.239)	169.47 (753.84)
STDEV	0.0036 (0.0906)	4.936 (21.96)	0.0500 (1.269)	2.753 (12.25)
COV	23%	2%	28%	2%

Table 5.14: 4G120S6(1/8) Specimen Crack Width Measurements.

Specimen	w_{ult}, in. (mm)	V_{ult}, kip (kN)	w_b, in. (mm)	V_b, kip (kN)
4G120S6(1/8)-1	0.0186 (0.4737)	220.12 (979.16)	0.1179 (2.995)	213.49 (949.65)
4G120S6(1/8)-2	0.0284 (0.7212)	261.45 (1163.0)	0.0937 (2.379)	218.05 (969.94)
4G120S6(1/8)-3	0.0151 (0.3835)	208.06 (925.50)	0.1220 (3.099)	208.56 (927.72)
Mean	0.0207 (0.5262)	229.88 (1022.5)	0.1112 (2.824)	213.37 (949.10)
Median	0.0186 (0.4737)	220.12 (979.16)	0.1179 (2.995)	213.49 (949.65)
STDEV	0.0069 (0.1750)	28.00 (124.54)	0.0153 (0.3889)	4.746 (21.11)
COV	33%	12%	14%	2%

Table 5.15: Summary of Crack Width Readings for Specimens Analyzing Influence of Reinforcing Steel Grade.

Specimen	w_{ult}, in. (mm)	V_{ult}, kip (kN)	w_b, in. (mm)	V_b, kip (kN)
4G60S6(1/8)	0.0106 (0.2692)	196.34 (873.38)	0.1110 (2.820)	123.65 (550.01)
4G80S6(1/8)	0.0297 (0.7532)	238.70 (1061.8)	0.2039 (5.178)	148.87 (662.20)
4G100S6(1/8)	0.0152 (0.3857)	213.33 (948.93)	0.1813 (4.605)	169.42 (753.63)
4G120S6(1/8)	0.0207 (0.5262)	229.88 (1022.5)	0.1112 (2.824)	213.37 (949.10)

5.3 INFLUENCE OF REIFORCING BAR SPACING

This section presents the experimental results and discussion for test specimens constructed with reinforcing steel U-bars spaced at 4 in. (101.6 mm), 6 in. (152.4 mm), and 12 in. (304.8 mm), labeled 4G80S4(1/8), 4G80S6(1/8), and 4G80S12(1/8), respectively. Specimen groups 4G80S4(1/8), 4G80S6(1/8), and 4G80S12(1/8) contain four, three, and two bars across the shear interface, respectively. All specimens discussed in this section have an interface preparation of 1/8 in. (3.175 mm) interface roughness, contain #4 (#13M) Grade 80 ksi (550 MPa) reinforcing steel U-bars, and a nominal concrete strength of 5000 psi (35 MPa). Details of the specimens such as bar size, bar spacing, and interface preparation can be found in section (c) of Table 3.1, while drawings showing dimensions, as well as location of the reinforcing steel U-bars are shown in Chapter 3.

5.3.1 Interface Shear Force versus Interface Shear Displacement

Figure 5.13 and Figure 5.14 show the interface shear force versus interface shear displacement curves for the three specimens within each test specimen group containing reinforcing steel U-bars spaced at 4 in. (101.6 mm), and 12 in. (304.8 mm), labeled as 4G80S4(1/8), and 4G80S12(1/8), respectively. The interface shear force versus interface shear displacement response for the specimen group with reinforcing steel U-bars of 6 in. (152.4 mm), labeled as 4G80S6(1/8) is shown in Figure 5.2.

In Figure 5.13 and Figure 5.14, it can be observed that in general, the peak load increased as the spacing between reinforcing steel crossing the interface decreased, which is somewhat tied to the increased number of bars crossing the interface for the specimens with rebar spaced at 4 in versus the 12 in spacing. In Figure 5.13 specimen 4G80S4(1/8)-3 shows a significantly lower interface shear load at cracking and peak load compared to the other specimens in the group. These results indicate that the behavior displayed by this test specimen may be due to a weak concrete-to-concrete bond created at the shear interface. Figure 5.14 shows that specimen 4G80S12(1/8)-1 exhibits a significantly lower peak load, but it reaches a similar interface shear load at cracking compared to the other specimens in the group. These results indicate that the behavior observed in specimen 4G80S12(1/8)-1 may be caused by the variability originating from the shear interface preparation of 1/8 in. (3.175 mm) interface roughness. Table 5.16 and Table 5.17 show values of the main points of study discussed in Figure 5.13 and Figure 5.14. Results in these tables and figures indicate that the behavior of all tested specimens is similar beginning with a linear force-displacement response until initial cracking occurs at V_{cr}. The COV for V_{cr} range from 9% to 23%, meanwhile the COV for Δ_{cr} range from 5% to 19%. After cracking, the slope is slightly reduced as the load continues to increase until peak load, V_{ult}, is reached. The respective COV ranges from 16% to 28%, meanwhile the COV for Δ_{ult} ranges from 8% to 23%. Following the peak load, the force-displacement response exhibits a rapid loss of interface shear load accompanied by a rapid increase in interface shear displacement. The post-peak response is characterized by a steady increase in interface shear load and interface shear displacement until first bar fracture.

Table 5.18 shows a summary of the mean values for the three specimens in each group. Analysis of the values in the table indicates that there is a correlation between peak interface shear capacity and spacing of reinforcing steel U-bars. Specimens with less spacing between reinforcing steel U-bars exhibited higher mean peak interface shear loads. The mean peak interface shear loads for 4G80S4(1/8), 4G80S6(1/8), and 4G80S12(1/8) specimens are 238.56 kip (1061.2 kN), 238.70 kip (1061.8 kN), and 160.46 kip (713.78 kN), respectively. This indicates that there is a 49% increase in capacity when the spacing is reduced from 12 in. (304.8 mm) to 4 in. (101.6 mm). These results indicate that reinforcing steel U-bars have a significant impact on interface shear force capacity, even though the capacity remained essentially the same when reducing the spacing from 6 in. (152.4 mm) to 4 in. (101.6 mm). On the other hand, the results do not show a clear influence on the interface shear force at cracking, V_{cr}, which is expected because cohesion controls the initial response prior to cracking. After cracking, the reinforcing steel U-bars begin to engage and strain readings from the strain gauges grow generating the clamping force necessary for aggregate interlock to engage.

From Table 5.18 it can be inferred that the post-peak sustained load increases as spacing between reinforcing steel U-bars is reduced. The maximum mean post-peak sustained loads at first bar fracture, V_b, are 196.79 kip (875.38 kN), 148.87 kip (662.19 kN), and 99.40 kip (442.17 kN) for specimens 4G80S4(1/8), 4G80S6(1/8), and 4G80S12(1/8), respectively. These values are expected, as dowel action is the controlling mechanism in post-peak behavior, and it is directly related to area of reinforcing steel present across the interface. The displacements at first bar fracture, Δ_b, do not show any evidence of being influenced by the spacing between reinforcing steel bars as they are 0.998 in. (25.36 mm), 1.018 in. (25.85 mm), and 0.917 in. (23.28 mm) for the 4G80S4(1/8), 4G80S6(1/8), and 4G80S12(1/8) specimens, respectively.

The energy dissipated by the specimens until first bar fracture, E_b, is calculated as the area under the force-displacement curve. This parameter increases as the spacing between reinforcing steel bars is reduced. The 4G80S4(1/8) specimens had the highest mean E_b at 14.39 kip-ft (19.51 kJ), followed by the 4G80S6(1/8) specimens at 12.61 kip-ft (17.10 kJ). The 4G80S12(1/8) specimens had the lowest mean E_b at 7.245 kip-ft (9.823 kJ). This could be expected as the specimens exhibit higher peak loads and higher sustained loads as reinforcing steel U-bar spacing is reduced.

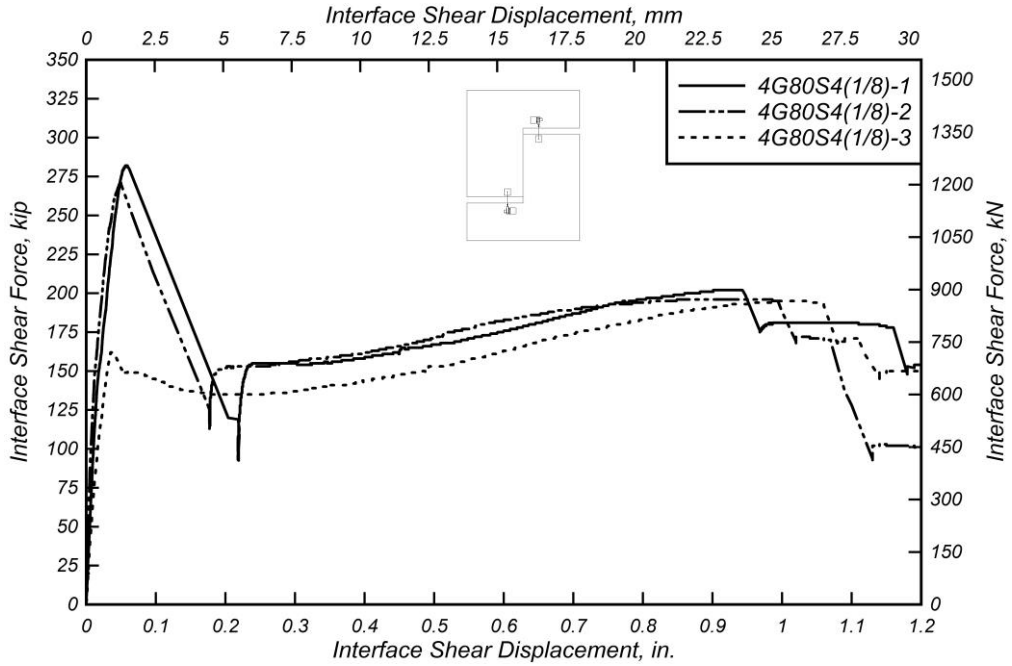

Figure 5.13: Interface shear force versus interface shear displacement for 4G80S4(1/8) specimens

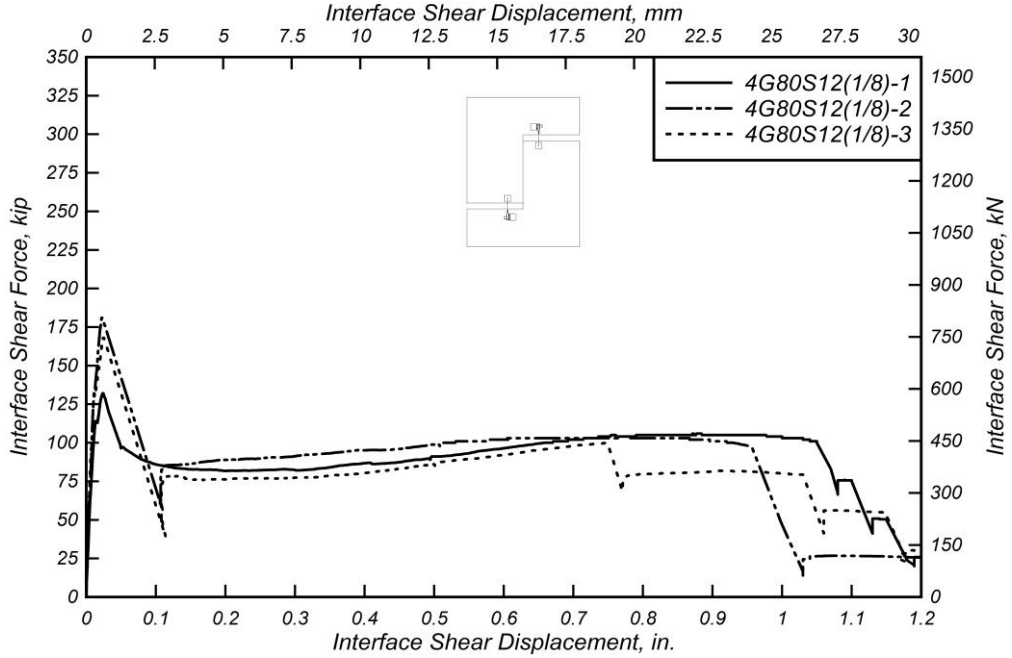

Figure 5.14: Interface shear force versus interface shear displacement for 4G80S12(1/8) specimens

Table 5.16: 4G80S4(1/8) Specimen Shear Test Results.

Specimen	Δ_{ult}, in. (mm)	V_{ult}, kip (kN)	σ_{ult}, ksi (MPa)	$V_{sus,min}$, kip (kN)	$V_{sus,max}$, kip (kN)	Δ_{cr}, in. (mm)	V_{cr}, kip (kN)	Δ_b, in. (mm)	V_b, kip (kN)	E_b, kip-ft (kJ)
4G80S4 (1/8)-1	0.058 (1.473)	282.25 (1255.5)	1.176 (8.109)	154.23 (686.05)	202.29 (899.83)	0.015 (0.389)	138.40 (615.63)	0.943 (23.95)	202.22 (899.52)	14.09 (19.11)
4G80S4 (1/8)-2	0.049 (1.245)	271.13 (1206.1)	1.130 (7.789)	152.46 (678.18)	196.16 (872.56)	0.011 (0.267)	135.80 (604.07)	0.994 (25.25)	194.67 (865.93)	14.94 (20.26)
4G80S4 (1/8)-3	0.036 (0.914)	162.30 (721.95)	0.676 (4.663)	134.63 (598.86)	194.84 (866.69)	0.014 (0.358)	88.34 (392.96)	1.058 (26.87)	193.49 (860.69)	14.13 (19.15)
Mean	0.048 (1.211)	238.56 (1061.2)	0.994 (6.853)	147.11 (654.36)	197.76 (879.69)	0.013 (0.338)	120.85 (537.55)	0.998 (25.36)	196.79 (875.38)	14.39 (19.51)
Median	0.049 (1.245)	271.13 (1206.1)	1.130 (7.789)	152.46 (678.18)	196.16 (872.56)	0.014 (0.358)	135.80 (604.07)	0.994 (25.25)	194.67 (865.93)	14.13 (19.15)
STDEV	0.0111 (0.281)	66.28 (294.81)	0.2762 (1.904)	10.84 (48.22)	3.975 (17.68)	0.0025 (0.063)	28.18 (125.36)	0.0576 (1.464)	4.737 (21.07)	0.479 (0.650)
COV	23%	28%	28%	7%	2%	19%	23%	6%	2%	3%

Table 5.17: 4G80S12(1/8) Specimen Shear Test Results.

Specimen	Δ_{ult}, in. (mm)	V_{ult}, kip (kN)	σ_{ult}, ksi (MPa)	$V_{sus,min}$, kip (kN)	$V_{sus,max}$, kip (kN)	Δ_{cr}, in. (mm)	V_{cr}, kip (kN)	Δ_b, in. (mm)	V_b, kip (kN)	E_b, kip-ft (kJ)
4G80S12 (1/8)-1	0.024 (0.610)	132.13 (587.74)	0.551 (3.796)	81.75 (363.64)	105.65 (469.95)	0.013 (0.338)	114.40 (508.88)	1.045 (26.54)	101.23 (450.29)	8.268 (11.21)
4G80S12 (1/8)-2	0.022 (0.559)	181.29 (806.42)	0.755 (5.208)	84.94 (377.83)	103.55 (460.61)	0.010 (0.252)	122.50 (544.91)	0.956 (24.28)	96.99 (431.43)	7.958 (10.79)
4G80S12 (1/8)-3	0.026 (0.660)	167.97 (747.17)	0.700 (4.825)	75.94 (337.80)	99.90 (444.38)	0.012 (0.292)	135.90 (604.51)	0.749 (19.02)	99.99 (444.78)	5.509 (7.469)
Mean	0.024 (0.610)	160.46 (713.78)	0.669 (4.610)	80.88 (359.76)	103.03 (458.31)	0.012 (0.294)	124.27 (552.77)	0.917 (23.28)	99.40 (442.17)	7.245 (9.823)
Median	0.024 (0.610)	167.97 (747.17)	0.700 (4.825)	81.75 (363.64)	103.55 (460.61)	0.012 (0.292)	122.50 (544.91)	0.956 (24.28)	99.99 (444.78)	7.958 (10.79)
STDEV	0.0020 (0.051)	25.43 (113.10)	0.1059 (0.730)	4.563 (20.30)	2.910 (12.94)	0.0017 (0.043)	10.86 (48.30)	0.1519 (3.857)	2.180 (9.697)	1.511 (2.049)
COV	8%	16%	16%	6%	3%	15%	9%	17%	2%	21%

Table 5.18: Summary of Mean Values for Specimen Groups (Influence of Reinforcing Steel bar Spacing).

Specimen	Δ_{ult}, in. (mm)	V_{ult}, kip (kN)	σ_{ult}, ksi (MPa)	$V_{sus,min}$, kip (kN)	$V_{sus,max}$, kip (kN)	Δ_{cr}, in. (mm)	V_{cr}, kip (kN)	Δ_b, in. (mm)	V_b, kip (kN)	E_b, kip-ft (kJ)
4G80S4 (1/8)	0.048 (1.211)	238.56 (1061.2)	0.994 (6.853)	147.11 (654.36)	197.76 (879.69)	0.013 (0.338)	120.85 (537.55)	0.998 (25.36)	196.79 (875.38)	14.39 (19.51)
4G80S6 (1/8)	0.073 (1.863)	238.70 (1061.8)	0.995 (6.858)	129.01 (573.86)	153.62 (683.35)	0.016 (0.395)	109.44 (486.80)	1.018 (25.85)	148.87 (662.19)	12.61 (17.10)
4G80S12 (1/8)	0.024 (0.610)	160.46 (713.78)	0.669 (4.610)	80.88 (359.76)	103.03 (458.31)	0.012 (0.294)	124.27 (552.77)	0.917 (23.28)	99.40 (442.17)	7.245 (9.823)

5.3.2 Interface Shear Force versus Strain

The interface shear force versus reinforcing steel strain relationship for 4G80S4(1/8) and 4G80S12(1/8) specimen groups are presented in Figure 5.15 and Figure 5.16. Figure 5.6 shows the interface shear force versus reinforcing steel strain relationship for specimen group 4G80S6(1/8). All tested specimens present a similar behavior in the initial stages, whereby the force-strain response is linear until the cracking shear force, V_{cr}, is reached. At this point the stiffness (slope) is reduced and the strain in the reinforcing steel U-bars begins to increase at a higher rate, which indicates that the reinforcing steel U-bars engage most once cohesion is lost.

As seen in Figure 5.15, strain in specimen 4G80S4(1/8)-3 begins to grow rapidly at a much lower load compared to the other specimens in the group. This result may suggest that the cohesion bond at the shear interface was significantly weaker, which can be attributed to the variability originating from creating the 1/8 in. (3.175 mm) interface preparation. Figure 5.16 shows that strain in specimen 4G80S12(1/8)-1 begins to grow rapidly at a shear load slightly lower than the other specimens in the group do. However, it does reach peak load at significantly lower strains. These results indicate that the behavior observed may be related to the aggregate interlock mechanism, possibly weakened by the variability originating from creating the 1/8 in. (3.175 mm) interface roughness.

The force-strain response begins to show differences in the post-cracking stage, where specimens in group 4G80S12(1/8) present a much lower post-cracking stiffness until the peak load, V_{ult}. After the peak load is reached, there is a steep drop in interface shear load followed by a sustained load as strain continues to grow. This steep drop is significantly different from the force-strain response of specimen groups 4G80S4(1/8) and 4G80S6(1/8), which exhibit a smooth softening curve leading to the sustained load phase. The abrupt loss of capacity in the 4G80S12(1/8) specimens indicates that the larger the spacing of the reinforcing steel bars across the interface the more brittle the interface shear response becomes.

Table 5.19 and Table 5.20 list the strain measurements at peak load for the strain gauges contained in each test specimen. Table 5.21 summarizes the mean values of strain gauge readings for strain gauges in the same location for all test specimens within each group. Values in the tables indicate that specimen group 4G80S6(1/8) exhibited higher strains at peak load. Note that in the tables, the strain gauges that were damaged before reaching peak load are labeled "-". Table cells containing "N/A" indicate that the corresponding strain gauges was not installed. Refer to Section 3.5 for strain gauges configurations.

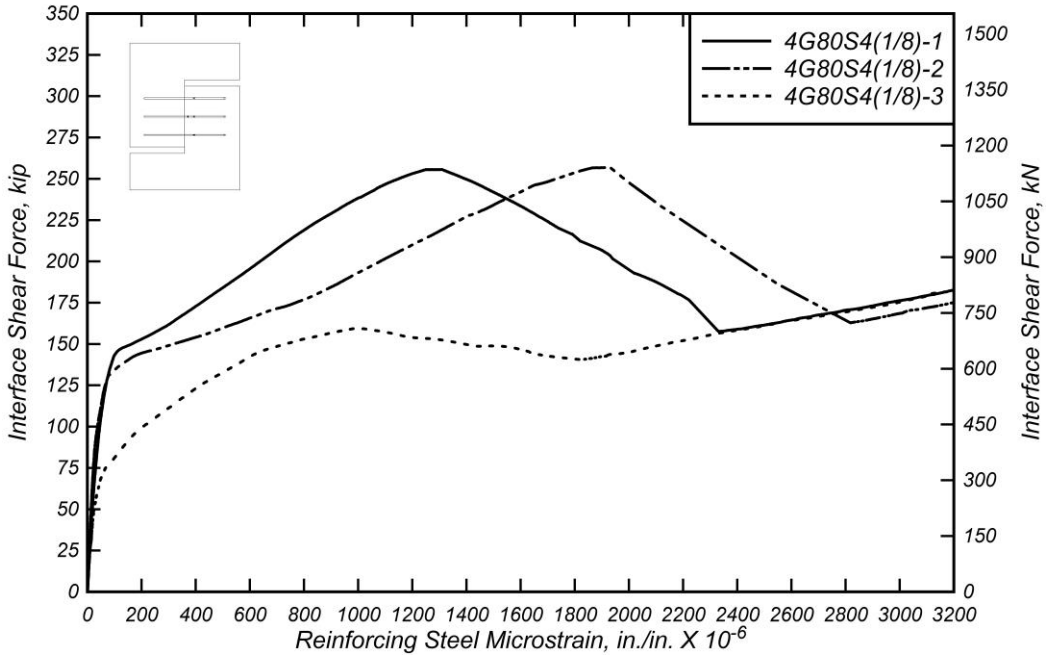

Figure 5.15: Interface shear force versus mean reinforcing steel microstrain for 4G80S4(1/8) specimens

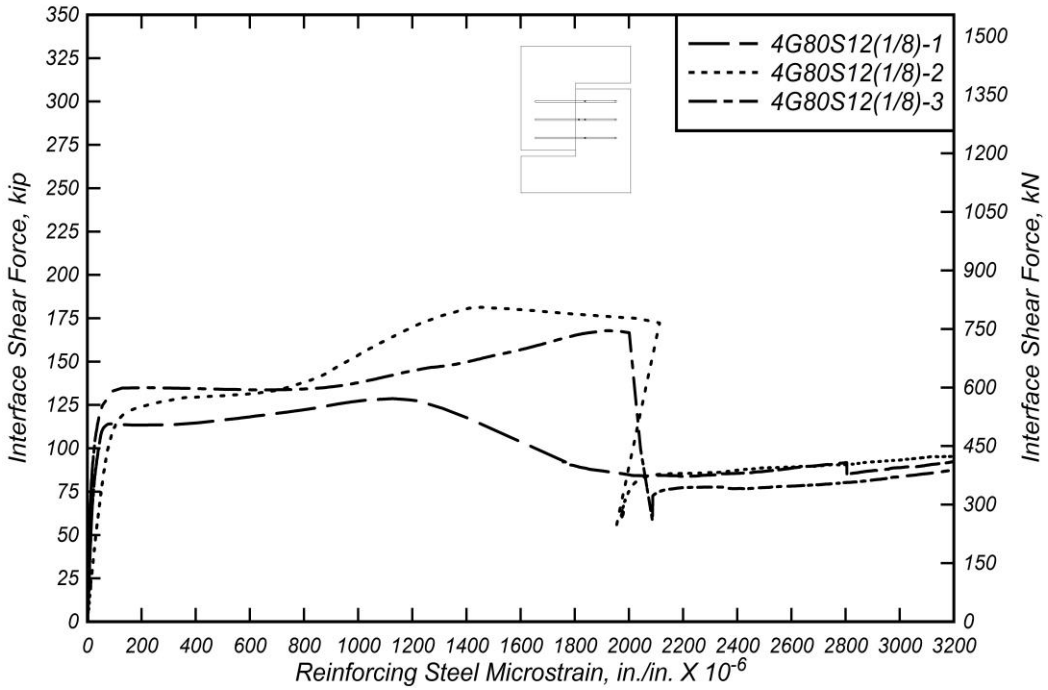

Figure 5.16: Interface shear force versus mean reinforcing steel microstrain for 4G80S12(1/8) specimens

Table 5.19: 4G80S4(1/8) Specimen Strain Gauge Readings at Peak Interface Shear Force.

Specimen	s_1, in./in. (mm/mm)	s_2, in./in. (mm/mm)	s_3, in./in. (mm/mm)	s_4, in./in. (mm/mm)	s_5, in./in. (mm/mm)	s_6, in./in. (mm/mm)	s_7, in./in. (mm/mm)	s_8, in./in. (mm/mm)	s_9, in./in. (mm/mm)
4G80S4(1/8)-1	0.0024	-	0.0018	0.0011	0.0018	-	0.0016	0.0012	-
4G80S4(1/8)-2	0.0026	-	-	-	-	-	0.0019	-	-
4G80S4(1/8)-3	0.0008	-	0.0010	-	-	-	-	-	0.0007
Mean	0.0019	-	0.0014	0.0011	0.0018	-	0.0017	0.0012	0.0007
Median	0.0024	-	0.0014	0.0011	0.0018	-	0.0017	0.0012	0.0007
STDEV	0.0010	-	0.0006	-	-	-	0.0002	-	-
COV	52%	-	39%	-	-	-	12%	-	-

Table 5.20: 4G80S12(1/8) Specimen Strain Gauge Readings at Peak Interface Shear Force.

Specimen	s_1, in./in. (mm/mm)	s_2, in./in. (mm/mm)	s_3, in./in. (mm/mm)	s_4, in./in. (mm/mm)	s_5, in./in. (mm/mm)
4G80S12(1/8)-1	0.0011	-	0.0014	0.0012	0.0008
4G80S12(1/8)-2	-	-	0.0013	-	0.0014
4G80S12(1/8)-3	0.0020	-	0.0014	0.0019	-
Mean	0.0015	-	0.0014	0.0016	0.0011
Median	0.0015	-	0.0014	0.0016	0.0011
STDEV	0.0006	-	0.00006	0.0005	0.0004
COV	38%	-	4%	30%	40%

Table 5.21: Summary of Mean Values of Strain Readings at Peak Interface Sheer Force of Specimen Groups Analyzing Influence of Reinforcing Steel bar Spacing.

Specimen	s_1, in./in. (mm/mm)	s_2, in./in. (mm/mm)	s_3, in./in. (mm/mm)	s_4, in./in. (mm/mm)	s_5, in./in. (mm/mm)	s_6, in./in. (mm/mm)	s_7, in./in. (mm/mm)	s_8, in./in. (mm/mm)	s_9, in./in. (mm/mm)
4G80S4 (1/8)	0.0019	-	0.0014	0.0011	0.0018	-	0.0017	0.0012	0.0007
4G80S6 (1/8)	-	0.0022	0.0019	0.0026	0.0028	0.0021	0.0015	N/A	N/A
4G80S12 (1/8)	0.0015	-	0.0014	0.0016	0.0011	N/A	N/A	N/A	N/A

5.3.3 Interface Shear Force versus Crack Width

The interface shear force versus crack width response for specimen groups 4G80S4(1/8), and 4G80S12(1/8) can be observed in Figure 5.17 and Figure 5.18. Figure 5.10 shows the interface shear force versus crack width response for specimen group 4G80S6(1/8). Each figure shows the force-crack width response for all specimens in each group. Tabulated values of points of interest such as crack width at peak load and crack width at first bar fracture, for each specimen group are presented in Table 5.22 and Table 5.23. A summary for comparison purposes of the three specimen groups is presented in Table 5.24.

The comparison between specimen groups in Table 5.24 shows a clear difference in post-cracked behavior. This difference reflects a greater capacity achieved by the 4G80S4(1/8) and 4G80S6(1/8) specimens, which indicates that reducing the spacing between reinforcing steel U-bars increases the capacity of specimens. This can be attributed to aggregate interlock controlling the post-cracking response, and thus the development of higher clamping forces allows the specimens to achieve a higher peak load in specimens with a larger reinforcing steel ratio. Results indicate that a significant increase in peak load capacity can be achieved by increasing the number of reinforcing steel U-bars and reducing the spacing.

The post-peak behavior is controlled by dowel action in the reinforcing steel U-bars. Figure 5.17 and Figure 5.18 show that the 4G80S4(1/8) specimens exhibit the highest post-peak mean sustained load, while the 4G80S12(1/8) specimens exhibit the lowest post-peak mean sustained load. This behavior is expected, as the 4G80S4(1/8) specimens contain a higher reinforcing steel ratio, which directly affects the force generated to dowel action. It is worth noting that the increase in post-peak mean sustained load is proportional to the inverse of the spacing and therefore linearly proportional to the reinforcing steel ratio across the interface.

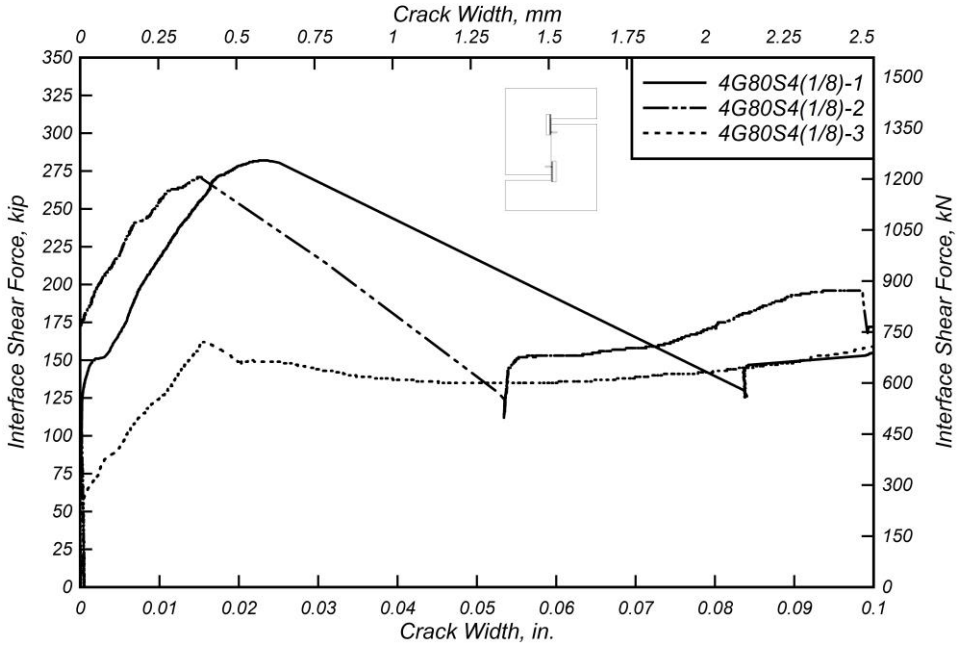

Figure 5.17: Interface shear force versus crack width for 4G80S4(1/8) specimens

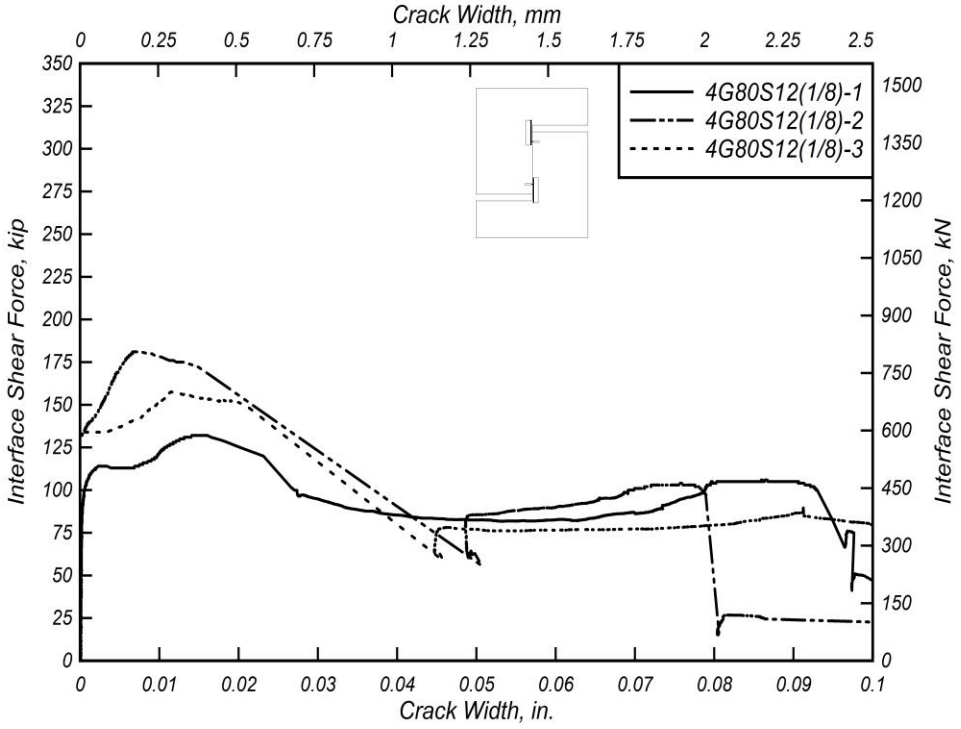

Figure 5.18: Interface shear force versus crack width for 4G80S12(1/8) specimens

Table 5.22: 4G80S4(1/8) Specimen Crack Width Measurements.

Specimen	w_{ult}, in. (mm)	V_{ult}, kip (kN)	w_b, in. (mm)	V_b, kip (kN)
4G80S4(1/8)-1	0.0234 (0.5937)	282.25 (1255.5)	0.2061 (5.236)	202.22 (899.51)
4G80S4(1/8)-2	0.0149 (0.3794)	271.13 (1206.0)	0.0986 (2.504)	194.67 (865.92)
4G80S4(1/8)-3	0.0156 (0.3962)	162.30 (721.95)	0.1358 (3.449)	193.49 (860.70)
Mean	0.0180 (0.4565)	238.56 (1061.2)	0.1468 (3.730)	196.79 (875.38)
Median	0.0156 (0.3962)	271.13 (1206.0)	0.1358 (3.449)	194.67 (865.92)
STDEV	0.0047 (0.1192)	66.28 (294.81)	0.0546 (1.387)	4.735 (21.06)
COV	26%	28%	37%	2%

Table 5.23: 4G80S12(1/8) Specimen Crack Width Measurements.

Specimen	w_{ult}, in. (mm)	V_{ult}, kip (kN)	w_b, in. (mm)	V_b, kip (kN)
4G80S12(1/8)-1	0.0154 (0.3910)	132.13 (587.74)	0.0928 (2.356)	101.23 (450.28)
4G80S12(1/8)-2	0.0070 (0.1768)	181.29 (806.42)	0.0790 (2.006)	96.99 (431.42)
4G80S12(1/8)-3	0.0160 (0.4062)	167.97 (747.19)	0.1070 (2.719)	99.99 (444.79)
Mean	0.0128 (0.3247)	160.47 (713.78)	0.0929 (2.360)	99.40 (442.16)
Median	0.0154 (0.3910)	167.97 (747.19)	0.0928 (2.356)	99.99 (444.79)
STDEV	0.0051 (0.1283)	25.43 (113.10)	0.0140 (0.356)	2.181 (9.701)
COV	40%	16%	15%	2%

Table 5.24: Summary of crack width readings for specimens analyzing influence of reinforcing steel bar spacing.

Specimen	w_{ult}, in. (mm)	V_{ult}, kip (kN)	w_b, in. (mm)	V_b, kip (kN)
4G80S4(1/8)	0.0180 (0.4565)	238.56 (1061.2)	0.1468 (3.730)	196.79 (875.38)
4G80S6(1/8)	0.0297 (0.7532)	238.70 (1061.8)	0.2039 (5.178)	148.87 (662.20)
4G80S12(1/8)	0.0128 (0.3247)	160.47 (713.78)	0.0929 (2.360)	99.40 (442.16)

5.4 INFLUENCE OF REINFORCING BAR SIZE

This section presents the experimental results and discussion for test specimens reinforced with #4 (#13M) and #5 (#16M) reinforcing steel U-bars. All specimens discussed in this section have three Grade 80 ksi (550 MPa) reinforcing steel U-bars spaced at 6 in. (152.4 mm) and a specified nominal concrete strength of 5000 psi (35 MPa). The effect of bar size is discussed separately for four types of interface roughness: As Cast, 1/8 in (3.175 mm), 1/4 in (6.35 mm), and Exposed Aggregate (EA). The general observations of the influence of bar size on the shear interface are discussed. Details of the specimens and how the surface roughness was prepared can be found in section (d) of Table 3.1 and Section 3.2.2, respectively. Detailed drawings showing dimensions of the specimens, as well as location of the reinforcing steel U-bars, are presented in Chapter 3.

5.4.1 Interface Shear Force versus Interface Shear Displacement

5.4.1.1 Interface Preparation: As Cast

Figure 5.19 and Figure 5.20 show the interface shear force versus interface shear displacement response curves for specimen groups 4G80S6(AC) and 5G80S6(AC), respectively. All specimens in these specimen groups are constructed with an As Cast interface preparation. The behavior of all specimens is similar except for specimen 4G80S6(AC)-3, which exhibits a lower peak load when compared to the other specimens in the group. The peak load, Vult, and displacement at peak load, Δult, are approximately 26% and 33% lower compared to the other specimens in the group. This reduction, however, does not repeat itself when analyzing the interface shear load and displacement when cracking occurs. Therefore, the lower peak load of the 4G80S6(AC)-3 specimen cannot be attributed to a weak concrete-to-concrete bond, but rather to a lower aggregate interlock influence, possibly caused by the variability generated during the interface preparation process. Table 5.25 and Table 5.26 present tabulated values of the main points of study for specimen groups 4G80S6(AC) and 5G80S6(AC), respectively.

Table 5.27 presents a summary of the tabulated values of the main points of interest for specimen groups 4G80S6(AC) and 5G80S6(AC). In the initial loading stages, specimen group 4G80S6(AC) exhibits a slightly larger mean interface shear load at cracking, V_{cr}, with 142.83 kip (635.35 kN) compared to the 5G80S6(AC) specimen group with 127.53 kip (567.30 kN) and a larger mean peak load capacity with 262.65 kip (1168.3 kN) compared to the 5G80S6(AC) group with 259.87 kip (1156.0 kN). Specimen group 5G80S6(AC) exhibits a larger post-peak mean sustained load at first bar fracture than the 4G80S6(AC) specimens, with values of 224.37 kip (998.05 kN) and 149.63 kip (665.60 kN) for specimen groups 5G80S6(AC) and 4G80S6(AC), respectively. This indicates a 50% increase in mean sustained load capacity when the reinforcing steel bars across the interface increases in size from #4 (#13M) to #5 (#16M). This increase is directly related to the reinforcing steel ratio across the interface, as the increase in reinforcing steel bar size across the interface results in a 55% increase in the reinforcing steel ratio. The

higher sustained load capacity is attributed to the larger reinforcing steel ratio across the interface, which is directly related to the dowel action mechanism controlling the post-peak response.

The mean dissipated energy up to bar fracture for the 5G80S6(AC) specimens, E_b, is 20.26 kip-ft (27.47 kJ) and 11.74 kip-ft (15.92 kJ) for 4G80S6(AC) specimens. This corresponds to a 68% increase in E_b when increasing the reinforcing steel bar size from #4 (#13M) to #5 (#16M). Shear displacement at first bar fracture, Δ_b, was 1.242 in. (31.55 mm) and 0.919 in. (23.35 mm) for 5G80S6(AC) and 4G80S6(AC), respectively; a 35% increase in Δ_b.

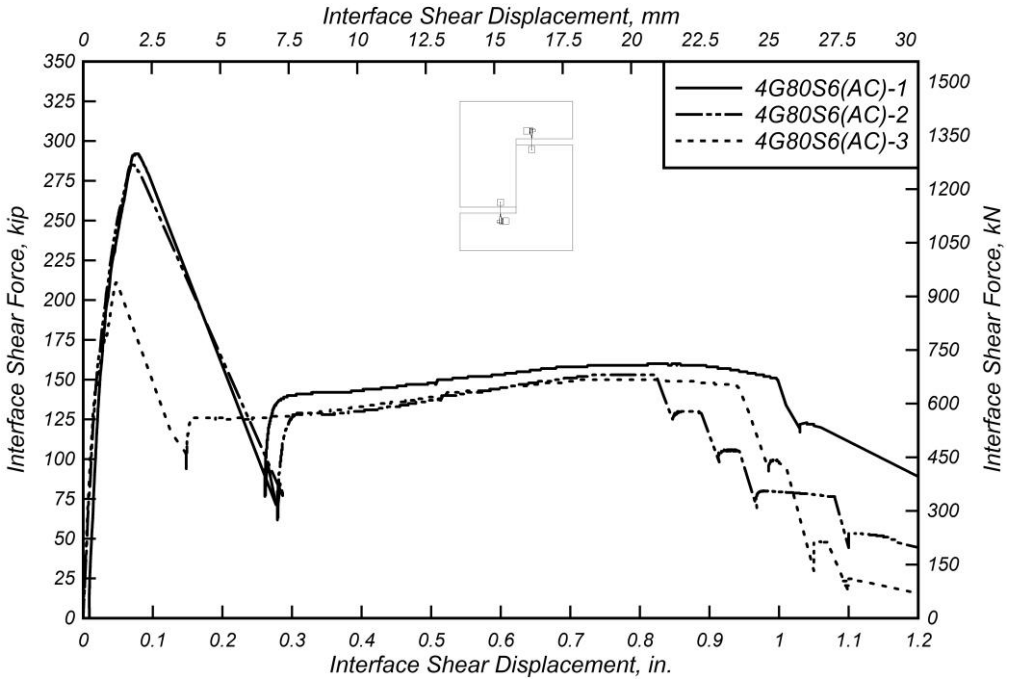

Figure 5.19: Interface shear force versus interface shear displacement for 4G80S6(AC) specimens

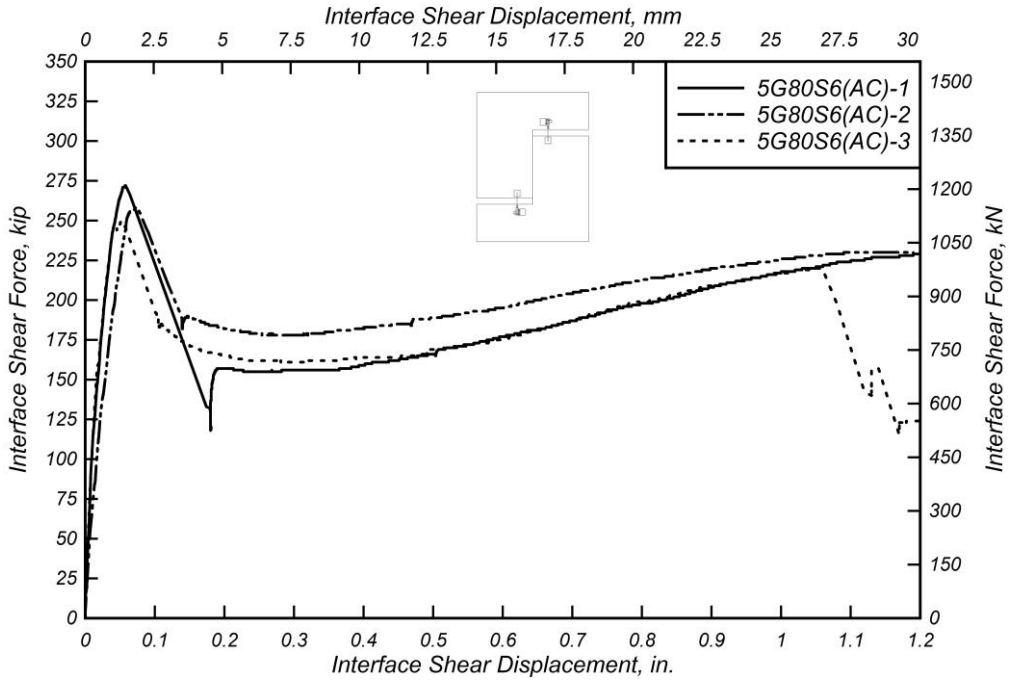

Figure 5.20: Interface shear force versus interface shear displacement for 5G80S6(AC) specimens

Table 5.25: 4G80S6(AC) Specimen Shear Test Results.

Specimen	Δ_{ult}, in. (mm)	V_{ult}, kip (kN)	σ_{ult}, ksi (MPa)	$V_{sus,min}$, kip (kN)	$V_{sus,max}$, kip (kN)	Δ_{cr}, in. (mm)	V_{cr}, kip (kN)	Δ_b, in. (mm)	V_b, kip (kN)	E_b, kip-ft (kJ)
4G80S6 (AC)-1	0.077 (1.956)	292.03 (1299.0)	1.217 (8.389)	140.31 (624.13)	159.75 (710.60)	0.021 (0.541)	132.20 (588.05)	0.995 (25.27)	150.66 (670.17)	13.43 (18.21)
4G80S6 (AC)-2	0.072 (1.829)	284.98 (1267.7)	1.187 (8.187)	128.36 (570.97)	153.38 (682.27)	0.020 (0.495)	153.40 (682.36)	0.822 (20.88)	152.78 (679.60)	10.73 (14.55)
4G80S6 (AC)-3	0.048 (1.219)	210.93 (938.26)	0.879 (6.060)	125.31 (557.41)	150.42 (669.10)	0.017 (0.427)	142.90 (635.65)	0.941 (23.90)	145.46 (647.04)	11.07 (15.01)
Mean	0.066 (1.668)	262.65 (1168.3)	1.094 (7.545)	131.33 (584.17)	154.52 (687.32)	0.019 (0.488)	142.83 (635.35)	0.919 (23.35)	149.63 (665.60)	11.74 (15.92)
Median	0.072 (1.829)	284.98 (1267.7)	1.187 (8.187)	128.36 (570.97)	153.38 (682.27)	0.020 (0.495)	142.90 (635.65)	0.941 (23.90)	150.66 (670.17)	11.07 (15.01)
STDEV	0.0155 (0.394)	44.93 (199.84)	0.1872 (1.291)	7.928 (35.26)	4.768 (21.21)	0.0023 (0.058)	10.60 (47.15)	0.0885 (2.248)	3.766 (16.75)	1.470 (1.993)
COV	24%	17%	17%	6%	3%	12%	7%	10%	3%	13%

Table 5.26: 5G80S6(AC) Specimen Shear Test Results.

Specimen	Δ_{ult}, in. (mm)	V_{ult}, kip (kN)	σ_{ult}, ksi (MPa)	$V_{sus,min}$, kip (kN)	$V_{sus,max}$, kip (kN)	Δ_{cr}, in. (mm)	V_{cr}, kip (kN)	Δ_b, in. (mm)	V_b, kip (kN)	E_b, kip-ft (kJ)
5G80S6 (AC)-1	0.058 (1.473)	271.63 (1208.3)	1.132 (7.803)	155.04 (689.65)	232.39 (1033.7)	0.0102 (0.259)	108.00 (480.41)	1.456 (36.98)	225.46 (1002.9)	23.88 (32.38)
5G80S6 (AC)-2	0.071 (1.803)	257.72 (1146.4)	1.074 (7.404)	177.97 (791.65)	230.47 (1025.2)	0.0197 (0.500)	116.50 (518.22)	1.215 (30.86)	228.09 (1014.6)	20.59 (27.92)
5G80S6 (AC)-3	0.052 (1.321)	250.26 (1113.2)	1.043 (7.190)	161.17 (716.92)	219.77 (977.59)	0.0171 (0.434)	158.10 (703.26)	1.055 (26.80)	219.56 (976.65)	16.30 (22.10)
Mean	0.0603 (1.532)	259.87 (1156.0)	1.083 (7.466)	164.73 (732.74)	227.54 (1012.2)	0.0157 (0.398)	127.53 (567.30)	1.242 (31.55)	224.37 (998.05)	20.26 (27.47)
Median	0.0580 (1.473)	257.72 (1146.4)	1.074 (7.404)	161.17 (716.92)	230.47 (1025.2)	0.0171 (0.434)	116.50 (518.22)	1.215 (30.86)	225.46 (1002.9)	20.59 (27.92)
STDEV	0.0097 (0.247)	10.85 (48.25)	0.0452 (0.312)	11.87 (52.81)	6.800 (30.25)	0.0049 (0.127)	26.81 (119.26)	0.2019 (5.127)	4.368 (19.43)	3.803 (5.157)
COV	16%	4%	4%	7%	3%	31%	21%	16%	2%	19%

Table 5.27: Summary of Mean Values of 4G80S6(AC) and 5G80S6(AC) Specimens with As Cast Interface Finish.

Specimen	Δ_{ult}, in. (mm)	V_{ult}, kip (kN)	σ_{ult}, ksi (MPa)	$V_{sus,min}$, kip (kN)	$V_{sus,max}$, kip (kN)	Δ_{cr}, in. (mm)	V_{cr}, kip (kN)	Δ_b, in. (mm)	V_b, kip (kN)	E_b, kip-ft (kJ)
4G80S6 (AC)	0.066 (1.668)	262.65 (1168.3)	1.094 (7.545)	131.33 (584.17)	154.52 (687.32)	0.019 (0.488)	142.83 (635.35)	0.919 (23.35)	149.63 (665.60)	11.74 (15.92)
5G80S6 (AC)	0.060 (1.532)	259.87 (1156.0)	1.083 (7.466)	164.73 (732.74)	227.54 (1012.2)	0.0157 (0.398)	127.53 (567.30)	1.242 (31.55)	224.37 (998.05)	20.26 (27.47)

5.4.1.2 Interface Preparation: Roughened with 1/8 in. (3.175 mm)

Figure 5.2 (presented earlier) and Figure 5.21 present the interface shear force versus interface shear displacement response curves for specimen groups 4G80S6(1/8) and 5G80S6(1/8), respectively. All specimens in both specimen groups are constructed with a surface intentionally roughened to an amplitude of 1/8 in. (3.175 mm). The behavior in all specimens is similar, although specimen 5G80S6(1/8)-2 exhibited a considerably larger mean peak-load, V_{ult}, as seen in Figure 5.21.

In general, specimen group 5G80S6(1/8) reinforced with #5 (#16M) steel bars crossing the interface exhibited a larger capacity, as can be observed from the tabulated values shown in

Table 5.29. Initially, a higher stiffness and a 13% higher peak-load, V_{ult}, can be observed in the 5G80S6(1/8) specimens. The main differences between the performance of the two specimen groups becomes more apparent in the post-cracked stage of the force-displacement response, with the larger capacity and energy dissipated by the 5G80S6(1/8) specimens when compared to the 4G80S6(1/8) specimens. This indicates that for specimens with the surface intentionally roughened to an amplitude of 1/8 in. (3.175 mm), increasing the reinforcing steel bar size from #4 (#13M) to #5 (#16M) results in an increase in capacity.

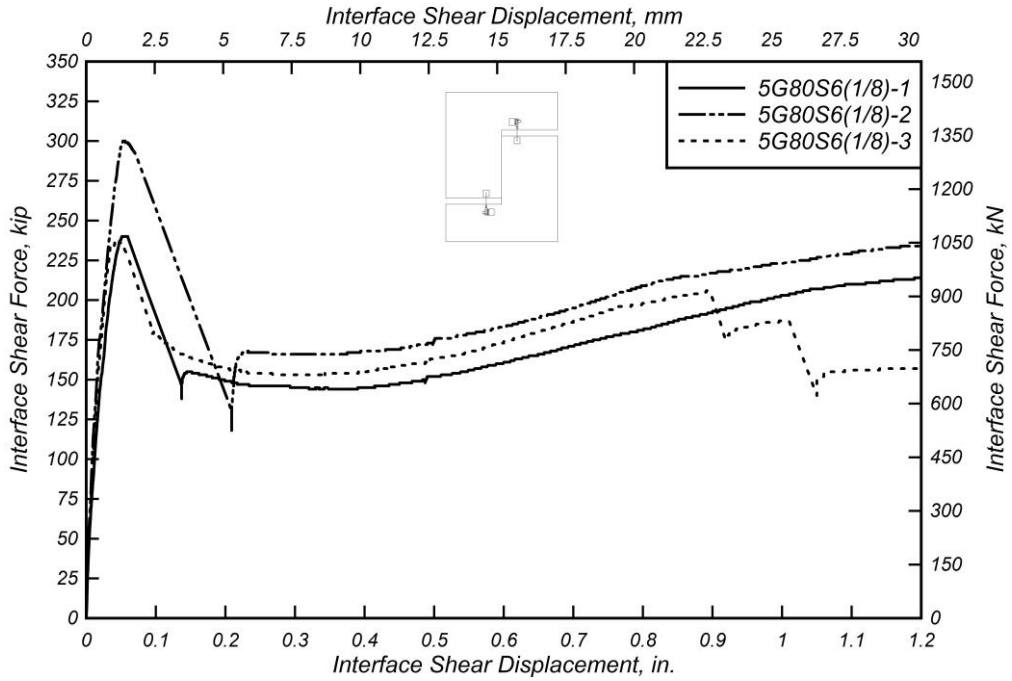

Figure 5.21: Interface shear force versus interface shear displacement for 5G80S6(1/8) specimens.

Table 5.28: 5G80S6(1/8) Specimen Shear Test Results.

Specimen	Δ_{ult}, in. (mm)	V_{ult}, kip (kN)	σ_{ult}, ksi (MPa)	$V_{sus,min}$, kip (kN)	$V_{sus,max}$, kip (kN)	Δ_{cr}, in. (mm)	V_{cr}, kip (kN)	Δ_b, in. (mm)	V_b, kip (kN)	E_b, kip-ft (kJ)
5G80S6 (1/8)-1	0.053 (1.346)	240.38 (1069.3)	1.002 (6.906)	144.04 (640.72)	221.13 (983.63)	0.021 (0.544)	151.70 (674.79)	1.385 (35.18)	220.63 (981.41)	20.82 (28.23)
5G80S6 (1/8)-2	0.054 (1.372)	300.13 (1335.0)	1.251 (8.622)	165.55 (736.40)	234.51 (1043.2)	0.018 (0.457)	171.60 (763.31)	1.315 (33.40)	225.72 (1004.1)	22.29 (30.22)
5G80S6 (1/8)-3	0.044 (1.118)	238.06 (1058.9)	0.992 (6.839)	152.81 (679.73)	205.95 (916.11)	0.017 (0.432)	155.30 (690.81)	0.895 (22.73)	205.82 (915.53)	12.96 (17.57)
Mean	0.050 (1.278)	259.52 (1154.4)	1.081 (7.456)	154.13 (685.62)	220.53 (980.97)	0.019 (0.478)	159.53 (709.64)	1.198 (30.44)	217.39 (967.00)	18.69 (25.34)
Median	0.053 (1.346)	240.38 (1069.3)	1.002 (6.906)	152.81 (679.73)	221.13 (983.63)	0.018 (0.457)	155.30 (690.81)	1.315 (33.40)	220.63 (981.41)	20.82 (28.23)
STDEV	0.0055 (0.140)	35.19 (156.51)	0.1466 (1.011)	10.82 (48.11)	14.29 (63.56)	0.0023 (0.059)	10.60 (47.17)	0.2650 (6.731)	10.34 (45.99)	5.019 (6.805)
COV	11%	14%	14%	7%	6%	12%	7%	22%	5%	27%

Table 5.29: Summary of Mean Values of 4G80S6(1/8) and 5G80S6(1/8) Specimens with 1/8 in. (3.175 mm) Interface Finish.

Specimen	Δ_{ult}, in. (mm)	V_{ult}, kip (kN)	σ_{ult}, ksi (MPa)	$V_{sus,min}$, kip (kN)	$V_{sus,max}$, kip (kN)	Δ_{cr}, in. (mm)	V_{cr}, kip (kN)	Δ_b, in. (mm)	V_b, kip (kN)	E_b, kip-ft (kJ)
4G80S6 (1/8)	0.073 (1.863)	238.70 (1061.8)	0.995 (6.858)	129.01 (573.86)	153.62 (683.35)	0.016 (0.395)	109.44 (486.80)	1.018 (25.85)	148.87 (662.19)	12.61 (17.10)
5G80S6 (1/8)	0.050 (1.278)	259.52 (1154.4)	1.081 (7.456)	154.13 (685.62)	220.53 (980.97)	0.019 (0.478)	159.53 (709.64)	1.198 (30.44)	217.39 (967.00)	18.69 (25.34)

5.4.1.3 Interface Preparation: Roughened with 1/4 in. (6.35 mm)

Figure 5.22 and Figure 5.23 present the interface shear force versus interface shear displacement response curves for specimen groups 4G80S6(1/4) and 5G80S6(1/4), respectively. All specimens in both specimen groups are constructed with a surface roughened to an amplitude of 1/4 in. (6.35 mm). Significant variability can be observed in the pre-peak force-displacement response of specimen group 4G80S6(1/4), as shown in Figure 5.22, where the displacements at peak-load, Δ_{ult}, range from 0.030 in. (0.762 mm) to 0.063 in. (1.60 mm) with a COV of 38% as shown in Table 5.30. Specimens from the group 5G80S6(1/4) exhibit a slightly lower variability with Δ_{ult} ranging from 0.054 in. (1.372 mm) to 0.083 in. (2.108 mm) and a COV of 22%, as shown in Table 5.31.

In general, specimen group 5G80S6(1/4) reinforced with #5 (#16M) steel bars exhibited a larger capacity (see Table 5.35). In this case, Δ_{ult} and V_{ult} are 43% and 29% higher, respectively, for specimen group 5G80S6(1/4) compared to the 4G80S6(1/4) specimen group. Additionally, the energy dissipated before first bar fracture, E_b, is 79% higher in specimen group 5G80S6(1/4). The mean sustained load at first bar fracture in specimen group 4G80S6(1/4) is 153.56 kip (683.07 kN) and 227.31 kip (1011.1 kN) for specimen group 5G80S6(1/4), indicating a 48% increase in mean sustained load capacity. This large increase in capacity is directly related to the 55% increase in reinforcing steel ratio across the interface when the reinforcing steel bar size is increased from #4 (#13M) to #5 (#16M).

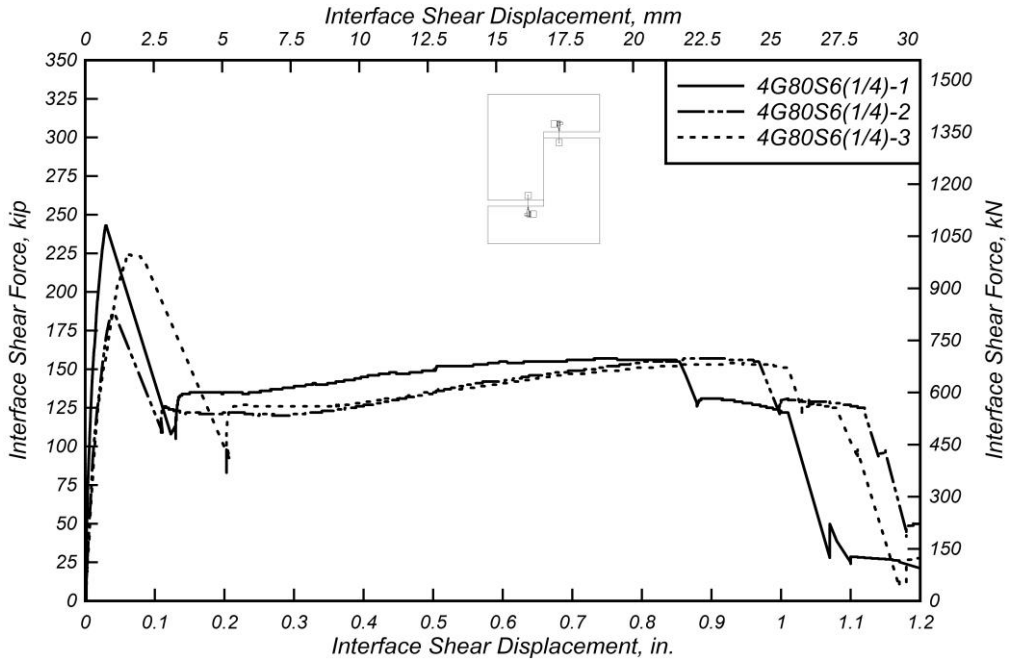

Figure 5.22: Interface shear force versus interface shear displacement for 4G80S6(1/4) specimens

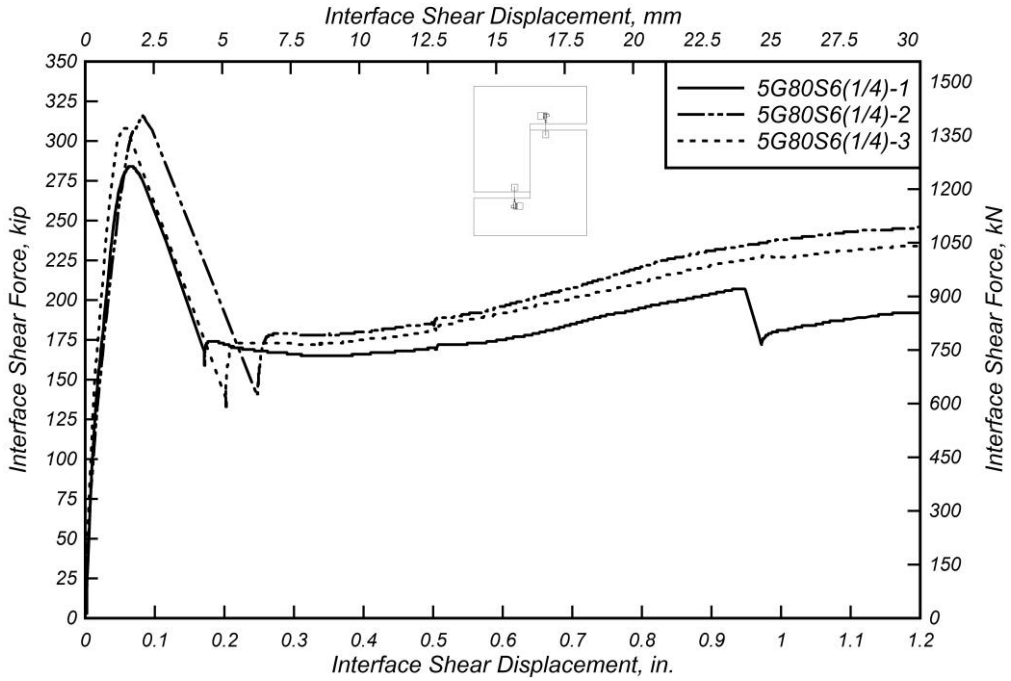

Figure 5.23: Interface shear force versus interface shear displacement for 5G80S6(1/4) specimens

Table 5.30: 4G80S6(1/4) Specimen Shear Test Results.

Specimen	$\Delta_{ult,}$ in. (mm)	V_{ult}, kip (kN)	σ_{ult}, ksi (MPa)	$V_{sus,min}$, kip (kN)	$V_{sus,max}$, kip (kN)	$\Delta_{cr,}$ in. (mm)	V_{cr}, kip (kN)	Δ_{b}, in. (mm)	V_{b}, kip (kN)	E_{b}, kip-ft (kJ)
4G80S6 (1/4)-1	0.030 (0.762)	243.07 (1081.2)	1.013 (6.983)	134.34 (597.57)	156.75 (697.26)	0.0068 (0.1727)	105.70 (470.18)	0.854 (21.69)	154.52 (687.34)	10.73 (14.55)
4G80S6 (1/4)-2	0.041 (1.041)	186.03 (827.50)	0.775 (5.344)	119.82 (532.99)	157.04 (698.55)	0.0139 (0.3531)	109.60 (487.52)	0.968 (24.59)	154.86 (688.85)	11.13 (15.09)
4G80S6 (1/4)-3	0.063 (1.600)	224.61 (999.11)	0.936 (6.453)	125.59 (558.65)	153.71 (683.74)	0.0170 (0.4318)	118.80 (528.45)	1.006 (25.55)	151.30 (673.02)	12.19 (16.52)
Mean	0.045 (1.135)	217.90 (969.28)	0.908 (6.260)	126.58 (563.07)	155.83 (693.18)	0.013 (0.319)	111.37 (495.38)	0.943 (23.94)	153.56 (683.07)	11.35 (15.39)
Median	0.041 (1.041)	224.61 (999.11)	0.936 (6.453)	125.59 (558.65)	156.75 (697.26)	0.014 (0.353)	109.60 (487.52)	0.968 (24.59)	154.52 (687.34)	11.13 (15.09)
STDEV	0.0168 (0.427)	29.11 (129.47)	0.1213 (0.836)	7.311 (32.52)	1.845 (8.205)	0.0052 (0.133)	6.726 (29.92)	0.0791 (2.009)	1.965 (8.739)	0.751 (1.018)
COV	38%	13%	13%	6%	1%	42%	6%	8%	1%	7%

Table 5.31: 5G80S6(1/4) Specimen Shear Test Results.

Specimen	Δ_{ult}, in. (mm)	V_{ult}, kip (kN)	σ_{ult}, ksi (MPa)	$V_{sus,min}$, kip (kN)	$V_{sus,max}$, kip (kN)	Δ_{cr}, in. (mm)	V_{cr}, kip (kN)	Δ_b, in. (mm)	V_b, kip (kN)	E_b, kip-ft (kJ)
5G80S6 (1/4)-1	0.064 (1.626)	283.85 (1262.6)	1.183 (8.154)	164.97 (733.82)	207.40 (922.56)	0.018 (0.4674)	152.60 (678.80)	0.948 (24.08)	206.76 (919.71)	14.71 (19.94)
5G80S6 (1/4)-2	0.083 (2.108)	315.53 (1403.5)	1.315 (9.065)	177.92 (791.43)	246.02 (1094.4)	0.014 (0.3480)	112.80 (501.76)	1.289 (32.74)	245.51 (1092.1)	23.18 (31.43)
5G80S6 (1/4)-3	0.054 (1.372)	308.23 (1371.1)	1.284 (8.855)	171.56 (763.14)	235.51 (1047.6)	0.012 (0.3073)	138.90 (617.86)	1.359 (34.52)	229.67 (1021.6)	23.57 (31.95)
Mean	0.067 (1.702)	302.54 (1345.7)	1.261 (8.691)	171.48 (762.80)	229.64 (1021.5)	0.015 (0.3742)	134.77 (599.47)	1.199 (30.45)	227.31 (1011.1)	20.48 (27.77)
Median	0.064 (1.626)	308.23 (1371.1)	1.284 (8.855)	171.56 (763.14)	235.51 (1047.6)	0.014 (0.3480)	138.90 (617.86)	1.289 (32.74)	229.67 (1021.6)	23.18 (31.43)
STDEV	0.0147 (0.374)	16.59 (73.79)	0.0691 (0.477)	6.475 (28.80)	19.97 (88.82)	0.0033 (0.0832)	20.22 (89.94)	0.2199 (5.585)	19.48 (86.66)	5.008 (6.790)
COV	22%	5%	5%	4%	9%	22%	15%	18%	9%	24%

Table 5.32: Summary of Mean Values of 4G80S6(1/4) and 5G80S6(1/4) Specimens with 1/4 in. (6.35 mm) Interface Finish.

Specimen	Δ_{ult}, in. (mm)	V_{ult}, kip (kN)	σ_{ult}, ksi (MPa)	$V_{sus,min}$, kip (kN)	$V_{sus,max}$, kip (kN)	Δ_{cr}, in. (mm)	V_{cr}, kip (kN)	Δ_b, in. (mm)	V_b, kip (kN)	E_b, kip-ft (kJ)
4G80S6 (1/4)	0.045 (1.135)	217.90 (969.28)	0.908 (6.260)	126.58 (563.07)	155.83 (693.18)	0.013 (0.319)	111.37 (495.38)	0.943 (23.94)	153.56 (683.07)	11.35 (15.39)
5G80S6 (1/4)	0.067 (1.702)	302.54 (1345.7)	1.261 (8.691)	171.48 (762.80)	229.64 (1021.5)	0.015 (0.3742)	134.77 (599.47)	1.199 (30.45)	227.31 (1011.1)	20.48 (27.77)

5.4.1.4 Interface Preparation: Exposed Aggregate

Figure 5.24 presents the interface shear force versus interface shear displacement response curve for specimen group 4G80S6(EA). In this figure specimen 4G80S6(EA)-1 exhibits a different force-displacement response characterized by higher values of Δ_{ult} and V_{ult}, but lower post-peak capacity. Additionally, specimens 4G80S6(EA)-2 and 4G80S6(EA)-3 present a "double peak" response, where the maximum sustained shear interface load, $V_{sus,max}$, is similar-to or higher-than the peak-load, V_{ult}. These results indicate that two out of the three specimens tested, exposing the aggregate of the shear interface may allow the aggregate interlock mechanism to contribute to the force-displacement response during the post-peak stage. It is important to note that bleed water moves upwards to the shear interface during the vibration of the fresh concrete, thus creating a weak layer of concrete on the shear interface during the first casting. The process of exposing the aggregate removes this weak layer, allowing for stronger aggregate interlock. This may explain the "double peak" behavior exhibited by test specimens 4G80S6(EA)-2 and 4G80S6(EA)-3.

The specimens in group 5G80S6(EA) exhibit different behavior, as can be observed in Figure 5.25. Specimen 5G80S6(EA)-1 reached a peak load approximately 20% higher than the other specimens did. In the initial stages, the behavior is similar in all specimens. During the post-cracking stage, however, specimen 5G80S6(EA)-1 also exhibited a higher stiffness. This indicates that the different behavior exhibited by this specimen can also be attributed to the aggregate interlock mechanism having a higher influence on the response, again since exposing the aggregate increases the propensity to enhance aggregate interlock. Nonetheless, the limited testing performed indicates that this increased strength and stiffness due to the aggregate interlock may not always develop, and additional testing and surface preparation trials using different aggregates and surface preparation mechanisms to develop the EA finishing should be investigated.

Table 5.35 shows comparative values of the main points of study between both specimen groups. A higher post-crack stiffness can be observed when #5 (#16M) bars are used. On the other hand, specimens reinforced with #4 (#13M) bars display a higher post-peak performance, which may be explained by the variability of the exposed aggregate shear interface preparation.

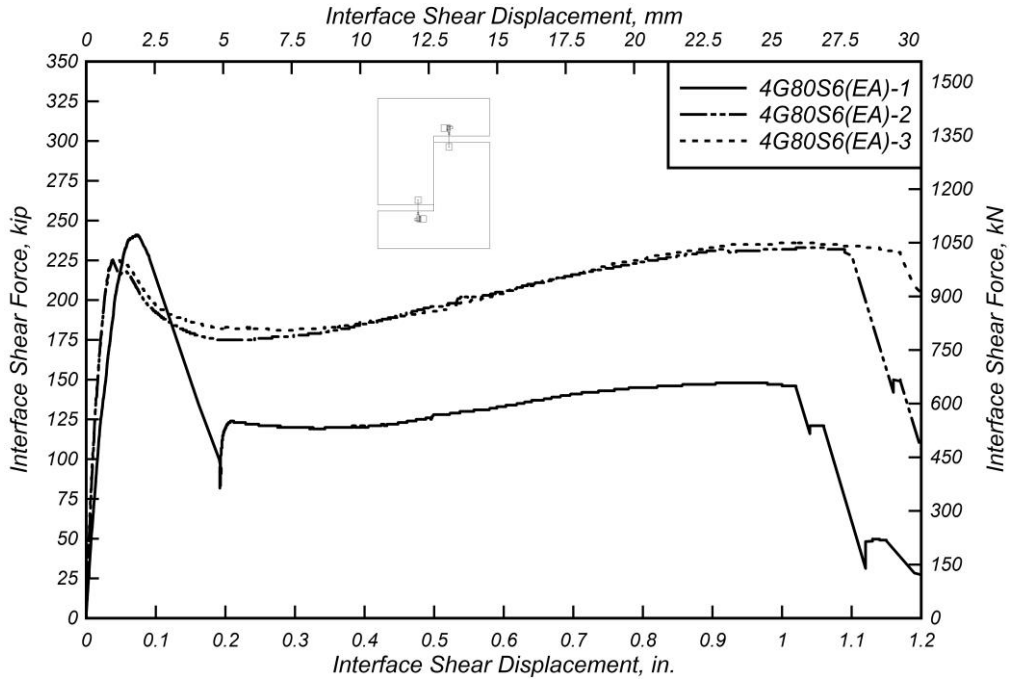

Figure 5.24: Interface shear force versus interface shear displacement for 4G80S6(EA) specimens

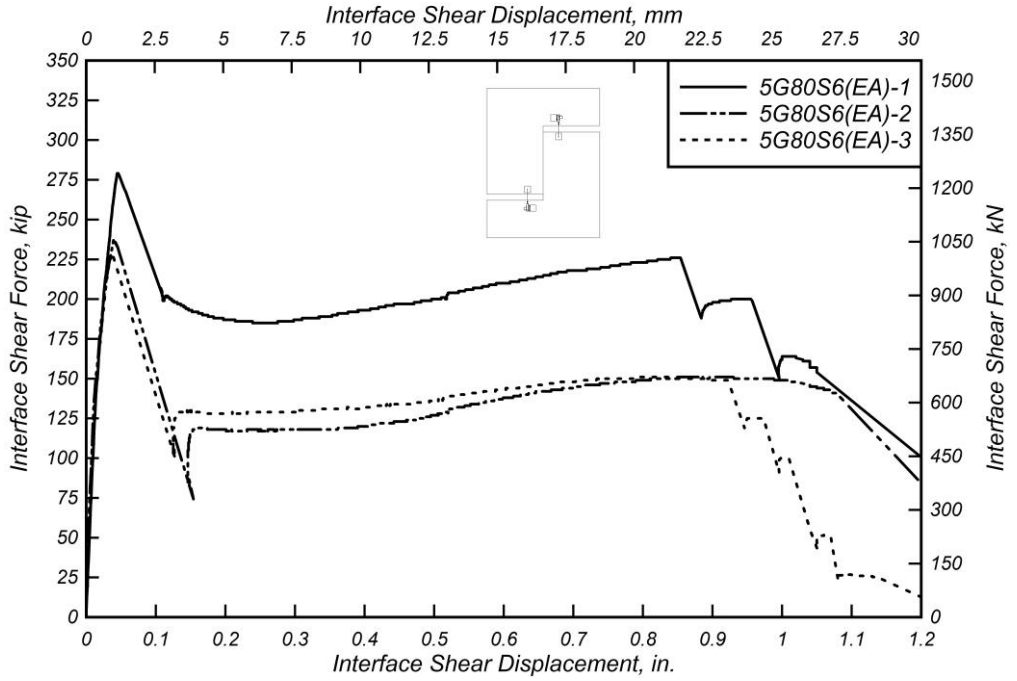

Figure 5.25: Interface shear force versus interface shear displacement for 5G80S6(EA) specimens

Table 5.33: 4G80S6(EA) Specimen Shear Test Results.

Specimen	Δ_{ult}, in. (mm)	V_{ult}, kip (kN)	σ_{ult}, ksi (MPa)	$V_{sus,min}$, kip (kN)	$V_{sus,max}$, kip (kN)	Δ_{cr}, in. (mm)	V_{cr}, kip (kN)	Δ_b, in. (mm)	V_b, kip (kN)	E_b, kip-ft (kJ)
4G80S6 (EA)-1	0.073 (1.854)	241.11 (1072.5)	1.005 (6.927)	119.20 (530.23)	148.28 (659.58)	0.0174 (0.4420)	107.90 (635.35)	1.023 (25.98)	145.13 (645.57)	11.93 (16.17)
4G80S6 (EA)-2	0.038 (0.965)	225.49 (1003.0)	0.940 (6.478)	174.99 (778.39)	232.89 (1035.9)	0.0128 (0.3251)	129.90 (465.53)	1.094 (27.79)	230.33 (1024.6)	18.45 (25.01)
4G80S6 (EA)-3	0.040 (1.016)	226.29 (1006.6)	0.943 (6.501)	180.92 (804.77)	235.67 (1048.3)	0.0079 (0.1994)	91.96 (495.38)	1.173 (29.79)	227.54 (1012.1)	20.21 (27.40)
Mean	0.050 (1.278)	230.96 (1027.4)	0.962 (6.635)	158.37 (704.46)	205.61 (914.61)	0.013 (0.322)	109.92 (488.95)	1.097 (27.86)	201.00 (894.09)	16.86 (22.86)
Median	0.040 (1.016)	226.29 (1006.6)	0.943 (6.501)	174.99 (778.39)	232.89 (1035.9)	0.013 (0.325)	107.90 (635.35)	1.094 (27.79)	227.54 (1012.1)	18.45 (25.01)
STDEV	0.0197 (0.499)	8.796 (39.13)	0.0367 (0.253)	34.05 (151.47)	49.67 (220.95)	0.0048 (0.1213)	19.05 (84.74)	0.0750 (1.906)	48.40 (215.32)	4.363 (5.916)
COV	39%	4%	4%	22%	24%	38%	17%	7%	24%	26%

Table 5.34: 5G80S6(EA) Specimen Shear Test Results.

Specimen	Δ_{ult}, in. (mm)	V_{ult}, kip (kN)	σ_{ult}, ksi (MPa)	$V_{sus,min}$, kip (kN)	$V_{sus,max}$, kip (kN)	Δ_{cr}, in. (mm)	V_{cr}, kip (kN)	Δ_b, in. (mm)	V_b, kip (kN)	E_b, kip-ft (kJ)
5G80S6 (EA)-1	0.045 (1.143)	279.43 (1243.0)	1.164 (8.028)	185.15 (823.59)	226.21 (1006.2)	0.012 (0.2946)	120.50 (567.30)	0.854 (21.69)	226.26 (1006.5)	14.52 (19.69)
5G80S6 (EA)-2	0.040 (1.016)	236.33 (1051.2)	0.985 (6.789)	117.23 (521.46)	150.66 (670.17)	0.013 (0.3353)	148.60 (709.64)	1.076 (27.33)	140.96 (627.02)	12.49 (16.93)
5G80S6 (EA)-3	0.037 (0.940)	229.12 (1019.2)	0.955 (6.582)	128.03 (569.51)	151.17 (672.44)	0.011 (0.2692)	126.20 (599.47)	0.923 (23.44)	148.27 (659.54)	10.95 (14.85)
Mean	0.041 (1.033)	248.29 (1104.5)	1.035 (7.133)	143.47 (638.19)	176.01 (782.95)	0.012 (0.300)	131.77 (625.47)	0.951 (24.16)	171.83 (764.34)	12.65 (17.16)
Median	0.040 (1.016)	236.33 (1051.2)	0.985 (6.789)	128.03 (569.51)	151.17 (672.44)	0.012 (0.295)	126.20 (599.47)	0.923 (23.44)	148.27 (659.54)	12.49 (16.93)
STDEV	0.0040 (0.103)	27.21 (121.01)	0.1134 (0.782)	36.50 (162.35)	43.47 (193.37)	0.0013 (0.033)	14.85 (74.65)	0.1136 (2.886)	47.28 (210.31)	1.790 (2.427)
COV	10%	11%	11%	25%	25%	11%	11%	12%	28%	14%

Table 5.35: Summary of Mean Values of 4G80S6(EA) and 5G80S6(EA) Specimens with Exposed Aggregate Interface Finish.

Specimen	Δ_{ult}, in. (mm)	V_{ult}, kip (kN)	σ_{ult}, ksi (MPa)	$V_{sus,min}$, kip (kN)	$V_{sus,max}$, kip (kN)	Δ_{cr}, in. (mm)	V_{cr}, kip (kN)	Δ_b, in. (mm)	V_b, kip (kN)	E_b, kip-ft (kJ)
4G80S6 (EA)	0.050 (1.278)	230.96 (1027.4)	0.962 (6.635)	158.37 (704.46)	205.61 (914.61)	0.013 (0.322)	109.92 (488.95)	1.097 (27.86)	201.00 (894.09)	16.86 (22.86)
5G80S6 (EA)	0.041 (1.033)	248.29 (1104.5)	1.035 (7.133)	143.47 (638.19)	176.01 (782.95)	0.012 (0.300)	131.77 (625.47)	1.097 (27.86)	201.00 (894.09)	12.65 (17.16)

5.4.2 Interface Shear Force versus Strain

5.4.2.1 Interface Preparation: As Cast

Figure 5.26 and Figure 5.27 present the interface shear force versus reinforcing steel bar strain relationship for specimen groups 4G80S6(AC) and 5G80S6(AC), respectively. The curves shown correspond to the mean strain measurements from all strain gauges contained in each test specimen plotted versus the interface shear force. As shown in Figure 5.26, all specimens present similar behavior except specimen 4G80S6(AC)-3. The initial behavior is characterized by a linear force-strain response with similar stiffness for all specimens until the cracking shear load is reached. After cracking occurs, the specimens experience a rapid increase in strain on the reinforcing steel U-bars as the load continues to grow until peak load. The force-strain response of specimen 4G80S6(AC)-3 shows that it reaches a significantly lower peak load and shows a steep reduction in shear load in the post-peak response, unlike the other specimens which show a smooth softening curve moving into the sustained load phase of the force-strain response. The behavior of test specimen group 5G80S6(AC) is similar across all specimens, as shown in Figure 5.27.

Table 5.36 and Table 5.37 present values of strain measurements at peak load for all strain gauges in specimen groups 4G80S6(AC) and 5G80S6(AC), respectively. Table 5.38 presents a summary of mean strain gauges measurements at peak load for both specimen groups. From these values it can be observed that specimen group 4G80S6(AC) achieved higher strains at peak load when compared to specimen group 5G80S6(AC).

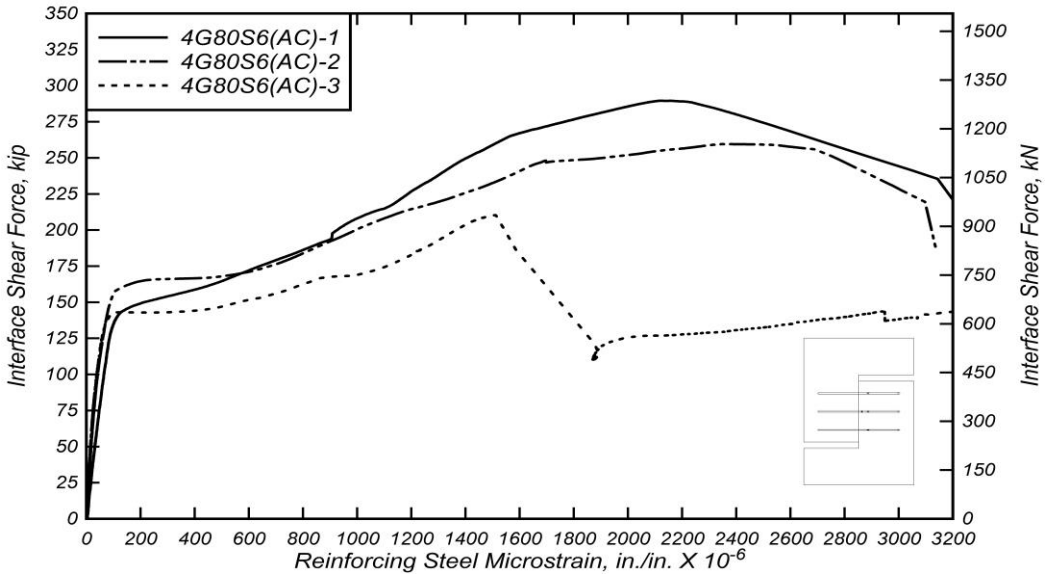

Figure 5.26: Interface shear force versus mean reinforcing steel microstrain for 4G80S6(AC) specimens

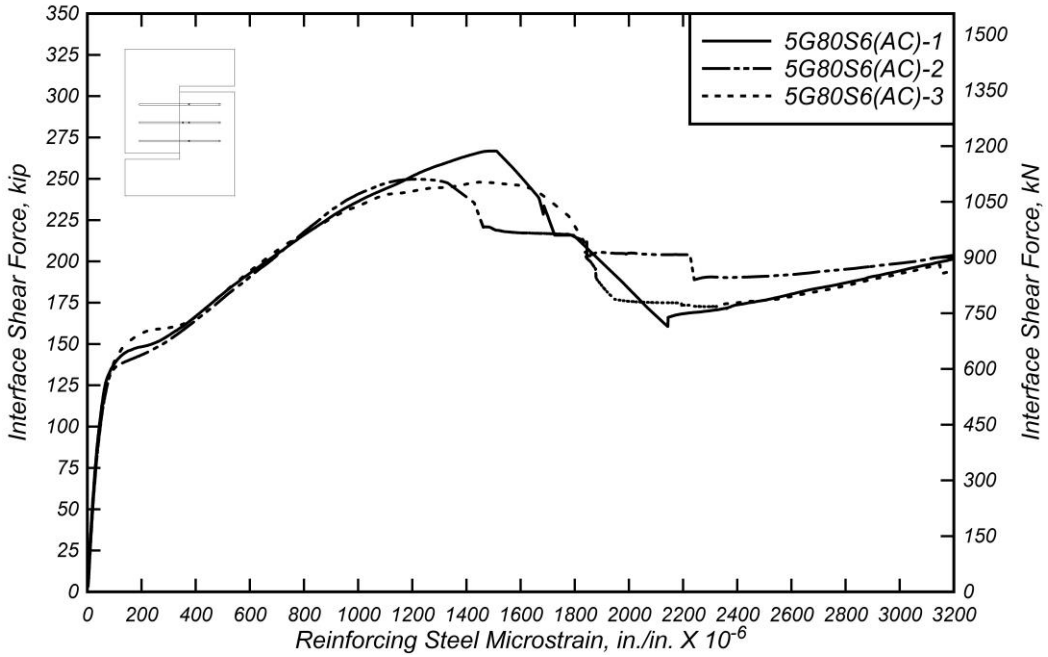

Figure 5.27: Interface shear force versus mean reinforcing steel microstrain for 5G80S6(AC) specimens

Table 5.36: 4G80S6(AC) Specimen Strain Gauge Readings at Peak Interface Shear Force.

Specimen	s_1, in./in. (mm/mm)	s_2, in./in. (mm/mm)	s_3, in./in. (mm/mm)	s_4, in./in. (mm/mm)	s_5, in./in. (mm/mm)	s_6, in./in. (mm/mm)	s_7, in./in. (mm/mm)
4G80S6(AC)-1	-	-	-	0.0027	-	0.0023	0.0017
4G80S6(AC)-2	0.0027	0.0023	-	-	0.0031	-	0.0017
4G80S6(AC)-3	-	-	0.0018	0.0025	0.0015	-	0.0015
Mean	0.0027	0.0023	0.0018	0.0026	0.0023	0.0023	0.0016
Median	0.0027	0.0023	0.0018	0.0026	0.0023	0.0023	0.0017
STDEV	-	-	-	0.0002	0.0011	-	0.0001
COV	-	-	-	7%	47%	-	9%

Table 5.37: 5G80S6(AC) Specimen Strain Gauge Readings at Peak Interface Shear Force.

Specimen	s_1, in./in. (mm/mm)	s_2, in./in. (mm/mm)	s_3, in./in. (mm/mm)	s_4, in./in. (mm/mm)	s_5, in./in. (mm/mm)	s_6, in./in. (mm/mm)	s_7, in./in. (mm/mm)
5G80S6(AC)-1	0.0017	0.0015	-	0.0021	0.0014	0.0016	0.0018
5G80S6(AC)-2	0.0011	-	0.0018	-	0.0011	0.0014	-
5G80S6(AC)-3	0.0016	0.0016	-	0.0023	0.0014	0.0014	0.0015
Mean	0.0015	0.0016	0.0018	0.0022	0.0013	0.0015	0.0016
Median	0.0016	0.0016	0.0018	0.0022	0.0014	0.0014	0.0016
STDEV	0.00031	5.12E-05	-	0.00011	0.00021	9.29E-05	0.00020
COV	21%	3%	-	5%	16%	6%	13%

Table 5.38: Summary of Strain Gauge Readings at Peak Interface Shear Force for 4G80S6(AC) and 5G80S6(AC) Specimens.

Specimen	s_1, in./in. (mm/mm)	s_2, in./in. (mm/mm)	s_3, in./in. (mm/mm)	s_4, in./in. (mm/mm)	s_5, in./in. (mm/mm)	s_6, in./in. (mm/mm)	s_7, in./in. (mm/mm)
4G80S6 (AC)	0.0027	0.0023	0.0018	0.0026	0.0023	0.0023	0.0016
5G80S6 (AC)	0.0015	0.0016	0.0018	0.0022	0.0013	0.0015	0.0016

5.4.2.2 Interface Preparation: Roughened to 1/8 in. (3.175 mm)

The interface shear force versus reinforcing steel U-bar strain relationship for specimen group 4G80S6(1/8) was shown earlier in Figure 5.6 and is shown in Figure 5.28 for specimen group 5G80S6(1/8). These curves correspond to the mean strain measurements from all strain gauges contained in each test specimen plotted versus the interface shear force. The behavior is similar in most specimens. There is an initial linear branch up until the interface shear cracking force is reached. The post-crack force-strain response is characterized by a reduction in stiffness resulting in a more rapid increase in strain until peak load. Post-peak behavior begins with a softening curve, followed by a hardening branch.

In Figure 5.28 specimen 5G80S6(1/8)-2 exhibits a significantly higher peak load compared to the other specimens in the group, which has already been discussed in previous sections of this report. Table 5.7 and Table 5.39 presents tabulated values of strain measurements at peak load for all strain gauges in specimen groups 4G80S6(1/8) and 5G80S6(1/8), respectively. Section 0 provides a description of the behavior exhibited by specimen group 4G80S6(1/8). From the comparison of both specimen groups it can be observed that specimen group 4G80S6(1/8) show larger mean strains at lower peak load values.

Table 5.40 shows a summary of strain measurements for both specimen groups for comparison. From this table, the discussion in the previous paragraph can be confirmed to show that specimen group 4G80S6(1/8), which is constructed with #4 (#13M) reinforcing steel bars across the interface, exhibits higher mean strains at peak load.

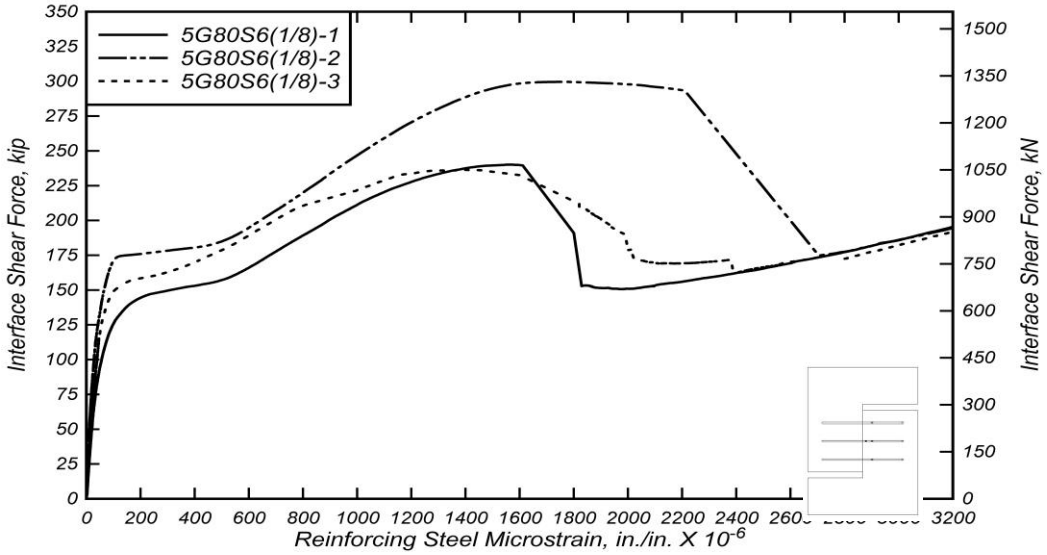

Figure 5.28: Interface shear force versus mean reinforcing steel microstrain for 5G80S6(1/8) specimens

Table 5.39: 5G80S6(1/8) Specimen Strain Gauge Readings at Peak Interface Shear Force.

Specimen	s_1, in./in. (mm/mm)	s_2, in./in. (mm/mm)	s_3, in./in. (mm/mm)	s_4, in./in. (mm/mm)	s_5, in./in. (mm/mm)	s_6, in./in. (mm/mm)	s_7, in./in. (mm/mm)
5G80S6(1/8)-1	0.0013	0.0016	0.0015	-	-	0.0015	0.0011
5G80S6(1/8)-2	0.0012	-	0.0016	-	-	-	0.0018
5G80S6(1/8)-3	0.0012	0.0013	-	0.0016	-	0.0015	-
Mean	0.0012	0.0015	0.0015	-	-	0.0015	0.0014
Median	0.0012	0.0015	0.0015	-	-	0.0015	0.0014
STDEV	7.7E-05	1.7E-04	7.1E-05	-	-	1.9E-05	4.8E-04
COV	9%	12%	5%	-	-	1%	34%

Table 5.40: Summary of Strain Gauge Readings at Peak Interface Shear Force for 4G80S6(1/8) and 5G80S6(1/8) (1/8 in. (3.175 mm)) Specimens.

Specimen	s_1, in./in. (mm/mm)	s_2, in./in. (mm/mm)	s_3, in./in. (mm/mm)	s_4, in./in. (mm/mm)	s_5, in./in. (mm/mm)	s_6, in./in. (mm/mm)	s_7, in./in. (mm/mm)
4G80S6(1/8)	-	0.0022	0.0019	0.0026	0.0028	0.0021	0.0015
5G80S6(1/8)	0.0012	0.0015	0.0015	-	-	0.0015	0.0014

5.4.2.3 Interface Preparation: Roughened to 1/4 in. (6.35 mm)

The interface shear force versus reinforcing steel U-bar strain relationship for specimen groups 4G80S6(1/4) and 5G80S6(1/4) are shown in Figure 5.29 and Figure 5.30, respectively. These curves correspond to the mean strain measurements from all strain gauges contained in each test specimen plotted versus the interface shear force and general trends of the responses have been discussed previously. Worth noting in Figure 5.29 is that specimen 4G80S6(1/4)-2 exhibits a significantly lower peak load and strain at peak load, although there were no observations or indications in the construction of the specimen or during testing that could suggest a reason for this lower performance. Table 5.41 presents values of strain measurements at peak load for all strain gauges in specimen group 4G80S6(1/4) where the underperformance of specimen 4G80S6(1/4)-2 can be confirmed by the significantly lower strain values at peak load.

Table 5.43 shows a summary of strain measurements for specimen groups 4G80S6(1/4) and 5G80S6(1/4). The values in this table show that, in general, specimen group 5G80S6(1/4) exhibits lower mean strain values at peak load, but also exhibits significantly larger peak load values, which can be related to the larger stiffness of the specimens with larger bars.

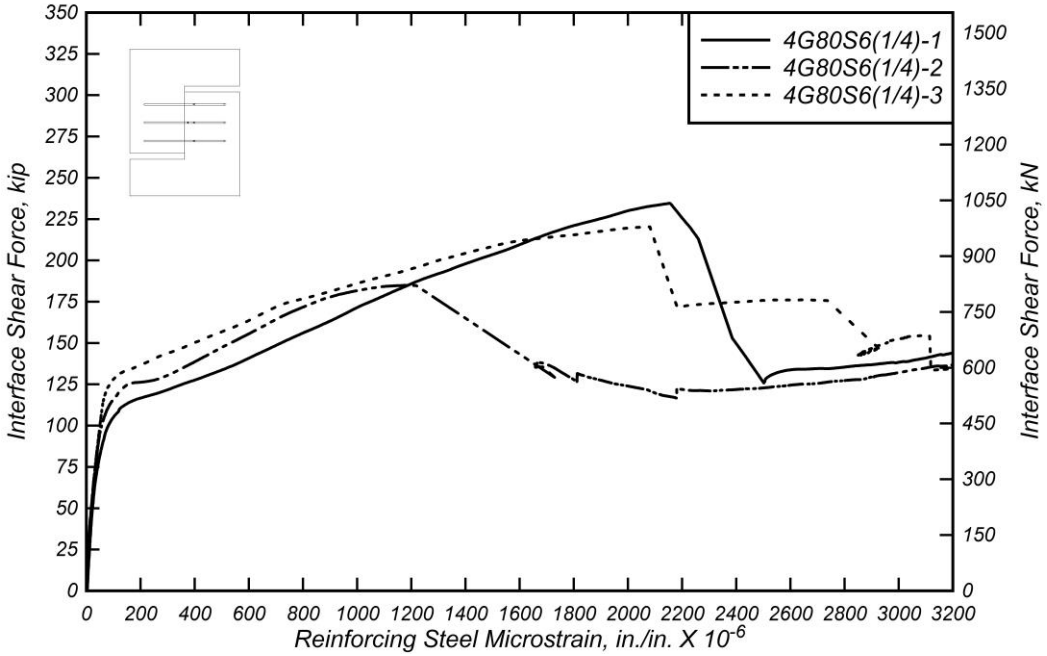

Figure 5.29: Interface shear force versus mean reinforcing steel microstrain for 4G80S6(1/4) specimens.

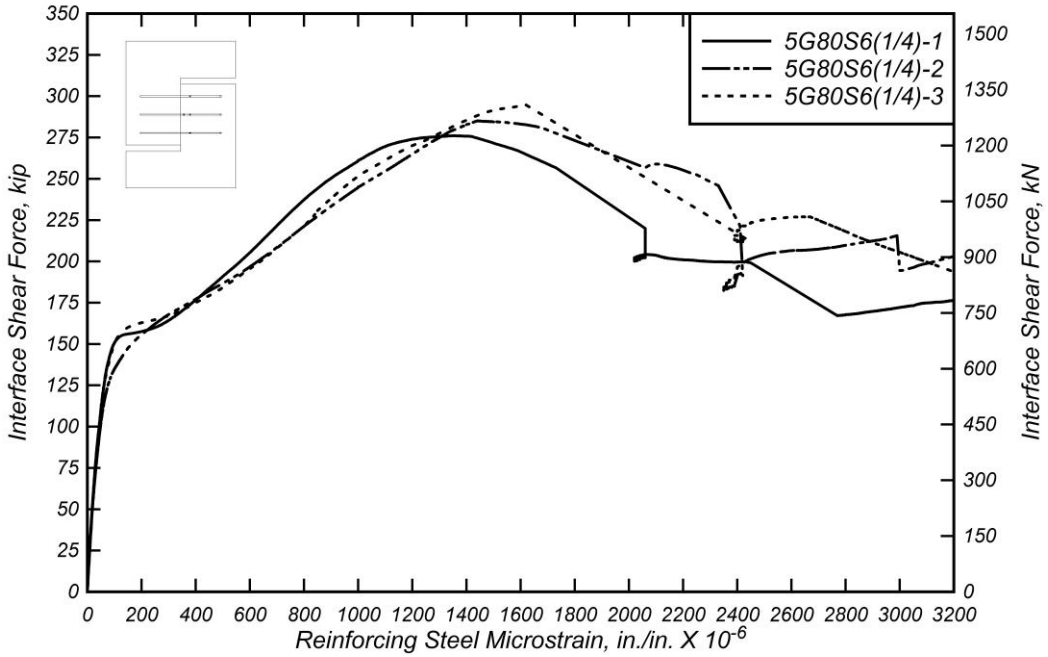

Figure 5.30: Interface shear force versus mean reinforcing steel microstrain for 5G80S6(1/4) specimens.

Table 5.41: 4G80S6(1/4) Specimen Strain Gauge Readings at Peak Interface Shear Force.

Specimen	s_1, in./in. (mm/mm)	s_2, in./in. (mm/mm)	s_3, in./in. (mm/mm)	s_4, in./in. (mm/mm)	s_5, in./in. (mm/mm)	s_6, in./in. (mm/mm)	s_7, in./in. (mm/mm)
4G80S6(1/4)-1	0.0026	-	-	0.0026	0.0024	0.0021	-
4G80S6(1/4)-2	0.0011	-	-	-	0.0012	0.0014	-
4G80S6(1/4)-3	-	0.0021	-	-	0.0025	0.0016	0.0013
Mean	0.0018	0.0021	-	0.0026	0.0020	0.0017	0.0013
Median	0.0018	0.0021	-	0.0026	0.0024	0.0016	0.0013
STDEV	0.0010	-	-	-	0.0007	0.0004	-
COV	55%	-	-	-	36%	21%	-

Table 5.42: 5G80S6(1/4) Specimen Strain Gauge Readings at Peak Interface Shear Force.

Specimen	s_1, in./in. (mm/mm)	s_2, in./in. (mm/mm)	s_3, in./in. (mm/mm)	s_4, in./in. (mm/mm)	s_5, in./in. (mm/mm)	s_6, in./in. (mm/mm)	s_7, in./in. (mm/mm)
5G80S6(1/4)-1	0.0014	0.0011	-	0.0018	0.0012	0.0019	-
5G80S6(1/4)-2	0.0022	0.0024	0.0020	0.0020	0.0013	0.0018	0.002205
5G80S6(1/4)-3	0.0012	0.0017	-	-	0.0022	-	-
Mean	0.0016	0.0017	0.0020	0.0019	0.0016	0.0018	0.0022
Median	0.0014	0.0017	0.0020	0.0019	0.0013	0.0018	0.0022
STDEV	0.00053	0.00063	-	0.00019	0.00058	5.55E-05	-
COV	33%	36%	-	10%	37%	3%	-

Table 5.43: Summary of Strain Gauge Readings at Peak Interface Shear Force for 4G80S6(1/4) and 5G80S6(1/4) (1/4 in. (6.35 mm)) Specimens.

Specimen	s_1, in./in. (mm/mm)	s_2, in./in. (mm/mm)	s_3, in./in. (mm/mm)	s_4, in./in. (mm/mm)	s_5, in./in. (mm/mm)	s_6, in./in. (mm/mm)	s_7, in./in. (mm/mm)
4G80S6 (1/4)	0.0018	0.0021	-	0.0026	0.0020	0.0017	0.0013
5G80S6 (1/4)	0.0016	0.0017	0.0020	0.0019	0.0016	0.0018	0.0022

5.4.2.4 Interface Preparation: Exposed Aggregate

The interface shear force versus reinforcing steel U-bar strain response for specimen groups 4G80S6(EA) and 5G80S6(EA) are shown in Figure 5.31 and Figure 5.32, respectively. In Figure 5.31 specimen 4G80S6(EA)-1 reaches its peak load at a higher strain value, which also indicates a larger crack width. The reason for this will be explained in the following section. Figure 5.32 shows that specimen 5G80S6(EA)-1 reaches a higher peak load for slightly lower strain values compared to the other specimens in the group. Both highlight the variability of the results observed, especially when the surface is roughened to a nominal amplitude of 1/4 in. (6.35 mm). Table 5.44 and Table 5.45 present strain gauge measurements at peak load for all strain gauges in specimen group 4G80S6(EA) and 5G80S6(EA), respectively. In Table 5.44 it can be observed that the strain gauge measurements at peak load are significantly higher for specimen 4G80S6(EA)-1 when compared to the other specimens within its group. Meanwhile Table 5.45 shows that specimen 5G80S6(EA)-1 exhibits lower strain gauge measurements at peak load when compared to the other specimens within its group.

Table 5.46 summarizes the average strain gauge measurements at peak load for specimen groups 4G80S6(EA) and 5G80S6(EA). The strain gauge measurements presented in this table show that specimen group 4G80S6(EA) exhibited lower average strains at peak load.

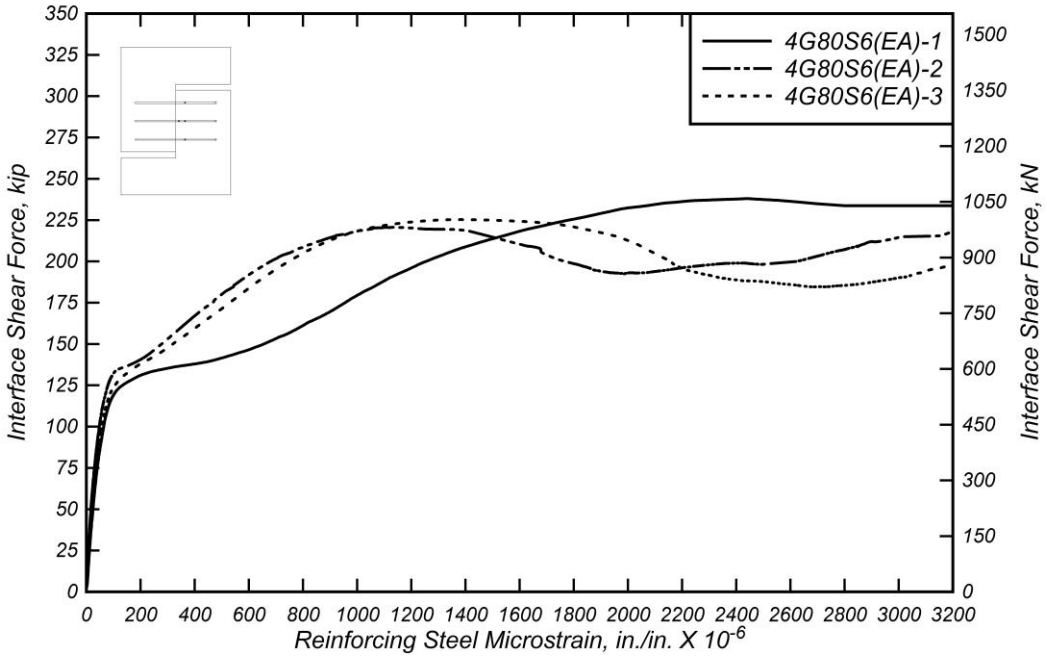

Figure 5.31: Interface shear force versus average reinforcing steel microstrain for 4G80S6(EA) specimens.

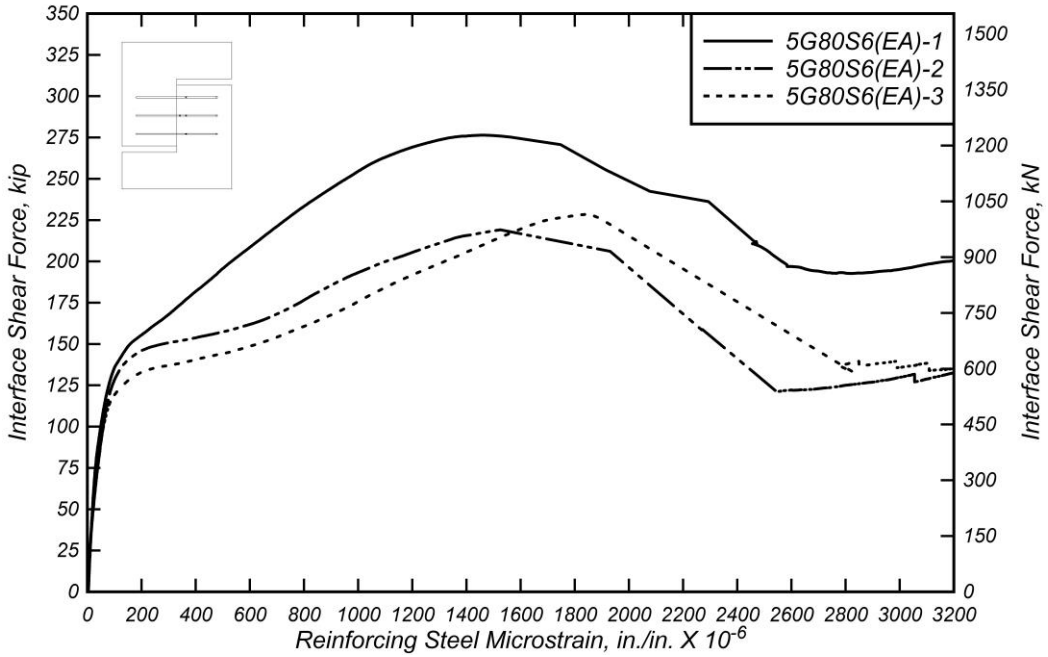

Figure 5.32: Interface shear force versus mean reinforcing steel microstrain for 5G80S6(EA) specimens.

Table 5.44: 4G80S6(EA) Specimen Strain Gauge Readings at Peak Interface Shear Force.

Specimen	s_1, in./in. (mm/mm)	s_2, in./in. (mm/mm)	s_3, in./in. (mm/mm)	s_4, in./in. (mm/mm)	s_5, in./in. (mm/mm)	s_6, in./in. (mm/mm)	s_7, in./in. (mm/mm)
4G80S6(EA)-1	0.0016	0.0025	0.0024	0.0023	0.0017	0.0024	0.0028
4G80S6(EA)-2	-	0.0012	0.0011	0.0018	-	0.0015	0.0009
4G80S6(EA)-3	0.0014	0.0016	0.0013	0.0019	0.0011	0.0013	0.0013
Mean	0.0015	0.0018	0.0016	0.0020	0.0014	0.0017	0.0017
Median	0.0015	0.0016	0.0013	0.0019	0.0014	0.0015	0.0013
STDEV	0.0001	0.0006	0.0007	0.0003	0.0004	0.0006	0.0010
COV	9%	37%	44%	14%	33%	35%	59%

Table 5.45: 5G80S6(EA) Specimen Strain Gauge Readings at Peak Interface Shear Force.

Specimen	s_1, in./in. (mm/mm)	s_2, in./in. (mm/mm)	s_3, in./in. (mm/mm)	s_4, in./in. (mm/mm)	s_5, in./in. (mm/mm)	s_6, in./in. (mm/mm)	s_7, in./in. (mm/mm)
5G80S6(EA)-1	0.0014	-	0.0011	0.0018	0.0015	0.0015	-
5G80S6(EA)-2	0.0017	0.0021	-	0.0025	0.0014	0.0024	0.0021
5G80S6(EA)-3	0.0013	0.0019	0.0019	0.0026	0.0017	0.0019	0.0018
Mean	0.0015	0.0020	0.0015	0.0023	0.0015	0.0019	0.0020
Median	0.0014	0.0020	0.0015	0.0025	0.0015	0.0019	0.0020
STDEV	0.0002	0.0001	0.0006	0.0005	0.0002	0.0004	0.0002
COV	14%	7%	37%	21%	11%	24%	11%

Table 5.46: Summary of Strain Gauge Readings at Peak Interface Shear Force for 4G80S6(EA) and 5G80S6(EA) (Exposed Aggregate) Specimens.

Specimen	s_1, in./in. (mm/mm)	s_2, in./in. (mm/mm)	s_3, in./in. (mm/mm)	s_4, in./in. (mm/mm)	s_5, in./in. (mm/mm)	s_6, in./in. (mm/mm)	s_7, in./in. (mm/mm)
4G80S6(EA)	0.0015	0.0018	0.0016	0.0020	0.0014	0.0017	0.0017
5G80S6(EA)	0.0015	0.0020	0.0015	0.0023	0.0015	0.0019	0.0020

5.4.3 Interface Shear Force versus Crack Width

5.4.3.1 Interface Preparation: As Cast

Figure 5.33 and Figure 5.34 present the interface shear force versus crack width response for specimen groups 4G80S6(AC) and 5G80S6(AC). All specimens discussed in this section were constructed with an As Cast interface preparation. Each figure shows the force-crack width response for all specimens in each group. Tabulated values of points of interest such as crack width at peak load and crack width at first bar fracture for each specimen group are presented in Table 5.47 and Table 5.48.

In Figure 5.33 it can be observed that most specimens behave similarly with negligible crack width in the initial stages. Following cracking, crack width begins to steadily increase until peak load is reached. During this stage, specimen 4G80S6(AC)-3 reaches a significantly lower peak load, V_{ult}, and lower crack width at peak load, w_{ult}, compared to the other specimens within the specimen group. As discussed in Section 5.4.1, these lower values can attributed to the variability that originates from the process implemented to obtain the As Cast interface preparation. This process may have weakened the aggregate interlock mechanism, thus preventing the test specimen from achieving a larger peak value. Figure 5.34 shows that specimen 5G80S6(AC)-1 exhibited larger post-cracked stiffness (slope) and it reached a higher peak load compared to the other specimens in the group. In the post-peak stage, a sudden increase in interface shear load can be observed. This behavior is attributed to a sensor malfunction, as the interface shear force versus interface shear displacement, seen in Figure 5.20, does not show any indication that this specimen is an outlier.

Table 5.49 presents a summary of mean crack width points of interest for specimen groups 4G80S6(AC) and 5G80S6(AC). Specimens reinforced with #4 (#13M) bars presented a slightly larger capacity than specimens reinforced with #5 (#16M), which was not expected behavior. This may be explained by the variability of the interface preparation process to obtain an As Cast surface preparation. Additionally, specimens reinforced with #5 (#16M) reinforcing steel U-bars displayed a smooth post-peak descending branch compared to the more abrupt behavior shown by the specimens reinforced with #4 (#13M) reinforcing steel U-bars.

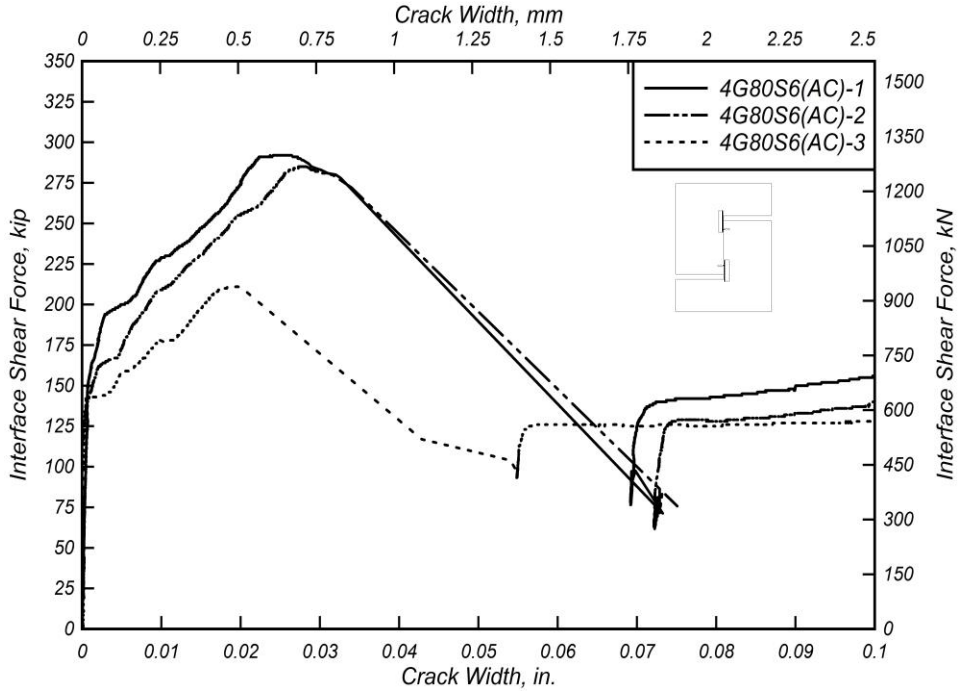

Figure 5.33: Interface shear force versus crack width for 4G80S6(AC) specimens

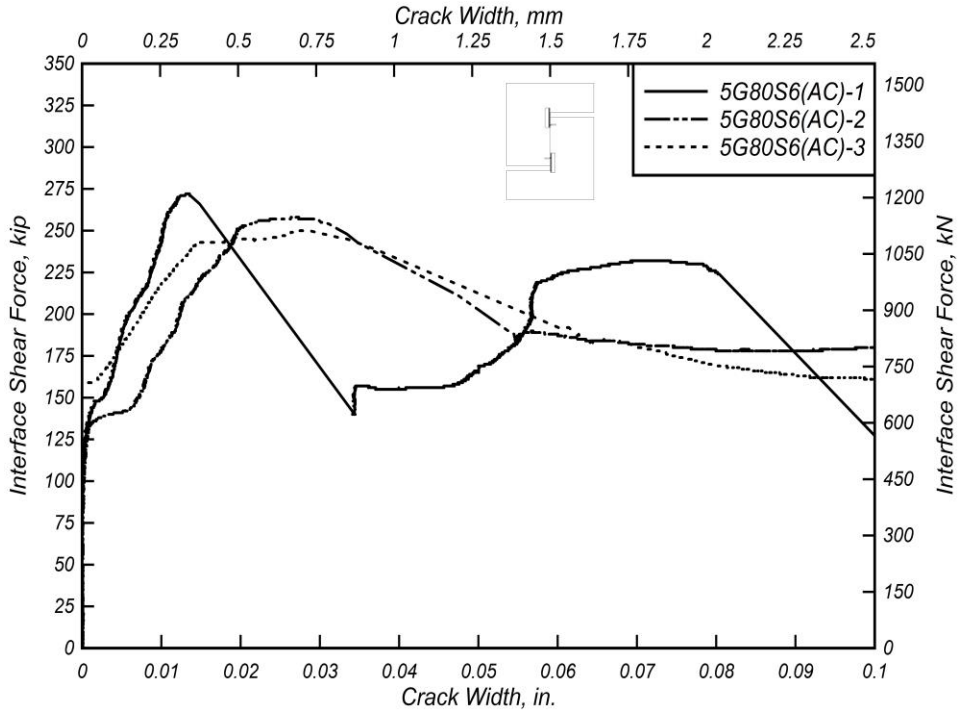

Figure 5.34: Interface shear force versus crack width for 5G80S6(AC) specimens

Table 5.47: 4G80S4(AC) Specimen Crack Width Measurements.

Specimen	w_{ult}, in. (mm)	V_{ult}, kip (kN)	w_b, in. (mm)	V_b, kip (kN)
4G80S6(AC)-1	0.0260 (0.6603)	292.03 (1299.0)	0.1239 (3.147)	150.66 (670.18)
4G80S6(AC)-2	0.0279 (0.7084)	284.98 (1267.7)	0.1372 (3.485)	152.78 (679.61)
4G80S6(AC)-3	0.0193 (0.4896)	210.93 (938.25)	0.2245 (5.702)	145.46 (647.04)
Mean	0.0244 (0.6194)	262.64 (1168.3)	0.1619 (4.112)	149.64 (665.61)
Median	0.0260 (0.6603)	284.98 (1267.7)	0.1372 (3.485)	150.66 (670.18)
STDEV	0.0045 (0.1150)	44.93 (199.85)	0.0546 (1.388)	3.767 (16.76)
COV	19%	17%	34%	3%

Table 5.48: 5G80S6(AC) Specimen Crack Width Measurements.

Specimen	w_{ult}, in. (mm)	V_{ult}, kip (kN)	w_b, in. (mm)	V_b, kip (kN)
5G80S6(AC)-1	0.0134 (0.3401)	271.63 (1208.3)	0.0800 (2.032)	225.46 (1002.9)
5G80S6(AC)-2	0.0267 (0.6786)	257.72 (1146.4)	0.1728 (4.388)	228.09 (1014.6)
5G80S6(AC)-3	0.0276 (0.7012)	250.26 (1113.2)	0.1615 (4.103)	219.56 (976.65)
Mean	0.0272 (0.6899)	253.99 (1129.8)	0.1671 (4.245)	223.82 (995.62)
Median	0.0272 (0.6899)	253.99 (1129.8)	0.1671 (4.245)	223.82 (995.62)
STDEV	0.0006 (0.0160)	5.274 (23.46)	0.0079 (0.2016)	6.029 (26.82)
COV	2%	2%	5%	3%

Table 5.49: Summary of Crack Width Measurements for 4G80S6(AC) and 5G80S6(AC) Specimens.

Specimen	w_{ult}, in. (mm)	V_{ult}, kip (kN)	w_b, in. (mm)	V_b, kip (kN)
4G80S6(AC)	0.0244 (0.6194)	262.64 (1168.3)	0.1619 (4.112)	149.64 (665.61)
5G80S6(AC)	0.0272 (0.6899)	253.99 (1129.8)	0.1671 (4.245)	223.82 (995.62)

5.4.3.2 Interface Preparation: Roughened to 1/8 in. (3.175 mm)

Figure 5.2 presented the interface shear force versus crack width response for specimen group 4G80S6(1/8). Figure 5.35 presents the interface shear force versus crack width response for specimen group 5G80S6(1/8). All specimens discussed in this section were constructed with a surface intentionally roughened to an amplitude of 1/8 in. (3.175 mm). Tabulated values of points of interest, such as crack width at peak load and crack width at first bar fracture for specimen group 5G80S6(1/8), are presented in Table 5.50. In the figure, it can be observed that all specimens exhibit similar behavior, showing negligible crack width in the initial stages before the interface shear force at cracking, V_{cr}, is reached. After the shear interface is cracked, the crack width begins to steadily increase until peak load is reached. The post-peak response is characterized by a smooth softening branch, followed by a sustained load phase until first bar fracture. An exception to the behavior is shown by specimen 5G80S6(1/8)-2. This specimen 5G80S6(1/8)-2 exhibits similar post-cracked stiffness, but it reaches a peak load approximately 25% higher than the other specimens in the group do. This behavior is believed to be caused by the variability of the process used to obtain an interface roughness of 1/8 in. (3.175 mm). A description of the interface shear force versus crack width behavior shown by specimen group 4G80S6(1/8) is presented in Section 0.

Table 5.51 presents a summary of mean crack width points of interest for specimen groups 4G80S6(1/8) and 5G80S6(1/8). Specimens reinforced with #5 (#16M) reinforcing steel U-bars reach a larger mean peak load, V_{ult}, and a value of mean crack width at peak load, w_{ult}, 50% lower compared to specimens constructed with #4 (#13M) reinforcing steel bars. This behavior is expected due to the reinforcing steel ratio being 50% higher in specimen group 5G80S6(1/8). The clamping force is directly related to the area of reinforcing steel, therefore test specimens with a higher reinforcing steel ratio are expected to show lower values of crack width.

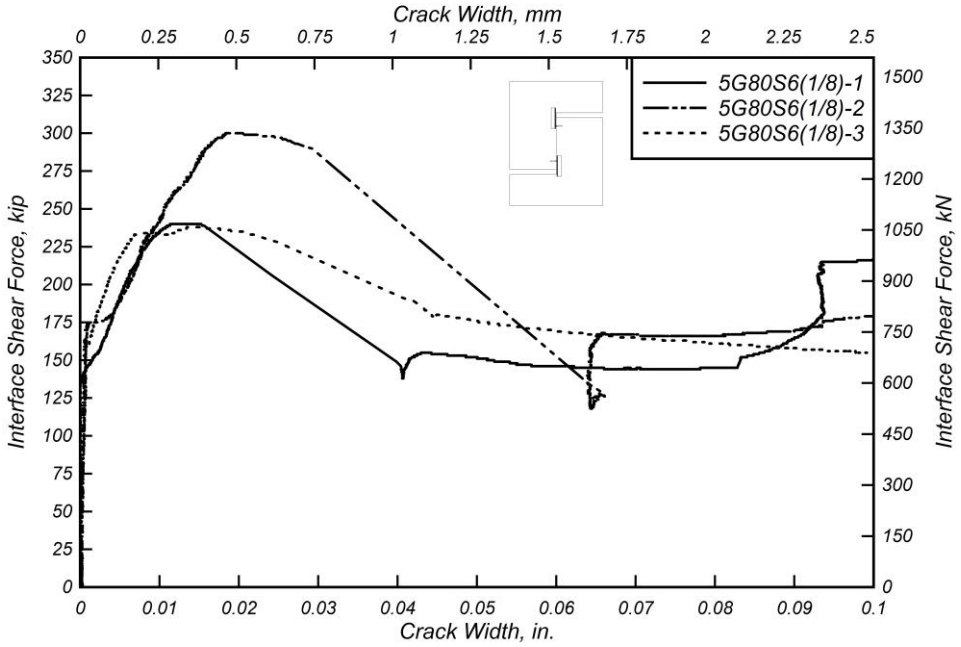

Figure 5.35: Interface shear force versus crack width for 5G80S6(1/8) specimens

Table 5.50: 5G80S6(1/8) Specimen Crack Width Measurements.

Specimen	w_{ult}, in. (mm)	V_{ult}, kip (kN)	w_b, in. (mm)	V_b, kip (kN)
5G80S6(1/8)-1	0.0123 (0.3117)	240.38 (1069.3)	0.1160 (2.947)	220.63 (981.40)
5G80S6(1/8)-2	0.0186 (0.4720)	300.13 (1335.0)	0.1755 (4.459)	225.72 (1004.1)
5G80S6(1/8)-3	0.0141 (0.3586)	238.06 (1059.0)	0.2171 (5.514)	205.82 (915.52)
Mean	0.0150 (0.3808)	259.52 (1154.4)	0.1696 (4.307)	217.39 (967.00)
Median	0.0141 (0.3586)	240.38 (1069.3)	0.1755 (4.459)	220.63 (981.40)
STDEV	0.0032 (0.0824)	35.18 (156.50)	0.0508 (1.291)	10.34 (46.00)
COV	22%	14%	30%	5%

Table 5.51: Summary of Crack Width Measurements for 4G80S6(1/8) and 5G80S6(1/8) (1/8 in. (3.175 mm)) Specimens.

Specimen	w_{ult}, in. (mm)	V_{ult}, kip (kN)	w_b, in. (mm)	V_b, kip (kN)
4G80S6(1/8)	0.0297 (0.7532)	238.70 (1061.8)	0.2039 (5.178)	148.87 (662.20)
5G80S6(1/8)	0.0150 (0.3808)	259.52 (1154.4)	0.1696 (4.307)	217.39 (967.00)

5.4.3.3 Interface Preparation: 1/4 in. (6.35 mm)

Figure 5.36 and Figure 5.37 present the interface shear force versus crack width response for specimen groups 4G80S6(1/4) and 5G80S6(1/4). All specimens discussed in this section were constructed with a surface roughened to an amplitude of 1/4 in. (6.35 mm). Each figure shows the force-crack width response for all specimens in each group. Tabulated values of points of interest such as crack width at peak load and crack width at first bar fracture for each specimen group are presented in Table 5.52 and Table 5.53.

Significant variability in the force-crack width response can be observed in Figure 5.36. Specimens 4G80S6(1/4)-1 and 4G80S6(1/4)-3 reach similar peak load values, but their response curves display significantly different behavior. Specimen 4G80S6(1/4)-1 reaches a larger peak load, V_{ult}, at smaller crack width, w_{ult}. Specimen 4G80S6(1/4)-1 also shows negligible crack width measurements until it reaches a load of approximately 200 kip (890 kN), which is approximately double of that shown by specimen 4G80S6(1/4)-3. This behavior exhibited by specimen 4G80S6(1/4)-1 may be attributed to a stronger concrete-to-concrete cohesion bond at the shear interface, thus resulting in a response with larger stiffness. This in consistent with results presented in Figure 5.22 where specimen 4G80S6(1/4)-1 exhibited a significantly larger stiffness in the force-displacement response when compared to specimen 4G80S6(1/4)-3. Additionally, specimen 4G80S6(1/4)-2 exhibits a different force-crack width response reaching a peak load 20% and 30% lower compared to specimens 4G80S6(1/4)-3 and 4G80S6(1/4)-1, respectively. The sensitivity in the behavior may be a result of the variability introduced by the process to roughen the surface to an amplitude of 1/4 in. (6.35 mm).

Figure 5.37 presents the interface shear force versus crack width response for specimen group 5G80S6(1/4). Significant variability of crack width values at peak load, w_{ult}, is observed, ranging from 0.010 in. (0.2533 mm) to 0.0275 in. (0.6985 mm) with a COV of 46%. Peak load values, V_{ult}, show less variability, however, ranging from 283.85 kip (1262.6 kN) to 315.53 kip (1403.6 kN) with a COV of 5%. The variability observed in w_{ult} values for specimens 5G80S6(1/4)-1 and 5G80S6(1/4)-2 may be related to the variability created by the intentional roughening of the interface surface. The response of specimen 5G80S6(1/4)-3, however, may be related to a stronger concrete-to-concrete cohesion bond formed at the shear interface, as this specimen shows negligible crack width until an interface shear load significantly larger is reached.

Table 5.54 presents a summary of the mean values for the points of interest for specimen groups 4G80S6(1/4) and 5G80S6(1/4). From the table it can be observed that specimens reinforced with #5 (#16M) reinforcing steel U-bars show a crack width at peak load 13% lower and peak load 30% larger than in specimens constructed with #4 (#13M) reinforcing steel bars. This larger capacity may be related to the higher reinforcing steel ratio crossing the interface in specimens reinforced with #5 (#16M) bars. A larger reinforcing steel ratio can produce a larger clamping force that is directly related to the aggregate interlock mechanism controlling this phase of the response.

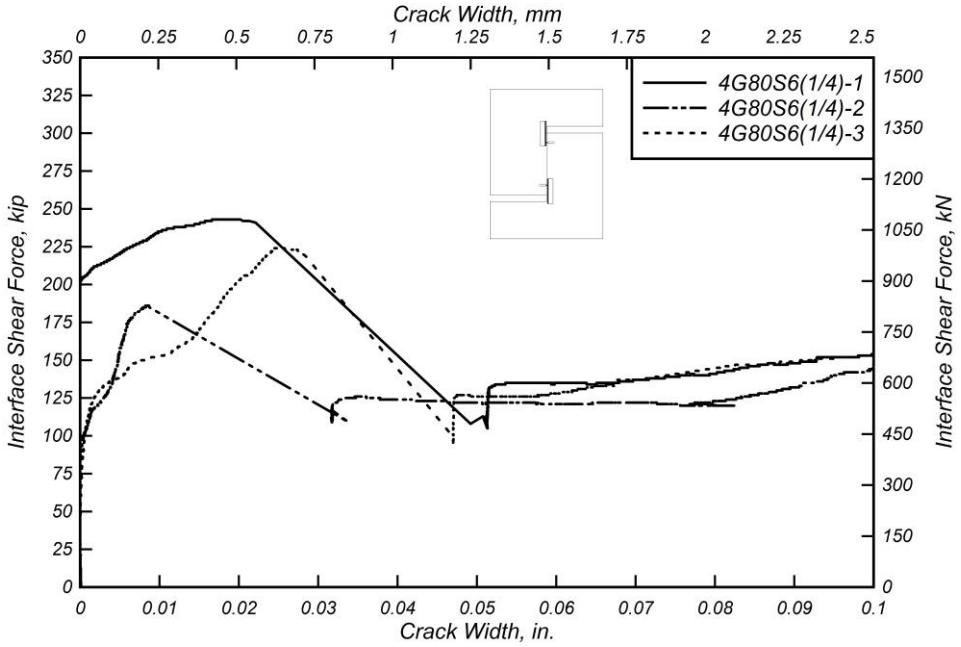

Figure 5.36: Interface shear force versus crack width for 4G80S6(1/4) specimens

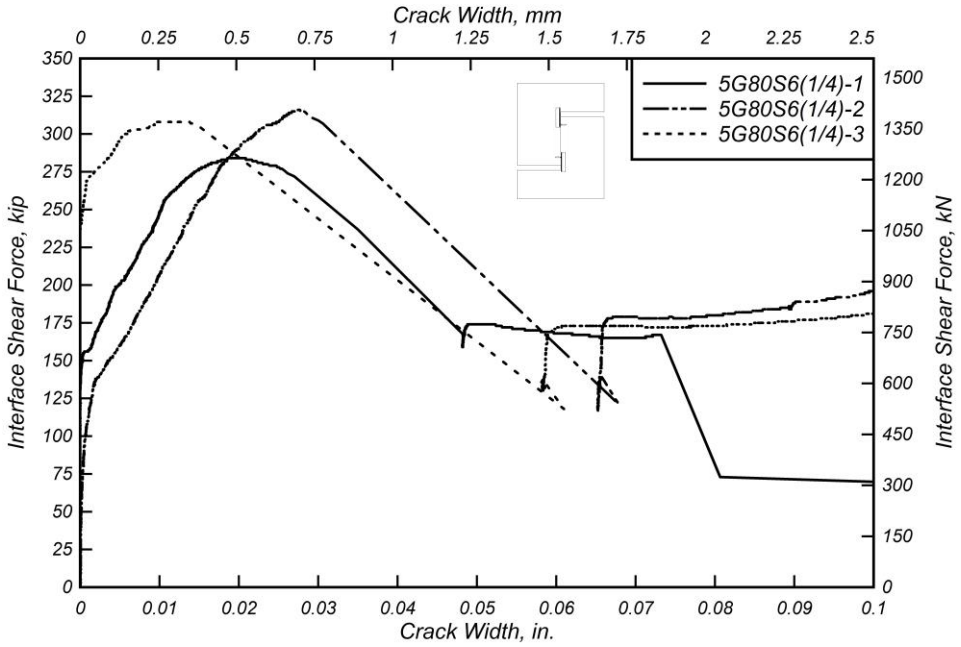

Figure 5.37: Interface shear force versus crack width for 5G80S6(1/4) specimens

Table 5.52: 4G80S4(1/4) Specimen Crack Width Measurements.

Specimen	w_{ult}, in. (mm)	V_{ult}, kip (kN)	w_b, in. (mm)	V_b, kip (kN)
4G80S6(1/4)-1	0.0188 (0.4767)	243.07 (1081.2)	0.1163 (2.955)	154.52 (687.35)
4G80S6(1/4)-2	0.0084 (0.2146)	186.03 (827.52)	0.1163 (2.953)	154.86 (688.84)
4G80S6(1/4)-3	0.0249 (0.6313)	224.61 (999.11)	0.1131 (2.874)	151.30 (673.03)
Mean	0.0174 (0.4409)	217.90 (969.28)	0.1152 (2.927)	153.56 (683.07)
Median	0.0188 (0.4767)	224.61 (999.11)	0.1163 (2.953)	154.52 (687.35)
STDEV	0.0083 (0.2106)	29.10 (129.45)	0.0018 (0.046)	1.962 (8.728)
COV	48%	13%	2%	1%

Table 5.53: 5G80S6(1/4) Specimen Crack Width Measurements.

Specimen	w_{ult}, in. (mm)	V_{ult}, kip (kN)	w_b, in. (mm)	V_b, kip (kN)
5G80S6(1/4)-1	0.0194 (0.4928)	283.85 (1262.6)	0.0672 (1.707)	206.76 (919.73)
5G80S6(1/4)-2	0.0275 (0.6985)	315.53 (1403.6)	0.1367 (3.472)	245.51 (1092.1)
5G80S6(1/4)-3	0.0100 (0.2533)	308.23 (1371.1)	0.1762 (4.477)	229.67 (1021.6)
Mean	0.0190 (0.4815)	302.54 (1345.7)	0.1267 (3.219)	227.31 (1011.1)
Median	0.0194 (0.4928)	308.23 (1371.1)	0.1367 (3.472)	229.67 (1021.6)
STDEV	0.0088 (0.2228)	16.59 (73.79)	0.0552 (1.402)	19.48 (86.65)
COV	46%	5%	44%	9%

Table 5.54: Summary of Crack Width Measurements for 4G80S6(1/4) and 5G80S6(1/4) (1/4 in. (6.35 mm)) Specimens.

Specimen	w_{ult}, in. (mm)	V_{ult}, kip (kN)	w_b, in. (mm)	V_b, kip (kN)
4G80S6(1/4)	0.0174 (0.4409)	217.90 (969.28)	0.1152 (2.927)	153.56 (683.07)
5G80S6(1/4)	0.0190 (0.4815)	302.54 (1345.7)	0.1267 (3.219)	227.31 (1011.1)

5.4.3.4 Interface Preparation: Exposed Aggregate

Figure 5.38 and Figure 5.39 present the interface shear force versus crack width response for specimen groups 4G80S6(EA) and 5G80S6(EA). All specimens discussed in this section were constructed with an EA interface preparation. Each figure shows the force-crack width response for all specimens in each group. Tabulated values of points of interest such as crack width at peak load and crack width at first bar fracture for each specimen group are presented in Table 5.55 and Table 5.56.

In Figure 5.38 specimen 4G80S6(EA)-1 shows a significantly lower post-crack stiffness compared to the other specimens in the group. As discussed in Section 0, these results indicate that exposing the aggregate of the interface surface may allow the aggregate interlock mechanism to contribute to the force-crack width response during the post-peak stage as is the case for specimens 4G80S6(EA)-2 and 4G80S6(EA)-3. However, this extended contribution by the aggregate interlock mechanism may not always develop, as it does not appear in the force-crack width response of specimen 4G80S6(EA)-1. During the sustained load phase of the force-crack width response it can be observed that specimens 4G80S6(EA)-2 and 4G80S6(EA)-3 maintained higher sustained loads. This appears to be related to the higher contribution of the aggregate interlock mechanism in these specimens, which may extend its contribution further into the post-peak phase of the response.

Figure 5.39 shows the interface shear force versus crack width response of specimen group 5G80S6(EA). In this figure specimen 5G80S6(EA)-1 exhibits similar behavior to specimens 4G80S6(EA)-2 and 4G80S6(EA)-3, exhibiting a high post-cracked stiffness and larger sustained load compared to the other specimens in the group. These results indicate that by using an Exposed Aggregate interface preparation, it may be possible to increase the contribution of the aggregate interlock mechanism not only in peak load capacity, but also in post-peak sustained load capacity. Additional testing and surface preparation trials using different aggregates and surface preparation mechanisms to develop the Exposed Aggregate surface finishing should be investigated.

Table 5.57 presents a summary of mean crack width points of interest for specimen groups 4G80S6(EA) and 5G80S6(EA). In this table specimens reinforced with #5 (#16M) reinforcing steel U-bars reach a higher peak load, V_{ult}, at lower crack width, w_{ult}. However, based on results from specimens 4G80S6(EA)-2, 4G80S6(EA)-3, and 5G80S6(EA)-1, it is important to perform further research into the use of an Exposed Aggregate shear interface.

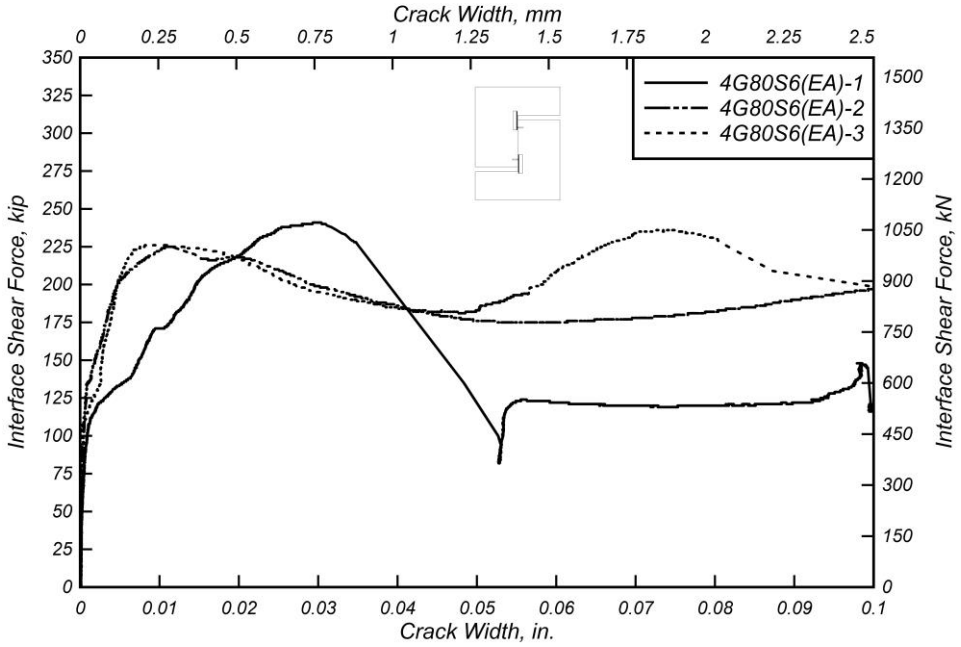

Figure 5.38: Interface shear force versus crack width for 4G80S6(EA) specimens

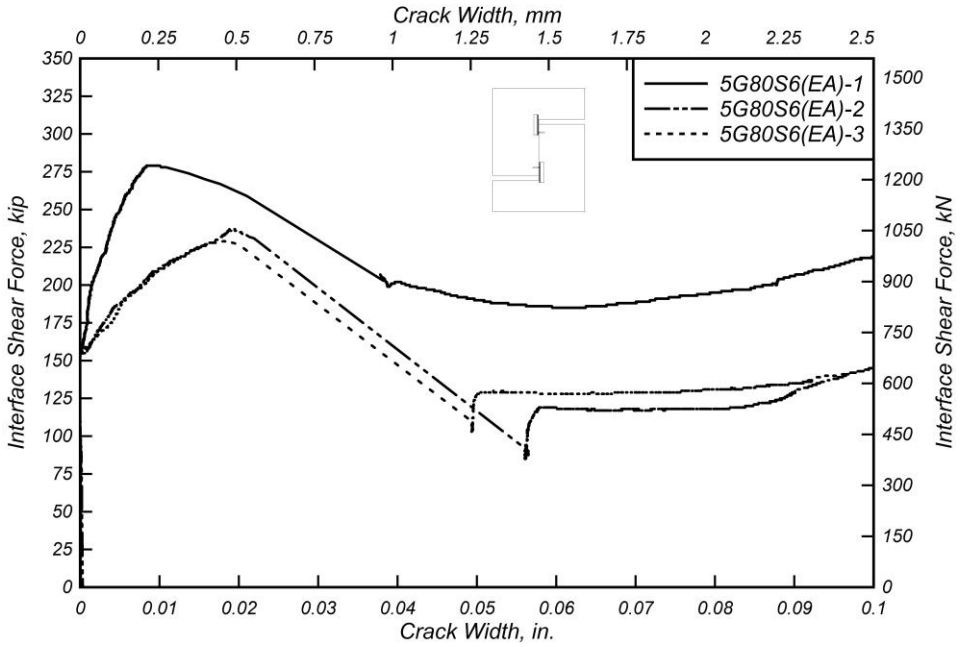

Figure 5.39: Interface shear force versus crack width for 5G80S6(EA) specimens

Table 5.55: 4G80S6(EA) Specimen Crack Width Measurements.

Specimen	w_{ult}, in. (mm)	V_{ult}, kip (kN)	w_b, in. (mm)	V_b, kip (kN)
4G80S6(EA)-1	0.0300 (0.7625)	241.11 (1072.5)	0.0993 (2.522)	145.13 (645.55)
4G80S6(EA)-2	0.0114 (0.2905)	225.49 (1003.0)	0.1432 (3.686)	230.33 (1024.6)
4G80S6(EA)-3	0.0093 (0.2371)	226.29 (1006.6)	0.0806 (2.048)	227.54 (1012.1)
Mean	0.0169 (0.4300)	230.96 (1027.4)	0.1077 (2.736)	201.00 (894.08)
Median	0.0114 (0.2905)	226.29 (1006.6)	0.0993 (2.522)	227.54 (1012.1)
STDEV	0.0114 (0.2829)	8.798 (39.13)	0.0321 (0.8158)	48.41 (215.32)
COV	67%	4%	30%	24%

Table 5.56: 5G80S6(EA) Specimen Crack Width Measurements.

Specimen	w_{ult}, in. (mm)	V_{ult}, kip (kN)	w_b, in. (mm)	V_b, kip (kN)
5G80S6(EA)-1	0.0090 (0.2290)	279.43 (1243.0)	0.1053 (2.675)	226.26 (1006.4)
5G80S6(EA)-2	0.0193 (0.4897)	236.63 (1052.6)	0.1200 (3.047)	140.96 (627.03)
5G80S6(EA)-3	0.0180 (0.4584)	229.12 (1019.2)	0.1259 (3.197)	148.27 (659.53)
Mean	0.0154 (0.3924)	248.39 (1104.9)	0.1170 (2.973)	171.83 (764.33)
Median	0.0180 (0.4584)	236.63 (1052.6)	0.1200 (3.047)	148.27 (659.53)
STDEV	0.0056 (0.1423)	27.14 (120.71)	0.0106 (0.2688)	47.28 (210.30)
COV	36%	11%	9%	28%

Table 5.57: Summary of Crack Width Measurements for 4G80S6(EA) and 5G80S6(EA) (Exposed Aggregate) Specimens.

Specimen	w_{ult}, in. (mm)	V_{ult}, kip (kN)	w_b, in. (mm)	V_b, kip (kN)
4G80S6(EA)	0.0169 (0.4300)	230.96 (1027.4)	0.1077 (2.736)	201.00 (894.08)
5G80S6(EA)	0.0154 (0.3924)	248.39 (1104.9)	0.1170 (2.973)	171.83 (764.33)

5.5 SUMMARY AND MAIN FINDINGS

This section provides a summary of experimental findings and a discussion on main findings regarding: (i) influence of reinforcing steel grade on shear interface capacity, (ii) influence of reinforcing steel bar spacing on shear interface capacity, and (iii) influence of reinforcing steel bar size on shear interface capacity. A comparison between experimentally measured capacity and calculated capacities per AASHTO and ACI 318-14 code provisions is also presented.

Figure 5.40 shows the peak shear stress (V_{ult}/A_c) normalized by actual concrete strength (f_c') versus the reinforcing steel ratio normalized by the concrete strength and the elastic modulus of the reinforcing steel. The effect analyzed in this figure is the influence of reinforcing steel grade, including data corresponding to test specimen groups 4G60S6(1/8), 4G80S6(1/8), 4G100S6(1/8), and 4G120S6(1/8) reinforced with Grade 60 (420 MPa), Grade 80 (550 MPa), Grade 100 (690 MPa), and Grade 120 (830 MPa), respectively. Note that all data points presented in this figure correspond to specimens with a shear interface roughened to an amplitude of 1/8 in. (3.175 mm). The figure also shows a thick line representing the AASHTO (2015) shear friction design equation (Equation 2-1), and a thin line representing the AASHTO (2015) shear friction design equation considering f_y = 80 ksi (550 MPa) nominal yield strength. Note that the thin line exceeds the current allowed limit of f_y = 60 ksi (420 MPa) yield strength. As observed in the figure, the data points are all above the lines, which indicates that increasing the nominal yield strength limit to 80 ksi (550 MPa) will maintain the conservative nature of the design equation. In the figure, it can be observed that one 4G80S6(1/8) specimen and one 4G120S6(1/8) specimen exhibited higher normalized peak shear stress compared to the rest of the specimens in the figure. However, the data points do not display an overall trend to show increased capacity as reinforcing steel grade increases.

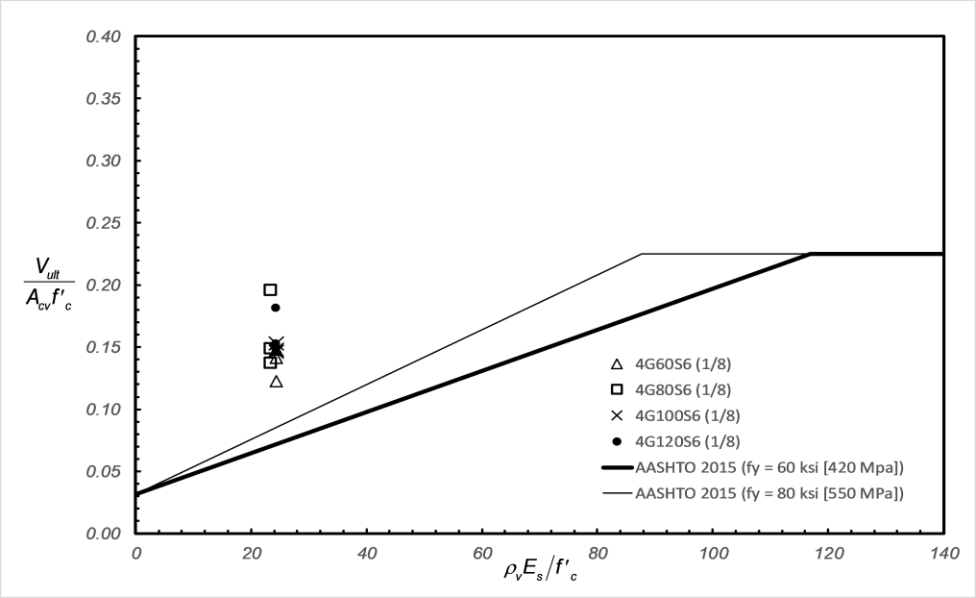

Figure 5.40: Experimental normalized peak shear stress versus normalized reinforcement stiffness across the interface – influence of reinforcing steel grade

Figure 5.41 shows the peak shear stress (V_{ult}/A_c) normalized by actual concrete strength (f_c') versus the reinforcing steel ratio normalized by the concrete strength and the elastic modulus of the reinforcing steel for specimens with different U-bar spacings. The figure presents data corresponding to test specimens 4G80S4(1/8), 4G80S6(1/8), and 4G80S12(1/8) constructed with reinforcing steel bars spaced at 4 in. (101.6 mm), 6 in. (152.4 mm), and 12 in. (304.8 mm), respectively. Additionally, this figure shows two lines. The first line corresponds to AASHTO (2015) shear friction design equation for a surface roughened to an amplitude of 1/8 in. (3.175 mm). The second line (thin line) corresponds to the same design equation with a nominal yield strength limit of f_y = 80 ksi (550 MPa). The figure shows that all data points are above the line, which is an indication that the design equation remains conservative when the nominal yield strength limit is increased to 80 ksi (550 MPa). Additionally, it can be observed that there is a trend of reaching larger peak loads as the reinforcing steel ratio increases. This indicates that steel reinforcement ratio significantly impacts the shear capacity, as it is directly related to the clamping force generated by the reinforcing steel bars crossing the interface.

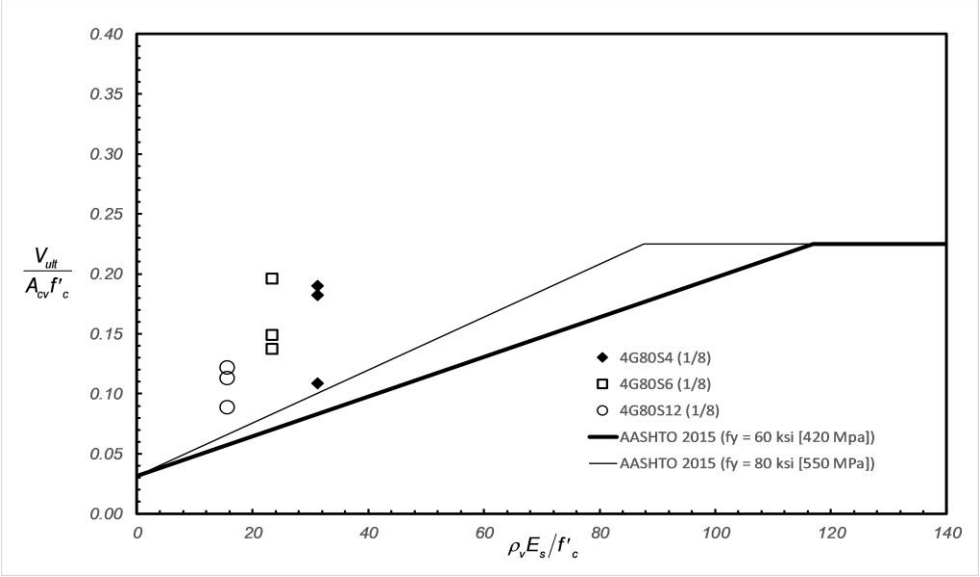

Figure 5.41: Experimental normalized peak shear stress versus normalized reinforcement stiffness across the interface – influence of reinforcing steel bar spacing.

Figure 5.42 shows the peak shear stress normalized by concrete strength versus the reinforcing steel ratio normalized by the concrete strength and the elastic modulus of the reinforcing steel for specimens with different bar sizes. The figure shows test data corresponding to test specimens constructed with reinforcing steel bars size #4 (#13M) and #5 (#16M). This figure includes AASHTO (2015) shear friction design equations curves corresponding to surface roughened to an amplitude of 1/4 in. (6.35 mm), surface not intentionally roughened (As Cast) and an EA surface. AASHTO (2015) does not include provisions for Exposed Aggregate. Therefore, it was taken as an interpolation between the 1/8 in. (3.175 mm) curve and the As Cast curve. Additionally, the figure includes the AASHTO (2015) mentioned considering a nominal yield strength of 80 ksi (550 MPa). It can be observed in the figure that all data points are above the

lines corresponding to each surface preparation. This indicates that the design equation will remain conservative if the nominal yield strength is increased to 80 ksi (550 MPa). The figure also shows a distinct pattern of increased interface shear capacity as the reinforcing steel bar size increases from #4 (#13M) to #5 (#16M).

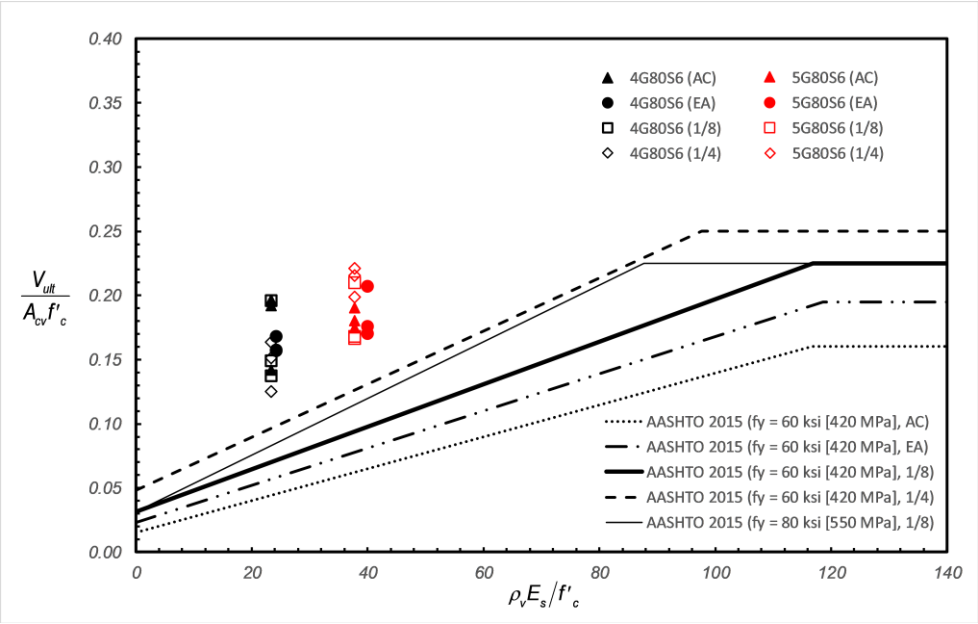

Figure 5.42: Experimental normalized peak shear stress versus normalized reinforcement stiffness across the interface – influence of reinforcing steel bar size.

Figure 5.43 and Figure 5.44 present the ratio of the experimentally measured peak loads, V_{ult}, to the shear capacity per AASHTO (2015) and ACI 318-14 code provisions, respectively. In these figures, each data set consists of two columns. The first column corresponds to the ratio considering the nominal yield strength of f_y = 80 ksi (550 MPa), or f_y = 100 ksi (690 MPa) and f_y = 120 ksi (830 MPa), for specimen groups 4G100S6(1/8) and 4G120S6(1/8), respectively. The second column corresponds to using the ratio considering the nominal yield strength limit of f_y = 60 ksi (420 MPa). Table 5.58 shows a summary of the ratio of experimentally measured shear resistance to nominal interface shear resistance per AASHTO (2015) and ACI 318-14, V_{ult}/V_{ni}. As seen in the table, increasing the nominal yield strength to 80 ksi (550 MPa) reduces the V_{ult}/V_{ni} ratio in all cases for both code provisions. These results indicate that an increase in the nominal yield strength limit to 80 ksi (550 MPa) will provide a more efficient design while remaining conservative for both AASHTO (2015) and ACI 318-14 code provisions. It is important to note that when considering f_y = 80 ksi (550 MPa) all specimen groups indicate V_{ult}/V_{ni} ratios greater than 1.5, except for specimen groups 4G120S6(1/8), 4G80S6(1/4), and 5G80S6(1/4), per AASHTO (2015) code provisions. All specimen groups indicate V_{ult}/V_{ni} ratios greater that 1.5 when considering f_y = 80 ksi (550 MPa), per ACI 318-14 code provisions.

From the presented data, the ACI 318-14 provisions result in higher V_{ult}/V_{ni} ratios when compared to the AASHTO (2015) provisions, therefore, increasing the nominal yield strength

limit to f_y = 80 ksi (550 MPa) would increase the efficiency while maintaining a conservative design. It is important to note that test specimens constructed with #4 (#13M) reinforcing steel bars and an As Cast surface preparation exhibited the highest V_{ult}/V_{ni} ratios. These results indicate that the interface shear capacity of this type of surface preparation may be underestimated which results in an overly conservative design.

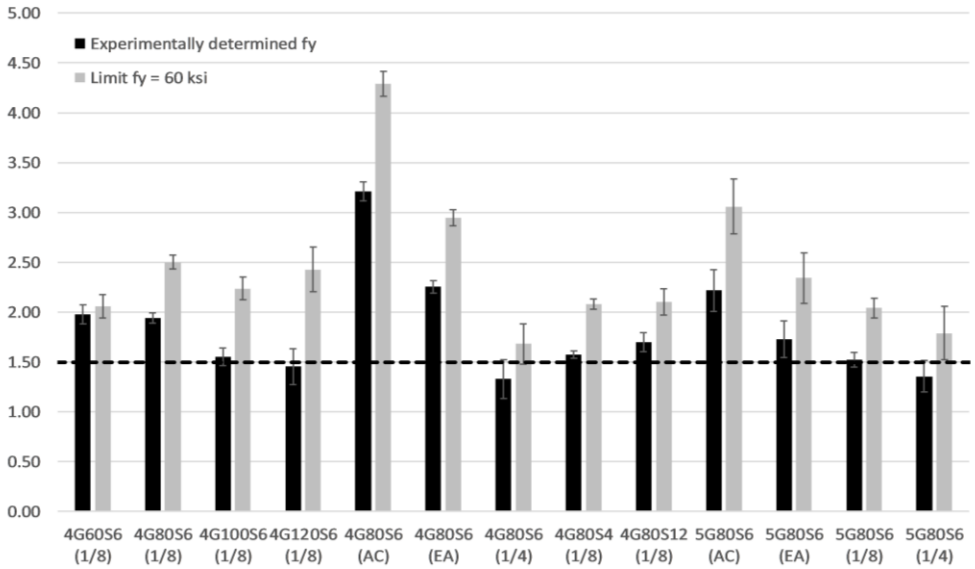

Figure 5.43: Comparison of experimentally measured strength with AASHTO (2015) calculated strength

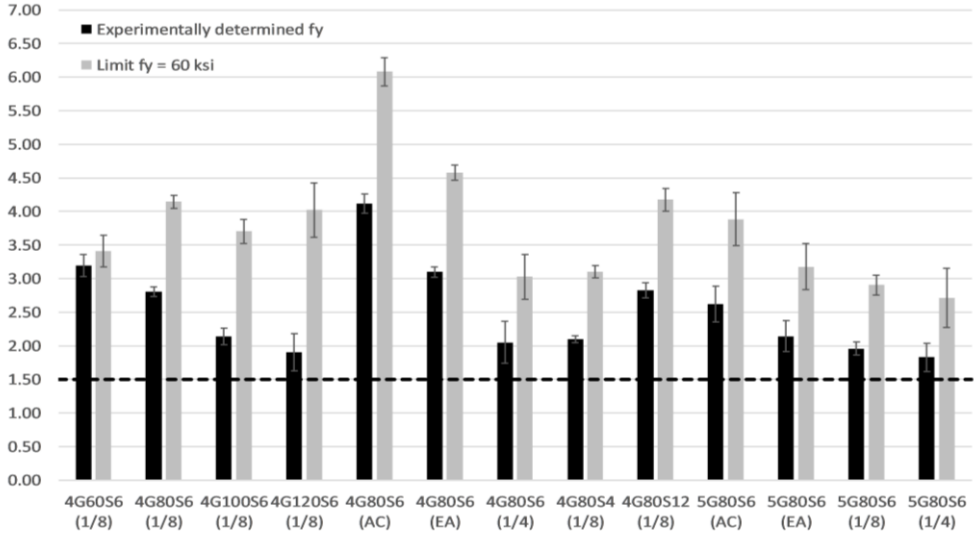

Figure 5.44: Comparison of experimentally measured strength with ACI 318-14 calculated strength

Table 5.58: Ratio of Measured Strength, V_{ult}, to Probable Strength, V_{ni}

Specimen label	V_{ult}, kip (kN)	AASHTO (2015) Section 5.8.4				ACI 318-14 Section 22.9			
		Experimental f_y		Limit f_y = 60 ksi (420 MPa)		Experimental f_y		Limit f_y = 60 ksi (420 MPa)	
		V_{ni}, kip (kN)	V_{ult}/V_{ni}	V_{ni}, kip (kN)	V_{ult}/V_{ni}	V_{nh}, kip (kN)	V_{ult}/V_{nh}	V_{nh}, kip (kN)	V_{ult}/V_{nh}
4G60S6(1/8)	196.33 (873.33)	99.28 (441.61)	1.98	95.40 (424.36)	2.06	61.48 (273.47)	3.19	57.60 (256.22)	3.41
4G80S6(1/8)	238.67 (1061.6)	122.88 (546.62)	1.94	95.40 (424.36)	2.50	85.08 (378.48)	2.81	57.60 (256.22)	4.14
4G100S6(1/8)	213.33 (948.95)	137.56 (611.91)	1.55	95.40 (424.36)	2.24	99.76 (443.77)	2.14	57.60 (256.22)	3.70
4G120S6(1/8)	231.67 (1030.5)	159.36 (708.89)	1.45	95.40 (424.36)	2.43	121.56 (540.75)	1.91	57.60 (256.22)	4.02
4G80S6(AC)	262.67 (1168.4)	81.81 (363.92)	3.21	61.20 (272.23)	4.29	63.81 (283.86)	4.12	43.20 (192.16)	6.08
4G80S6(EA)	230.67 (1026.1)	102.35 (455.27)	2.25	78.30 (348.30)	2.95	74.45 (331.17)	3.10	50.40 (224.19)	4.58
4G80S6(1/4)	218.00 (969.71)	163.96 (729.31)	1.33	129.60 (576.49)	1.68	106.36 (473.09)	2.05	72.00 (320.27)	3.03
4G80S4(1/8)	238.33 (1060.2)	151.25 (672.78)	1.58	114.60 (509.77)	2.08	113.45 (504.63)	2.10	76.80 (341.62)	3.10
4G80S12(1/8)	160.33 (713.20)	94.52 (420.46)	1.70	76.20 (338.95)	2.10	56.72 (252.32)	2.83	38.40 (170.81)	4.18
5G80S6(AC)	260.00 (1156.5)	117.26 (521.59)	2.22	84.96 (377.92)	3.06	99.26 (441.52)	2.62	66.96 (297.85)	3.88
5G80S6(EA)	248.33 (1104.6)	143.70 (639.21)	1.73	106.02 (471.60)	2.34	115.80 (515.10)	2.14	78.12 (347.49)	3.18
5G80S6(1/8)	259.33 (1153.6)	170.14 (756.83)	1.52	127.08 (565.28)	2.04	132.34 (588.69)	1.96	89.28 (397.14)	2.90
5G80S6(1/4)	302.67 (1346.3)	223.03 (992.08)	1.36	169.20 (752.64)	1.79	165.43 (735.86)	1.83	111.60 (496.42)	2.71

6.0 EFFECT OF SURFACE PREPARATION AND CONCRETE STRENGTH ON SHEAR FRICTION

6.1 INTRODUCTION

This chapter presents test results from push-off test specimens with a focus on establishing the effect of (1) surface preparation and (2) nominal concrete strength on shear friction. The details of each push-off test specimen discussed in this chapter can be found in the test matrix presented in Table 3.1, section (b) and (e). The discussion in this chapter focuses on results for interface shear force versus interface shear displacement, interface shear force versus strain, and interface shear force versus crack width. The methods implemented for data collection and the instrumentation utilized are presented in Section 3.5.

6.2 INFLUENCE OF SURFACE PREPARATION

This section focusses on the influence of interface preparation. All specimens discussed in this section are reinforced with three (3) #4 (#13M) or #5 (#16M) Grade 80 ksi (550 MPa) reinforcing steel U-bars spaced at 6 in. (152.4 mm) with a nominal design concrete strength of 5000 psi (35 MPa). Because the variable of interest in this discussion is interface preparation, the test specimens discussed in this section are constructed with As Cast, 1/8 in. (3.175 mm), 1/4 in. (6.35 mm), and Exposed Aggregate interface preparations. Details of the specimens such as bar size, bar spacing, and interface preparation can be found in section (b) of Table 3.1; drawings showing dimensions of the specimens, as well as location of the reinforcing steel U-bars are presented in Chapter 3. Properties of the reinforcing steel and the concrete used are presented in Section 4.1 and Section 4.2, respectively.

6.2.1 Interface Shear Force versus Interface Shear Displacement

6.2.1.1 Reinforcing Steel U-bar Size: #4 (#13M)

Figure 6.1 to Figure 6.4 present the interface shear force versus interface shear displacement response curves for specimen groups 4G80S6(AC), 4G80S6(1/8), 4G80S6(1/4), and 4G80S6(EA), respectively. Table 6.1 to Table 6.4 present tabulated values for the main characteristic points of the test results for the specimens. Discussions regarding Figure 6.1 to Figure 6.4 and Table 6.1 to Table 6.4 are presented in Section 5.4.1.

Table 6.5 presents mean values of the main points of interest of the interface shear force versus interface shear displacement response for specimen groups 4G80S6(AC), 4G80S6(1/8), 4G80S6(1/4), and 4G80S6(EA). From this table it can be observed that the

mean peak load, V_{ult}, is larger for specimen group 4G80S6(AC) with a V_{ult} value of 262.65 kip (1168.3 kN). The other specimen groups present mean peak load values ranging from 217.90 kip (969.28 kN) to 238.70 kip (1061.8 kN). A similar trend is observed when comparing V_{cr}, where the mean interface shear load at cracking is similar for specimen groups 4G80S6(1/8), 4G80S6(EA), and 4G80S6(1/4), with V_{cr} values 109.44 kip (486.80 kN), 109.92 kip (488.95 kN), and 111.37 kip (495.38 kN), respectively, while specimen group 4G80S6(AC) reaches a larger V_{cr} value of 142.83 kip (635.35 kN). These results indicate that specimens with an As Cast interface preparation not only formed a stronger concrete-to-concrete cohesion bond, thus reaching a larger V_{cr}, but also had a larger aggregate interlock contribution to the force-displacement response.

Specimen groups constructed with an interface preparation of 1/8 in. (3.175 mm) and 1/4 in. (6.35 mm) reached lower peak load values when compared to specimens constructed with an As Cast surface preparation, as mentioned in the previous paragraph. These results may be explained by comparing the maximum aggregate size and the size of the ridges present on the shear interface. The maximum aggregate size is 3/8 in. (9.525 mm), whereas the ridges on the shear interface have a depth of 1/8 in. (3.175 mm) and 1/4 in. (6.35 mm). The larger size of the maximum aggregates may cause voids to form, as they will not fit inside the ridges, thus weakening the concrete-to-concrete cohesion bond between the top and bottom layer of concrete.

From Table 6.5 it can be inferred that during post-peak stage of the force-displacement response, specimen groups 4G80S6(EA) outperforms all other specimen groups in terms of mean sustained load at first bar fracture, V_b, and energy dissipated by the specimen until first bar fracture, E_b. Specimen group 4G80S6(EA) reaches a V_b value of 201.00 kip (894.09 kN), which is 31% larger than the second highest V_b value. Additionally, specimen group 4G80S6(EA) reaches an E_b value of 16.86 kip-ft (22.86 kJ), which is 34% larger than the second highest E_b value. This significant increase in post-peak capacity appears to be related to the Exposed Aggregate interface preparation, as it may cause the aggregate interlock mechanism to extend its contribution to the post-peak shear capacity into the sustained load stage of the force-displacement response, as previously discussed in Section 0.

It is worth noting that, per current AASHTO and ACI design provisions, test specimens with an As Cast interface preparation are expected to perform at lower levels than test specimens do with an interface intentionally roughened. The results discussed in this section may indicate that the shear interface capacity of specimens constructed with an As Cast interface preparation is underestimated and, therefore, is unnecessarily conservative. Additional testing and surface preparation trials using different methods to obtain an As Cast surface preparation should be investigated.

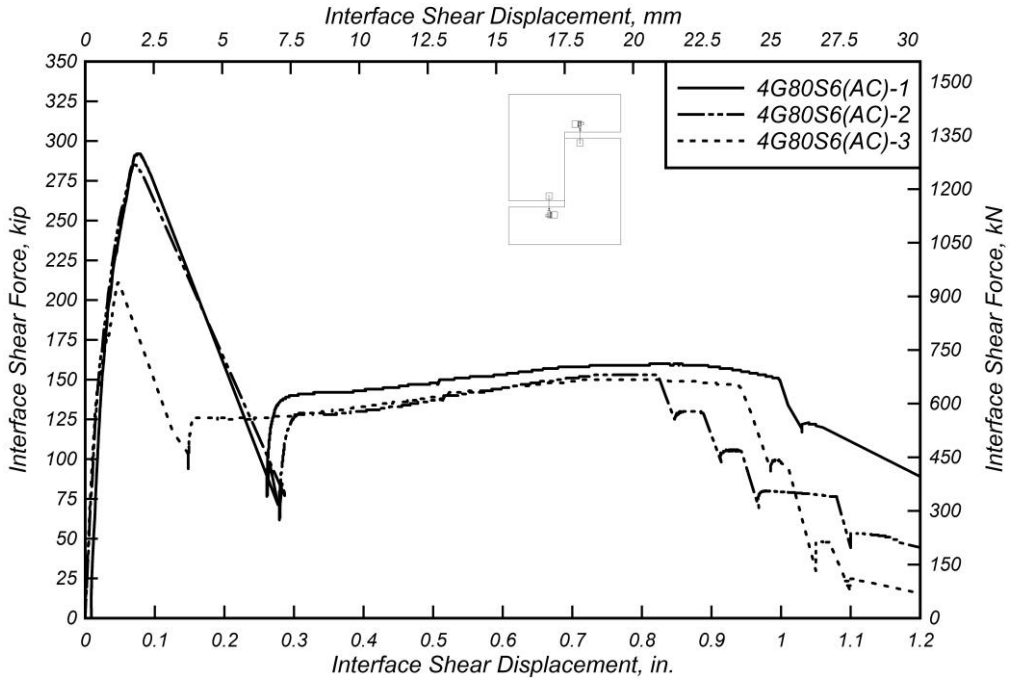

Figure 6.1: Interface shear force versus interface shear displacement for 4G80S6(AC) specimens.

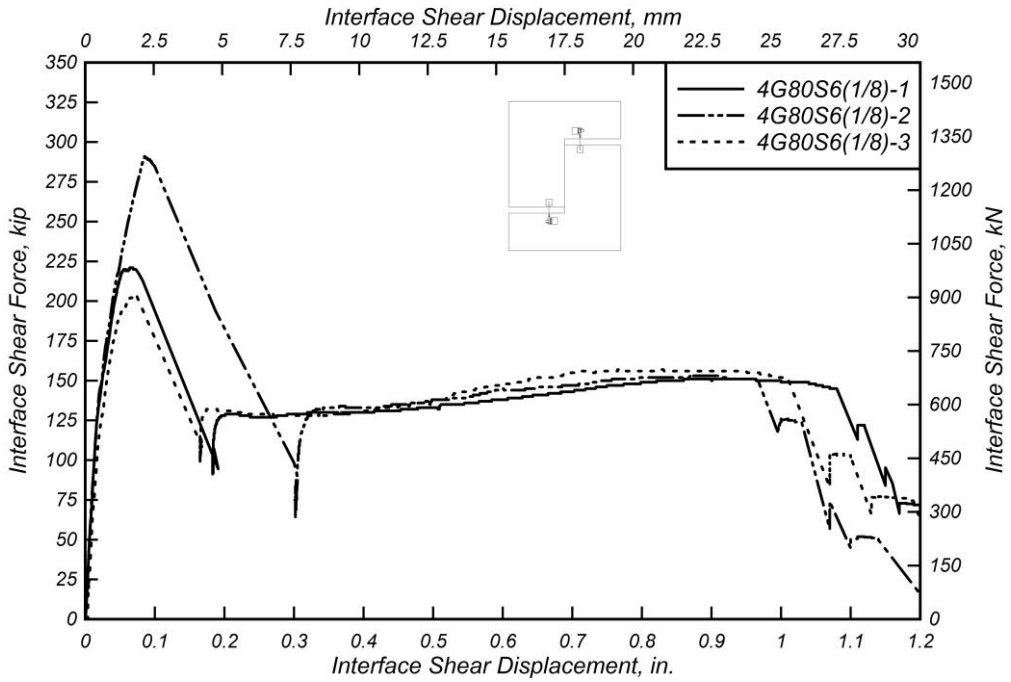

Figure 6.2: Interface shear force versus interface shear displacement the 4G80S6(1/8) specimens.

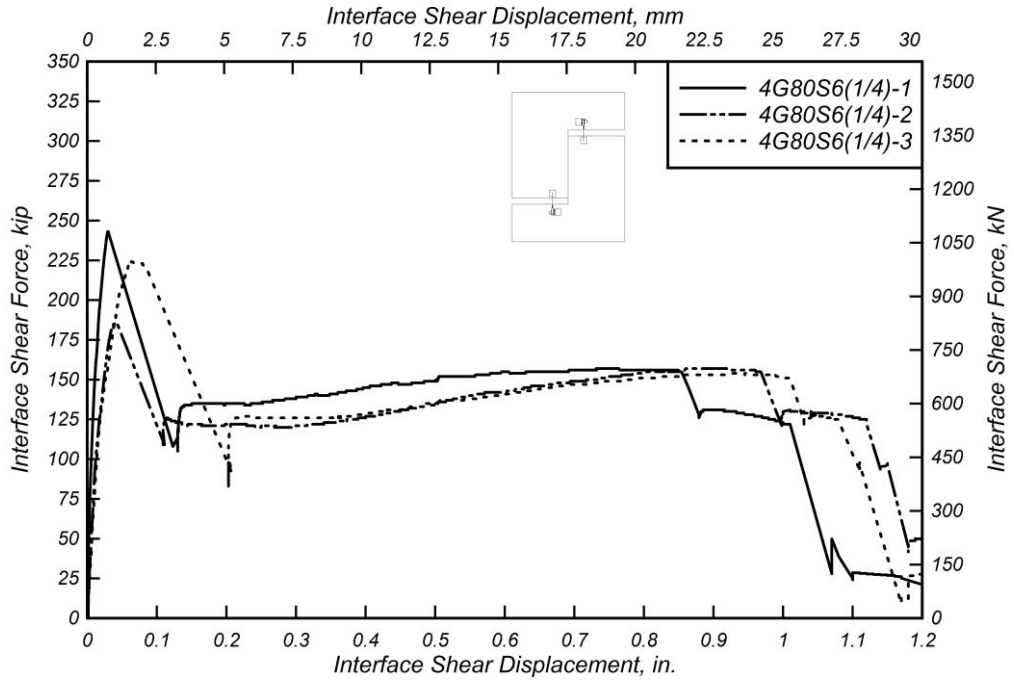

Figure 6.3: Interface shear force versus interface shear displacement for 4G80S6(1/4) specimens.

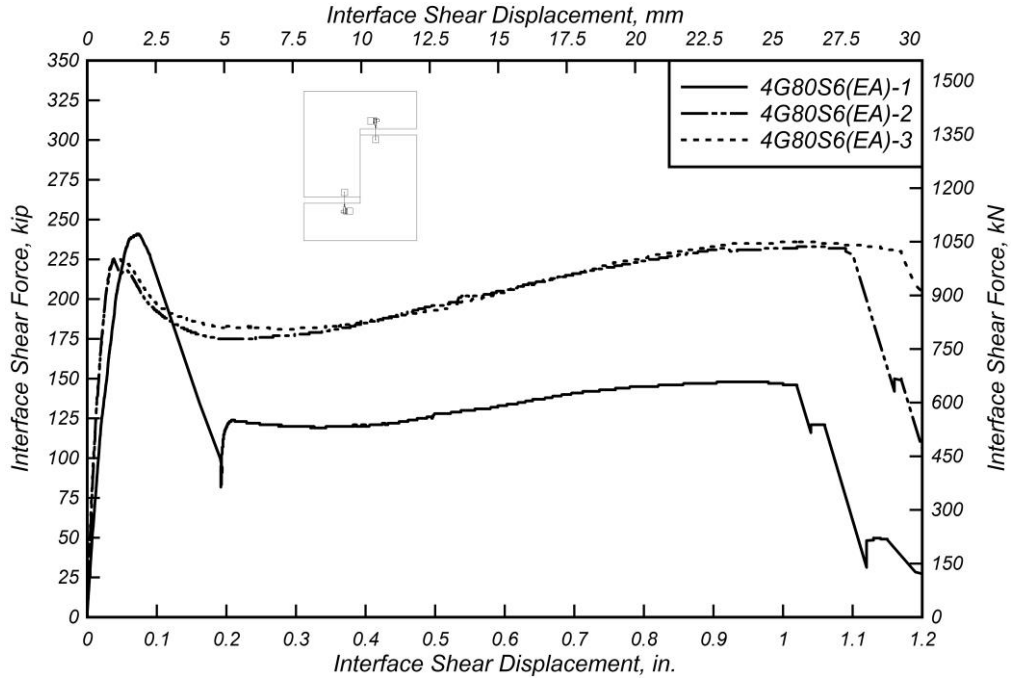

Figure 6.4: Interface shear force versus interface shear displacement for 4G80S6(EA) specimens.

Table 6.1: 4G80S6(AC) Specimen Shear Test Results.

Specimen	Δ_{ult}, in. (mm)	V_{ult}, kip (kN)	σ_{ult}, ksi (MPa)	$V_{sus,min}$, kip (kN)	$V_{sus,max}$, kip (kN)	Δ_{cr}, in. (mm)	V_{cr}, kip (kN)	Δ_b, in. (mm)	V_b, kip (kN)	E_b, kip-ft (kJ)
4G80S6 (AC)-1	0.077 (1.956)	292.03 (1299.0)	1.217 (8.389)	140.31 (624.13)	159.75 (710.60)	0.0213 (0.5410)	132.20 (588.05)	0.995 (25.27)	150.66 (670.17)	13.43 (18.21)
4G80S6 (AC)-2	0.072 (1.829)	284.98 (1267.7)	1.187 (8.187)	128.36 (570.97)	153.38 (682.27)	0.0195 (0.4953)	153.40 (682.36)	0.822 (20.88)	152.78 (679.60)	10.73 (14.55)
4G80S6 (AC)-3	0.048 (1.219)	210.93 (938.26)	0.879 (6.060)	125.31 (557.41)	150.42 (669.10)	0.0168 (0.4267)	142.90 (635.65)	0.941 (23.90)	145.46 (647.04)	11.07 (15.01)
Mean	0.066 (1.668)	262.65 (1168.3)	1.094 (7.545)	131.33 (584.17)	154.52 (687.32)	0.019 (0.488)	142.83 (635.35)	0.919 (23.35)	149.63 (665.60)	11.74 (15.92)
Median	0.072 (1.829)	284.98 (1267.7)	1.187 (8.187)	128.36 (570.97)	153.38 (682.27)	0.020 (0.495)	142.90 (635.65)	0.941 (23.90)	150.66 (670.17)	11.07 (15.01)
STDEV	0.0155 (0.394)	44.93 (199.84)	0.1872 (1.291)	7.928 (35.26)	4.768 (21.21)	0.0023 (0.058)	10.60 (47.15)	0.0885 (2.248)	3.766 (16.75)	1.470 (1.993)
COV	24%	17%	17%	6%	3%	12%	7%	10%	3%	13%

Table 6.2: 4G80S6(1/8) Specimen Shear Test Results.

Specimen	Δ_{ult}, in. (mm)	V_{ult}, kip (kN)	σ_{ult}, ksi (MPa)	$V_{sus,min}$, kip (kN)	$V_{sus,max}$, kip (kN)	Δ_{cr}, in. (mm)	V_{cr}, kip (kN)	Δ_b, in. (mm)	V_b, kip (kN)	E_b, kip-ft (kJ)
4G80S6 (1/8)-1	0.065 (1.651)	221.21 (983.99)	0.922 (6.355)	126.72 (563.68)	151.44 (673.64)	0.015 (0.373)	112.5 (500.42)	1.079 (27.41)	145.00 (644.99)	12.92 (17.52)
4G80S6 (1/8)-2	0.085 (2.159)	290.99 (1294.4)	1.212 (8.360)	132.37 (588.81)	152.83 (679.82)	0.016 (0.396)	119.00 (529.34)	0.962 (24.43)	150.57 (669.77)	12.73 (17.26)
4G80S6 (1/8)-3	0.070 (1.778)	203.91 (907.04)	0.850 (5.858)	127.94 (569.11)	156.60 (696.59)	0.016 (0.414)	96.81 (430.63)	1.012 (25.70)	151.03 (671.81)	12.19 (16.53)
Mean	0.073 (1.863)	238.70 (1061.8)	0.995 (6.858)	129.01 (573.86)	153.62 (683.35)	0.016 (0.395)	109.44 (486.80)	1.018 (25.85)	148.87 (662.19)	12.61 (17.10)
Median	0.070 (1.778)	221.21 (983.99)	0.922 (6.355)	127.94 (569.11)	152.83 (679.82)	0.016 (0.396)	112.50 (500.42)	1.012 (25.70)	150.57 (669.77)	12.73 (17.26)
STDEV	0.0104 (0.264)	46.10 (205.06)	0.1921 (1.324)	2.973 (13.22)	2.670 (11.88)	0.0008 (0.020)	11.41 (50.74)	0.0587 (1.491)	3.357 (14.93)	0.377 (0.512)
COV	14%	19%	19%	2%	2%	5%	10%	6%	2%	3%

Table 6.3: 4G80S6(1/4) Specimen Shear Test Results.

Specimen	Δ_{ult}, in. (mm)	V_{ult}, kip (kN)	σ_{ult}, ksi (MPa)	$V_{sus,min}$, kip (kN)	$V_{sus,max}$, kip (kN)	Δ_{cr}, in. (mm)	V_{cr}, kip (kN)	Δ_b, in. (mm)	V_b, kip (kN)	E_b, kip-ft (kJ)
4G80S6 (1/4)-1	0.030 (0.762)	243.07 (1081.2)	1.013 (6.983)	134.34 (597.57)	156.75 (697.26)	0.0068 (0.1727)	105.70 (470.18)	0.854 (21.69)	154.52 (687.34)	10.73 (14.55)
4G80S6 (1/4)-2	0.041 (1.041)	186.03 (827.50)	0.775 (5.344)	119.82 (532.99)	157.04 (698.55)	0.0139 (0.3531)	109.60 (487.52)	0.968 (24.59)	154.86 (688.85)	11.13 (15.09)
4G80S6 (1/4)-3	0.063 (1.600)	224.61 (999.11)	0.936 (6.453)	125.59 (558.65)	153.71 (683.74)	0.0170 (0.4318)	118.80 (528.45)	1.006 (25.55)	151.30 (673.02)	12.19 (16.52)
Mean	0.045 (1.135)	217.90 (969.28)	0.908 (6.260)	126.58 (563.07)	155.83 (693.18)	0.013 (0.319)	111.37 (495.38)	0.943 (23.94)	153.56 (683.07)	11.35 (15.39)
Median	0.041 (1.041)	224.61 (999.11)	0.936 (6.453)	125.59 (558.65)	156.75 (697.26)	0.014 (0.353)	109.60 (487.52)	0.968 (24.59)	154.52 (687.34)	11.13 (15.09)
STDEV	0.0168 (0.427)	29.11 (129.47)	0.1213 (0.836)	7.311 (32.52)	1.845 (8.205)	0.0052 (0.133)	6.726 (29.92)	0.0791 (2.009)	1.965 (8.739)	0.751 (1.018)
COV	38%	13%	13%	6%	1%	42%	6%	8%	1%	7%

Table 6.4: 4G80S6(EA) Specimen Shear Test Results.

Specimen	Δ_{ult}, in. (mm)	V_{ult}, kip (kN)	σ_{ult}, ksi (MPa)	$V_{sus,min}$, kip (kN)	$V_{sus,max}$, kip (kN)	Δ_{cr}, in. (mm)	V_{cr}, kip (kN)	Δ_b, in. (mm)	V_b, kip (kN)	E_b, kip-ft (kJ)
4G80S6 (EA)-1	0.073 (1.854)	241.11 (1072.5)	1.005 (6.927)	119.20 (530.23)	148.28 (659.58)	0.0174 (0.4420)	107.90 (635.35)	1.023 (25.98)	145.13 (645.57)	11.93 (16.17)
4G80S6 (EA)-2	0.038 (0.965)	225.49 (1003.0)	0.940 (6.478)	174.99 (778.39)	232.89 (1035.9)	0.0128 (0.3251)	129.90 (465.53)	1.094 (27.79)	230.33 (1024.6)	18.45 (25.01)
4G80S6 (EA)-3	0.040 (1.016)	226.29 (1006.6)	0.943 (6.501)	180.92 (804.77)	235.67 (1048.3)	0.0079 (0.1994)	91.96 (495.38)	1.173 (29.79)	227.54 (1012.1)	20.21 (27.40)
Mean	0.050 (1.278)	230.96 (1027.4)	0.962 (6.635)	158.37 (704.46)	205.61 (914.61)	0.013 (0.322)	109.92 (488.95)	1.097 (27.86)	201.00 (894.09)	16.86 (22.86)
Median	0.040 (1.016)	226.29 (1006.6)	0.943 (6.501)	174.99 (778.39)	232.89 (1035.9)	0.013 (0.325)	107.90 (635.35)	1.094 (27.79)	227.54 (1012.1)	18.45 (25.01)
STDEV	0.0197 (0.499)	8.796 (39.13)	0.0367 (0.253)	34.05 (151.47)	49.67 (220.95)	0.0048 (0.1213)	19.05 (84.74)	0.0750 (1.906)	48.40 (215.32)	4.363 (5.916)
COV	39%	4%	4%	22%	24%	38%	17%	7%	24%	26%

Table 6.5: Summary of Mean Values for each Specimen Group Analyzing Influence of Interface Preparation.

Specimen	Δ_{ult}, in. (mm)	V_{ult}, kip (kN)	σ_{ult}, ksi (MPa)	$V_{sus,min}$, kip (kN)	$V_{sus,max}$, kip (kN)	Δ_{cr}, in. (mm)	V_{cr}, kip (kN)	Δ_b, in. (mm)	V_b, kip (kN)	E_b, kip-ft (kJ)
4G80S6 (AC)	0.066 (1.668)	262.65 (1168.3)	1.094 (7.545)	131.33 (584.17)	154.52 (687.32)	0.019 (0.488)	142.83 (635.35)	0.919 (23.35)	149.63 (665.60)	11.74 (15.92)
4G80S6 (1/8)	0.073 (1.863)	238.70 (1061.8)	0.995 (6.858)	129.01 (573.86)	153.62 (683.35)	0.016 (0.395)	109.44 (486.80)	1.018 (25.85)	148.87 (662.19)	12.61 (17.10)
4G80S6 (1/4)	0.045 (1.135)	217.90 (969.28)	0.908 (6.260)	126.58 (563.07)	155.83 (693.18)	0.013 (0.319)	111.37 (495.38)	0.943 (23.94)	153.56 (683.07)	11.35 (15.39)
4G80S6 (EA)	0.050 (1.278)	230.96 (1027.4)	0.962 (6.635)	158.37 (704.46)	205.61 (914.61)	0.013 (0.322)	109.92 (488.95)	1.097 (27.86)	201.00 (894.09)	16.86 (22.86)

6.2.1.2 Reinforcing Steel U-bar size: #5 (#16M)

Figure 6.5 to Figure 6.6 present the interface shear force versus interface shear displacement response curves for specimen groups 5G80S6(AC), 5G80S6(1/8), 5G80S6(1/4), and 5G80S6(EA), respectively. Table 6.6 to Table 6.9 present tabulated values for the main points of interest regarding the mentioned specimen groups. Discussions regarding Figure 6.5 to Figure 6.8 and Table 6.6 to Table 6.9 are presented in Section 5.4.1.

Table 6.10 compares values of the main points of interest for specimen groups 5G80S6(AC), 5G80S6(1/8), 5G80S6(1/4), and 5G80S6(EA). As with Table 6.5, all data were used for the analysis and it can be seen that specimen group 5G80S6(1/4) exhibits a significantly large peak load, V_{ult}, at 302.54 kip (1345.7 kN). Values of V_{ult} for specimen groups 5G80S6(AC), 5G80S6(1/8), and 5G80S6(EA) are 259.87 kip (1156.0 kN), 259.52 kip (1154.4 kN), and 248.29 kip (11 kN), respectively. These results indicate that an interface roughness of 1/4 in. (6.35 mm) significantly increased the interface shear capacity compared to the other three types of interface preparation. It is worth noting that in test specimens constructed with #4 (#13M) reinforcing steel bars, specimens with an interface roughness of 1/4 in. (6.35 mm) reached the lowest peak load compared to the specimens with the three other surface preparations. In test specimens constructed with #5 (#16M) reinforcing steel bars, specimens with an interface roughness of 1/4 in. (6.35 mm) exhibited the largest peak load when compared to the specimens with the three other surface preparations. This indicates that the process of roughening the interface causes significant variability in test results. It is also worth noting that increasing reinforcing steel U-bar size from #4 (#13M) to #5 (#16M) increased V_{ult} in all cases of interface preparation, except for As Cast interface preparation.

During the post-peak stage of the force-displacement response, specimen groups 5G80S6(AC), 5G80S6(1/8), and 5G80S6(1/4) exhibited similar mean values of sustained loads at first bar fracture, V_b, ranging from 217.39 kip (967.00 kN) to 227.31 kip (1011.1 kN). Specimen group 5G80S6(EA) exhibited a significantly lower V_b of 171.83 kip (764.34 kN).

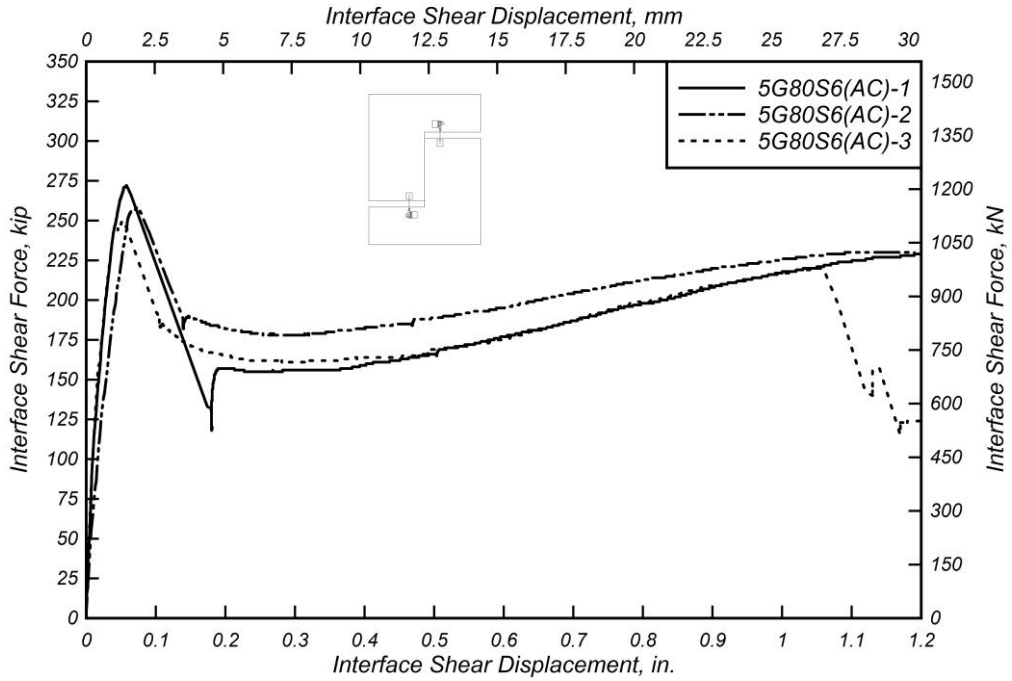

Figure 6.5: Interface shear force versus interface shear displacement for 5G80S6(AC) specimens.

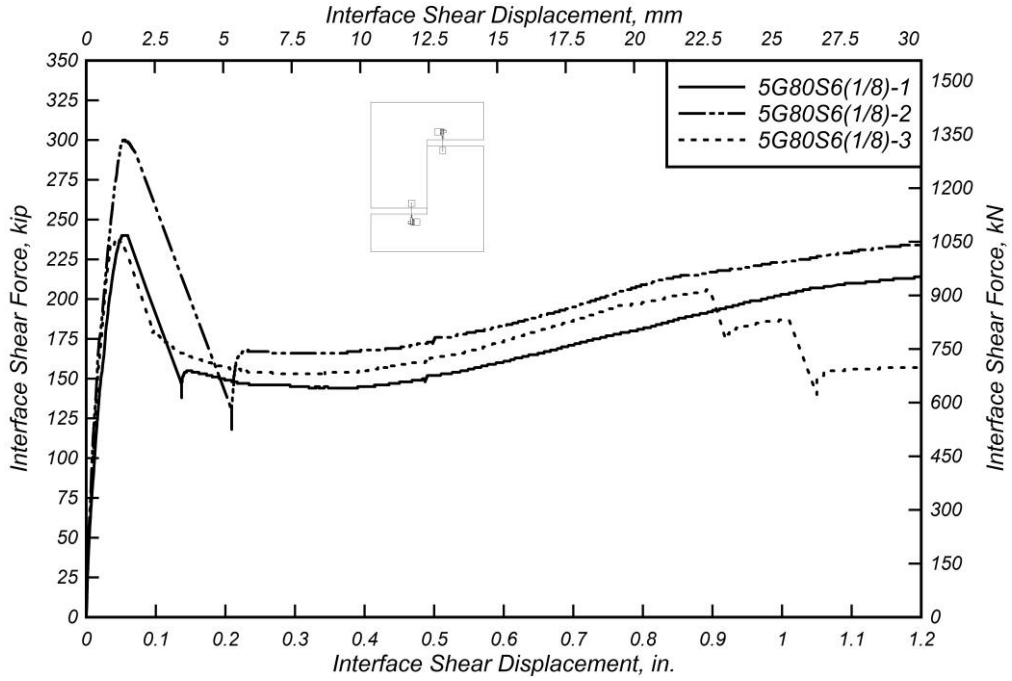

Figure 6.6: Interface shear force versus interface shear displacement the 5G80S6(1/8) specimens.

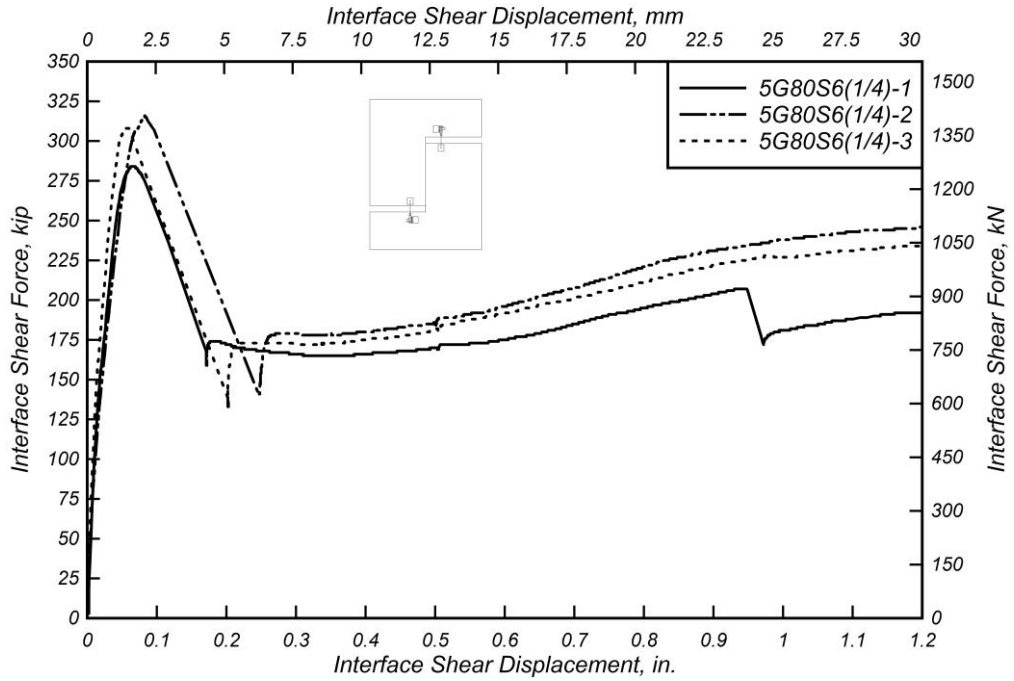

Figure 6.7: Interface shear force versus interface shear displacement for 5G80S6(1/4) specimens.

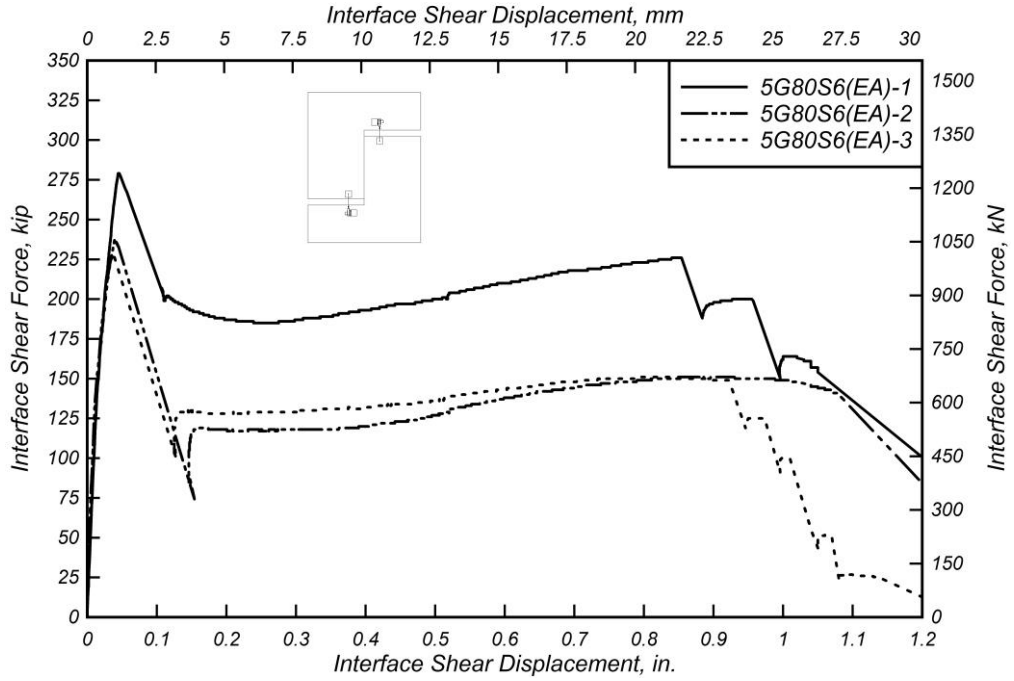

Figure 6.8: Interface shear force versus interface shear displacement for 5G80S6(EA) specimens.

Table 6.6: 5G80S6(AC) Specimen Shear Test Results.

Specimen	Δ_{ult}, in. (mm)	V_{ult}, kip (kN)	σ_{ult}, ksi (MPa)	$V_{sus,min}$, kip (kN)	$V_{sus,max}$, kip (kN)	Δ_{cr}, in. (mm)	V_{cr}, kip (kN)	Δ_b, in. (mm)	V_b, kip (kN)	E_b, kip-ft (kJ)
5G80S6 (AC)-1	0.058 (1.473)	271.63 (1208.3)	1.132 (7.803)	155.04 (689.65)	232.39 (1033.7)	0.0102 (0.2591)	108.00 (480.41)	1.456 (36.98)	225.46 (1002.9)	23.88 (32.38)
5G80S6 (AC)-2	0.071 (1.803)	257.72 (1146.4)	1.074 (7.404)	177.97 (791.65)	230.47 (1025.2)	0.0197 (0.5004)	116.50 (518.22)	1.215 (30.86)	228.09 (1014.6)	20.59 (27.92)
5G80S6 (AC)-3	0.052 (1.321)	250.26 (1113.2)	1.043 (7.190)	161.17 (716.92)	219.77 (977.59)	0.0171 (0.4343)	158.10 (703.26)	1.055 (26.80)	219.56 (976.65)	16.30 (22.10)
Mean	0.0603 (1.532)	259.87 (1156.0)	1.083 (7.466)	164.73 (732.74)	227.54 (1012.2)	0.0157 (0.3979)	127.53 (567.30)	1.242 (31.55)	224.37 (998.05)	20.26 (27.47)
Median	0.0580 (1.473)	257.72 (1146.4)	1.074 (7.404)	161.17 (716.92)	230.47 (1025.2)	0.0171 (0.4343)	116.50 (518.22)	1.215 (30.86)	225.46 (1002.9)	20.59 (27.92)
STDEV	0.0097 (0.247)	10.85 (48.25)	0.0452 (0.312)	11.87 (52.81)	6.800 (30.25)	0.0049 (0.1274)	26.81 (119.26)	0.2019 (5.127)	4.368 (19.43)	3.803 (5.157)
COV	16%	4%	4%	7%	3%	31%	21%	16%	2%	19%

Table 6.7: 5G80S6(1/8) Specimen Shear Test Results.

Specimen	$\Delta_{ult,}$ in. (mm)	V_{ult}, kip (kN)	σ_{ult}, ksi (MPa)	$V_{sus,min}$, kip (kN)	$V_{sus,max}$, kip (kN)	$\Delta_{cr,}$ in. (mm)	V_{cr}, kip (kN)	Δ_{b}, in. (mm)	V_{b}, kip (kN)	E_{b}, kip-ft (kJ)
5G80S6 (1/8)-1	0.053 (1.346)	240.38 (1069.3)	1.002 (6.906)	144.04 (640.72)	221.13 (983.63)	0.021 (0.544)	151.70 (674.79)	1.385 (35.18)	220.63 (981.41)	20.82 (28.23)
5G80S6 (1/8)-2	0.054 (1.372)	300.13 (1335.0)	1.251 (8.622)	165.55 (736.40)	234.51 (1043.2)	0.018 (0.457)	171.60 (763.31)	1.315 (33.40)	225.72 (1004.1)	22.29 (30.22)
5G80S6 (1/8)-3	0.044 (1.118)	238.06 (1058.9)	0.992 (6.839)	152.81 (679.73)	205.95 (916.11)	0.017 (0.432)	155.30 (690.81)	0.895 (22.73)	205.82 (915.53)	12.96 (17.57)
Mean	0.049 (1.232)	239.22 (1064.1)	0.997 (6.872)	148.43 (660.23)	213.54 (949.87)	0.019 (0.488)	153.50 (682.80)	1.140 (28.96)	213.23 (948.47)	16.89 (22.90)
Median	0.049 (1.232)	239.22 (1064.1)	0.997 (6.872)	148.43 (660.23)	213.54 (949.87)	0.019 (0.488)	153.50 (682.80)	1.140 (28.96)	213.23 (948.47)	16.89 (22.90)
STDEV	0.0064 (0.162)	1.640 (7.297)	0.0068 (0.047)	6.201 (27.58)	10.73 (47.75)	0.0031 (0.079)	2.546 (11.32)	0.3465 (8.801)	10.47 (46.58)	5.563 (7.542)
COV	13%	1%	1%	4%	5%	16%	2%	30%	5%	33%

Table 6.8: 5G80S6(1/4) Specimen Shear Test Results.

Specimen	Δ_{ult}, in. (mm)	V_{ult}, kip (kN)	σ_{ult}, ksi (MPa)	$V_{sus,min}$, kip (kN)	$V_{sus,max}$, kip (kN)	Δ_{cr}, in. (mm)	V_{cr}, kip (kN)	Δ_b, in. (mm)	V_b, kip (kN)	E_b, kip-ft (kJ)
5G80S6 (1/4)-1	0.064 (1.626)	283.85 (1262.6)	1.183 (8.154)	164.97 (733.82)	207.40 (922.56)	0.018 (0.4674)	152.60 (678.80)	0.948 (24.08)	206.76 (919.71)	14.71 (19.94)
5G80S6 (1/4)-2	0.083 (2.108)	315.53 (1403.5)	1.315 (9.065)	177.92 (791.43)	246.02 (1094.4)	0.014 (0.3480)	112.80 (501.76)	1.289 (32.74)	245.51 (1092.1)	23.18 (31.43)
5G80S6 (1/4)-3	0.054 (1.372)	308.23 (1371.1)	1.284 (8.855)	171.56 (763.14)	235.51 (1047.6)	0.012 (0.3073)	138.90 (617.86)	1.359 (34.52)	229.67 (1021.6)	23.57 (31.95)
Mean	0.067 (1.702)	302.54 (1345.7)	1.261 (8.691)	171.48 (762.80)	229.64 (1021.5)	0.015 (0.3742)	134.77 (599.47)	1.199 (30.45)	227.31 (1011.1)	20.48 (27.77)
Median	0.064 (1.626)	308.23 (1371.1)	1.284 (8.855)	171.56 (763.14)	235.51 (1047.6)	0.014 (0.3480)	138.90 (617.86)	1.289 (32.74)	229.67 (1021.6)	23.18 (31.43)
STDEV	0.0147 (0.374)	16.59 (73.79)	0.0691 (0.477)	6.475 (28.80)	19.97 (88.82)	0.0033 (0.0832)	20.22 (89.94)	0.2199 (5.585)	19.48 (86.66)	5.008 (6.790)
COV	22%	5%	5%	4%	9%	22%	15%	18%	9%	24%

Table 6.9: 5G80S6(EA) Specimen Shear Test Results.

Specimen	Δ_{ult}, in. (mm)	V_{ult}, kip (kN)	σ_{ult}, ksi (MPa)	$V_{sus,min}$, kip (kN)	$V_{sus,max}$, kip (kN)	Δ_{cr}, in. (mm)	V_{cr}, kip (kN)	Δ_b, in. (mm)	V_b, kip (kN)	E_b, kip-ft (kJ)
5G80S6 (EA)-1	0.045 (1.143)	279.43 (1243.0)	1.164 (8.028)	185.15 (823.59)	226.21 (1006.2)	0.0116 (0.2946)	120.50 (567.30)	0.854 (21.69)	226.26 (1006.5)	14.52 (19.69)
5G80S6 (EA)-2	0.040 (1.016)	236.33 (1051.2)	0.985 (6.789)	117.23 (521.46)	150.66 (670.17)	0.0132 (0.3353)	148.60 (709.64)	1.076 (27.33)	140.96 (627.02)	12.49 (16.93)
5G80S6 (EA)-3	0.037 (0.940)	229.12 (1019.2)	0.955 (6.582)	128.03 (569.51)	151.17 (672.44)	0.0106 (0.2692)	126.20 (599.47)	0.923 (23.44)	148.27 (659.54)	10.95 (14.85)
Mean	0.039 (0.978)	232.73 (1035.2)	0.970 (6.686)	122.63 (545.49)	150.92 (671.30)	0.012 (0.302)	137.40 (641.14)	1.000 (25.39)	144.62 (643.28)	11.72 (15.89)
Median	0.039 (0.978)	232.73 (1035.2)	0.970 (6.686)	122.63 (545.49)	150.92 (671.30)	0.012 (0.302)	137.40 (641.14)	1.000 (25.39)	144.62 (643.28)	11.72 (15.89)
STDEV	0.0021 (0.054)	5.098 (22.68)	0.0212 (0.147)	7.637 (33.97)	0.3606 (1.604)	0.0018 (0.0467)	15.84 (58.92)	0.1082 (2.748)	5.169 (22.99)	1.087 (1.474)
COV	6%	2%	2%	6%	0%	15%	12%	11%	4%	9%

Table 6.10: Summary of Mean Values for Specimen Groups Analyzing Influence of Interface Preparation.

Specimen	Δ_{ult}, in. (mm)	V_{ult}, kip (kN)	σ_{ult}, ksi (MPa)	$V_{sus,min}$, kip (kN)	$V_{sus,max}$, kip (kN)	Δ_{cr}, in. (mm)	V_{cr}, kip (kN)	Δ_b, in. (mm)	V_b, kip (kN)	E_b, kip-ft (kJ)
5G80S6 (AC)	0.0603 (1.532)	259.87 (1156.0)	1.083 (7.466)	164.73 (732.74)	227.54 (1012.2)	0.0157 (0.3979)	127.53 (567.30)	1.242 (31.55)	224.37 (998.05)	20.26 (27.47)
5G80S6 (1/8)	0.049 (1.232)	239.22 (1064.1)	0.997 (6.872)	148.43 (660.23)	213.54 (949.87)	0.019 (0.488)	153.50 (682.80)	1.140 (28.96)	213.23 (948.47)	16.89 (22.90)
5G80S6 (1/4)	0.067 (1.702)	302.54 (1345.7)	1.261 (8.691)	171.48 (762.80)	229.64 (1021.5)	0.015 (0.3742)	134.77 (599.47)	1.199 (30.45)	227.31 (1011.1)	20.48 (27.77)
5G80S6 (EA)	0.039 (0.978)	232.73 (1035.2)	0.970 (6.686)	122.63 (545.49)	150.92 (671.30)	0.012 (0.302)	137.40 (641.14)	1.000 (25.39)	144.62 (643.28)	11.72 (15.89)

6.2.2 Interface Shear Force versus Strain

6.2.2.1 Reinforcing Steel U-bar Size: #4 (#13M)

Figure 6.9 to Figure 6.12 show the interface shear force versus reinforcing steel U-bar strain relationships for specimen groups 4G80S6(AC), 4G80S6(1/8), 4G80S6(1/4), and 4G80S6(EA), respectively. The curves shown correspond to the mean strain measurements from all strain gauges contained in each test specimen plotted versus the interface shear force. Table 6.11 to Table 6.14 presents tabulated values for the main points of interest regarding the mentioned specimen groups. As can be observed in these tables, several strain gauges were damaged before the peak load was reached, thus limiting the analysis that can be carried out with the strain gauge data. Additionally, significant variability was observed in the strain gauge measurements with COV values ranging from 7% to 59%. Discussions regarding Figure 6.9 to Figure 6.12 and Table 6.11 to Table 6.14 are presented in Section 5.4.2.

Table 6.15 shows a comparison of the mean interface shear strain for specimen groups 4G80S6(AC), 4G80S6(1/8), 4G80S6(1/4), and 4G80S6(EA). It can be inferred from this table that specimen group 4G80S6(EA) reaches its peak load at a significantly lower strain value compared to the other specimen groups. This behavior is consistent with results discussed in Section 6.2.1 and Section 0, as the Exposed Aggregate interface preparation appears to reduce the interface shear displacement and crack width at peak load. Note that for specimens discussed in this section, the reinforcing steel strain only surpasses the nominal yield strain of 2760 microstrain after the peak interface shear load is reached.

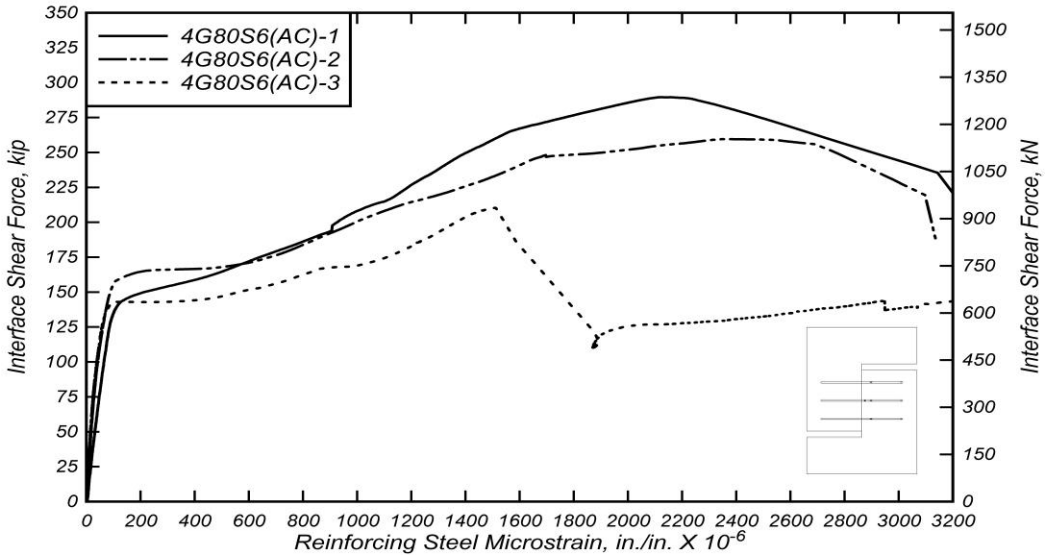

Figure 6.9: Interface shear force versus mean reinforcing steel microstrain for 4G80S6(AC) specimens.

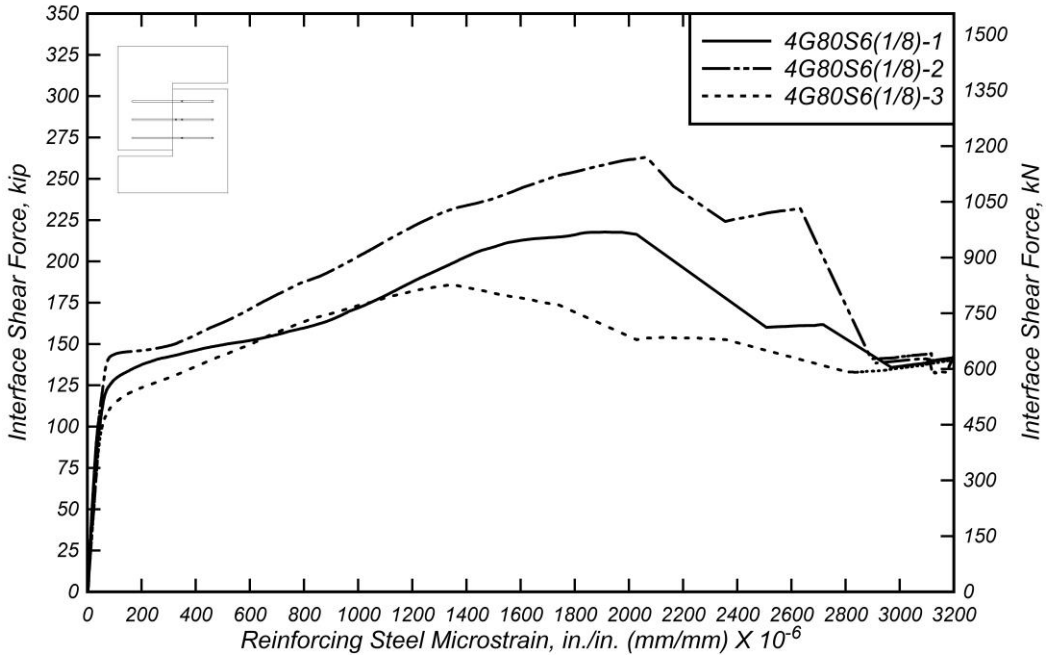

Figure 6.10: Interface shear force versus mean reinforcing steel microstrain for 4G80S6(1/8) specimens.

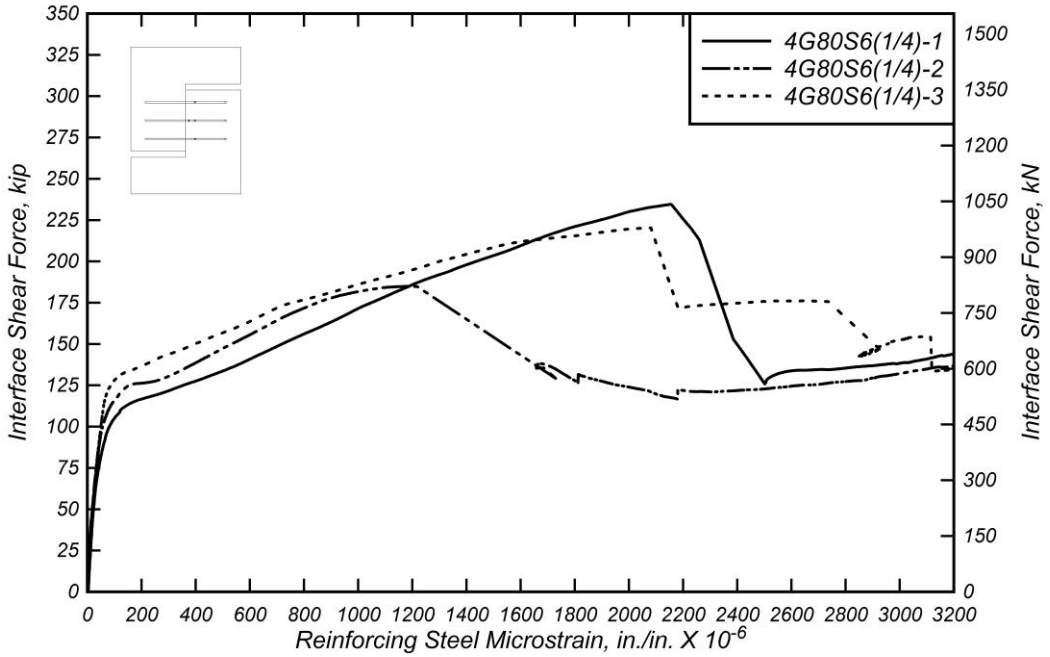

Figure 6.11: Interface shear force versus mean reinforcing steel microstrain for 4G80S6(1/4) specimens.

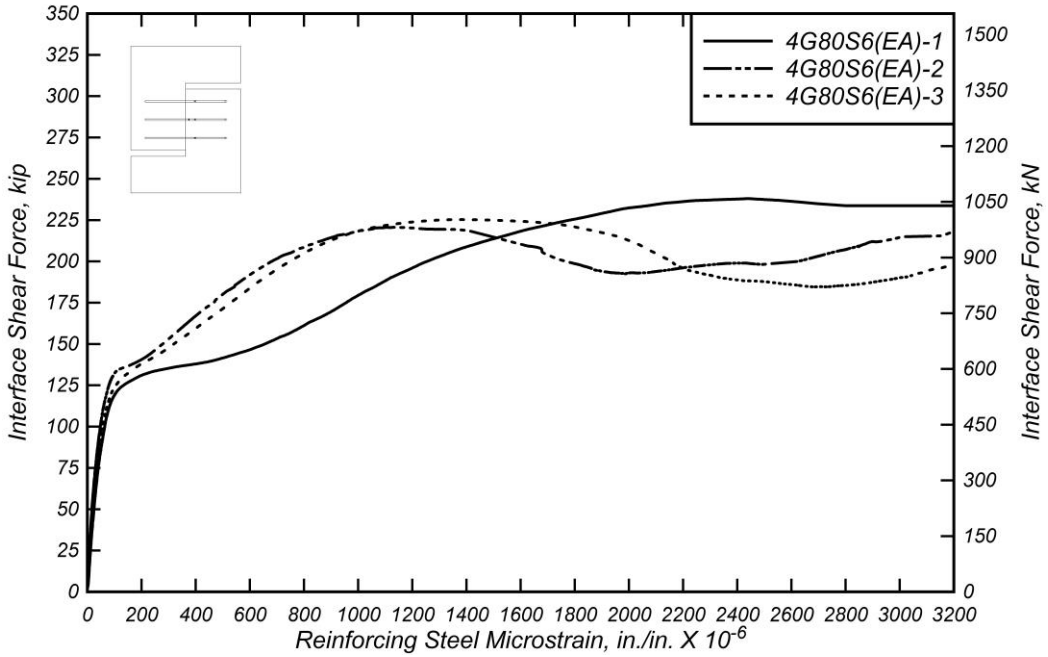

Figure 6.12: Interface shear force versus mean reinforcing steel microstrain for 4G80S6(EA) specimens.

Table 6.11: 4G80S6(AC) Specimen Strain Gauge Readings at Peak Interface Shear Force.

Specimen	s_1, in./in. (mm/mm)	s_2, in./in. (mm/mm)	s_3, in./in. (mm/mm)	s_4, in./in. (mm/mm)	s_5, in./in. (mm/mm)	s_6, in./in. (mm/mm)	s_7, in./in. (mm/mm)
4G80S6(AC)-1	-	-	-	0.0027	-	0.0023	0.0017
4G80S6(AC)-2	0.0027	0.0023	-	-	0.0031	-	0.0017
4G80S6(AC)-3	-	-	0.0018	0.0025	0.0015	-	0.0015
Mean	0.0027	0.0023	0.0018	0.0026	0.0023	0.0023	0.0016
Median	0.0027	0.0023	0.0018	0.0026	0.0023	0.0023	0.0017
STDEV	-	-	-	0.0002	0.0011	-	0.0001
COV	-	-	-	7%	47%	-	9%

Table 6.12: 4G80S6(1/8) Specimen Strain Gauge Readings at Peak Interface Shear Force.

Specimen	s_1, in./in. (mm/mm)	s_2, in./in. (mm/mm)	s_3, in./in. (mm/mm)	s_4, in./in. (mm/mm)	s_5, in./in. (mm/mm)	s_6, in./in. (mm/mm)	s_7, in./in. (mm/mm)
4G80S6(1/8)-1	-	-	0.0019	-	0.0025	0.0018	-
4G80S6(1/8)-2	-	-	-	-	0.0030	0.0025	0.0017
4G80S6(1/8)-3	-	0.0022	-	0.0026	-	0.0018	0.0012
Mean	-	0.0022	0.0019	0.0026	0.0028	0.0021	0.0015
Median	-	0.0022	0.0019	0.0026	0.0028	0.0018	0.0015
STDEV	-	-	-	-	0.0004	0.0004	0.0004
COV	-	-	-	-	13%	19%	26%

Table 6.13: 4G80S6(1/4) Specimen Strain Gauge Readings at Peak Interface Shear Force.

Specimen	s_1, in./in. (mm/mm)	s_2, in./in. (mm/mm)	s_3, in./in. (mm/mm)	s_4, in./in. (mm/mm)	s_5, in./in. (mm/mm)	s_6, in./in. (mm/mm)	s_7, in./in. (mm/mm)
4G80S6(1/4)-1	0.0026	-	-	0.0026	0.0024	0.0021	-
4G80S6(1/4)-2	0.0011	-	-	-	0.0012	0.0014	-
4G80S6(1/4)-3	-	0.0021	-	-	0.0025	0.0016	0.0013
Mean	0.0018	0.0021	-	0.0026	0.0020	0.0017	0.0013
Median	0.0018	0.0021	-	0.0026	0.0024	0.0016	0.0013
STDEV	0.0010	-	-	-	0.0007	0.0004	-
COV	55%	-	-	-	36%	21%	-

Table 6.14: 4G80S6(EA) Specimen Strain Gauge Readings at Peak Interface Shear Force.

Specimen	s_1, in./in. (mm/mm)	s_2, in./in. (mm/mm)	s_3, in./in. (mm/mm)	s_4, in./in. (mm/mm)	s_5, in./in. (mm/mm)	s_6, in./in. (mm/mm)	s_7, in./in. (mm/mm)
4G80S6(EA)-1	0.0016	0.0025	0.0024	0.0023	0.0017	0.0024	0.0028
4G80S6(EA)-2	-	0.0012	0.0011	0.0018	-	0.0015	0.0009
4G80S6(EA)-3	0.0014	0.0016	0.0013	0.0019	0.0011	0.0013	0.0013
Mean	0.0015	0.0018	0.0016	0.0020	0.0014	0.0017	0.0017
Median	0.0015	0.0016	0.0013	0.0019	0.0014	0.0015	0.0013
STDEV	0.0001	0.0006	0.0007	0.0003	0.0004	0.0006	0.0010
COV	9%	37%	44%	14%	33%	35%	59%

Table 6.15: Summary of Mean Values of Strain Gauge Readings of each Specimen Group Analyzing Influence of Interface Preparation.

Specimen	s_1, in./in. (mm/mm)	s_2, in./in. (mm/mm)	s_3, in./in. (mm/mm)	s_4, in./in. (mm/mm)	s_5, in./in. (mm/mm)	s_6, in./in. (mm/mm)	s_7, in./in. (mm/mm)
4G80S6(AC)	0.0027	0.0023	0.0018	0.0026	0.0023	0.0023	0.0016
4G80S6(1/8)	-	0.0022	0.0019	0.0026	0.0028	0.0021	0.0015
4G80S6(1/4)	0.0018	0.0021	-	0.0026	0.0020	0.0017	0.0013
4G80S6(EA)	0.0015	0.0018	0.0016	0.0020	0.0014	0.0017	0.0017

6.2.2.2 Reinforcing Steel U-bar Size: #5 (#16M)

Figure 6.13 to Figure 6.16 present the interface shear force versus reinforcing steel U-bar strain relationship for specimen groups 5G80S6(AC), 5G80S6(1/8), 5G80S6(1/4), and 5G80S6(EA), respectively. The curves shown correspond to the mean values of strain measurements from all strain gauges contained in each test specimen plotted versus the interface shear force (when available). Table 6.16 to Table 6.19 present tabulated values for the main points of interest regarding the mentioned specimen groups. Note that the "-" in the tables indicates no data were available from the strain gauges (or no strain gauge was installed at this location). As noted earlier, several strain gauges were damaged before the peak load was reached, thus limiting the analysis that can be carried out with the strain gauges data. Additionally, significant variability was observed in the strain gauge measurements with COV values ranging from 3% to 37%. Discussions regarding Figure 6.13 to Figure 6.16 and Table 6.16 to Table 6.19 are presented in Section 5.4.2.

Table 6.20 shows a comparison of strain gauge measurements at peak load for specimen groups 5G80S6(AC), 5G80S6(1/8), 5G80S6(1/4), and 5G80S6(EA). From this table it can be observed that all specimen groups exhibited similar mean strain values at peak load. Note that for specimens discussed in this section, the reinforcing steel strain only surpasses the nominal yield strain of 2760 microstrain after the peak interface shear load is reached.

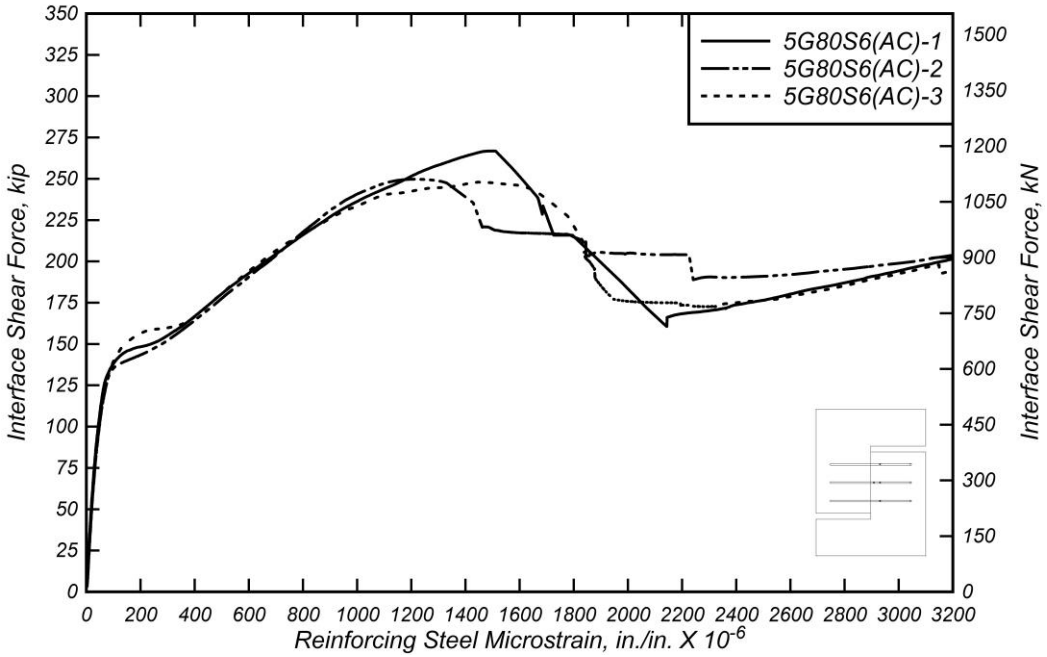

Figure 6.13: Interface shear force versus mean reinforcing steel microstrain for 5G80S6(AC) specimens.

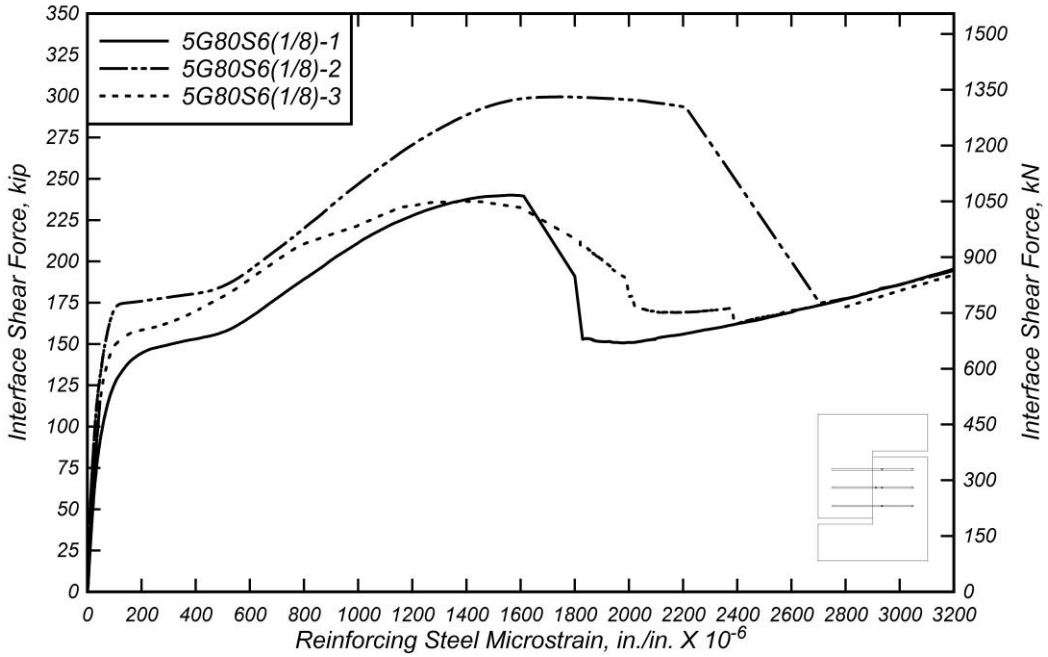

Figure 6.14: Interface shear force versus mean reinforcing steel microstrain for 5G80S6(1/8) specimens.

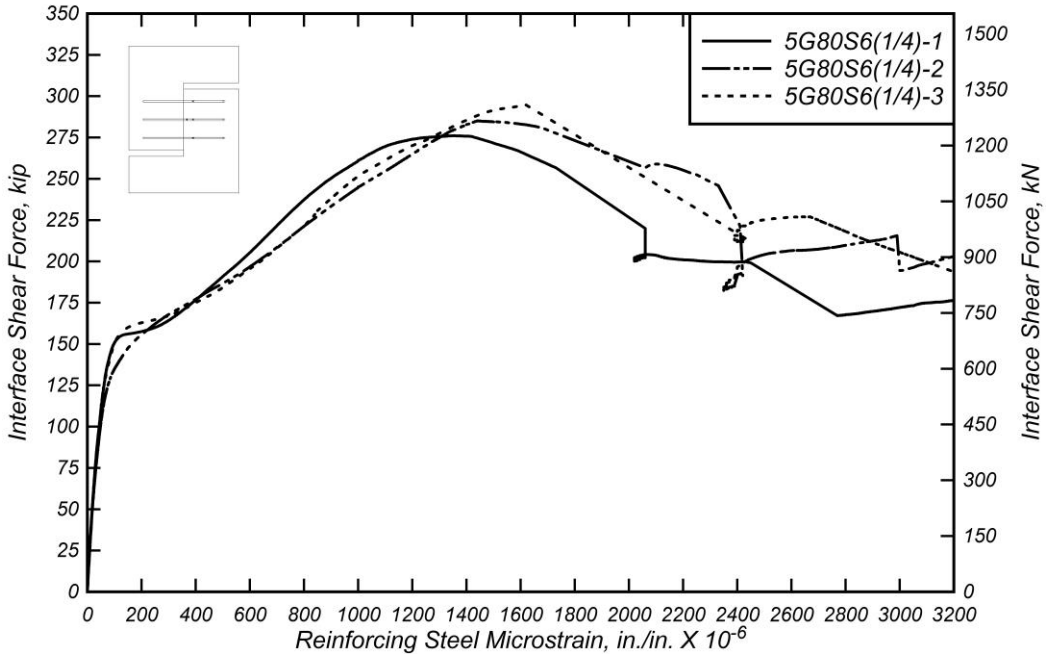

Figure 6.15: Interface shear force versus mean reinforcing steel microstrain for 5G80S6(1/4) specimens.

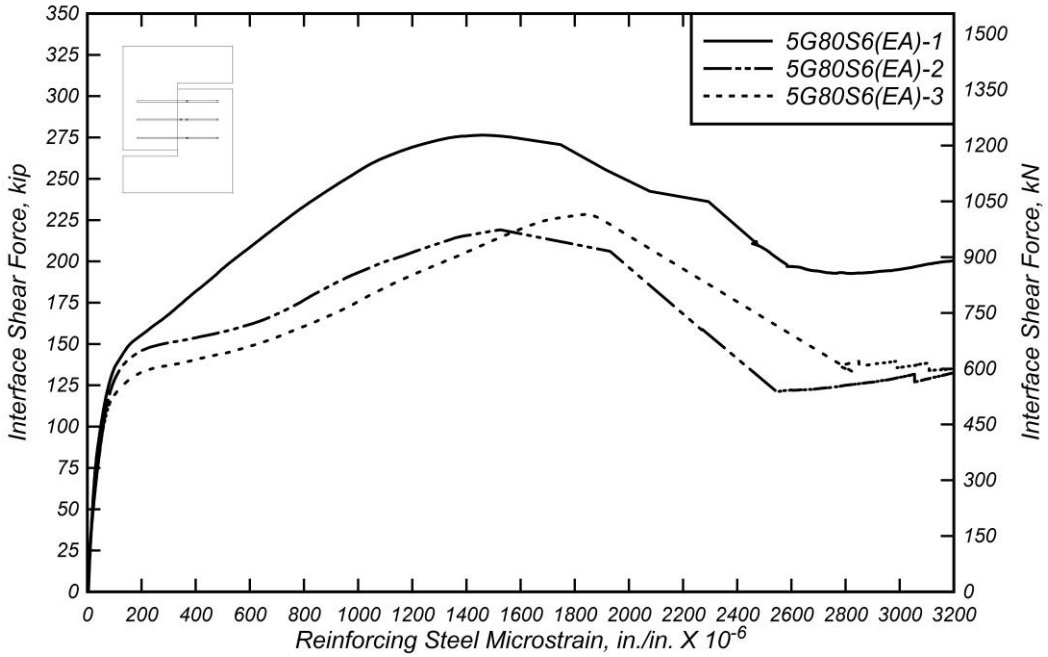

Figure 6.16: Interface shear force versus mean reinforcing steel microstrain for 5G80S6(EA) specimens.

Table 6.16: 5G80S6(AC) Specimen Strain Gauge Readings at Peak Interface Shear Force.

Specimen	s_1, in./in. (mm/mm)	s_2, in./in. (mm/mm)	s_3, in./in. (mm/mm)	s_4, in./in. (mm/mm)	s_5, in./in. (mm/mm)	s_6, in./in. (mm/mm)	s_7, in./in. (mm/mm)
5G80S6(AC)-1	0.0017	0.0015	-	0.0021	0.0014	0.0016	0.0018
5G80S6(AC)-2	0.0011	-	0.0018	-	0.0011	0.0014	-
5G80S6(AC)-3	0.0016	0.0016	-	0.0023	0.0014	0.0014	0.0015
Mean	0.0015	0.0016	0.0018	0.0022	0.0013	0.0015	0.0016
Median	0.0016	0.0016	0.0018	0.0022	0.0014	0.0014	0.0016
STDEV	0.00031	5.12E-05	-	0.00011	0.00021	9.29E-05	0.00020
COV	21%	3%	-	5%	16%	6%	13%

Table 6.17: 5G80S6(1/8) Specimen Strain Gauge Readings at Peak Interface Shear Force.

Specimen	s_1, in./in. (mm/mm)	s_2, in./in. (mm/mm)	s_3, in./in. (mm/mm)	s_4, in./in. (mm/mm)	s_5, in./in. (mm/mm)	s_6, in./in. (mm/mm)	s_7, in./in. (mm/mm)
5G80S6(1/8)-1	0.0013	0.0016	0.0015	-	-	0.0015	0.0011
5G80S6(1/8)-2	0.0012	-	0.0016	-	-	-	0.0018
5G80S6(1/8)-3	0.0012	0.0013	-	0.0016	-	0.0015	-
Mean	0.0012	0.0015	0.0015	-	-	0.0015	0.0014
Median	0.0012	0.0015	0.0015	-	-	0.0015	0.0014
STDEV	7.7E-05	1.7E-04	7.1E-05	-	-	1.9E-05	4.8E-04
COV	9%	12%	5%	-	-	1%	34%

Table 6.18: 5G80S6(1/4) Specimen Strain Gauge Readings at Peak Interface Shear Force.

Specimen	s_1, in./in. (mm/mm)	s_2, in./in. (mm/mm)	s_3, in./in. (mm/mm)	s_4, in./in. (mm/mm)	s_5, in./in. (mm/mm)	s_6, in./in. (mm/mm)	s_7, in./in. (mm/mm)
5G80S6(1/4)-1	0.0014	0.0011	-	0.0018	0.0012	0.0019	-
5G80S6(1/4)-2	0.0022	0.0024	0.0020	0.0020	0.0013	0.0018	0.0022
5G80S6(1/4)-3	0.0012	0.0017	-	-	0.0022	-	-
Mean	0.0016	0.0017	0.0020	0.0019	0.0016	0.0018	0.0022
Median	0.0014	0.0017	0.0020	0.0019	0.0013	0.0018	0.0022
STDEV	0.00053	0.00063	-	0.00019	0.00058	5.55E-05	-
COV	33%	36%	-	10%	37%	3%	-

Table 6.19: 5G80S6(EA) Specimen Strain Gauge Readings at Peak Interface Shear Force.

Specimen	s_1, in./in. (mm/mm)	s_2, in./in. (mm/mm)	s_3, in./in. (mm/mm)	s_4, in./in. (mm/mm)	s_5, in./in. (mm/mm)	s_6, in./in. (mm/mm)	s_7, in./in. (mm/mm)
5G80S6(EA)-1	0.0014	-	0.0011	0.0018	0.0015	0.0015	-
5G80S6(EA)-2	0.0017	0.0021	-	0.0025	0.0014	0.0024	0.0021
5G80S6(EA)-3	0.0013	0.0019	0.0019	0.0026	0.0017	0.0019	0.0018
Mean	0.0015	0.0020	0.0015	0.0023	0.0015	0.0019	0.0020
Median	0.0014	0.0020	0.0015	0.0025	0.0015	0.0019	0.0020
STDEV	0.0002	0.0001	0.0006	0.0005	0.0002	0.0004	0.0002
COV	14%	7%	37%	21%	11%	24%	11%

Table 6.20: Summary of Mean Values of Strain Gauge Readings of each Specimen Group Analyzing Influence of Interface Preparation.

Specimen	s_1, in./in. (mm/mm)	s_2, in./in. (mm/mm)	s_3, in./in. (mm/mm)	s_4, in./in. (mm/mm)	s_5, in./in. (mm/mm)	s_6, in./in. (mm/mm)	s_7, in./in. (mm/mm)
5G80S6(AC)	0.0015	0.0016	0.0018	0.0022	0.0013	0.0015	0.0016
5G80S6(1/8)	0.0012	0.0015	0.0015	-	-	0.0015	0.0014
5G80S6(1/4)	0.0016	0.0017	0.0020	0.0019	0.0016	0.0018	0.0022
5G80S6(EA)	0.0015	0.0020	0.0015	0.0023	0.0015	0.0019	0.0020

6.2.3 Interface Shear Force versus Crack Width

6.2.3.1 Reinforcing Steel U-bar Size: #4 (#13M)

Figure 6.17 to Figure 6.20 present the interface shear force versus crack width response for specimen groups 4G80S6(AC), 4G80S6(1/8), 4G80S6(1/4), and 4G80S6(EA). Each figure shows the force-crack width response for all specimens in each group. Tabulated values of points of interest are presented in Table 6.21 to Table 6.24.

Table 6.25 presents a comparison of the mean crack width values for specimen groups 4G80S6(AC), 4G80S6(1/8), 4G80S6(1/4), and 4G80S6(EA). From the table it can be inferred that specimen groups 4G80S6(AC) and 4G80S6(1/8) reach similar mean crack width at peak load, although, specimens with an As Cast interface preparation reached peak loads slightly larger than specimens with 1/8 in. (3.175 mm) interface preparation. Specimen group 4G80S6(1/4) exhibited smaller mean crack width at peak load, but for significantly lower peak load values. Specimens with an Exposed Aggregate interface preparation show the lowest mean crack width at peak load compared to the other specimen groups. These results are consistent with the discussion presented in Section 6.2.2.1 where it was observed that specimen group 4G80S6(EA) showed lower strain values compared to the other specimen groups. The smaller crack width at peak load reached by specimen group 4G80S6(EA) is beneficial and therefore additional testing to get further insight into the behavior of an Exposed Aggregate interface preparation is needed.

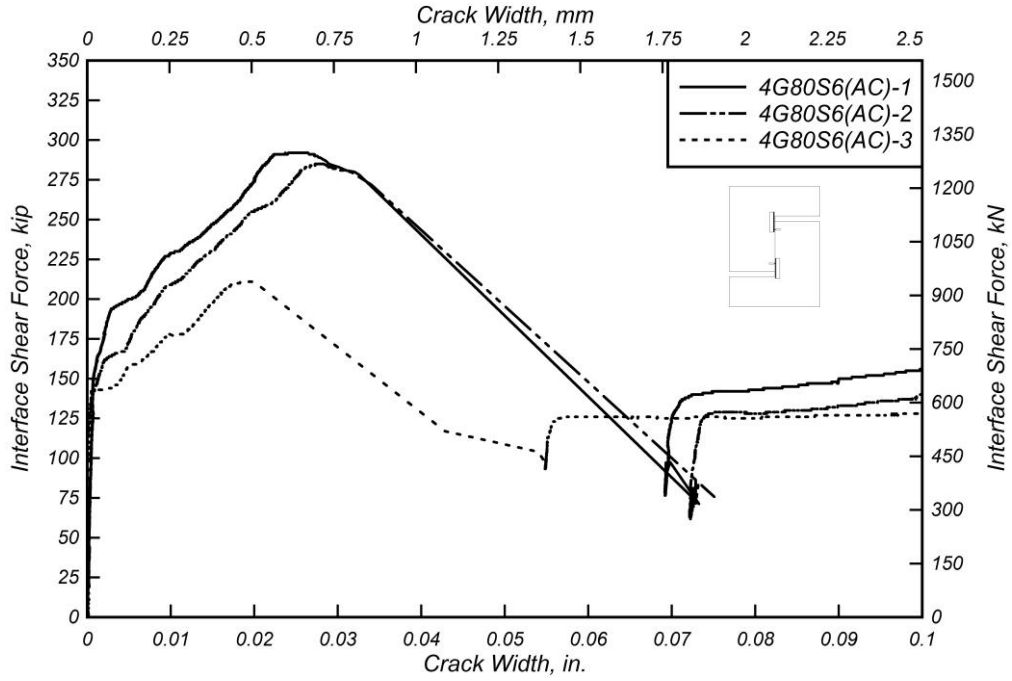

Figure 6.17: Interface shear force versus crack width for 4G80S6(AC) specimens.

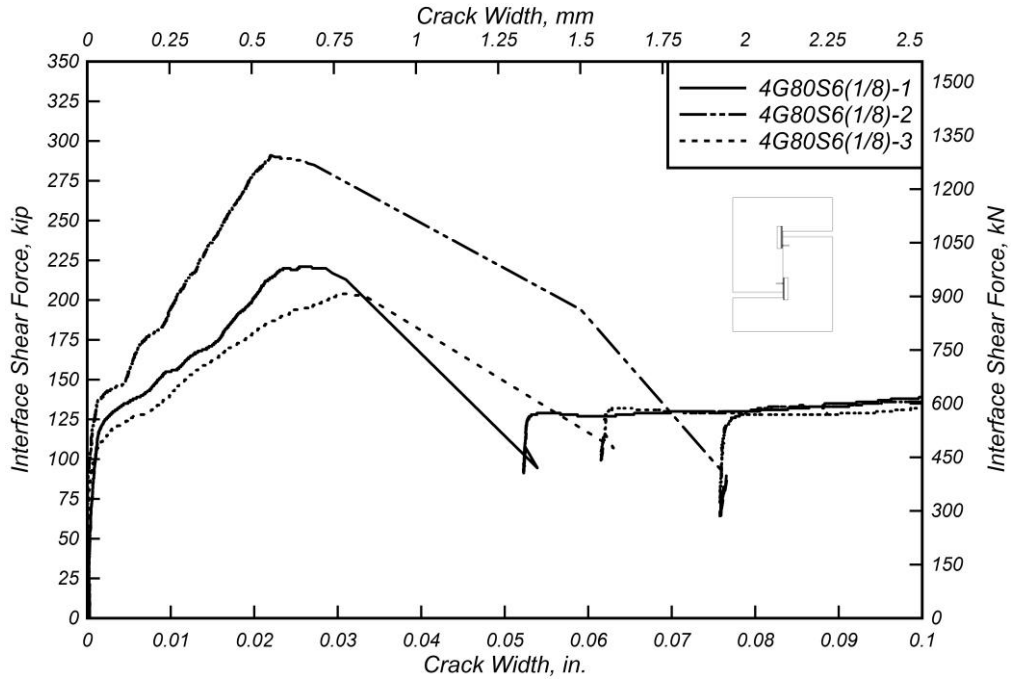

Figure 6.18: Interface shear force versus crack width for 4G80S6(1/8) specimens.

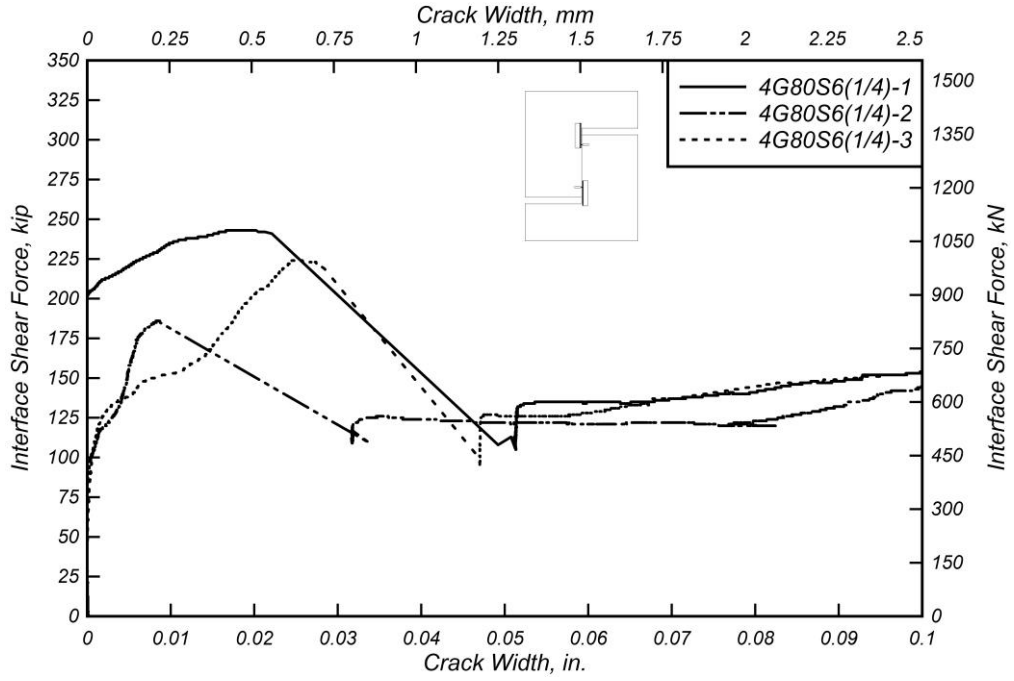

Figure 6.19: Interface shear force versus crack width for 4G80S6(1/4) specimens.

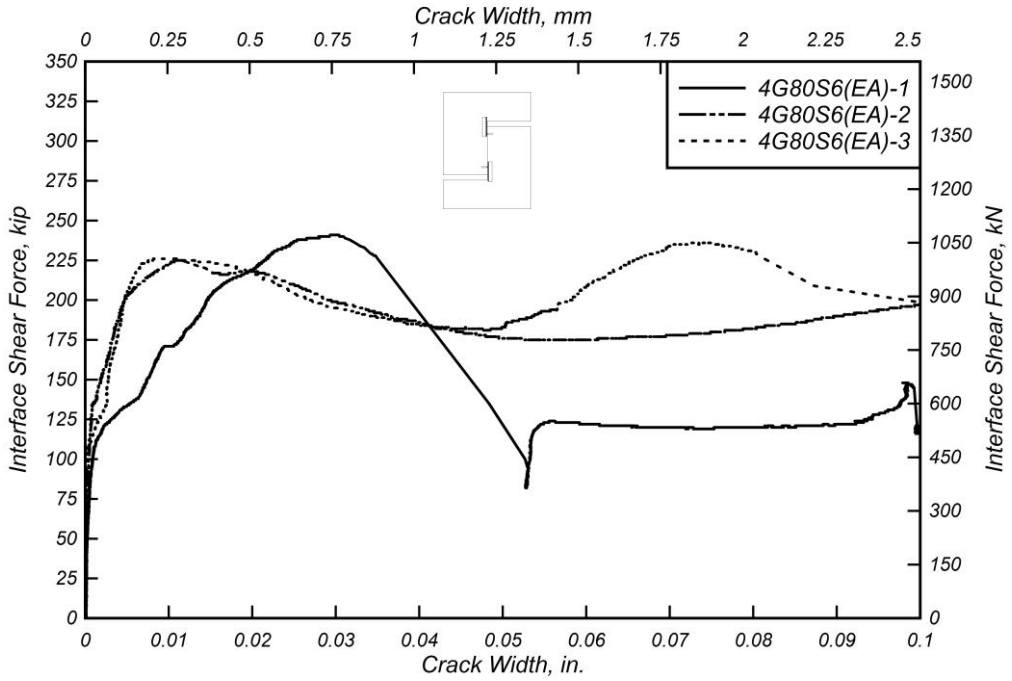

Figure 6.20: Interface shear force versus crack width for 4G80S6(EA) specimens.

Table 6.21: 4G80S6(AC) Specimen Crack Width Measurements.

Specimen	w_{ult}, in. (mm)	V_{ult}, kip (kN)	w_b, in. (mm)	V_b, kip (kN)
4G80S6(AC)-1	0.0260 (0.6603)	292.03 (1299.0)	0.1239 (3.147)	150.66 (670.18)
4G80S6(AC)-2	0.0279 (0.7084)	284.98 (1267.7)	0.1372 (3.485)	152.78 (679.61)
4G80S6(AC)-3	0.0193 (0.4896)	210.93 (938.25)	0.2245 (5.702)	145.46 (647.04)
Mean	0.0244 (0.6194)	262.64 (1168.3)	0.1619 (4.112)	149.64 (665.61)
Median	0.0260 (0.6603)	284.98 (1267.7)	0.1372 (3.485)	150.66 (670.18)
STDEV	0.0045 (0.1150)	44.93 (199.85)	0.0546 (1.388)	3.767 (16.76)
COV	19%	17%	34%	3%

Table 6.22: 4G80S6(1/8) Specimen Crack Width Measurements.

Specimen	w_{ult}, in. (mm)	V_{ult}, kip (kN)	w_b, in. (mm)	V_b, kip (kN)
4G80S6(1/8)-1	0.0256 (0.6510)	221.21 (983.98)	0.1732 (4.398)	145.00 (645.01)
4G80S6(1/8)-2	0.0327 (0.8314)	290.99 (1294.4)	0.2602 (6.610)	150.57 (669.77)
4G80S6(1/8)-3	0.0306 (0.7771)	203.91 (907.04)	0.1782 (4.526)	151.03 (671.81)
Mean	0.0297 (0.7532)	238.70 (1061.8)	0.2039 (5.178)	148.87 (662.20)
Median	0.0306 (0.7771)	221.21 (983.98)	0.1782 (4.526)	150.57 (669.77)
STDEV	0.0036 (0.0926)	46.10 (205.07)	0.0489 (1.242)	3.354 (14.92)
COV	12%	19%	24%	2%

Table 6.23: 4G80S6(1/4) Specimen Crack Width Measurements.

Specimen	w_{ult}, in. (mm)	V_{ult}, kip (kN)	w_b, in. (mm)	V_b, kip (kN)
4G80S6(1/4)-1	0.0188 (0.4767)	243.07 (1081.2)	0.1163 (2.955)	154.52 (687.35)
4G80S6(1/4)-2	0.0084 (0.2146)	186.03 (827.52)	0.1163 (2.953)	154.86 (688.84)
4G80S6(1/4)-3	0.0249 (0.6313)	224.61 (999.11)	0.1131 (2.874)	151.30 (673.03)
Mean	0.0174 (0.4409)	217.90 (969.28)	0.1152 (2.927)	153.56 (683.07)
Median	0.0188 (0.4767)	224.61 (999.11)	0.1163 (2.953)	154.52 (687.35)
STDEV	0.0083 (0.2106)	29.10 (129.45)	0.0018 (0.046)	1.962 (8.728)
COV	48%	13%	2%	1%

Table 6.24: 4G80S6(EA) Specimen Crack Width Measurements.

Specimen	w_{ult}, in. (mm)	V_{ult}, kip (kN)	w_b, in. (mm)	V_b, kip (kN)
4G80S6(EA)-1	0.0300 (0.7625)	241.11 (1072.5)	0.0993 (2.522)	145.13 (645.55)
4G80S6(EA)-2	0.0114 (0.2905)	225.49 (1003.0)	0.1432 (3.637)	230.33 (1024.6)
4G80S6(EA)-3	0.0093 (0.2371)	226.29 (1006.6)	0.0806 (2.048)	227.54 (1012.1)
Mean	0.0169 (0.4300)	230.96 (1027.4)	0.1077 (2.736)	201.00 (894.08)
Median	0.0114 (0.2905)	226.29 (1006.6)	0.0993 (2.522)	227.54 (1012.1)
STDEV	0.0114 (0.2829)	8.798 (39.13)	0.0321 (0.8158)	48.41 (215.30)
COV	67%	4%	30%	24%

Table 6.25: Summary of Mean Values of Crack Width Measurements for As Cast, 1/8 in. (3.175 mm), 1/4 in. (6.35 mm), and Exposed Aggregate Specimens.

Specimen	w_{ult}, in. (mm)	V_{ult}, kip (kN)	w_b, in. (mm)	V_b, kip (kN)
4G80S6(AC)	0.0244 (0.6194)	262.64 (1168.3)	0.1619 (4.112)	149.64 (665.61)
4G80S6(1/8)	0.0297 (0.7532)	238.70 (1061.8)	0.2039 (5.178)	148.87 (662.20)
4G80S6(1/4)	0.0174 (0.4409)	217.90 (969.28)	0.1152 (2.927)	153.56 (683.07)
4G80S6(EA)	0.0169 (0.4300)	230.96 (1027.4)	0.1077 (2.736)	201.00 (894.08)

6.2.3.2 Reinforcing Steel U-bar Size: #5 (#16M)

Figure 6.21 to Figure 6.24 present the interface shear force versus crack width response for specimen groups 5G80S6(AC), 5G80S6(1/8), 5G80S6(1/4), and 5G80S6(EA). Each figure shows the force-crack width response for all specimens in each group. Tabulated values of points of interest, such as crack width at peak load and crack width at first bar fracture for each specimen group are presented in Table 6.26 to Table 6.29. A discussion regarding Figure 6.21 to Figure 6.24, and Table 6.26 to Table 6.29is presented in Section 5.4.3.

Table 6.30 presents a comparison of the mean crack width values for specimen groups 5G80S6(AC), 5G80S6(1/8), 5G80S6(1/4), and 5G80S6(EA). From the table it can be seen that specimen group 5G80S6(1/8) reached the lowest mean crack width, w_{ult}, at 0.0150 in. (0.3808 mm) with a corresponding peak load of 259.52 kip (1154.4 kN). Specimen groups 5G80S6(EA) reached a similar value of w_{ult} with 0.0154 in. (0.3924 mm) with a corresponding peak load of 248.39 kip (1104.9 kN), exhibiting similar post-crack stiffness as specimen group 5G80S6(1/8). Additionally, specimen group 5G80S6(1/4) reached larger w_{ult} with a corresponding larger mean peak load, thus displaying similar stiffness as specimen groups 5G80S6(1/8) and 5G80S6(EA).

It is important to note that for specimens with an interface preparation of 1/8 in. (3.175 mm) and Exposed Aggregate, the mean crack width at peak load decreased when increasing the size of reinforcing steel bars crossing the interface from #4 (#13M) to #5 (#16M). Specimens with an As Cast and 1/4 in. (6.35 mm) interface preparation exhibited increased mean crack width when increasing reinforcing steel bar size from #4 (#13M) to #5 (#16M).

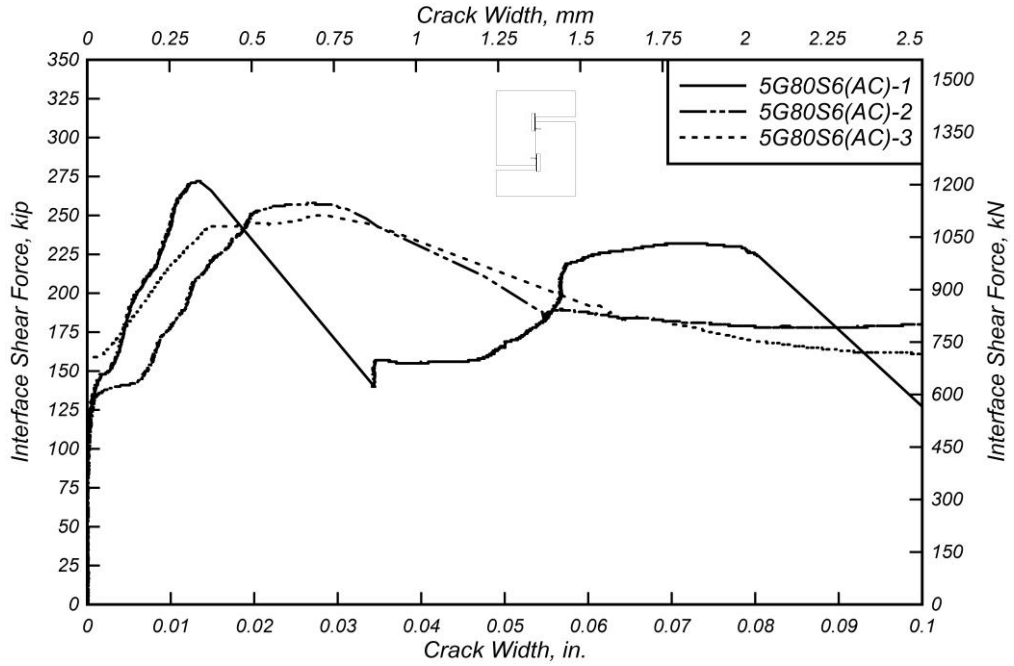

Figure 6.21: Interface shear force versus crack width for 5G80S6(AC) specimens.

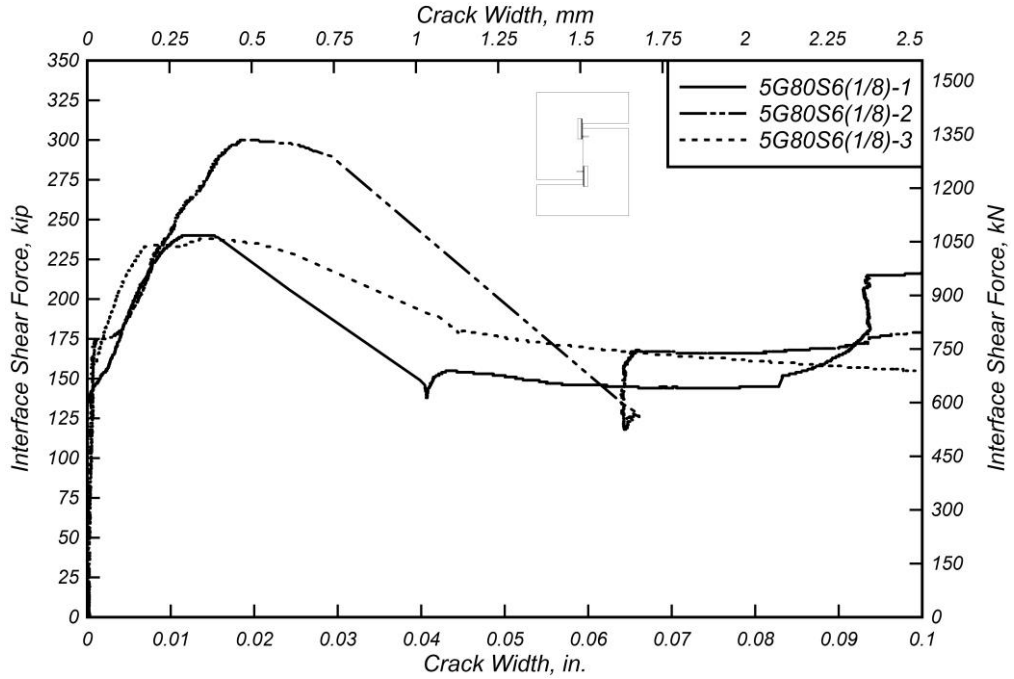

Figure 6.22: Interface shear force versus crack width for 5G80S6(1/8) specimens.

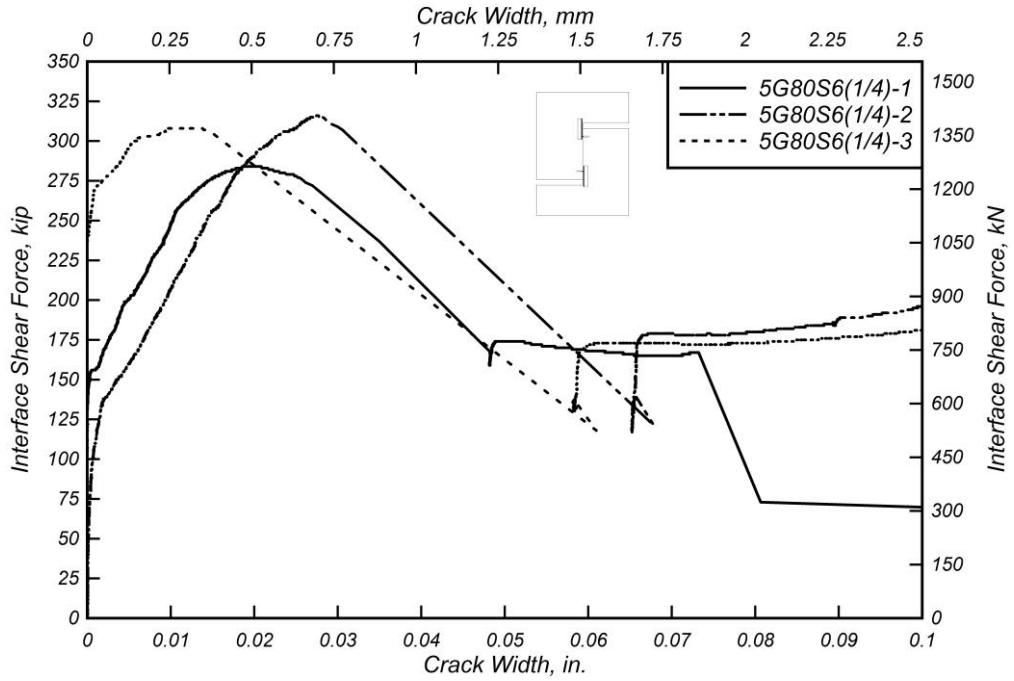

Figure 6.23: Interface shear force versus crack width for 5G80S6(1/4) specimens.

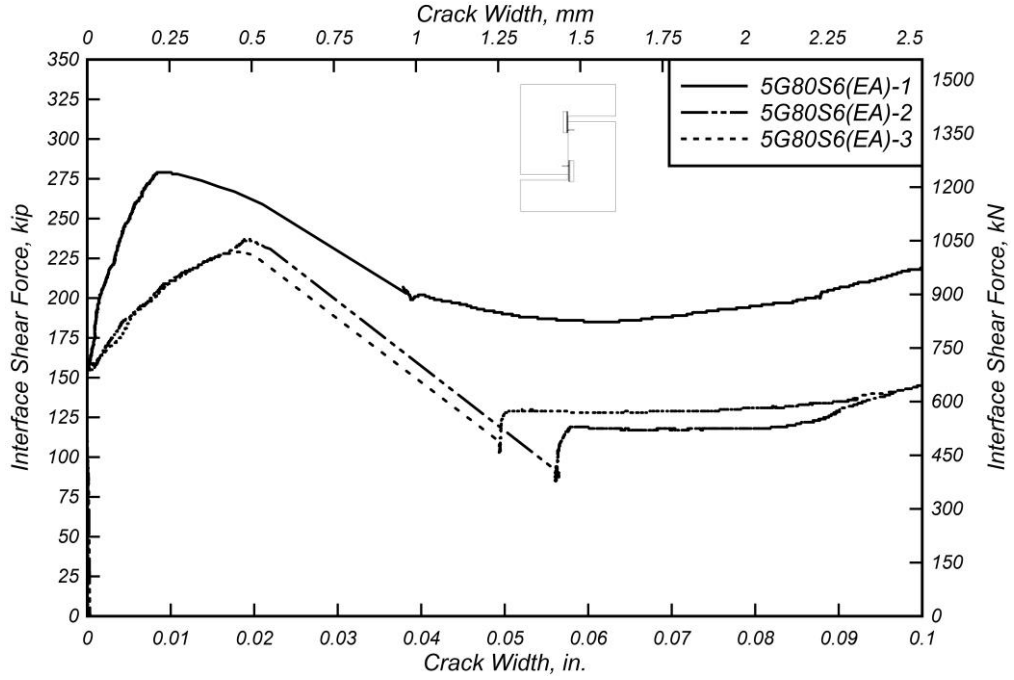

Figure 6.24: Interface shear force versus crack width for 5G80S6(EA) specimens.

Table 6.26: 5G80S6(AC) Specimen Crack Width Measurements.

Specimen	w_{ult}, in. (mm)	V_{ult}, kip (kN)	w_b, in. (mm)	V_b, kip (kN)
5G80S6(AC)-1	0.0134 (0.3401)	271.63 (1208.3)	0.0800 (2.032)	225.46 (1002.9)
5G80S6(AC)-2	0.0267 (0.6786)	257.72 (1146.4)	0.1728 (4.388)	228.09 (1014.6)
5G80S6(AC)-3	0.0276 (0.7012)	250.26 (1113.2)	0.1615 (4.103)	219.56 (976.65)
Mean	0.0272 (0.6899)	253.99 (1129.8)	0.1671 (4.245)	223.82 (995.62)
Median	0.0272 (0.6899)	253.99 (1129.8)	0.1671 (4.245)	223.82 (995.62)
STDEV	0.0006 (0.0160)	5.274 (23.46)	0.0079 (0.2016)	6.029 (26.82)
COV	2%	2%	5%	3%

Table 6.27: 5G80S6(1/8) Specimen Crack Width Measurements.

Specimen	w_{ult}, in. (mm)	V_{ult}, kip (kN)	w_b, in. (mm)	V_b, kip (kN)
5G80S6(1/8)-1	0.0123 (0.3117)	240.38 (1069.3)	0.1160 (2.947)	220.63 (981.40)
5G80S6(1/8)-2	0.0186 (0.4720)	300.13 (1335.0)	0.1755 (4.459)	225.72 (1004.1)
5G80S6(1/8)-3	0.0141 (0.3586)	238.06 (1059.0)	0.2171 (5.514)	205.82 (915.52)
Mean	0.0150 (0.3808)	259.52 (1154.4)	0.1696 (4.307)	217.39 (967.00)
Median	0.0141 (0.3586)	240.38 (1069.3)	0.1755 (4.459)	220.63 (981.40)
STDEV	0.0032 (0.0824)	35.18 (156.50)	0.0508 (1.291)	10.34 (46.00)
COV	22%	14%	30%	5%

Table 6.28: 5G80S6(1/4) Specimen Crack Width Measurements.

Specimen	w_{ult}, in. (mm)	V_{ult}, kip (kN)	w_b, in. (mm)	V_b, kip (kN)
5G80S6(1/4)-1	0.0194 (0.4928)	283.85 (1262.6)	0.0672 (1.707)	206.76 (919.73)
5G80S6(1/4)-2	0.0275 (0.6985)	315.53 (1403.6)	0.1367 (3.472)	245.51 (1092.1)
5G80S6(1/4)-3	0.0100 (0.2533)	308.23 (1371.1)	0.1762 (4.477)	229.67 (1021.6)
Mean	0.0190 (0.4815)	302.54 (1345.7)	0.1267 (3.219)	227.31 (1011.1)
Median	0.0194 (0.4928)	308.23 (1371.1)	0.1367 (3.472)	229.67 (1021.6)
STDEV	0.0088 (0.2228)	16.59 (73.79)	0.0552 (1.402)	19.48 (86.65)
COV	46%	5%	44%	9%

Table 6.29: 5G80S6(EA) Specimen Crack Width Measurements.

Specimen	w_{ult}, in. (mm)	V_{ult}, kip (kN)	w_b, in. (mm)	V_b, kip (kN)
5G80S6(EA)-1	0.0090 (0.2290)	279.43 (1243.0)	0.1053 (2.675)	226.26 (1006.4)
5G80S6(EA)-2	0.0193 (0.4897)	236.63 (1052.6)	0.1200 (3.047)	140.96 (627.03)
5G80S6(EA)-3	0.0180 (0.4584)	229.12 (1019.2)	0.1259 (3.197)	148.27 (659.53)
Mean	0.0154 (0.3924)	248.39 (1104.9)	0.1170 (2.973)	171.83 (764.33)
Median	0.0180 (0.4584)	236.63 (1052.6)	0.1200 (3.047)	148.27 (659.53)
STDEV	0.0056 (0.1423)	27.14 (120.71)	0.0106 (0.2688)	47.28 (210.30)
COV	36%	11%	9%	28%

Table 6.30: Summary of Mean Values of Crack Width Measurements for As Cast, 1/8 in. (3.175 mm), 1/4 in. (6.35 mm), and Exposed Aggregate Specimens.

Specimen	w_{ult}, in. (mm)	V_{ult}, kip (kN)	w_b, in. (mm)	V_b, kip (kN)
5G80S6(AC)	0.0272 (0.6899)	253.99 (1129.8)	0.1671 (4.245)	223.82 (995.62)
5G80S6(1/8)	0.0150 (0.3808)	259.52 (1154.4)	0.1696 (4.307)	217.39 (967.00)
5G80S6(1/4)	0.0190 (0.4815)	302.54 (1345.7)	0.1267 (3.219)	227.31 (1011.1)
5G80S6(EA)	0.0154 (0.3924)	248.39 (1104.9)	0.1170 (2.973)	171.83 (764.33)

6.3 INFLUENCE OF NOMINAL CONCRETE STRENGTH

This section presents the experimental results and discussion for test specimens built with nominal design concrete strength of 3000 psi (20 MPa), 5000 psi (35 MPa), and 6000 psi (40 MPa). All specimens discussed in this section are reinforced with three #4 (#13M) Grade 80 ksi (550 MPa) reinforcing steel U-bars spaced at 6 in. (152.4 mm) with an interface preparation of 1/8 in. (3.175 mm) roughness. Details of the specimens such as bar size, bar spacing, and interface preparation can be found in section (e) of Table 3.1, while drawings showing specimen dimensions, as well as location of the reinforcing steel U-bars are presented in Chapter 3.

6.3.1 Interface Shear Force versus Interface Shear Displacement

The interface shear force versus interface shear displacement response for specimen groups 4G80S6F3(1/8), 4G80S6(1/8), and 4G80S6F6(1/8) are presented in Figure 6.25 to Figure 6.27, respectively, which correspond to specimens with the same finishing, same reinforcing steel bar size and spacing, and the only difference between them being the concrete strength. The design parameters of the tests for these three groups are listed in Table 3.1(e). Some of the results relative to the 4G80S6(1/8) specimen group were already shown in Figure 6.26 and Table 6.32 for comparison purposes and were already been discussed in Section 5.2.1. The tabulated values of the main points of study are presented in Table 6.31 to Table 6.33.

In Figure 6.25 it can be observed that all specimens present similar behavior except for specimen 4G80S6F3(1/8)-1 where the displacement at first bar fracture, Δ_b, was lower compared to the other two specimens in the group. Additionally, specimen group 4G80S6F3(1/8) exhibited displacements at peak load Δ_{ult} values ranging from 0.075 in. (1.905 mm) to 0.125 in. (3.175 mm) with a COV of 25%, which is still reasonable, but in general larger than that observed for other specimen groups. However, the peak loads V_{ult}, for specimen group 4G80S6F3(1/8) ranged from 223.26 kip (993.11 kN) to 229.31 kip (1020.0 kN) with a COV of 1%. Figure 6.27 shows the interface shear force versus interface shear displacement response of specimen group 4G80S6F6(1/8). In this figure it can be observed that all specimens exhibited similar behavior, except for specimen 4G80S6F6(1/8)-1, which reached a lower peak load. Additionally, the first bar fracture in specimen 4G80S6F6(1/8)-2 occurred at a lower displacement value compared to the other two specimens in the group.

Table 6.34 shows the mean tabulated values of the main points of interest for specimen groups 4G80S6F3(1/8), 4G80S6(1/8), and 4G80S6F6(1/8). From the table it can be observed that a correlation exists between peak load and nominal concrete strength, as the results show that mean peak load is proportional nominal concrete strength with V_{ult} values of 226.86 kip (1009.1 kN), 238.70 kip (1061.8 kN), and 260.28 kip (1157.8 kN) for specimen groups 4G80S6F3(1/8), 4G80S6(1/8), and 4G80S6F6(1/8), respectively. The same trend appears regarding interface shear load when cracking occurs where V_{cr} values are 98.53 kip (438.30 kN), 109.44 kip (486.80 kN), and 133.20 kip (592.50 kN), for specimen groups 4G80S6F3(1/8), 4G80S6(1/8), and 4G80S6F6(1/8), respectively. These results indicate that increasing the nominal concrete

strength increases the strength of the concrete-to-concrete cohesion bond created at the shear interface.

Additionally, Table 6.34 shows a trend regarding mean displacement at peak load, where it can be observed that mean displacement at peak load is inversely proportional to nominal concrete strength. That is as, as the concrete strength increases, mean displacement at peak load decreases, which is to be expected as the MOE also increases with concrete strength.

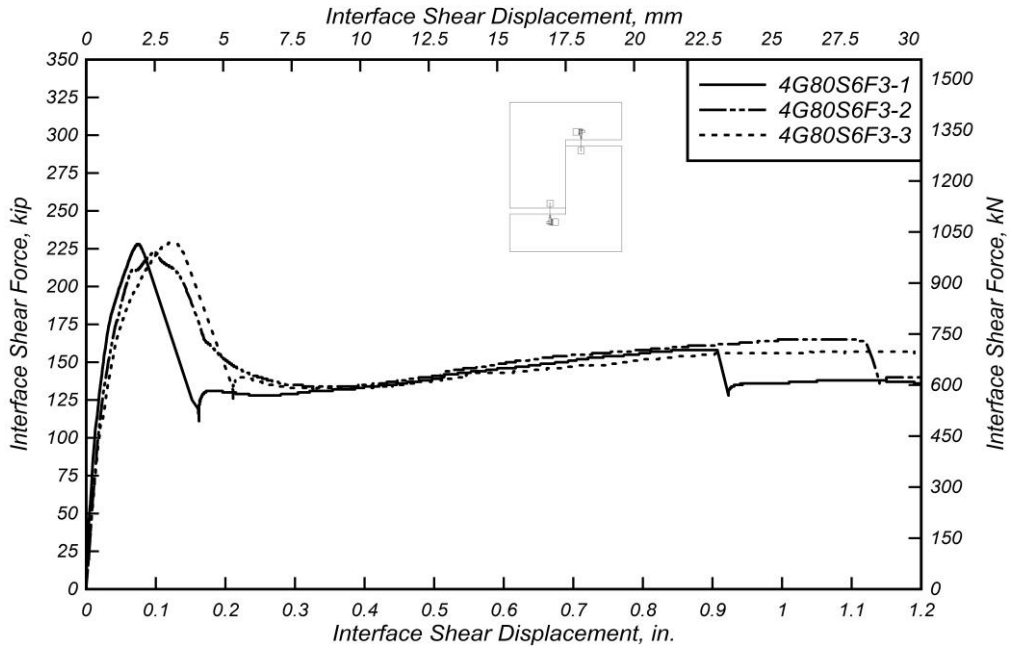

Figure 6.25: Interface shear force versus interface shear displacement for 4G80S6F3(1/8) specimens.

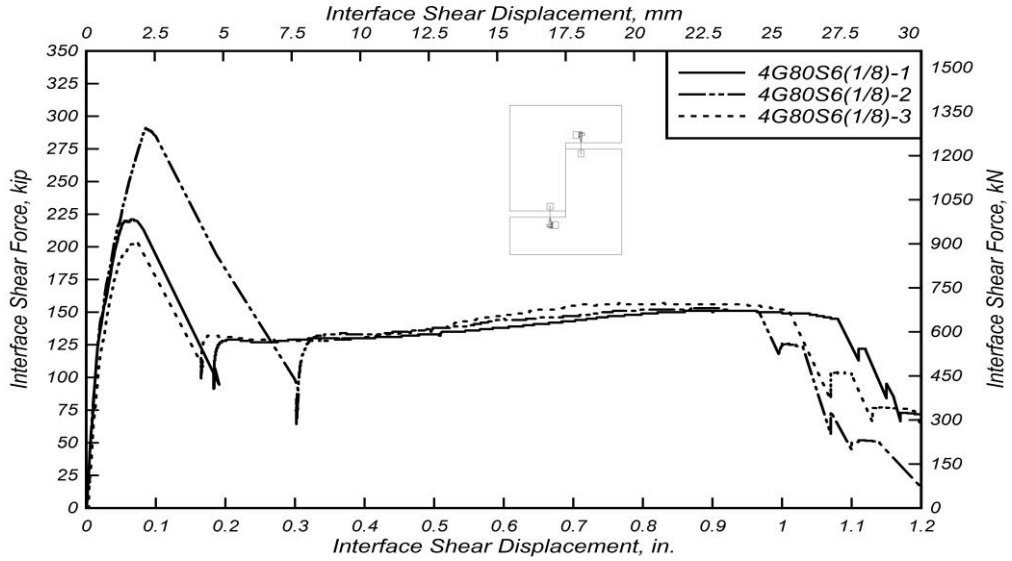

Figure 6.26: Interface shear force versus interface shear displacement the 4G80S6(1/8) specimens.

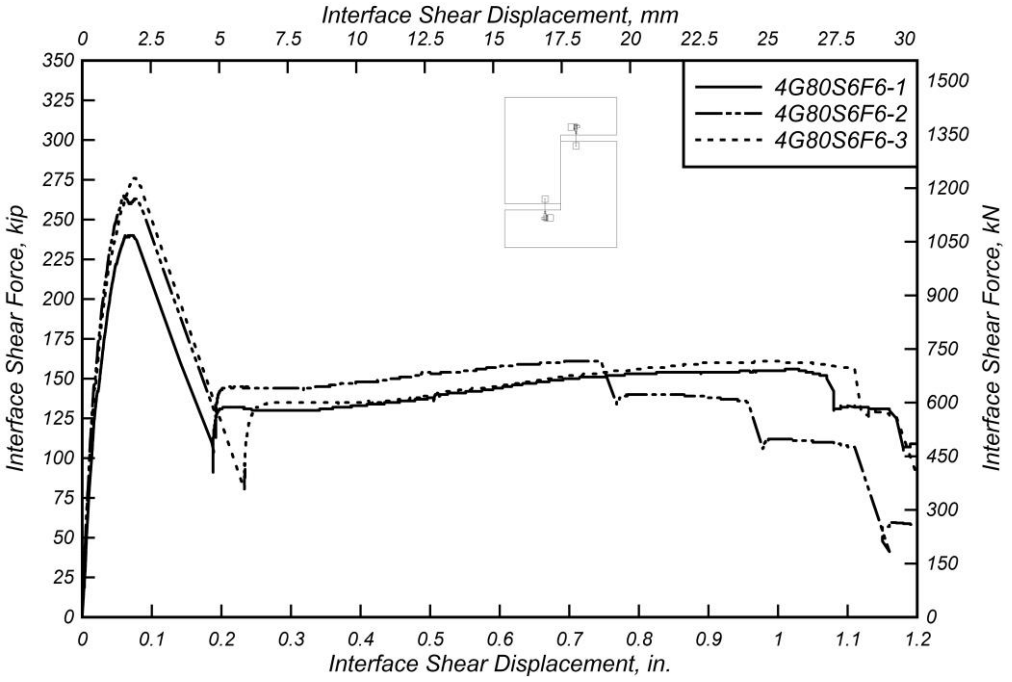

Figure 6.27: Interface shear force versus interface shear displacement for 4G80S6F6(1/8) specimens.

Table 6.31: 4G80S6F3(1/8) Specimen Shear Test Results.

Specimen	Δ_{ult}, in. (mm)	V_{ult}, kip (kN)	σ_{ult}, ksi (MPa)	$V_{sus,min}$, kip (kN)	$V_{sus,max}$, kip (kN)	Δ_{cr}, in. (mm)	V_{cr}, kip (kN)	Δ_b, in. (mm)	V_b, kip (kN)	E_b, kip-ft (kJ)
4G80S6F3 (1/8)-1	0.075 (1.905)	228.01 (1014.2)	0.950 (6.550)	128.19 (570.22)	158.35 (704.38)	0.013 (0.318)	102.40 (455.50)	0.907 (23.04)	158.03 (702.95)	11.10 (15.05)
4G80S6F3 (1/8)-2	0.099 (2.515)	223.26 (993.11)	0.930 (6.414)	133.76 (594.99)	165.34 (735.47)	0.015 (0.371)	87.50 (389.22)	1.115 (28.32)	164.01 (729.55)	14.50 (19.66)
4G80S6F3 (1/8)-3	0.125 (3.175)	229.31 (1020.0)	0.955 (6.588)	132.39 (588.90)	157.25 (699.48)	0.020 (0.503)	105.70 (470.18)	1.301 (33.05)	154.46 (687.07)	16.46 (22.31)
Mean	0.100 (2.532)	226.86 (1009.1)	0.945 (6.517)	131.45 (584.70)	160.31 (713.11)	0.016 (0.397)	98.53 (438.30)	1.108 (28.13)	158.83 (706.53)	14.02 (19.01)
Median	0.099 (2.515)	228.01 (1014.2)	0.950 (6.550)	132.39 (588.90)	158.35 (704.38)	0.015 (0.371)	102.40 (455.50)	1.115 (28.32)	158.03 (702.95)	14.50 (19.66)
STDEV	0.0250 (0.635)	3.185 (14.17)	0.0133 (0.092)	2.902 (12.91)	4.388 (19.52)	0.0038 (0.096)	9.697 (43.13)	0.1971 (5.006)	4.825 (21.46)	2.710 (3.675)
COV	25%	1%	1%	2%	3%	24%	10%	18%	3%	19%

Table 6.32: 4G80S6(1/8) Specimen Shear Test Results.

Specimen	Δ_{ult}, in. (mm)	V_{ult}, kip (kN)	σ_{ult}, ksi (MPa)	$V_{sus,min}$, kip (kN)	$V_{sus,max}$, kip (kN)	Δ_{cr}, in. (mm)	V_{cr}, kip (kN)	Δ_b, in. (mm)	V_b, kip (kN)	E_b, kip-ft (kJ)
4G80S6 (1/8)-1	0.065 (1.651)	221.21 (983.99)	0.922 (6.355)	126.72 (563.68)	151.44 (673.64)	0.015 (0.373)	112.5 (500.42)	1.079 (27.41)	145.00 (644.99)	12.92 (17.52)
4G80S6 (1/8)-2	0.085 (2.159)	290.99 (1294.4)	1.212 (8.360)	132.37 (588.81)	152.83 (679.82)	0.016 (0.396)	119.00 (529.34)	0.962 (24.43)	150.57 (669.77)	12.73 (17.26)
4G80S6 (1/8)-3	0.070 (1.778)	203.91 (907.04)	0.850 (5.858)	127.94 (569.11)	156.60 (696.59)	0.016 (0.414)	96.81 (430.63)	1.012 (25.70)	151.03 (671.81)	12.19 (16.53)
Mean	0.073 (1.863)	238.70 (1061.8)	0.995 (6.858)	129.01 (573.86)	153.62 (683.35)	0.016 (0.395)	109.44 (486.80)	1.018 (25.85)	148.87 (662.19)	12.61 (17.10)
Median	0.070 (1.778)	221.21 (983.99)	0.922 (6.355)	127.94 (569.11)	152.83 (679.82)	0.016 (0.396)	112.50 (500.42)	1.012 (25.70)	150.57 (669.77)	12.73 (17.26)
STDEV	0.0104 (0.264)	46.10 (205.06)	0.1921 (1.324)	2.973 (13.22)	2.670 (11.88)	0.0008 (0.020)	11.41 (50.74)	0.0587 (1.491)	3.357 (14.93)	0.377 (0.512)
COV	14%	19%	19%	2%	2%	5%	10%	6%	2%	3%

Table 6.33: 4G80S6F6(1/8) Specimen Shear Test Results.

Specimen	Δ_{ult}, in. (mm)	V_{ult}, kip (kN)	σ_{ult}, ksi (MPa)	$V_{sus,min}$, kip (kN)	$V_{sus,max}$, kip (kN)	Δ_{cr}, in. (mm)	V_{cr}, kip (kN)	Δ_b, in. (mm)	V_b, kip (kN)	E_b, kip-ft (kJ)
4G80S6F6 (1/8)-1	0.070 (1.778)	240.20 (1068.5)	1.001 (6.901)	129.89 (577.78)	155.80 (693.03)	0.015 (0.384)	111.70 (496.87)	1.065 (27.05)	151.96 (675.95)	13.28 (18.00)
4G80S6F6 (1/8)-2	0.060 (1.524)	264.66 (1177.3)	1.103 (7.603)	143.46 (638.14)	161.17 (716.92)	0.016 (0.409)	143.20 (636.99)	0.746 (18.95)	160.53 (714.07)	10.17 (13.79)
4G80S6F6 (1/8)-3	0.075 (1.905)	275.97 (1227.6)	1.150 (7.928)	134.46 (598.11)	160.87 (715.59)	0.019 (0.472)	144.70 (643.66)	1.105 (28.07)	155.85 (693.26)	14.41 (19.53)
Mean	0.068 (1.736)	260.28 (1157.8)	1.084 (7.477)	135.94 (604.68)	159.28 (708.51)	0.017 (0.422)	133.20 (592.50)	0.972 (24.69)	156.11 (694.43)	12.62 (17.11)
Median	0.070 (1.778)	264.66 (1177.3)	1.103 (7.603)	134.46 (598.11)	160.87 (715.59)	0.016 (0.409)	143.20 (636.99)	1.065 (27.05)	155.85 (693.26)	13.28 (18.00)
STDEV	0.0076 (0.194)	18.28 (81.33)	0.076 (0.525)	6.904 (30.71)	3.017 (13.42)	0.0018 (0.046)	18.63 (82.89)	0.1967 (4.997)	4.291 (19.09)	2.195 (2.976)
COV	11%	7%	7%	5%	2%	11%	14%	20%	3%	17%

Table 6.34: Summary of Mean Values of each Specimen Group Analyzing Influence of Nominal Concrete Strength.

Specimen	Δ_{ult}, in. (mm)	V_{ult}, kip (kN)	σ_{ult}, ksi (MPa)	$V_{sus,min}$, kip (kN)	$V_{sus,max}$, kip (kN)	Δ_{cr}, in. (mm)	V_{cr}, kip (kN)	Δ_b, in. (mm)	V_b, kip (kN)	E_b, kip-ft (kJ)
4G80S6F3 (1/8)	0.100 (2.532)	226.86 (1009.1)	0.945 (6.517)	131.45 (584.70)	160.31 (713.11)	0.016 (0.397)	98.53 (438.30)	1.108 (28.13)	158.83 (706.53)	14.02 (19.01)
4G80S6 (1/8)	0.073 (1.863)	238.70 (1061.8)	0.995 (6.858)	129.01 (573.86)	153.62 (683.35)	0.016 (0.395)	109.44 (486.80)	1.018 (25.85)	148.87 (662.19)	12.61 (17.10)
4G80S6F6 (1/8)	0.068 (1.736)	260.28 (1157.8)	1.084 (7.477)	135.94 (604.68)	159.28 (708.51)	0.017 (0.422)	133.20 (592.50)	0.972 (24.69)	156.11 (694.43)	12.62 (17.11)

6.3.2 Interface Shear Force versus Strain

The interface shear force versus reinforcing steel U-bar strain relationships are presented in Figure 6.28 to Figure 6.30 for specimen groups 4G80S6F3(1/8), 4G80S6(1/8), and 4G80S6F6(1/8), respectively. The curves shown correspond to the mean strain measurements from all strain gauges contained in each test specimen (when available) plotted versus the interface shear force. From these figures, it can be observed that all specimens present similar force-strain responses. Discussion pertaining to Figure 6.29 is presented in Section 5.2.2. Table 6.35 to Table 6.37 show strain readings from strain gauges in each specimen at peak load. The variability of strain gauge readings is observed with COV reaching 38%, which seems reasonable but is larger than others are. It is important to note that some strain gauges were damaged before the peak load was reached.

Table 6.38 shows a comparison of the mean interface shear strain relationship of the three specimen groups. From the table, in general, specimen group 4G80S6(1/8) shows the lowest strain values at peak load compared to specimen group 4G80S6F3(1/8) and 4G80S6F6(1/8). This may be attributed to the reinforcing steel U-bars crushing the concrete around them, thus reducing the strain.

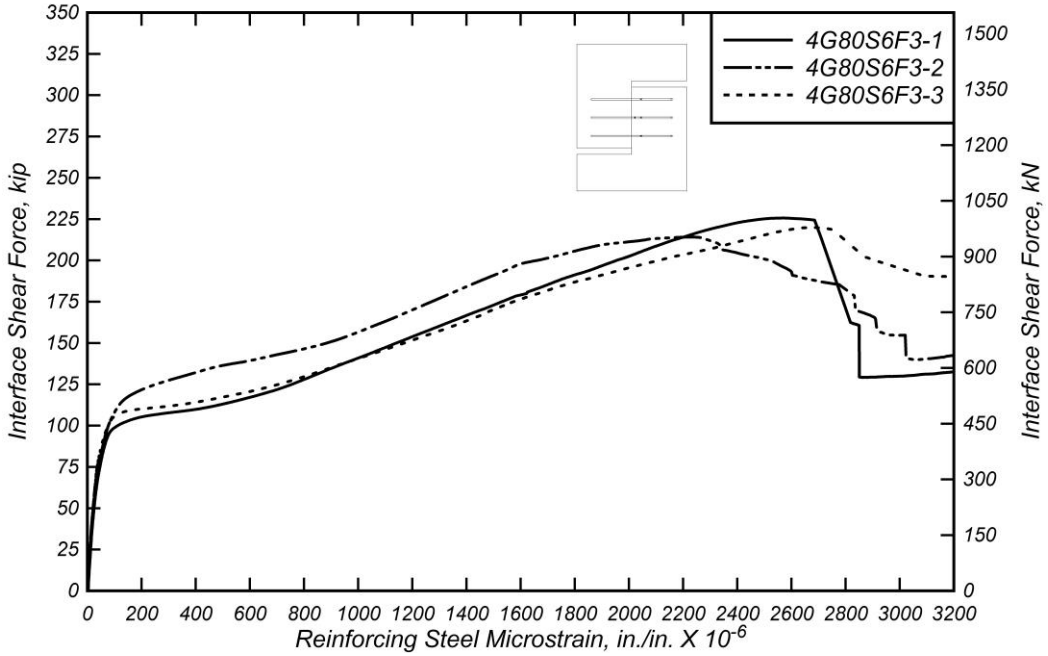

Figure 6.28: Interface shear force versus mean values of reinforcing steel microstrain for 4G80S6F3(1/8) specimens.

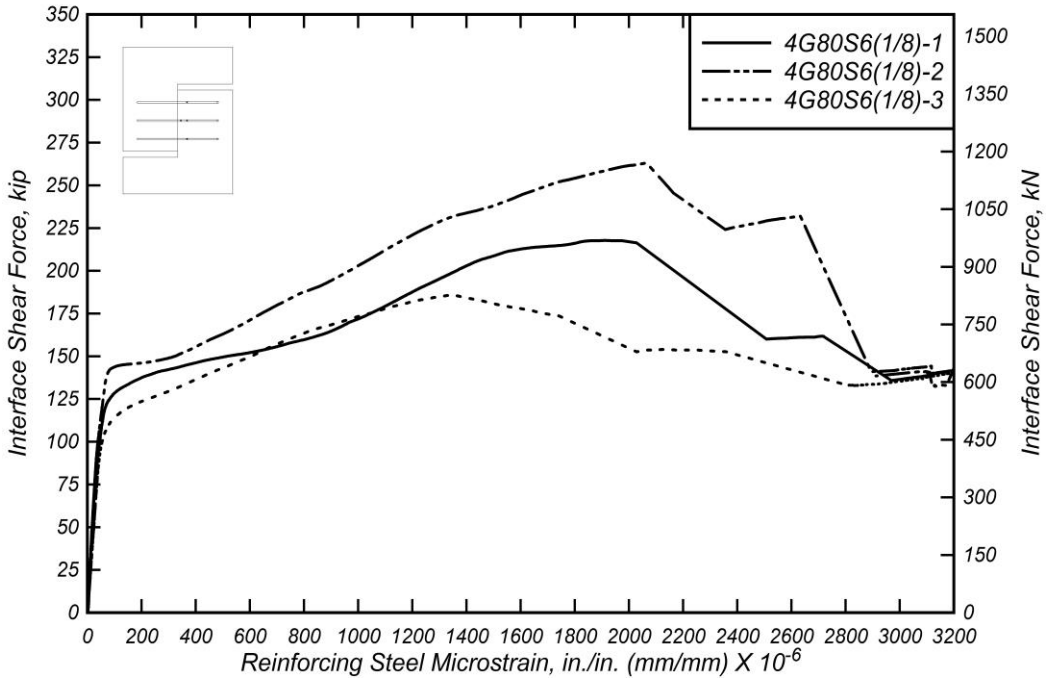

Figure 6.29: Interface shear force versus mean values of reinforcing steel microstrain for 4G80S6(1/8) specimens.

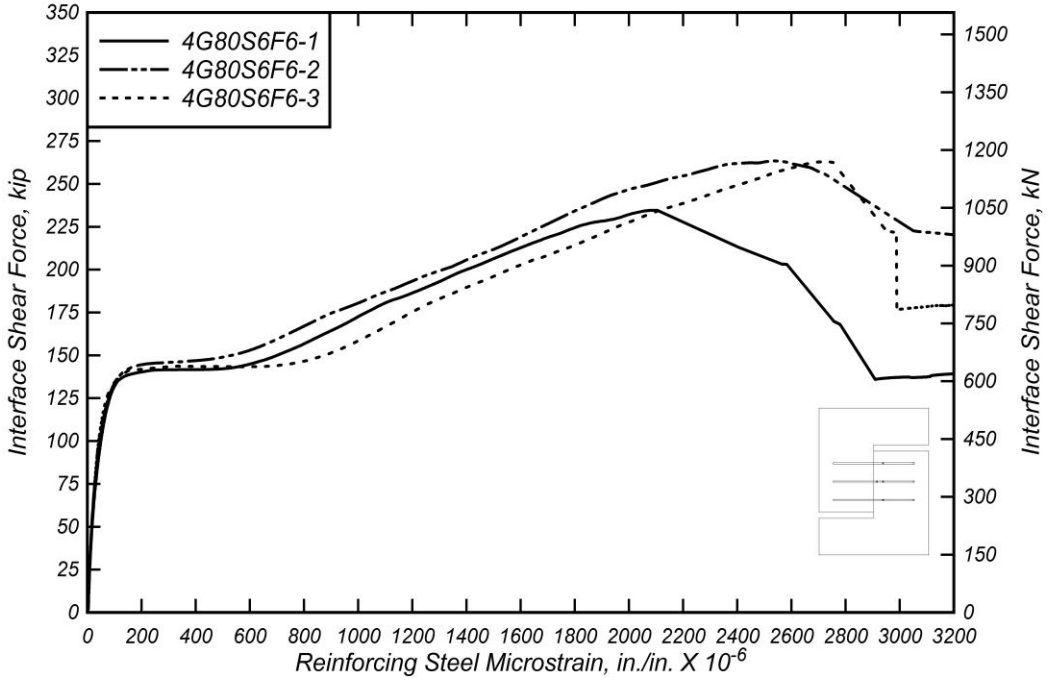

Figure 6.30: Interface shear force versus mean values of reinforcing steel microstrain for 4G80S6F6(1/8) specimens.

Table 6.35: 4G80S6F3(1/8) Specimen Strain Gauge Readings at Peak Interface Shear Force.

Specimen	s_1, in./in. (mm/mm)	s_2, in./in. (mm/mm)	s_3, in./in. (mm/mm)	s_4, in./in. (mm/mm)	s_5, in./in. (mm/mm)	s_6, in./in. (mm/mm)	s_7, in./in. (mm/mm)
4G80S6F3(1/8)-1	0.0012	0.0025	0.0027	0.0026	0.0015	0.0024	0.0025
4G80S6F3(1/8)-2	0.0025	0.0019	0.0019	0.0025	0.0024	0.0029	0.0023
4G80S6F3(1/8)-3	0.0028	0.0035	0.0026	0.0035	0.0025	0.0039	0.0027
Mean	0.0022	0.0026	0.0024	0.0029	0.0021	0.0030	0.0025
Median	0.0025	0.0025	0.0026	0.0026	0.0024	0.0029	0.0025
STDEV	0.000826	0.000779	0.000452	0.000555	0.000584	0.000761	0.000205
COV	38%	30%	19%	19%	28%	25%	8%

Table 6.36: 4G80S6(1/8) Specimen Strain Gauge Readings at Peak Interface Shear Force.

Specimen	s_1, in./in. (mm/mm)	s_2, in./in. (mm/mm)	s_3, in./in. (mm/mm)	s_4, in./in. (mm/mm)	s_5, in./in. (mm/mm)	s_6, in./in. (mm/mm)	s_7, in./in. (mm/mm)
4G80S6(1/8)-1	-	-	0.0019	-	0.0025	0.0018	-
4G80S6(1/8)-2	-	-	-	-	0.0030	0.0025	0.0017
4G80S6(1/8)-3	-	0.0022	-	0.0026	-	0.0018	0.0012
Mean	-	0.0022	0.0019	0.0026	0.0028	0.0021	0.0015
Median	-	0.0022	0.0019	0.0026	0.0028	0.0018	0.0015
STDEV	-	-	-	-	0.0004	0.0004	0.0004
COV	-	-	-	-	13%	19%	26%

Table 6.37: 4G80S6F6(1/8) Specimen Strain Gauge Readings at Peak Interface Shear Force.

Specimen	s_1, in./in. (mm/mm)	s_2, in./in. (mm/mm)	s_3, in./in. (mm/mm)	s_4, in./in. (mm/mm)	s_5, in./in. (mm/mm)	s_6, in./in. (mm/mm)	s_7, in./in. (mm/mm)
4G80S6F6(1/8)-1	0.0019	-	-	0.0028	0.0014	0.0024	0.0026
4G80S6F6(1/8)-2	0.0015	0.0024	0.0026	0.0025	-	0.0025	0.0024
4G80S6F6(1/8)-3	0.0014	-	0.0027	0.0033	0.0016	0.0035	0.0029
Mean	0.0016	0.0024	0.0026	0.0029	0.0015	0.0028	0.0026
Median	0.0015	0.0024	0.0026	0.0028	0.0015	0.0025	0.0026
Stdv	0.000284	-	5.43E-05	0.000394	0.000185	0.000643	0.000292
COV	18%	-	2%	14%	12%	23%	11%

Table 6.38: Summary of Mean Values of Strain Gauge Readings at Peak Interface Shear Load.

Specimen	s_1, in./in. (mm/mm)	s_2, in./in. (mm/mm)	s_3, in./in. (mm/mm)	s_4, in./in. (mm/mm)	s_5, in./in. (mm/mm)	s_6, in./in. (mm/mm)	s_7, in./in. (mm/mm)
4G80S6F3(1/8)	0.0022	0.0026	0.0024	0.0029	0.0021	0.0030	0.0025
4G80S6(1/8)	-	0.0022	0.0019	0.0026	0.0028	0.0021	0.0015
4G80S6F6(1/8)	0.0016	0.0024	0.0026	0.0029	0.0015	0.0028	0.0026

6.3.3 Interface Shear Force versus Crack Width

Figure 6.31 to Figure 6.33 show the interface shear force versus crack width relationship for specimen groups 4G80S6F3(1/8), 4G80S6(1/8), and 4G80S6F6(1/8). Table 6.39 to Table 6.41 show tabulated values for the main points of study for specimen groups 4G80S6F3(1/8), 4G80S6(1/8), and 4G80S6F6(1/8). All specimens exhibited similar behavior in the initial stages, characterized by negligible crack width due to the uncracked concrete-to-concrete bond. After the cohesion bond is exceeded, the force-crack width response is characterized by a hardening branch until peak load is reached. Table 6.39 to Table 6.41 list the variability of crack widths at peak load, w_{ult}, with COV ranging from 12% to 30%.

Table 6.42 shows a comparison between the mean crack width values for specimen groups 4G80S6F3(1/8), 4G80S6(1/8), and 4G80S6F6(1/8). From the table it can be seen that the mean crack widths at peak load, w_{ult}, tend to be reduced as concrete strength increases. Mean crack widths at peak load are 0.0436 in. (1.107 mm), 0.0297 in. (0.753 mm), and 0.0299 in. (0.758 mm), for specimen groups 4G80S6F3(1/8), 4G80S6(1/8), and 4G80S6F6(1/8) respectively. These results indicate that larger crack widths at peak load, w_{ult}, is likely to be expected when the concrete strength is lower.

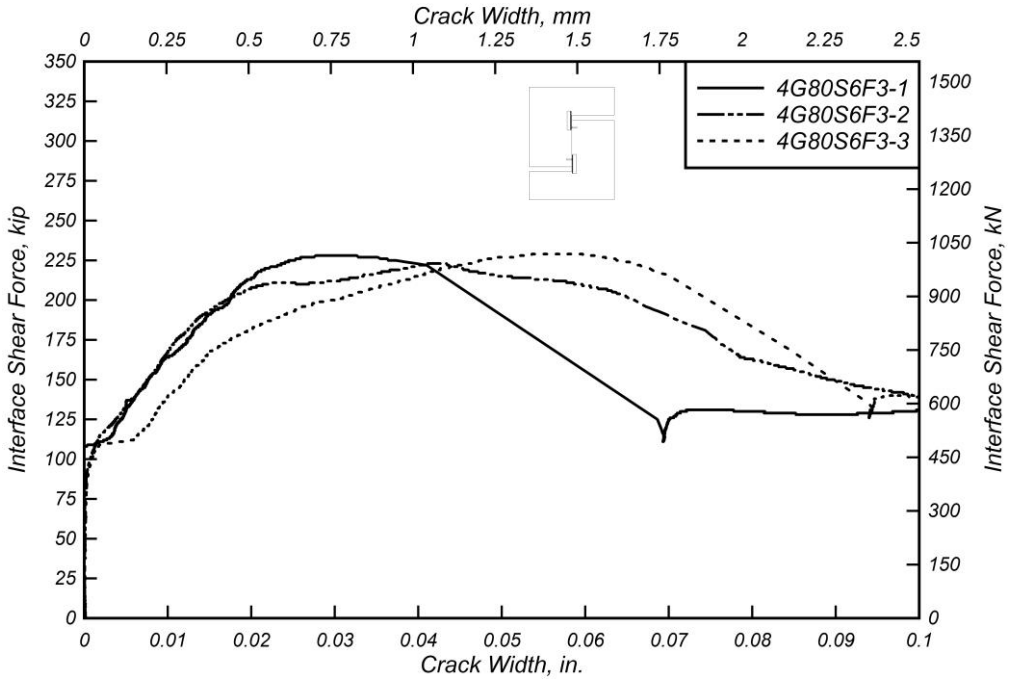

Figure 6.31: Interface shear force versus crack width for 4G80S6F3(1/8) specimens.

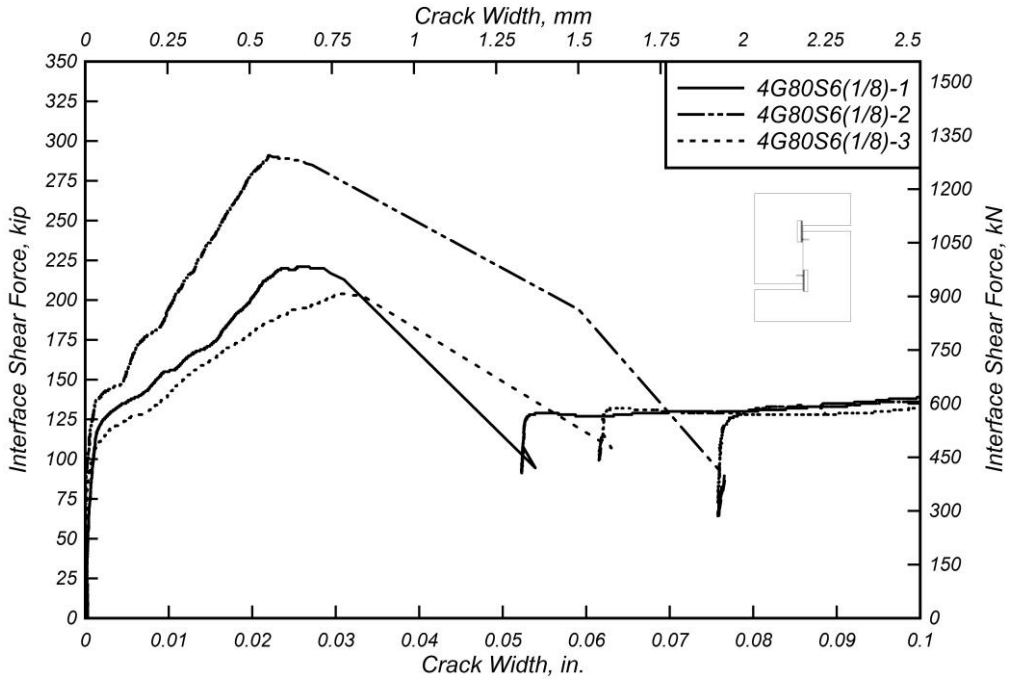

Figure 6.32: Interface shear force versus crack width for 4G80S6(1/8) specimens.

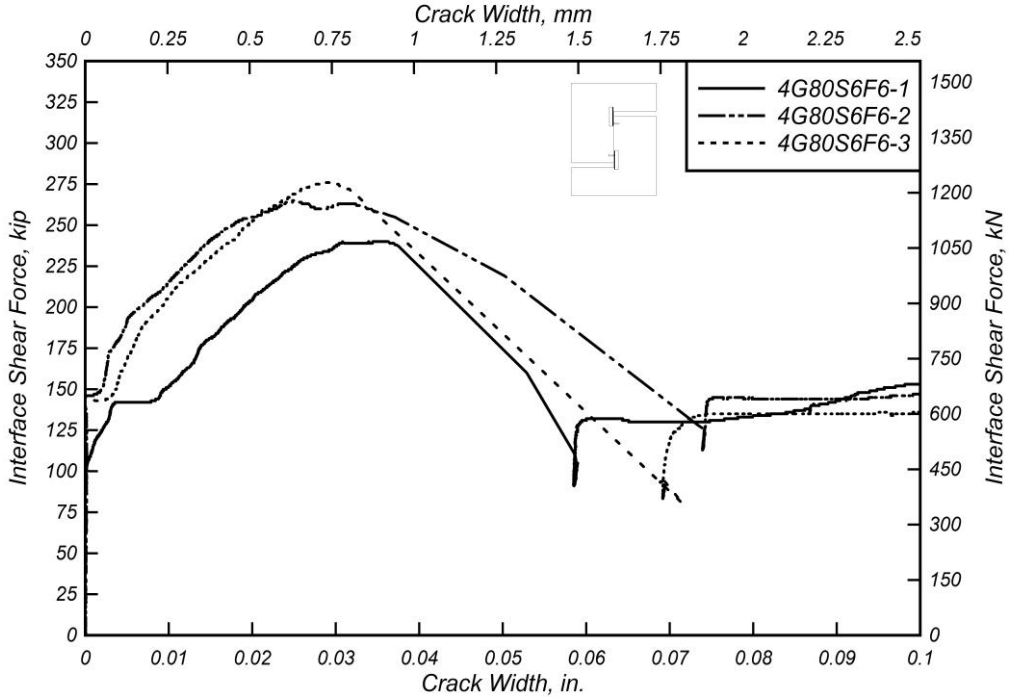

Figure 6.33: Interface shear force versus crack width for 4G80S6F6(1/8) specimens.

Table 6.39: 4G80S6F3(1/8) Specimen Crack Width Measurements.

Specimen	w_{ult}, in. (mm)	V_{ult}, kip (kN)	w_b, in. (mm)	V_b, kip (kN)
4G80S6F3(1/8)-1	0.0312 (0.7926)	228.01 (1014.2)	0.1652 (4.196)	158.03 (702.95)
4G80S6F3(1/8)-2	0.0426 (1.081)	223.16 (992.66)	0.1956 (4.969)	164.01 (729.55)
4G80S6F3(1/8)-3	0.0570 (1.447)	229.31 (1020.0)	0.2243 (5.698)	154.46 (687.07)
Mean	0.0436 (1.107)	226.83 (1009.0)	0.1951 (4.954)	158.83 (706.52)
Median	0.0426 (1.081)	228.01 (1014.2)	0.1956 (4.969)	158.03 (702.95)
STDEV	0.0129 (0.3278)	3.240 (14.41)	0.0296 (0.7515)	4.825 (21.46)
COV	30%	1%	15%	3%

Table 6.40: 4G80S6(1/8) Specimen Crack Width Measurements.

Specimen	w_{ult}, in. (mm)	V_{ult}, kip (kN)	w_b, in. (mm)	V_b, kip (kN)
4G80S6(1/8)-1	0.0256 (0.6510)	221.21 (983.98)	0.1732 (4.398)	145.00 (645.01)
4G80S6(1/8)-2	0.0327 (0.8314)	290.99 (1294.4)	0.2602 (6.610)	150.57 (669.77)
4G80S6(1/8)-3	0.0306 (0.7771)	203.91 (907.04)	0.1782 (4.526)	151.03 (671.81)
Mean	0.0297 (0.7532)	238.70 (1061.8)	0.2039 (5.178)	148.87 (662.20)
Median	0.0306 (0.7771)	221.21 (983.98)	0.1782 (4.526)	150.57 (669.77)
STDEV	0.0036 (0.0926)	46.10 (205.07)	0.0489 (1.242)	3.354 (14.92)
COV	12%	19%	24%	2%

Table 6.41: 4G80S6F6(1/8) Specimen Crack Width Measurements.

Specimen	w_{ult}, in. (mm)	V_{ult}, kip (kN)	w_b, in. (mm)	V_b, kip (kN)
4G80S6F6(1/8)-1	0.0356 (0.9042)	240.20 (1068.5)	0.1142 (2.900)	151.96 (675.95)
4G80S6F6(1/8)-2	0.0251 (0.6366)	264.66 (1177.3)	0.1449 (3.680)	160.53 (714.08)
4G80S6F6(1/8)-3	0.0289 (0.7341)	275.97 (1227.6)	0.1753 (4.452)	155.85 (693.25)
Mean	0.0299 (0.7583)	260.28 (1157.8)	0.1448 (3.678)	156.11 (694.42)
Median	0.0289 (0.7341)	264.66 (1177.3)	0.1449 (3.680)	155.85 (693.25)
STDEV	0.0053 (0.1354)	18.28 (81.33)	0.0305 (0.776)	4.292 (19.09)
COV	18%	7%	21%	3%

Table 6.42: Summary of Crack Width Measurements for 4G80S6F3(1/8), 4G80S6(1/8), and 4G80S6F6(1/8) Specimens.

Specimen	w_{ult}, in. (mm)	V_{ult}, kip (kN)	w_b, in. (mm)	V_b, kip (kN)
4G80S6F3(1/8)	0.0436 (1.107)	226.83 (1009.0)	0.1951 (4.954)	158.83 (706.52)
4G80S6(1/8)	0.0297 (0.7532)	238.70 (1061.8)	0.2039 (5.178)	148.87 (662.20)
4G80S6F6(1/8)	0.0299 (0.7583)	260.28 (1157.8)	0.1448 (3.678)	156.11 (694.42)

6.4 SUMMARY AND MAIN FINDINGS

This section provides a summary of experimental findings and a discussion on main findings regarding: (1) influence of shear interface preparation, and (2) influence of concrete strength on shear friction behavior. Comparisons between experimentally measured capacity and calculated capacities per AASHTO and ACI 318-14 code provisions are presented.

Figure 6.34 presents the peak shear stress normalized by measured concrete strength versus the reinforcing steel ratio normalized by the measured concrete strength and the elastic modulus of the reinforcing steel. The data points presented in this figure are experimentally determined peak loads for specimen groups compared to analyze the influence of shear interface preparation on shear friction for specimens constructed with #4 (#13M) reinforcing steel bars. Data points corresponding to test specimens 4G80S6(AC), 4G80S6(EA), 4G80S6(1/8), and 4G80S6(1/4) constructed with shear interface surface preparations As Cast, Exposed Aggregate, 1/8 in. (3.175 mm), and 1/4 in. (6.35 mm), respectively, are shown in this figure. Additionally, there are curves shown corresponding to AASHTO (2015) shear friction design equation (Equation 2-1), which limits the yield strength to f_y = 60 ksi (420 MPa), for a surface not intentionally roughened (As Cast), an Exposed Aggregate surface, a surface roughness of 1/4 in. (6.35 mm), a surface roughness of 1/8 in. (3.175 mm). In addition to the mentioned four curves using AASHTO (2015), an additional curve is shown in which a nominal yield strength limit of f_y = 80 ksi (550 MPa) for comparison with the test results shown in the figure. This indicates that the shear capacity design will remain conservative when allowing the nominal yield strength to be increased to 80 ksi (550 MPa).

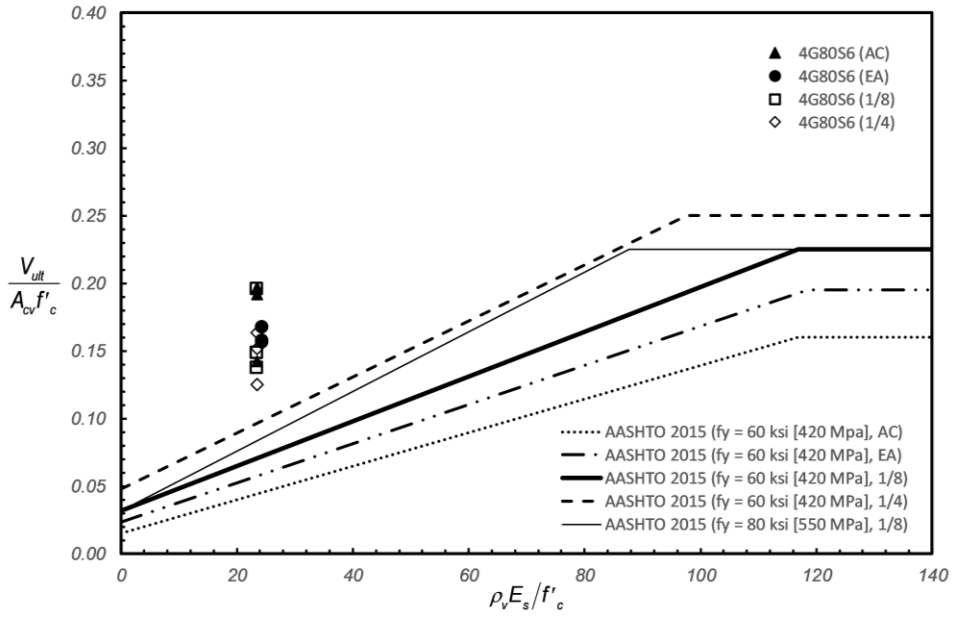

Figure 6.34: Experimental normalized peak shear stress versus normalized reinforcement stiffness across the interface – influence of interface preparation #4 (#13M) reinforcing steel bars.

Figure 6.35shows the peak shear stress normalized by measured concrete strength versus the reinforcing steel ratio normalized by the measured concrete strength and the elastic modulus of the reinforcing steel. The data points presented in this figure are experimentally determined peak loads for specimen groups compared to analyze the influence of shear interface preparation on shear friction for specimens constructed with #5 (#16M) reinforcing steel bars. Data points corresponding to test specimens 5G80S6(AC), 5G80S6(EA), 5G80S6(1/8), and 5G80S6(1/4) constructed with shear interface surface preparations As Cast, Exposed Aggregate, 1/8 in. (3.175 mm), and 1/4 in. (6.35 mm), respectively, are shown in this figure. As discussed in the previous paragraph, this figure also shows four AASHTO design equation curves corresponding to each surface preparation, and one additional one considering the AASHTO equation, but adjusted using a nominal yield strength of 80 ksi (550 MPa) for comparison purposes. All data points are above their respective AASHTO design equation curve. This indicates that allowing the nominal yield strength limit to be raised to 80 ksi (550 MPa) maintains a conservative design.

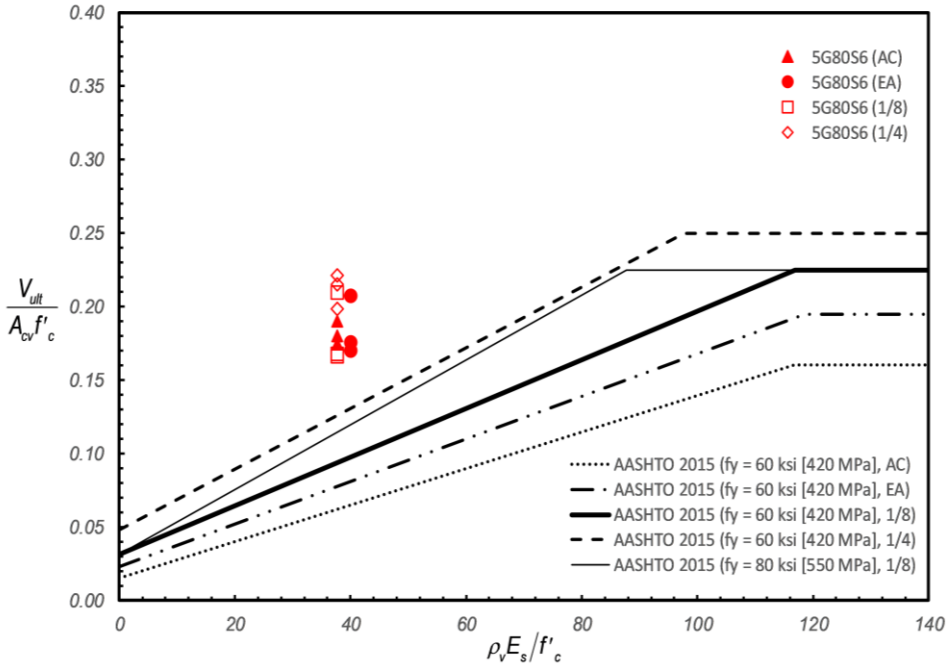

Figure 6.35: Experimental normalized peak shear stress versus normalized reinforcement stiffness across the interface – influence of interface preparation #5 (#16M) reinforcing steel bars.

Figure 6.36 presents the peak shear stress normalized by measured concrete strength versus the reinforcing steel ratio normalized by the measured concrete strength and the elastic modulus of the reinforcing steel. Data points corresponding to test results from specimens 4G80S6F3(1/8), 4G80S6(1/8), and 4G80S6F6(1/8) are presented in the figure.

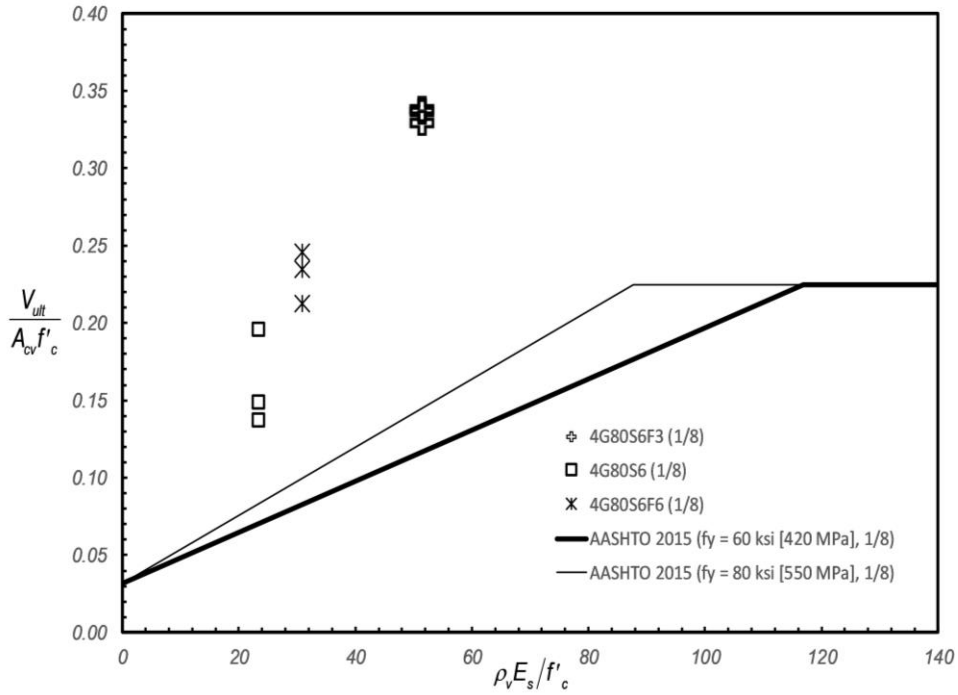

Figure 6.36: Experimental normalized peak shear stress versus normalized reinforcement stiffness across the interface – influence of nominal concrete strength.

Figure 6.37 and Figure 6.38 present the ratio of the experimentally measured peak loads, V_{max}, to the shear capacity per AASHTO (2015) and ACI 318-14 code provisions, respectively. In these figures, each data set consists of two columns. The first column corresponds to the ratio considering the nominal yield strength of f_y = 80 ksi (550 MPa). The second column corresponds to the ratio considering the nominal yield strength limit of f_y = 60 ksi (420 MPa). Table 6.43 shows a summary of the ratio of experimentally measured shear resistance to nominal interface shear resistance per AASHTO (2015) and ACI 318-14, V_{ult}/V_{ni}. As seen in the table, increasing the nominal yield strength to 80 ksi (550 MPa) reduces the V_{ult}/V_{ni} ratio in all cases for both code provisions. These results indicate that an increase in the nominal yield strength limit to 80 ksi (550 MPa) will provide a more efficient design while remaining conservative for both AASHTO (2015) and ACI 318-14 code provisions. It is important to note that when considering f_y = 80 ksi (550 MPa) all specimen groups indicate V_{ult}/V_{ni} ratios greater than 1.5, except for specimen groups 4G80S6(1/4) and 5G80S6(1/4). Additionally, the results show that ratios are larger when calculated per ACI 318-14 provisions, which indicates a higher level of conservatism.

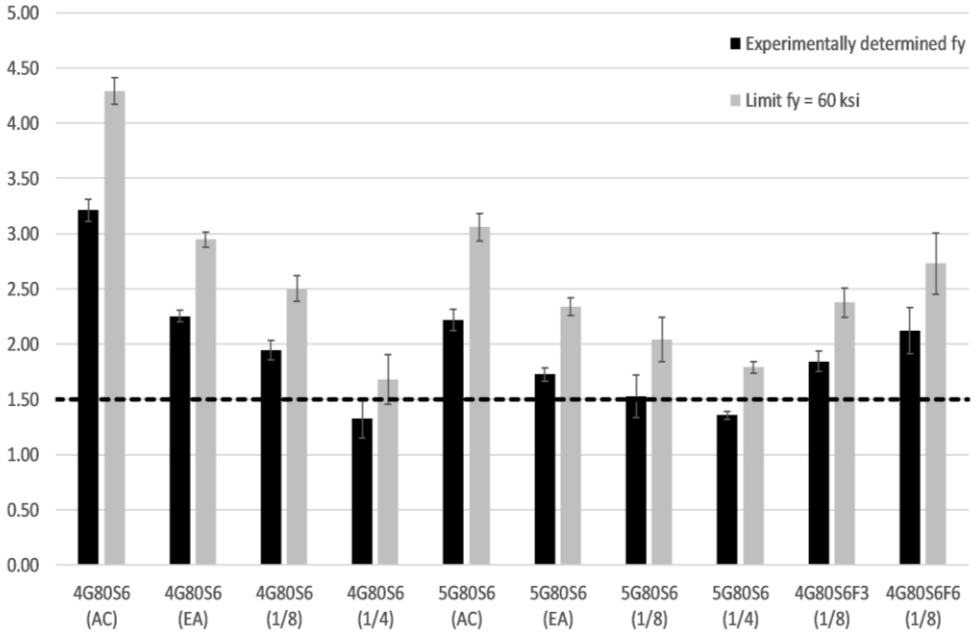

Figure 6.37: Comparison of experimentally measured strength with AASHTO (2015) calculated strength.

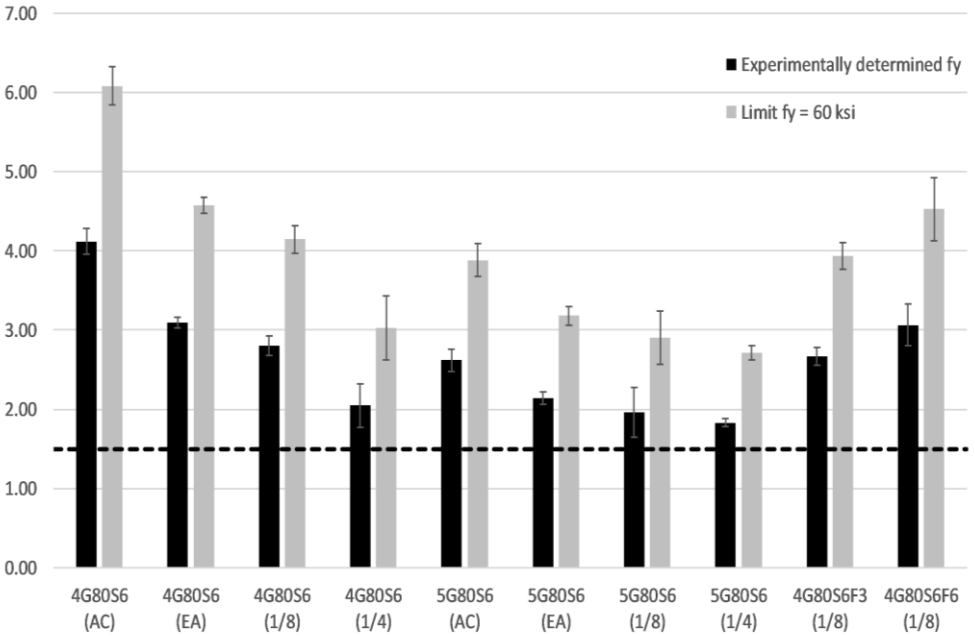

Figure 6.38: Comparison of experimentally measured strength with ACI 318-14 calculated strength.

Table 6.43: Ratio of Measured Strength, V_{ult}, to Probable Strength, V_p.

Specimen label	V_{ult}, kip (kN)	AASHTO (2015) Section 5.8.4				ACI 318-14 Section 22.9			
		Experimental f_y		Limit f_y = 60 ksi (420 MPa)		Experimental f_y		Limit f_y = 60 ksi (420 MPa)	
		V_{ni}, kip (kN)	V_{ult}/V_{ni}	V_{ni}, kip (kN)	V_{ult}/V_{ni}	V_{ni}, kip (kN)	V_{ult}/V_{ni}	V_{ni}, kip (kN)	V_{ult}/V_{ni}
4G80S6(AC)	262.67 (1168.4)	81.81 (363.92)	3.21	61.20 (272.23)	4.29	63.81 (283.86)	4.12	43.20 (192.16)	6.08
4G80S6(EA)	230.67 (1026.1)	102.35 (455.27)	2.25	78.30 (348.30)	2.95	74.45 (331.17)	3.10	50.40 (224.19)	4.58
4G80S6(1/8)	238.67 (1061.6)	122.88 (546.62)	1.94	95.40 (424.36)	2.50	85.08 (378.48)	2.81	57.60 (256.22)	4.14
4G80S6(1/4)	218.00 (969.71)	163.96 (729.31)	1.33	129.60 (576.49)	1.68	106.36 (473.09)	2.05	72.00 (320.27)	3.03
4G80S4(1/8)	238.33 (1060.2)	151.25 (672.78)	1.58	114.60 (509.77)	2.08	113.45 (504.63)	2.10	76.80 (341.62)	3.10
4G80S12(1/8)	160.33 (713.20)	94.52 (420.46)	1.70	76.20 (338.95)	2.10	56.72 (252.32)	2.83	38.40 (170.81)	4.18
5G80S6(AC)	260.00 (1156.5)	117.26 (521.59)	2.22	84.96 (377.92)	3.06	99.26 (441.52)	2.62	66.96 (297.85)	3.88
5G80S6(EA)	248.33 (1104.6)	143.70 (639.21)	1.73	106.02 (471.60)	2.34	115.80 (515.10)	2.14	78.12 (347.49)	3.18
5G80S6(1/8)	259.33 (1153.6)	170.14 (756.83)	1.52	127.08 (565.28)	2.04	132.34 (588.69)	1.96	89.28 (397.14)	2.90
5G80S6(1/4)	302.67 (1346.3)	223.03 (992.08)	1.36	169.20 (752.64)	1.79	165.43 (735.86)	1.83	111.60 (496.42)	2.71
4G80S6F3(1/8)	226.67 (1008.3)	122.88 (546.62)	1.84	95.40 (424.36)	2.38	85.08 (378.48)	2.66	57.60 (256.22)	3.94
4G80S6F6(1/8)	260.67 (1159.5)	122.88 (546.62)	2.12	95.40 (424.36)	2.73	85.08 (378.48)	3.06	57.60 (256.22)	4.53

7.0 CONCLUSION

The objective of this research was to evaluate and define the performance of concrete shear friction applications when designed with high strength steel (HSS) reinforcing steel bars. This was accomplished by implementing an experimental program that consisted in testing forty-five push-off test specimens. The experimental variables were reinforcing steel grade, interface surface preparation, reinforcing steel bar spacing, reinforcing steel bar size, and concrete strength. The test program included specimens with four reinforcing steel types (ASTM A706 Grade 60 (420 MPa), ASTM A708 Grade 80 (550 MPa), ASTM A615 Grade 100 (690 MPa), and ASTM A1035 Grade 120 (830 MPa)), four interface preparations (As Cast, Exposed Aggregate, 1/8 in. (3.175 mm), and 1/4 in. (6.35 mm)), three reinforcing steel bar spacings (4 in. (101.6 mm), 6 in. (152.4 mm), and 12 in. (304.8 mm)), two reinforcing steel bar sizes (#4 (#13M) and #5 (#16M)), and three specified concrete strengths (3 ksi (20.7 MPa), 5 ksi (34.5 MPa), and 6 ksi (41.4 MPa)).

The following conclusions can be drawn from the test results presented in this research report:

1. The use of HSS reinforcing bars as interface shear reinforcement had a minor increase on peak shear forces. However, the increase in peak forces were accompanied by an increase in crack width and interface shear displacement.

2. Higher peak shear forces were observed in specimens with reduced spacing between reinforcing steel bars crossing the shear interface. Specimens with the same concrete shear interface area were tested. The specimens with reinforcing steel bars spaced at 6 in. (152.4 mm) and reinforcing steel bars spaced at 4 in. (101.6 mm) exhibited similar peak shear forces when compared to specimens with reinforcing steel bars spaced at 12 in. (304.8 mm). In addition, specimens with 4 in. (101.6 mm) spacing between reinforcing steel bars presented lower interface shear displacement and crack width at peak shear force compared to specimens with 6 in. (152.4 mm) spacing between reinforcing steel bars. This is likely a result of the higher reinforcement ratio in specimens with lower spacings between reinforcing steel bars, as it is directly related to the clamping force.

3. An increase in peak shear load was observed in specimens reinforced with #5 (#16M) steel bars when compared to specimens reinforced with #4 (#13M) bars, except for specimens constructed with an As Cast shear interface surface preparation, which exhibited similar peak shear loads when reinforcing steel bar size was increased. Additionally, specimens with #5 (#16M) reinforcing steel bars exhibited smaller interface shear displacements at peak shear load when compared to specimens with #4 (#13M) reinforcing steel bars, except for specimens constructed with a shear interface surface roughened to an amplitude of 1/4 in. (6.35 mm).

4. Results indicate that surface preparation has an impact on shear friction performance. However, substantial variability was observed. While mean trends from testing results are clear in most cases, statistical significance of results was not assessed due to the limited number of test specimens tested per group.

5. Specimens reinforced with HSS bars exhibited higher sustained (i.e. post-peak) interface shear forces. Specimens with Grade 80 and Grade 100 reinforcing steel bars across the interface exhibited similar sustained post-peak interface shear forces, although specimens with Grade 120 reinforcing steel bars across the interface exhibited the largest sustained interface shear forces. Since the main mechanism involved with load transfer in the post-peak is due to dowel action, these results indicate that using higher strength steel reinforcement leads to the development of greater capacities due to dowel action and therefore larger sustained post-peak loads.

6. In some cases, Exposed Aggregate surface preparation on the shear interface enhanced the aggregate interlock and allowed it to contribute to the post-peak shear capacity. Nonetheless, the limited testing performed indicates that this aggregate interlock enhancement does not always develop. Additional testing and surface preparation trials are recommended to gain further insight into the Exposed Aggregate surface preparation, possible products, and impact on the behavior and performance of shear friction applications.

7. None of the measurements from the strain gauges indicated that the reinforcing steel bars reached the nominal yield strain. Even though results during a previous testing program (SPR762) had shown yielding forces being achieved before the peak shear force, similar results were not found in this research program.

8.0 REFERENCES

American Association of State Highway and Transportation Officials (1998). *AASHTO LRFD Bridge Design Specifications, Customary U.S. Units*. Washington, DC.

American Association of State Highway and Transportation Officials (2004). *AASHTO LRFD Bridge Design Specifications, Customary U.S. Units*. Washington, DC.

American Association of State Highway and Transportation Officials (2007). *AASHTO LRFD Bridge Design Specifications, Customary U.S. Units*. Washington, DC.

American Association of State Highway and Transportation Officials (2012). *AASHTO LRFD Bridge Design Specifications, Customary U.S. Units*. Washington, DC.

American Association of State Highway and Transportation Officials (2014). *AASHTO LRFD Bridge Design Specifications, Customary U.S. Units*. Washington, DC.

American Concrete Institute (2002). *Building Code Requirements for Structural Concrete and Commentary* (Standard No. ACI 318-02). Farmington Hills, MI.

American Concrete Institute (2011). *Building Code Requirements for Structural Concrete and Commentary* (Standard No. ACI 318-11). Farmington Hills, MI.

American Concrete Institute (2014). *Building Code Requirements for Structural Concrete and Commentary* (Standard No. ACI 318-14). Farmington Hills, MI.

ASTM International (2012). *Standard Practice for Making and Curing Concrete Test Specimens in the Field* (Standard No. C31/31M-12). West Conshohocken, PA, DOI: 10.1520/C0031_C0031M-12.

ASTM International (2012). *Standard Test Method for Compressive Strength of Cylindrical Concrete Specimens* (Standard No. C39/C39M-12a). West Conshohocken, PA, DOI: 10.1520/C0039_C0039M-12A.

ASTM International (2012). *Standard Test Method for slump of Hydraulic-Cement Concrete* (Standard No. C143/C143M-12). West Conshohocken, PA, DOI: 10.1520/C0143_C0143M-12.

ASTM International (2014). *Standard Specification for Deformed and Plain Carbon-Steel Bars for Concrete Reinforcement* (Standard No. A615/A615M-14). West Conshohocken, PA, DOI: 10.1520/A0615_A0615M-14.

ASTM International (2014). *Standard Specification for Low-Alloy Steel Deformed and Plain Bars for Concrete Reinforcement* (Standard No. A706/A706M-14) West Conshohocken, PA, DOI: 10.1520/A0706_A0706M-14.

ASTM International (2014). *Standard Test Method for Air Content of Freshly Mixed Concrete by the Pressure Method* (Standard No. C231/C231M-14). West Conshohocken, PA, DOI: 10.1520/C0231_C0231M-14.

ASTM International (2016). *Standard Specification for Deformed and Plain, Low-Carbon, Chromium, Steel Bars for Concrete Reinforcement* (Standard No. A1035/A1035M-16b). West Conshohocken, PA, DOI: 10.1520/A1035_A1035M-16B.

ASTM International (2016). *Standard Test Methods for Tension Testing of Metallic Materials* (Standard No. E8/E8M-16a) West Conshohocken, PA, DOI: 10.1520/E0008_E0008M-16a.

ASTM International (2016). *Standard Practice for Verification and Classification of Extensometer Systems* (Standard No. E83-10a). West Conshohocken, PA, DOI: 10.1520/E0083-10A.

Barbosa, A. R., Trejo, D., & Nielson, D. (2017). Effect of High-Strength Reinforcement Steel on Shear Friction Behavior. *Journal of Bridge Engineering, 22*(8). doi:10.1061/(asce)be.1943-5592.0001015

Barbosa, A., Trejo, D., & Nielson, D. (2017). *High Strength Reinforcing Steel Bars: Concrete Shear Friction Interface* (Publication No. FHWA-OR-RD-17-08). Salem, OR: Oregon Department of Transportation.

Birkeland, P., & Birkeland, H. (1966). Connections in Precast Concrete Construction. *ACI Journal Proceedings, 63*(3), 345-368. doi:10.14359/7627

Fang, Z., Jiang, H., Liu, A., Feng, J., & Chen, Y. (2018). Horizontal Shear Behaviors of Normal Weight and Lightweight Concrete Composite T-Beams. *International Journal of Concrete Structures and Materials, 12*(1). doi:10.1186/s40069-018-0274-3

Harries, K., Zeno, G., & Shahrooz, B. (2012). Toward an Improved Understanding of Shear-Friction Behavior. *ACI Structural Journal, 109*(6), 835-844. doi:10.14359/51684127

Hofbeck, J., Ibrahim, I., & Mattock, A. (1969). Shear Transfer in Reinforced Concrete. *ACI Journal Proceedings, 66*(2), 119-128. doi:10.14359/7349

Hwang, S., Yu, H., & Lee, H. (2000). Theory of interface shear capacity of reinforced concrete. *Journal of Structural Engineering, 126*(6), 700-707. doi:10.1061/(ASCE)0733-9445(2000)126:6(700)

Júlio, E. N., Branco, F. A., & Silva, V. D. (2004). Concrete-to-concrete bond strength. Influence of the roughness of the substrate surface. *Construction and Building Materials, 18*(9), 675-681. doi:10.1016/j.conbuildmat.2004.04.023

Kahn, L. F., & Mitchell, A. (2002). Shear Friction Tests with High-Strength Concrete. *ACI Structural Journal, 99*(1), 98-103. doi:10.14359/11040

Kahn, L. F., & Slapkus, A. (2004). Interface Shear in High Strength Composite T-Beams. *PCI Journal, 49*(4), 102-110. doi:10.15554/pcij.07012004.102.110

Kim, Y. H., Hueste, M. B., Trejo, D., & Cline, D. B. (2010). Shear Characteristics and Design for High-Strength Self-Consolidating Concrete. *Journal of Structural Engineering, 136*(8), 989-1000. doi:10.1061/(asce)st.1943-541x.0000194

Kovach, J., & Naito, C. (2008). *Horizontal Shear Capacity of Composite Concrete Beams without Interface Ties* (Working paper No. 08-05). Bethlehem, PA: Advanced Technology for Large Structural Systems. Retrieved from https://www.lehigh.edu/~cjn3/ATLSS-08-05.pdf.

Krc, K., Wermager, S., Sneed, L. H., & Meinheit, D. (2016). Examination of the Effective Coefficient of Friction for Shear Friction Design. *PCI Journal, 61*(6). doi:10.15554/pcij61.6-01

Li, C., Lequesne, R., & Matamoros, A. (2017). *Composite Action in Prestressed NU I-Girder Bridge Deck Systems Constructed with Bond Breakers to Facilitate Deck Removal* (Tech. No. K-TRAN: KU-15-1). Topeka, KS: Kansas Department of Transportation.

Loov, R. E., & Patnaik, A. K. (1994). Horizontal Shear Strength of Composite Concrete Beams with a Rough Interface. *PCI Journal, 39*(1), 48-69. doi:10.15554/pcij.01011994.48.69

Mattock, A. H., Li, W. K., & Wang, T. C. (1976). Shear transfer in lightweight reinforced concrete. *PCI Journal, 21*(1), 20-39. doi:10.15554/pcij.01011976.20.39

Mansur, M. A., Vinayagam, T., & Tan, K. (2008). Shear Transfer across a Crack in Reinforced High-Strength Concrete. *Journal of Materials in Civil Engineering, 20*(4), 294-302. doi:10.1061/(asce)0899-1561(2008)20:4(294)

Menzel, C. (1939). Some Factors Influencing Results Of Pull-Out Bond Tests. *ACI Journal Proceedings, 35*(6), 517-542. doi:10.14359/8507

Mirza, S., Hatzinikolas, M., & MacGregor, J. (1979). Statistical Descriptions of Strength of Concrete. *Journal of the Structural Division, 105*(ST6), 1021-1037.

Oregon Department of Transportation (2014). *Bridge Design and Drafting Manual*. Oregon Department of Transportation, Salem, OR. Retrieved from https://www.oregon.gov/odot/Bridge/Pages/Bridge-Design-Manual.aspx

Oregon Department of Transportation (2015). *Standard Specifications*. Oregon Department of Transportation, Salem, OR. Retrieved from https://www.oregon.gov/odot/Business/Pages/Standard_Specifications.aspx

Paulay, T., & Park, R. (1975). *Reinforced concrete structures*. New York, NY: John Wiley & Sons.

Patnaik, A. K. (2001). Behavior of Composite Concrete Beams with Smooth Interface. *Journal of Structural Engineering, 127*(4), 359-366. doi:10.1061/(asce)0733-9445(2001)127:4(359)

Saemann, J., & Washa, G. (1964). Horizontal Shear Connections between Precast Beams and Cast-in -Place. *ACI Journal Proceedings, 61*(11), 1383-1410. doi:10.14359/7832

Santos, P. M., & Júlio, E. N. (2012). A state-of-the-art review on shear-friction. *Engineering Structures, 45*, 435-448. doi:10.1016/j.engstruct.2012.06.036

Santos, P., & Julio, E. (2014). Interface shear transfer on composite concrete members. *ACI Structural Journal, 111*(1), 113-122.

Scholz, D., Wallenfelsz, J., Lijeron, C., & Roberts-Wollmann, C. (2007). *Recommendations for the Connection between Full-Depth Precast Bridge Deck Panel Systems and Precast I-Beams* (Tech. No. FHWA/VTRC 07-CR17). Richmond, VA: Virginia Department of Transportation.

Scott, J. (2010). *Interface shear strength in lightweight concrete bridge girders* (Master's thesis, Virginia Polytechnic Institute and State University, 2010). Blacksburg, VA.

Shaw, D. M., & Sneed, L. H. (2014). Interface shear transfer of lightweight-aggregate concretes cast at different times. *PCI Journal, 59*(3), 130-144. doi:10.15554/pcij.06012014.130.144

Soltani, M., & Ross, B. E. (2017). Database Evaluation of Interface Shear Transfer in Reinforced Concrete Members. *ACI Structural Journal, 114*(2). doi:10.14359/51689249

Trejo, D., Barbosa, A., & Link, T. (2014). *Seismic Performance of Circular Reinforced Concrete Bridge Columns Constructed with Grade 80 Reinforcement* (Publication No. FHWA-OR-RD-15-02). Salem, OR: Oregon Department of Transportation.

Trejo, D., Head, M., Mander, J., Mander, T., Henley, M., Scott, R., Patil, S. (2011). *Development of Precast Bridge Deck Overhang System: Technical Report* (Publication No. FHWA/TX-10/0-6100-1). Austin, TX: Texas Department of Transportation.

Wallenfelsz, J. A. (2006). *Horizontal shear transfer for full-depth precast concrete bridge deck panels* (Master's thesis, Virginia Polytechnic Institute and State University, 2006). Blacksburg, VA.

Walraven, J., & Reinhardt, H. (1981). Theory and experiments on the mechanical behaviour of cracks in plain and reinforced concrete subjected to shear loading. *HERON, 26*(1A), 1-68.

Waweru, R., Palacios, G., & Chao, S. (2014). Horizontal Shear Strength of Full-Scale Composite Box and Slab Bridge Beams Having Horizontal Shear Reinforcement with Limited Development Length. In *PCI Convention and National Bridge Conference*. Washington D.C.

Zeno, G. (2009). *Use of High-Strength Steel Reinforcement in Shear Friction Applications* (Unpublished master's thesis). University of Pittsburgh.